HTBS 2019

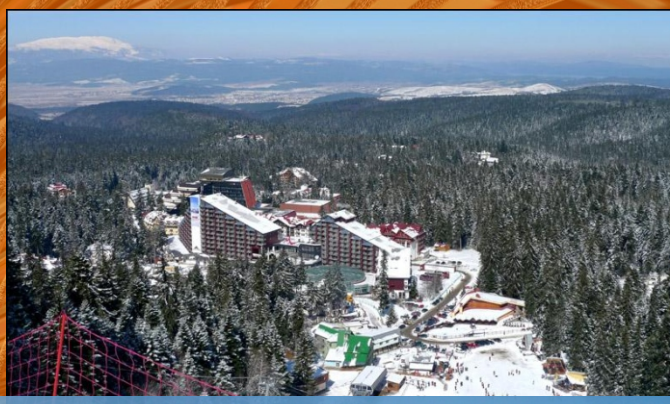

IV INTERNATIONAL SCIENTIFIC CONFERENCE

HIGH TECHNOLOGIES. BUSINESS. SOCIETY 2019

11-14.03.2019, BOROVETS, BULGARIA

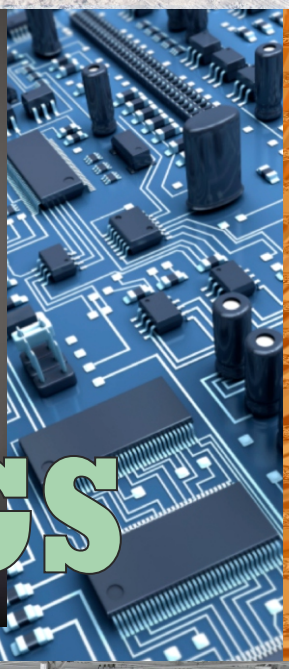

PROCEEDINGS

VOLUME I "HIGH TECHNOLOGIES"

ISSN 2535-0005 (PRINT)
ISSN 2535-0013 (ONLINE)

SCIENTIFIC-TECHNICAL UNION OF MECHANICAL ENGINEERING - INDUSTRY 4.0

INTERNATIONAL SCIENTIFIC CONFERENCE

HIGH TECHNOLOGIES. BUSINESS. SOCIETY

11-14.03.2019, BOROVETS, BULGARIA

PROCEEDINGS

YEAR III, ISSUE 1 (4), SOFIA, BULGARIA 2019

VOLUME I "HIGH TECHNOLOGIES"

ISSN 2535-0005(PRINT
ISSN 2535-0013 (ONLINE)

PUBLISHER:

**SCIENTIFIC TECHNICAL UNION OF MECHANICAL ENGINEERING
INDUSTRY-4.0**

108, Rakovski Str., 1000 Sofia, Bulgaria
tel. (+359 2) 987 72 90,
tel./fax (+359 2) 986 22 40**,**
office@hightechsociety.eu
www.hightechsociety.eu

INTERNATIONAL EDITORIAL BOARD

C O N T E N T S

GREEN CHEMISTRY: CARBON-BEARING MINERALS AS A SOURCE OF NANOCARBONS

Prof. Huczko A.[*1], Dr Dąbrowska A.[1], Dr Fronczak M.[1], Dr Strachowski P.[1], Sokołowski S.[1], Prof. Bystrzejewski M.[1], Prof. Subedi D.P. [2], Dr Kafle B.P.[2]

Department of Chemistry, Warsaw University, Warsaw, Poland[1]

School of Science, Kathmandu University, Dhulikhel, Kavre, Nepal[2]

[*]ahuczko@chem.uw.edu.pl

Abstract: *Natural abundant, cheap and widely used raw materials like calcite, magnesite and dolomite contain elemental carbon up to several wt percent. Such rocks have been chemically processed here using combustion synthesis route to yield novel nanocarbons including two-dimensional graphene-like structures. The fast and efficient reduction of powdered minerals with strong reducer (Mg) produces, after chemical wet purification, carbon nanomaterial which was analyzed using different techniques like XRD and SEM. This 'combustion' process was followed on-line to evaluate reaction duration (usually within 1 sec).*

Keywords: COMBUSTION SYNTHESIS, CARBOB-BEARING MINERALS, NANOCARBONS

1. Introduction

Carbon is one of the most important elements in the world as it builds both organic and inorganic matter. Till XX century only two allotropes of carbon were known, graphite and diamond (in addition to amorphous carbon, i.e. soot or carbon black). Recent decades brought into a daylight, however, new nanocarbon allotropes[1]. In 1985 the fullerenes were discovered[2], with the importance of the discovery honored with a Nobel Price (1996). Soon later, carbon nanotubes (even called the 'black diamonds of XX century') were shown to the world (1991)[3]. The very beginning of the XXI century brought one, even more important discovery of next new carbon allotrope – graphene[4]. Graphene and graphene-related nanomaterials are indeed a revolutionary materials. They have many applications replacing conventional materials as well as the ability to support applications previously not possible before the advent of two-dimensional materials. The applications of graphene are truly endless and many are yet to be conceived of[5].

Essentially, the nanomaterials are synthesized using either 'top-down' (miniaturization) or 'bottom-up' approach. The latter one makes the use of the smallest 'building blocks' (atoms, ions and molecules) which form nanostructures via coalescence and coagulation during quench. Those starting promoters are usually produced via high-energy activation of a bulk material (i.e. plasma, laser or high-temperature activation). Dyjak et al.[6] synthesized an intriguing carbon nitride C_3N_4 via high-temperature pyrolysis of melamine. In a search for novel nanocarbons, Manning et al.[7] prepared the exfoliated graphite (in minuscule, however, amounts) from fluorinated graphite already in 1999 using inductively coupled Ar plasma. High energy consumption is, however, a drawback of the listed routes.

Here we propose a SHS (Self-propagating High-temperature Synthesis) approach for the formation of nanocarbons. SHS also termed combustion synthesis (CS) is a strong high-temperature, exothermic and autothermic, and fast redox reaction that leads to the formation of new thermodynamically stable nanomaterials with structures often not obtained under conventional conditions[8]. We reported earlier[9] that silicon carbide nanowires were efficiently synthesized via silicon-polytetrafluoroethene thermolysis. Later on, the solid carbon nanomaterials were successfully obtained using the reduction of different carbon-bearing compounds. Thus, Dąbrowska et al.[10] atomized different carbonates by using strong reducers to obtain novel nanomaterials. Such research was later continued towards the heterogeneous autothermic reduction of CO_2 and CO to elements using the following reducers: Li, Mg, Ca, B, Ti, Zr, and Al[11]. The solid product contained the layered graphite and nanocarbides. Novel carbon nanostructures were also obtained by Huczko et al.[12] from the mixtures of strong metal reducers and strong oxidizers (fluorinated graphite, TEFLON®, PTFE and PVC). Few-layered graphene was also produced via reduction of graphite oxide and fluorinated graphite using different reducers[13]. Recently, Dyjak et al.[14] prepared porous graphenic nanomaterials through a self-sustaining magnesiothermic reduction of oxalic acid.

Here, we've extended such research into a field of 'Green Chemistry' – processing of cheap and abundant minerals (which contain elemental carbon) via combustion synthesis. Specifically, the minerals (natural carbonates) of Polish and Nepal origin were chosen as oxidants with a relatively high content of elemental carbon. A phthalic acid, as a pure carbon-bearing reference reactant, was also reduced with magnesium.

2. Experimental

The reduction of carbon-bearing compounds was carried out in the stainless-steel high-pressure vessel (volume 375 cm^3, Fig. 1) following the protocol outlined earlier[9]. The reactor (a modified bomb calorimeter) is resistant to extreme process parameters (very high temperature, pressure gradients, and chemically aggressive reaction environment) and was pre-tested at the pressure up to 10 MPa.

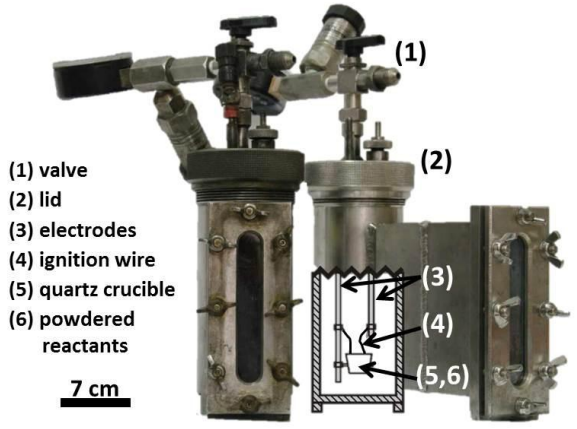

Fig. 1*. Modified bomb calorimeter as a CS reactor*

A stoichiometric mixture of the reactants (Mg powder/carbon-bearing oxidant) was powdered and loaded into the quartz crucible under the pre-planned atmosphere (Ar) and pressure. The reaction was started by the resistive heating of the crucible with the igniter (carbon thread). After combustion and cooling down the system the solid raw product was collected. The product was later purified (leaching of Mg/MgO compounds using hot 3M HCl). The final sample contained mostly carbon (its content was analyzed using the elemental analysis). Both raw and purified products were examined using SEM (morphology) and XRD (phase composition) analyses.

3. Results and Discussion

3.1. System $Mg/C_6H_4(COOH)_2$

The combustion of minerals was pre-tested (2 runs) with the magnesiothermic decomposition of the phthalic acid, a carbon-rich (58 wt% of C) commodity chemical produced on a large scale, following the reaction scheme

$$4\ Mg + C_6H_4(COOH)_2 = 8\ C + 4\ MgO + 3\ H_2$$

For a better conversion, 2-fold excess of a reducer (Mg powder, below 40 μm) was used. The operating parameters of combustions are shown in Table 1.

Table 1. Combustion of $Mg/C_6H_4(COOH)_2$ mixture

Run #	1 – 1	1 – 2
Combustion atmosphere/ Starting pressure, MPa	Ar, 0.1	Ar, 1.0
Peak pressure, MPa	1.1	3.2
Starting mass of reactants, g	6.55	7.21
Mass of solid product, g	6.08	6.57
Mass decrease, %	7.2	8.9
Starting mass of raw product, g	6.04	6.2
Mass of purified product, g	2.31	2.45
Mass decrease, %	61.8	60.5

The combustion was easily initiated and strongly exothermic reaction was accompanied by a distinct pressure increase. The mass decrease of reactants was relatively low (below 10%) thus confirming the desirable reaction scheme. Puffy, greyish/blackish product was collected and leached with HCl. Up to 40 wt% of the raw product was recovered as an insoluble blackish residue (carbon-containing phase). The change of the starting pressure does not seem to influence the process. Fig. 2 and 3 present the representative images (SEM observation) of the raw and purified products.

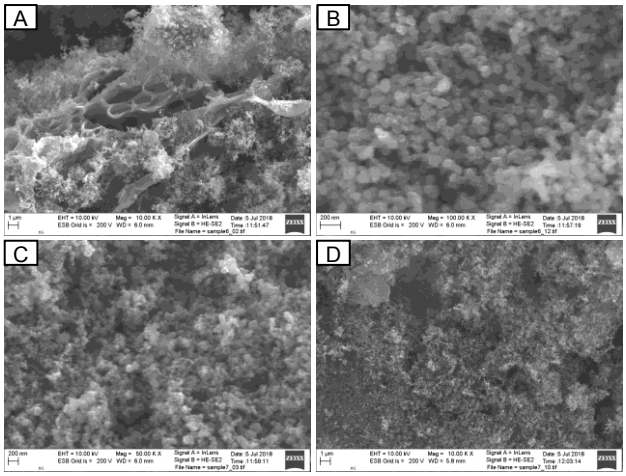

***Fig. 2**. Run # 1-1. SEM images of raw (A-B) and purified (C-D) product*

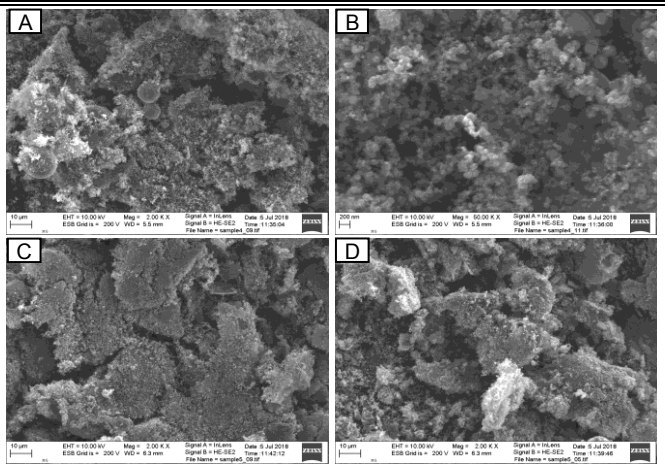

***Fig. 3**. Run # 1-2. SEM images of raw (A-B) and purified (C-D) product*

The raw product is dominated by nanometric crystallites of MgO, with some larger particles of un-reacted Mg. The leaching essentially does not change the product morphology thus confirming that the vast part of produced MgO is covered with a thin nanocarbon layer, insoluble in HCl. The EDX analyses of purified products fully confirmed that observation (Table 2).

Table 2. The results of EDX analyses of purified products

Run #	1 – 1	1 – 2
C content, wt%	61-63	72-75
O content, wt%	18-23	13-16
Mg content, wt%	15-19	10-11

The results of those reference combustions showed that magnesium effectively reduces oxygen-containing organic matter yielding the final nanopowder composed mostly of C (60-70 wt%). This nanocarbon material dominates the purified product which, however, still contains MgO nanocrystallites encapsulated in a carbon shell.

3.2. System Mg/magnesite $MgCO_3$ (Szklary, Poland)

The composition of magnesite (mostly nanometric powder, Fig. 4) was analyzed with EDX technique (the spectra not shown here). The results (C, Mg, O and Si content 7.7, 21.3, 49.8, and 20.3 wt %, respectively) confirmed that it is mostly composed of $MgCO_3$ with some silica/silicates admixtures, as expected for a mineral.

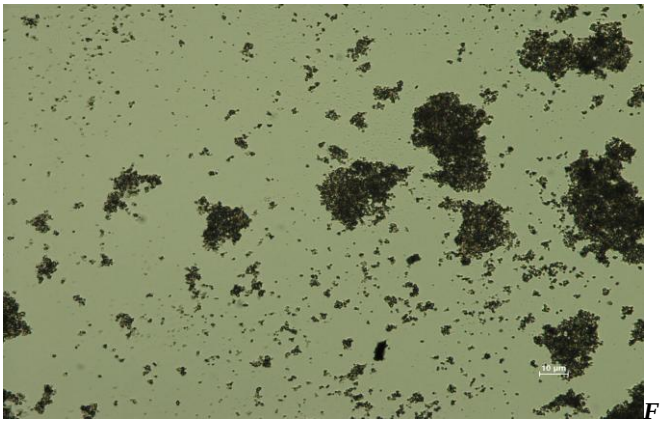

***Fig. 4**. Fine-grinded magnesite (Szklary, Poland)*

The mineral was reduced with magnesium (Mg powder, below 40 μm) following the reaction scheme

$$2\ Mg + MgCO_3 = C + 3\ MgO$$

This reaction can be, however, accompanied by the parallel thermal decomposition of magnesium carbonate with the evolution of carbon dioxide carrying away the carbon from the solid products

$$MgCO_3 \rightarrow MgO + CO_2$$

Thus, the final composition of the solid product is governed by the kinetics of both competing reactions. The operating parameters of all combustions (stoichiometric composition of reactants) are shown in Table 3. In runs 2-2 and 2-4 the starting mixture was additionally ball-milled (2 h) in hexane.

Table 3. Combustion of Mg/magnesite mixture

Run #	2 – 1	2 – 2	2 – 3	2 – 4
Combustion atmosphere/ Starting pressure, MPa	Ar, 0.1	Ar, 0.1	Ar, 1.0	Ar, 1.0
Peak pressure, MPa	0.4	0.3	1.9	1.9
Starting mass of reactants, g	5.47	3.46	6.91	3.38
Mass of solid product, g	5.24	3.16	6.07	3.16
Mass decrease, %	4.2	8.7	12.2	6.5
Starting mass of raw product, g	4.77	2.7	5.19	2.54
Mass of purified product, g	0.94	0.51	0.82	0.42
Mass decrease, %	80.3	81.1	84.2	83.5
Combustion duration, sec	2.52	3.34	1.3	2.27

The reaction mixture was easily and effectively combusted with a pressure jump caused by a heat-up of reactants and the evolution of hot gaseous by-products. The mass decrease of starting mixture was found to be within ca 10.0 wt%. Thus, one can conclude that the thermal pyrolysis of a carbonate (directly into MgO and CO_2) is responsible for the loss of only below 20 wt % of starting carbonate while its almost total conversion is dominated by a fast (well below 5 sec, Table 3) direct magnesiothermic reduction following the main reaction scheme. This conclusion was confirmed by the elemental analysis (C content) of reactants. Puffy, greyish/blackish product was collected and leached with HCl. The mass of purified product was monitored and compared to that of raw material. In agreement with the reduction stoichiometry up to 20 wt% of the raw product was insoluble (carbon phase). Neither the change of the starting pressure nor the prolonged milling in hexane influenced the process. Fig. 5 presents the representative images (SEM observation) of the reactants.

The starting reactants (A-B) are inhomogeneous mixture of micron-sized particles which, during the combustion, form mostly the conglomerates of nanosized MgO crystallites. Those are essentially removed during the acid leaching but the nanostructure of the solid residue (mostly carbon material) is still preserved. New structures are, however, also spotted in a purified product, i.e. nanowires (probably SiC[8]) and layered graphene-related nanomaterial. XRD spectra of selected samples are shown in Fig. 6.

Mg and $MgCO_3$ are the main components of starting mixture (A) with some silica/silicates as the minor impurity of a magnesite. The XRD spectrum of the raw product (B) is completely different thus confirming the deep transformation of the magnesite during the reduction. MgO dominates the product with some traces of un-reacted Mg. Carbon phase is also present while silicon elemental phase presence is the result of either silica/silicates or crucible material magnesiothermic reduction. Carbon phase dominates the

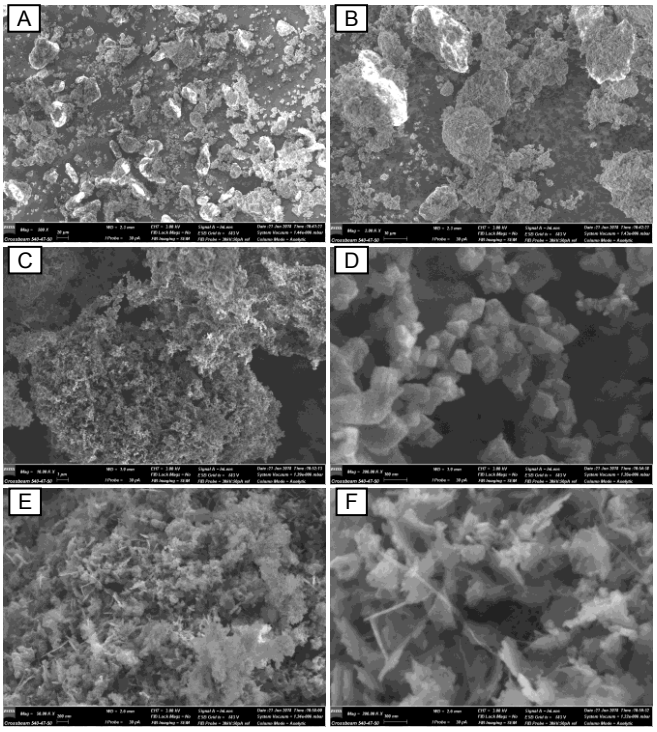

Fig. 5. *Run # 2-4. SEM images of starting mixture (A-B), raw (C-D) and purified (E-F) product*

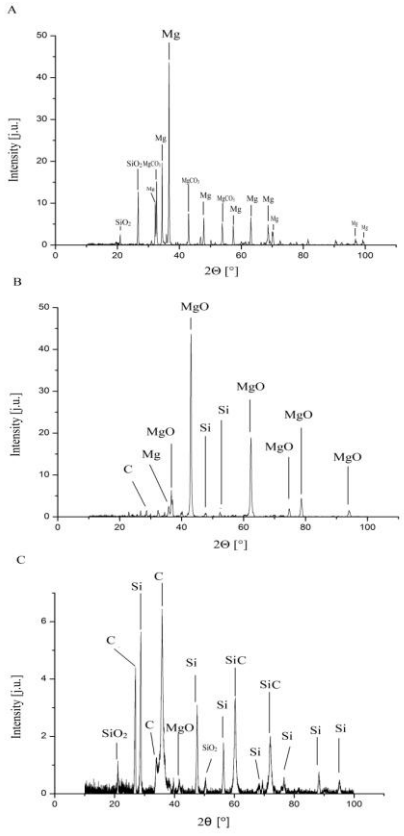

***Fig. 6**. XRD spectra (run # 2-2) of selected samples: A – starting mixture; B – raw product; C – purified product*

purified product (C) while SiO_2, Si, MgO, and SiC are the side admixtures still present in the sample. The composition of the purified product confirms that alkaline components have not been removed during the acid leaching while SiC was formed from elemental silicon and carbon which dominates the reactants.

The EDX analyses of a purified product fully confirmed that finding with the following content of the main elements: C – 51.7, Mg – 0.9, O – 16.5, and Si – 30.9 wt %.

3.3. System Mg/dolomite (Kavre,Nepal)

Powdered dolomite (calcium magnesium carbonate) was also reduced with Mg metal via combustion synthesis following the reaction scheme

$$4\ Mg + CaMg(CO_3)_2 = 2\ C + CaO + 5\ MgO$$

Again, the parallel high-temperature thermal decomposition of this complex carbonate is also possible. All combustions were easily initiated and greyish/blackish fine powder was collected for the purification and the following analyses. The operational parameters of those combustions are shown in Table 4.

Table 4. *Combustion of Mg/dolomite mixture*

Run #	3 – 1	3 – 2
Combustion atmosphere/ Starting pressure, MPa	Ar, 0.1	Ar, 1.0
Peak pressure, MPa	1.0	2.0
Starting mass of reactants, g	7.11	10.05
Mass of solid product, g	7.04	9.96
Mass decrease, %	1.0	0.9
Starting mass of raw product, g	6.78	9.61
Mass of purified product, g	0.71	1.3
Mass decrease, %	89.5	86.5

The very law mass decrease (ca 1 wt%) of solid reactants during combustion confirms practically the only reaction channel as shown in the desired scheme above. Above 10 % of the solid product (nanocarbon phase) was recovered after the purification stage. The change of the starting combustion pressure thus not seem to influence the process confirming its course entirely in solid-liquid phase. The representative SEM images of the selected products are shown in Fig. 7.

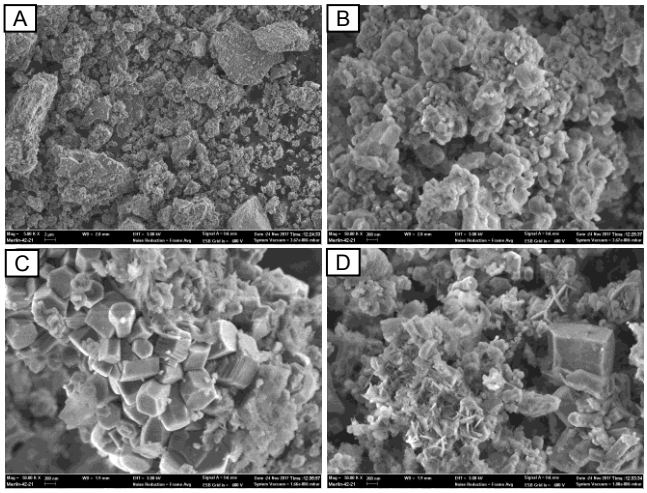

Fig. 7*. Run # 3-2. SEM images of raw (A-B) and purified (C-D) product*

The raw product (A-B) is an inhomogeneous mixture of un-reacted micron-sized Mg particles and agglomerates of nanostructured matter (mostly MgO). The purified blackish product (C-D) contains mostly MgO nanocrystallites covered with a thin carbon layer. Some intriguing one-dimensional and layered structures (nanocarbons?) can also be spotted in the product.

The non-linear course of combustion synthesis allows to obtain a nanomaterial, which may be impossible to obtain by conventional methods. The SHS processes, however, are susceptible to changing initial conditions and phase transformations of reactants disturbing heat and mass transport in the system. The consequence of such phenomena causes a difficulty in process modeling, which makes it impossible to predict the final synthesis product. The attempt to optimize the process involves time-consuming parametric studies, which makes the calculations of equilibrium thermodynamics often too much simplified. Lack of sufficient information on transient compounds prevents the modeling of process kinetics for higher orders of reaction. In the answers to these limitations the methods arose that investigate processes based on propagation combustion wave, using fractal analysis or identification of compounds at their stage follow-up reactions using time-variable analysis of the light signal on based on registered images.

In the combustion synthesis process, the heated reactants emit the radiation that is responsible for variable light signal. Optical and /or spectral registration of such a signal can be used in the process diagnostics to measure the duration of the flash or other parameters accompanying combustion.

The flash sequences for the synthesis # 2-1 and # 2-3 were photographically recorded by means of a Pentax digital camera with HD resolution of 1920x1800 and speed of 30 frames per second (duration of one frame is about 0.03s). Based on divided and selected frames, combustion maps have been made for each test from photos arranged in the progress sequence (from left to right). On the basis of these data it was possible to determine the flash time, maxima, qualitative mileage and occurrence of follow-up reactions. Fig. 8 and Fig. 9 present representative combustion maps for those synthesis with an initial pressure of 0.1 MPa and 1.0 MPa.

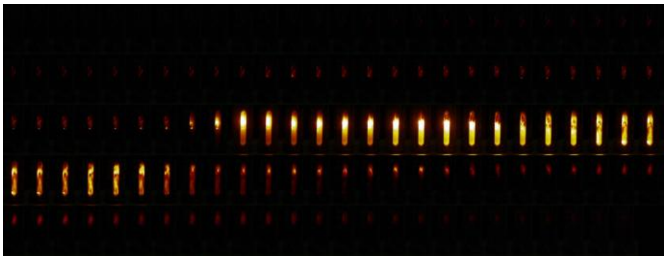

Fig. *8. Combustion map for run # 2 –*

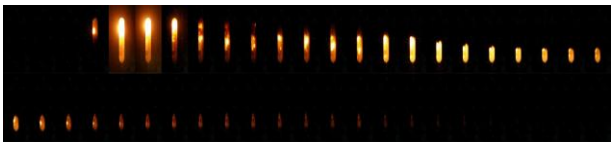

Fig. *9. Combustion map for run # 2-3*

For the run # 2-1 the flash lasted about 3.34s and the maximum reached after 0.81s. The observed extended flash-out times were slower and the passage of the combustion wave was smoother than in run # 2-3. For the run # 2-3 the flash lasted about 1.30s and the maximum reached after 0.07s. A rapid flash was observed and a greater scattering of the solid product was found within the reactor.

4. Conclusions

Carbon-bearing synthetic (phthalic acid) compound and natural minerals (magnesite of Polish and dolomite of Nepal origin) were processed via fast magesiothermic and autothermic reduction. The resulting solid product was chemically (wet chemistry) purified to yield mostly carbon-containing nanomaterial. The presence of silica/silicates in a purified product calls for the improvement of the purification protocol. Thus, the raw product should be leached not

only with HCl but also with NaOH. The produced nanosized carbon material should present the prospective applications, i.e. as an adsorbent, substrate for catalyst, and a component of electrodes in electrochemistry (lithium ion batteries and fuel cells).

5. References

1. Tiwari S.K., V. Kumar, A. Huczko, R. Oraon, A. De Adhikari, G.C. Nayak (2016) Magical Allotropes of Carbon: Prospects and Applications. Critical Reviews in Solid State Materials Science 41: 257–317

2. Kroro H.W., J. R. Heath, S. C. O'Brien, R. F. Curl & R. E. Smalley (1985) C_{60}: Buckminsterfullerene. Nature 318: 162–163

3. Iijima, S. (1991) Synthesis of Carbon Nanotubes. Nature 354: 56-58

4. Novoselov K.S., A. K. Geim, S. V. Morozov, D. Jiang, Y. Zhang, S. V. Dubonos, I. V. Grigorieva, A. A. Firsov (2004) Electric Field Effect in Atomically Thin Carbon Films. Science 306: 666-669

5. Zhao Y., X.G. Li , X. Zhou, Y.N. Zhang (2016) Review on the Graphene Based Optical Fiber Chemical and Biological Sensors. Sensors and Actuators B: Chemical 231: 324-340

6. Dyjak S., W. Kiciński, A. Huczko (2015) Thermite-driven Melamine Condensation to CxNyHz Graphite Ternary Polymers: Towards an Instant, Large-scale Synthesis of g-C_3N_4. J. Mater. Chem. A 3: 9621-9631

7. Manning T.J., M. Mitchell, J. Stach, T. Vickers (1999) Synthesis of Exfoliated Graphite from Fluorinated Graphite using an Atmospheric-pressure Argon Plasma. Carbon 37: 1159-1164

8. Morsi K. (2012) The Diversity of Combustion Synthesis Processing: a Review. J. Mater. Sci. 47: 68-92

9. Huczko, A., H. Lange, G. Chojecki, S. Cudziło, Y.Q. Zhu, H.W. Kroto, D.R.M. Walton (2003) Synthesis of Novel Nanostructures by Metal-Polytetrafluoroethene Thermolysis. J. Phys. Chem. B 107: 2519-2524

10. Dąbrowska A., A. Huczko, M. Soszyński, B. Bendjemil, F. Micciulla, I. Sacco, L. Coderoni, S. Bellucci (2011) Ultra-fast Efficient Synthesis of One-dimensional Nanostructures. Phys. Status Solidi B 248: 2704-2707

11. Dąbrowska A., A. Huczko, S. Dyjak (2012) Fast and Efficient Combustion Synthesis Route to Produce Novel Nanocarbons.Phys. Status Solidi B 249: 2373-2377

12. Huczko, A., A. Dąbrowska, O. Łabędź, M. Soszyński, M. Bystrzejewski, P. Baranowski, R. Bhatta, B. Pokhrel, B.P. Kafle, S. Stelmakh, S. Gierlotka, S. Dyjak (2014) Facile and Fast Combustion Synthesis and Characterization of Novel Carbon Nanostructures. Physica Status Solidi B 251: 2563-2568

13. Huczko A., O. Łabędź, A. Dąbrowska, M. Kurcz, M. Bystrzejewski, H. Lange, P. Baranowski, L. Stobiński, A. Małolepszy, A. Okotrub, M. Soszyński (2015) Efficient One-pot Combustion Synthesis of Few-layered Graphene. Physica Status Solidi B 252: 2412-2417

14. Dyjak S., W. Kiciński, M. Norek, A. Huczko, O. Łabędź, B. Budner, M. Polański (2016) Hierarchical, Nanoporous Graphenic Carbon Materials Through an Instant, Self-sustaining Magnesiothermic Reduction. Carbon 96: 937-946

SMART RESIDENTIAL HOUSE SAVING ENERGY SYSTEM

Salloom A. Al-Juboori, Prof., B.Sc, M.Sc, PhD, Leeds University, U.K[1,2] , Sana A. Al-Dmour[1] , B.Sc, M.Sc,

Ziyad AL-Majali , B.Sc, M.Sc, PhD[1]

[1]Engineering Faculty /Mutah University / AlKark/ Jordan,

[1,2]Email: sajibury@mutah.edu.jo

Abstract: *The special design process of an efficient residential house energy saving energy system is presented in this work. The main objectives are to achieve major energy cost reductions, providing safe house and reliable service. Thus, the essentials tool of the system will focus on providing useful information for the user by continuous monitoring and recording of the consumption behaviour of the operating appliances, also will raise early alarms in case of fault detection by high temperature monitoring. The outcomes of monitoring and analyzing the real power demand of group of typical house appliances is then used as a case-study for proposing further tools such as consumption forecast, tariff comparing and scheduling tools. Rule based system was designed for efficient and reliable operation control of house energy system with distributed energy source and storage units. Lab-View software package is used for implementation of most of the proposed algorithms which have been tested by variation of possible operating conditions. The results have shown that 22.75% energy savings can be achieved by applying the proposed tools and control strategies on typical home appliances. Modification of the system is recommended to include wide range of consumer's types such as industrial and commercial sectors and to include more than one type of distributed energy sources.*

Keywords: ENERGY SAVING, SMART HOUSE, ENERGY MANAGEMENT SYSTEM, LAB-VIEW

1-Introduction: Recent developments in information and communication technology such as intelligent meter technology, intelligent smart electrical appliances and intelligent storage systems, has led to the establishment of the smart home concept, and aid in building the energy management system infrastructure (Dounis&Caraiscos,2009). Energy Management Systems (EMS) technology such as home or building energy management system which is recognized as the most important element in the smart grid appear in response to the continuous requirement of high reliability and demand of increasing safety measures for the traditional power grid to meet customer satisfaction. Smart houses are expected to help power companies by dynamically adjusting power consumption in response to grid conditions, allowing for lower peak power costs as well as energy and maintenance costs. These savings help to reduce capital investment and the purchase of excess electricity from additional generators at peak time. The company's strategies to reduce the amount of fuel consumed to produce electricity are the pricing rates and demand response strategies (Li, 2013). Intelligent demand-side electricity use has a significant role in improving energy consumption by home users, and also effects on their daily behaviors and activities. The smart meter receives signals such as the maximum level of power allowed in a specified period or real-time price signals (Yoon et al., 2014). The flow of information between suppliers of electricity and consumers helps the energy management system play a role in demand response strategies. Where the demand response allows the consumer to reduce or convert their use of electricity during peak time in response to changes in prices by controlling the electrical devices manually or automatically, especially for the appliances of cooling, heating, air conditioners and water heaters, which considered the most used electrical appliances for electricity (Augean, et al, 2015). Real-time optimization and scheduling schemes for power storage systems and household electrical appliances are planned by the end-users. The object of the scheduling scheme of the home Energy Management System (EMS) is to manage the power consumption of the appliances during the peak and off-peak periods, to reduce consumption costs and to improve energy use (Shariatzadeha, et al, 2015).

2-Data collection: Dataset of house appliances operating conditions and power demand are to be available for the purpose of system testing and evaluating, for the purpose of saving time, effort and financial cost. When generating a log-file, two rules must be followed: The first rule is avoiding any appliances data with missing fragments. The second rule is selecting what local users are familiar with and avoid device duplicating. Table-1 shows the nine selected appliances for the present work house and figure-1 shows the suggested layout of the proposed house with appliances locations in addition to solar cells system with their storage batteries. When selecting development environment for the software, the followed rule was to search for a powerful programming software but user friendly at the same time, it is required to be able to communicate with external devices, able to send and receive data from the home system components. The Lab-View software package was selected for implementation of the system tools and functions.

3-Monitoring: Monitoring of house appliances will start form major part of the intended design objectives. Suitable monitoring tools are selected in this work for implementation. Their design criteria focus on automating instantaneous monitoring or saving data for later usage such as later analysis and comparisons for various appliances and delivering useful information quickly without effort even for beginner energy manager or ordinary user quite simply because it is going to be user every day partner. Figure-2 shows screen shot which represents the first system stage that the user will encounter when operating the software.

4-Individual consumptions: This feature is important and need to be included in any professional Energy Managing System (EMS). Although it could be difficult to be applied on all types and kinds of appliances in the house but at least it should be there for the important and heavy loads, those loads which need to be identified causing and driving the peak power demand and also it is important to identify cyclic loads whose operation could be delayed. In present work will simulate the case-study house which has nine major appliances, which are included in the individual loads power demand profile scheme. A small window of the registered devices list is included in the left side of the main window and shown in figure-3. Moving between the different items can be achieved easily using mouse clicks or moving by arrows in the key boards. One scheme of monitoring which is implemented in the main screen of the proposed system is the twenty-four-hour period of individual power consumption information. When an item name is selected, it will be highlighted and its load power demand profile will be updated automatically on the chart, which is shown to the right side of the list and on the upper side of the system main window. The chart will provide twenty-four-hour period of individual power consumption information. Continuous monitoring requires instantaneous updating with any change in the absorbed power values. The user will then have the freedom to select any device he

is interested in showing its load pattern. Following, some recordings examples are included for some loads to understand the general operating pattern and the power demand. The operating pattern of the fridge, kettle and freezer are illustrated in Error! Reference Source not found as shown in figures, 4, 5, and 6. The lines in the plot connect the data points and the data points were recorded at five minutes intervals. The figures show the active power consumed by the appliances. The operating patterns display the cyclic nature of the appliances and their energy demand. Another scheme of monitoring is suggested which is based on keeping record of each device cumulative consumption over a period of one day for example depending on the tariff type and details as shown in figure-7, which illustrates the system idea based on using the traditional total dayly cumulative consumption meter.

5-Total power demand profile consumptions: Another scheme is similar to the individual loads power demand profiles monitoring scheme but it is monitoring the total home consumptions instead. The consumption sum is calculated on a minute by minute basis. A chart is continually monitoring and showing a period of twenty-four hours of the home load profile. The total consumption reading data for each minute represents the summation of all appliances consumption data, the summation was performed internally by the system and the total consumption is plotted with the time on the x-axis as shown in figure-8. This figure shows the home uses approximately 250 W/h during low power demand times and this rise and reaches approximately 2 kWh during peak power demand times. This is approximately eight times as much power required during the low power demand time. A similar power profile exists for different days, the minimum and maximum values will vary slightly but still in the same ranges.

6-Alarming systems: The previous section focuses on monitoring of home appliances to achieve one major design objective of providing home owner with important management advices and information. Another major design objective of present work proposed system is to provide alarming services. These services can be categorized in two main groups; first group design criteria focuses on alarming of high temperature detection and this is mainly for supporting safety measures in addition to achieving power savings, the second group design criteria focus on alarming regard detecting of any high or up-normal power consumption and although this is mainly for achieving power savings purpose and bill payments reducing but could also be used for supporting safety measures as well. It is important for the proposed system to have the ability of raising alarms to warn house owners of dangerous situations.

6-1 High temperatures alarms: Unlike power consumption data, real operating temperature from the REFIT electrical load measurements data set was not recorded. Hazard scenarios are essential for testing of the proposed management system ability for providing alarm if required and thus hazard scenarios need also to be simulated and stored on the system for testing purposes. Figure-9 shows an example of this approach block diagram connections. Here, the alarm monitor will turn color to red if temperature found to reach any value between 24.5-25 degrees. Of course, these values and threshold constants can be altered easily by the system programmer. Figure-10 shows the front panel of present work proposed house.

6-2 High power consumption alarm:

High power consumption may occur in the system during daily operations and having early alarm raise when such increase occur will be an advantage over traditional homes with no monitoring facilities. The alarm will help mainly in reducing bills, aiding safety measures of home owners, and increasing expected life of some part of the home system. High power consumption may occur due to faulty conditions, some of these faults may not be detected by home protection systems such as current leakage in high resistance. Figures- 10 shows the front panel of present work proposed alarm and the monitoring meter, *Грешка! Източникът на препратката не е намерен.* Figure-10 shows an example where the consumed power is less than the preset threshold, while figure-11 show the same example when the consumed power exceeds the preset threshold. Alert is raised for the high consumption by converting its color from green to red.

7- Consumption forecast tools: The consumption forecast tool work on raising an alert to inform of possible high consumption. The tool is designed to involve current month usage and previous month consumption as well in its estimations. Figures-12-15 show the structure for the front screen of the designed consumption forecast tool and an example for the forecasting tool outcome. Figure -15 shows an example for the forecasting tool outcome, the selected block was 300kWh, the previous month used data was set to 500 kWh for testing and the calculated forecast is expected to exceed the allowance. Figure-16 shows a one day home consumption with peak time tariff, while table-2 shows the total cost reduction before and after dishwasher scheduling strategy. Figures-17 and 18 Illustrate the savings after applying scheduling on freezer and Scheduling savings calculations for freezer, respectively. Finally the Summary of estimated reduction percentage is shown in table-3.

8- Analyses and Discussion of Results: Extra reductions in bills for some tariff types can be achieved if some measures are considered at the time of the application, example of this application of the peak time tariff or the real-time tariff when combined with a well-designed scheduling strategy. To build the wanted scheduling strategy, some rules should be defined, starting by rules for appliances classification into two groups, namely; essential and nonessential load. Essential loads include loads where operation automatic control may negatively affects the user comfort, such as TV, PC or router. On the other hand, turning off or rescheduling some loads will not have big impact on the user regular life activity, these will be defined as the nonessential loads such as the dishwasher or the washing machine. For illustration example of the proposed scheduling tool, figure-***16*** shows a plot of a typical total home consumption for one day with details of the peak time tariff on the same figure. The plot found to be containing five major consumption spikes. The first three will be treated with by the shoulder rate and the last two will be paid by the peak rate. These spikes will effectively contribute to a large payment share of the expected bill. Information from the installed individual power meters will be passed on to the scheduling strategy in order to identify the source of these spikes. Error! Reference source not found, shows that the Dishwasher is responsible for the rest four of these spikes, the first two was during the shoulder rate period and due to the dishwasher usage, that starts at around 8:50am and finish at around 10:00am. The second usage of the dishwasher was encountered at a longer interval which starts at 6:00pm and continues until 7:40pm; the main point here to be noticed is that this usage was at the peak rate period. The scheduling tool function may be utilized regard the power spikes which was generated by the dishwasher as shown in tables-4. This device can be considered as a non-essential device since shifting its operation time will have no effect on the user. Error! Reference source not found, figure-19 is an example of this set power consumption. A simple control strategy is proposed for this set which is based on the master-slave principle. The TV will be the master device, the control strategy will be based on turning off the whole set if the master device was not in use and turning it on will signal the on-control order to the whole set of slave devices as shown in tables 5 and 6. Figures-20 and 21 show the already monitored freezer power consumptions profile (i.e. before and after suggested modification). Its cyclic operation is governed by two temperature limits; the total time for each cycle can be estimated to be in the range of two to two and half hours divided almost in half between the on-time and off-time. Similar cyclic operation behavior is also noticed in fridge power consumptions profile. The strategy algorithm can be built on the principle of controlling the on-times and off-times according to the rate of that period. Flowchart shown in figure-22 represent

summary of this proposed strategy steps. The idea is to keep fixed cycle time, monitoring the time will be used to identify the rate different periods and then selecting Ton1 for operating- time in the off-peak period, Ton2 for the shoulder peak period or Ton3 for the peak period. The following equations of 1,2 and 3 may be used to summarize the proposed algorithm.

$$\text{Time delay} = T_{on}+T_{off} \quad (1)$$

$$Ton_1 = 1.5*T_{on2} \quad (2)$$

$$Ton_1 = 3*T_{on3} \quad (3)$$

Although, following the previous strategy algorithm will serve achieving the scheduling purpose, but there are few aspects regard the safe operation of the device which if neglected may have serious negative consequences on the man life especially regard using of these vital appliances i.e. fridge and freezer. Healthy and food conserving safety serious issues may be encountered if operating of this equipment was determined and controlled by time constrains only. The low temperature limit in the shoulder time T_{low2}, will be little bit higher than T_{low1}, and the low temperature limit in the peak time T_{low3}, will be higher than both T_{low1} and Tlow2. The general rule will be to ensure that $T_{low3}>T_{low2}>T_{low1}$. Low temperature limits must be selected in a manner that ensure early turn off and thus means more power savings to avoid device long operation intervals in high rate periods. Flowchart shown in figure represent summary of this proposed strategy steps. For illustration, figure-17 shows an example of calculations for applying the peak tariff rate structure for day, month, year and ten years durations. The calculation is performed for normal operation without scheduling case and also on the scheduled operation of the device. Further increasing in the savings percentage may be achieved by further decrement in the shoulder and peak on times. For energy storing, a slight increase in the off-peak on-time duration may be suggested. Figure-18 shows a comparison between the previous example of time parameters set and a new set of time parameters and the increase in the savings percentage. Summary of estimated reduction percentage is included in year's durations. The calculation is performed for normal operation without scheduling case and also on the scheduled operation of the device. Further increasing in the savings percentage may be achieved by further decrement in the shoulder and peak on times. For energy storing, a slight increase in the off-peak on-time duration may be suggested. Summary of estimated reduction percentage is included in table-3.

9-Conclusions: The functionality of the proposed design system is demonstrated by modeling and simulation of various scenarios for reducing bill payments; appliances operation controlling strategies are investigated. For some of the appliances, such as the fridge and kettle, application of storage-based strategy can achieve 12.7% cost reduction. For the washing machine and the dishwasher, a peak clipping based strategy by operating time shifting can achieve 22.4% cost reduction. For the TV set and the PC set, a master and slave principle is selected. For the TV set, 44.4% consumption reduction can be achieved. The router controlling strategy is based on monitoring the presence of the home owner and calculating the expected reduction requires a study of his daily behavior. Applying suggested strategies can achieve total cost reduction of 22.75%.

Table 1: *List of appliances used in present work case-study*

Number	Registered devices
1	Fridge
2	Freezer
3	Microwave
4	TV
5	Kettle
6	Dishwasher
7	Washing machine
8	Computer
9	Router

References:

Dounis, A.I., Caraiscos, C., "Advanced control systems engineering for energy and comfort management in a building environment- A review", Renewable and Sustainable Energy Reviews 13 (2009) 1246-1261.

Elma, F., Selamogullari, U. S.,"A new home energy management algorithm with voltage control in smart home environment" Energy 91 (2015) 720-731.

Francisco, D., Moya, C., Juan, C., Lopez, A., Luiz, C. P., da, S., "Model For Smart Building Electrical Loads Scheduling" 978-1-5090-2320-2/16/$31.00 ©2016 IEEE

Li, Y., "Design of A Key Establishment Protocol for Smart Home Energy Management System"2013 Fifth International Conference on Computational Intelligence, Communication Systems and Networks. 5-7 June 2013, Madrid, Spain, DOI: 10.1109/CICSYN.2013.42.

Murray, D.; Stankovic, L.; Stankovic, V., " An electrical load measurements dataset of United Kingdom households from a two-year longitudinal study" Scientific Data; London Vol. 4, (Jan 2017): 160122

Ozkan, H. A."Appliances based control for power management systems" Energy 114(2016)693-707.

Shariatzadeha, F., Mandalb, P., Srivastavac, A. K., " Demand response for sustainable energy systems: A review, application and implementation strategy" Renewable and Sustainable Energy Reviews 45 (2015) 343–350.

Yoon, J. H., ladick, R. B., Novoselac, A., "Demand response for residential buildings based on dynamic price of electricity" energy and building 80 (2014) 531-541.

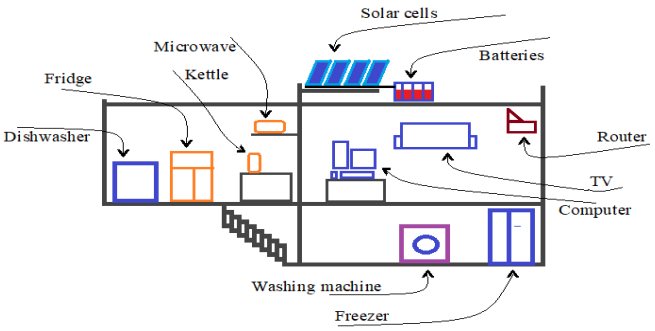

Figure 1: *Layout of proposed case-study house*

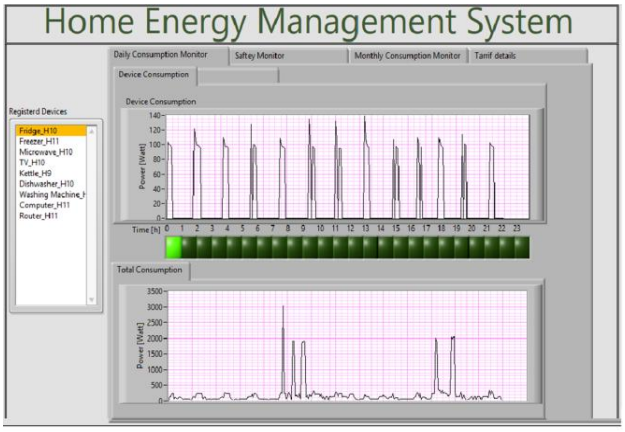

Figure 2: Desk top screen shot

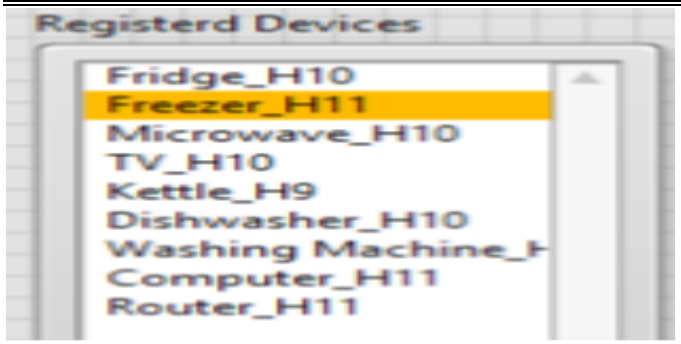

Figure 3: *Registered devices list*

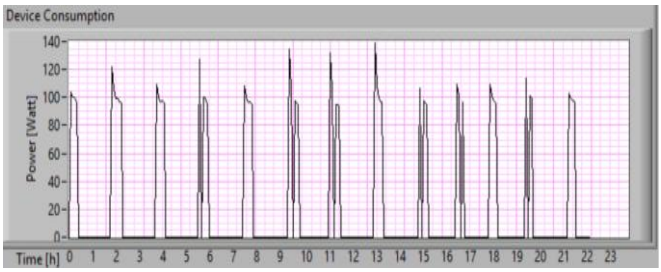

Figure 4: Example of the fridge consumption

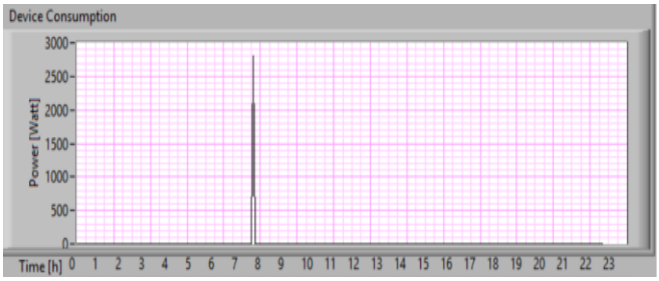

Figure 5: *Example of the kettle consumption*

Figure-7*: Cumulative consumption meter panel*

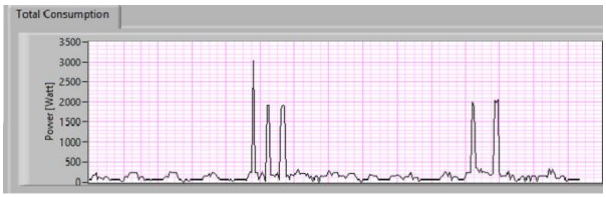

Figure-8: *Example 1 of total consumption for a day*

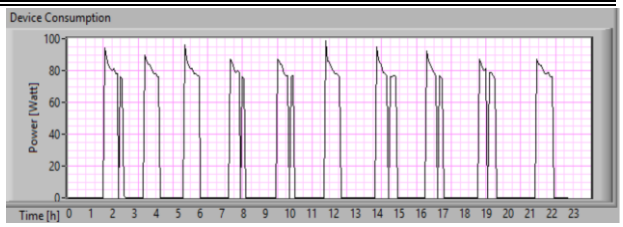

Figure 6: *Example of the freezer consumption*

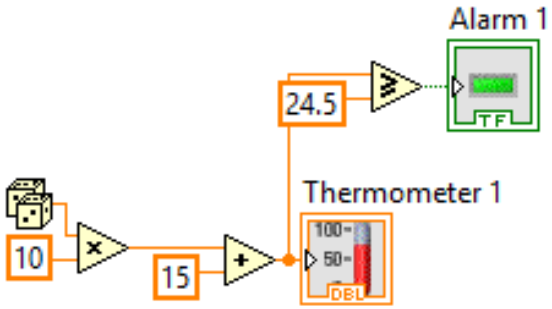

Figure-9: *first approach block diagram connections*

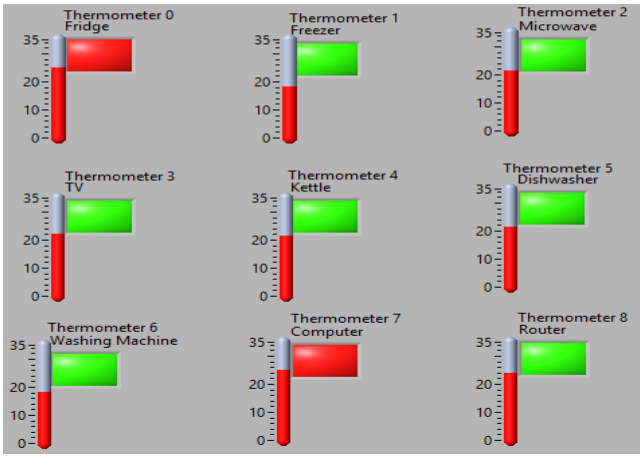

Figure -10: *Alarm system front panel*

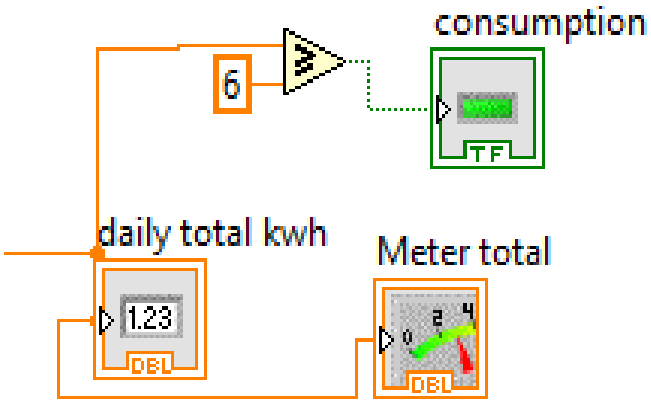

Figure 11: *High power consumption alarm Block diagram connections*

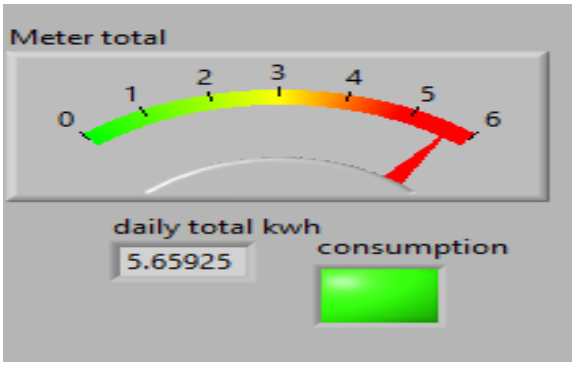

Figure 12: *Monitoring meter with proposed alarm*

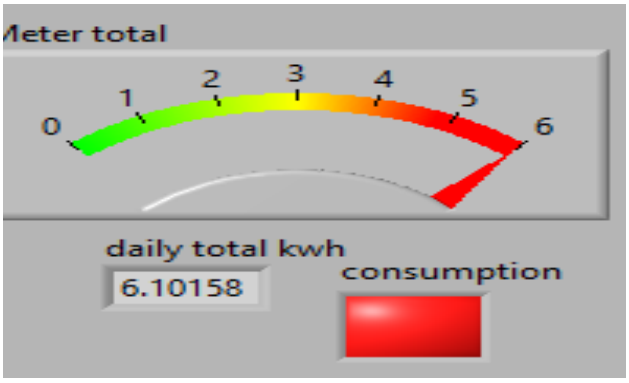

Figure 13: *Raised alert for high consumption*

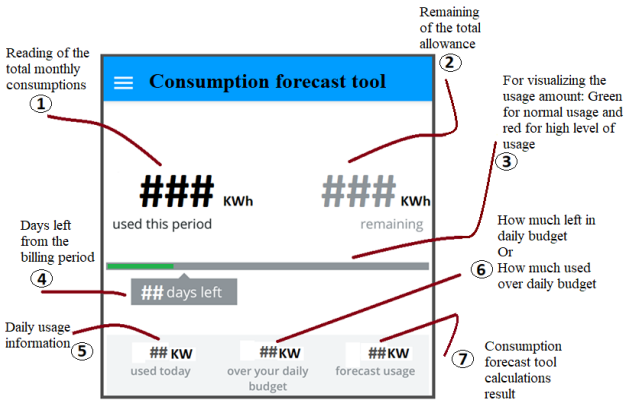

Figure 14: *Consumption forecast tool front screen structure*

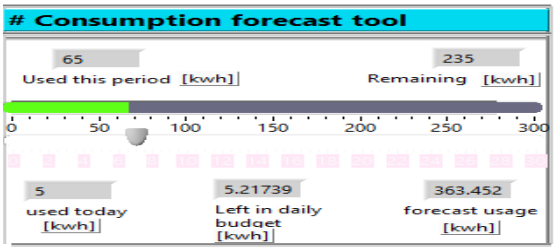

Figure 15: *Forecast if normal usage and previous month consumption was 500 kWh*

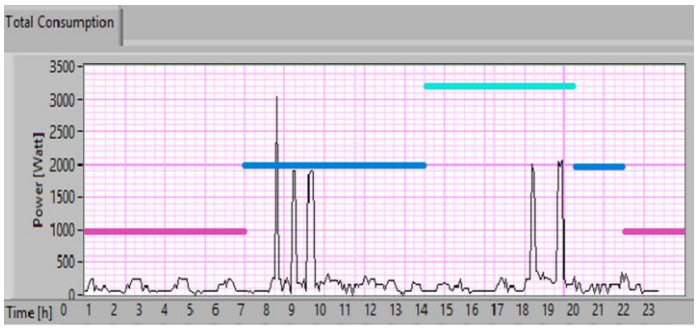

Figure -16: *One day home consumption with peak time tariff*

Table 2: *Total cost reduction before and after dishwasher scheduling strategy*

Total appliances operating cos with Time of da tariff	before Appling Dishwashe scheduling strategy	1.01 $
	after Appling Dishwashe scheduling strategy	0.91 $
		Reduction Percentage 9.9%

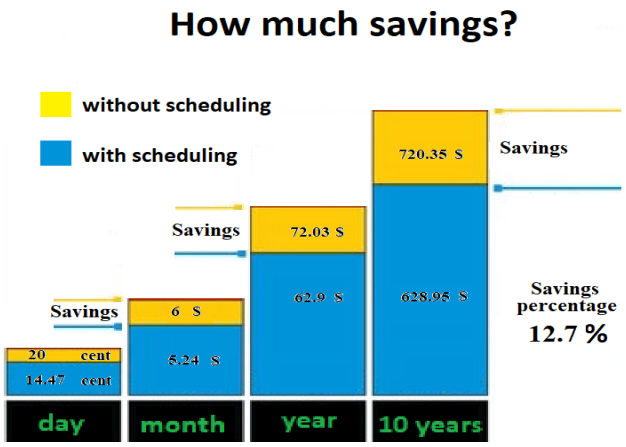

Figure-17: *Savings after applying scheduling on freezer*

Time parameter set		Total costs over 10 years	Savings percentage
T_{on1}=90 minutes T_{on2}=40 minutes T_{on3}=20 minutes	Without scheduling	720.34 $	12.7%
	With scheduling	628.95 $	
T_{on1}=100 minutes T_{on2}=35 minutes T_{on3}=15 minutes	Without scheduling	720.34 $	14.3%
	With scheduling	617.44 $	

Figure-18: *Scheduling savings calculations for freezer*

Table-3: *Summary of estimated reduction percentage*

Appliance	before	after	Reduction percentage estimation
Freezer	0.2001 $	0.1747 $	12.7%
Dishwasher	0.42 $	0.33$	22.4%
TV set	0.27 $	0.15 $	44.4%

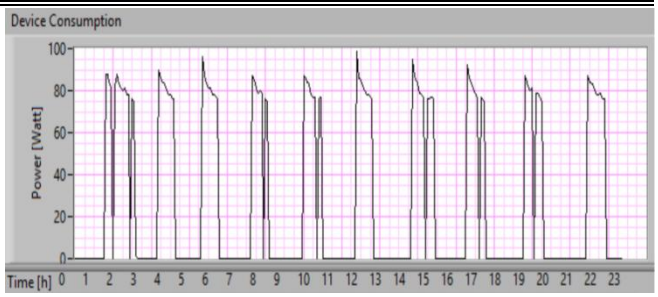

Figure-20: *Freezer power profile before suggested modification*

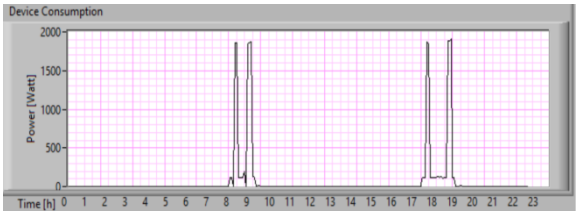

Figure-19: *Example of the dishwasher consumption*

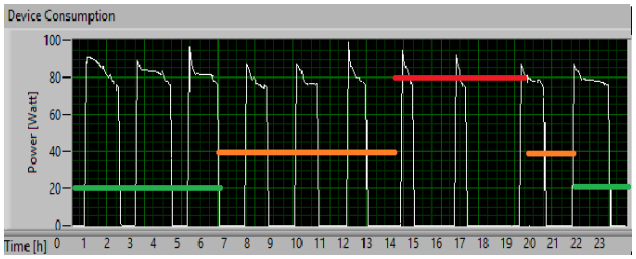

Figure-21*: Freezer power profile after with energy storage*

Table 4: *Dishwasher operating cost reduction before And after dishwasher scheduling strategy*

Dishwasher operating cost with Time of day tariff	before Appling Dishwasher scheduling strategy	0.42 $
	after Appling Dishwasher scheduling strategy	0.33 $
		Reduction Percentage 21.4%

Table-5*: TV control strategy consumption results*

TV operating kWh	before control strategy	1.322 kWh
	after control strategy	0.722 kWh
		Reduction Percentage 45.3 %

Table 6: *TV control strategy cost results*

TV operating kWh	before control strategy	0.27 $
	after control strategy	0.15 $
		Reduction Percentage 44.4 %

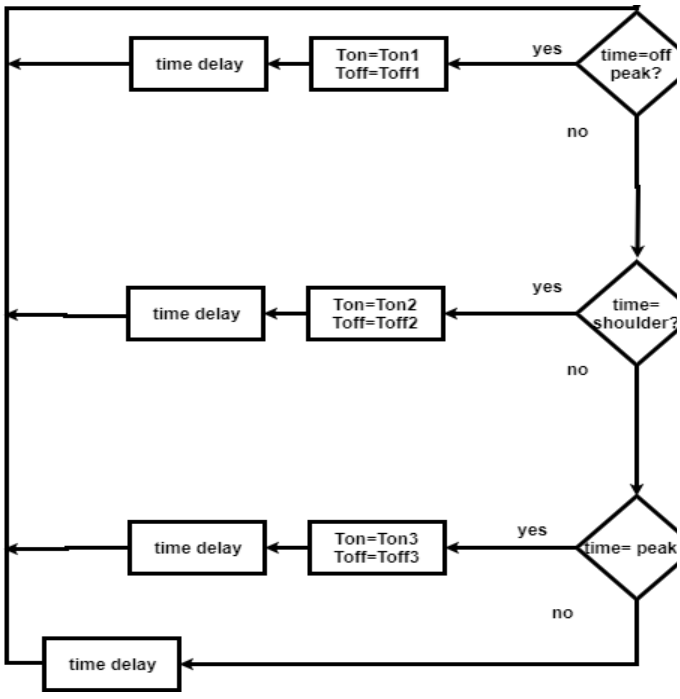

Figure 22: *Time constraint-based algorithm*

INDUSTRY 4.0 AND SUPPLY CHAIN INTERACTION ANALYSIS WITH FUZZY ANALYTICAL HIERARCHY PROCESS

Assoc. Prof. Dr. Erkan.T.E, MSc Student Calkin.S.
Faculty of Industrial Engineering, Atilim University, Ankara, Turkey
E-mail:erman.erkan@atilim.edu.tr, calkin.suayip@student.atilim.edu.tr

Abstract: *Industry revolution is not a new thing for the world and it has been coming up till the machines were invented. And now, Production authorities have discussed the Industry 4.0 which is combinations of the existing manufacturing and large technological innovations and also, Supply Chain perspective is changing that product flows will become regional. This research paper will firstly aim to clearly understand the Industry 4.0 and what kind of changes occurs into the Supply Chain Environment. The Second part of the Research will focus on the Performance Measurement and Decision Making Analyzing which comparison between before Industry 4.0 and after applications of Industry 4.0. Fuzzy Analytical Hierarchy Process Method is used for determination of comparison.*
KEYWORDS: INDUSTRY 4.0, SUPPLY CHAIN MANAGEMENT, FUZZY ANALYTICAL HIERARCHY PROCESS (FUZZY AHP)

1. Introduction

1.1 Understanding the New Supply Chain and Industry 4.0

In to close future, Factories will be relocated for being close to market that means product will not flow east to West and became regional product flows. Product will not travel to whole world to reach the consumer. This is a new Supply Chain model which manufacturing close to consumer market. They become smaller and more agile. Scale and make to stock does not understand as productivity anymore and Companies will be operating on a multi-product that made to order basis. Flexibility will be important that same production line able to manufacture the more customized products. Industry 4.0 is a main element for new Supply Chain Environment.

Industry 4.0 is not a new thing for World and it has been discussed in search in several years and mentioned in the first time in 2011 in the Hannover fair in Germany. This involves the main technological innovations applied to production processes in the field of automation, control and information technologies (Hermann, 2017)

Industry 4.0 is the fourth industrial revolution. The first one was about the steam engines that were around 1780. Second one consists of the electric motors and petroleum fuel that was around 1870. Third industrial revolution was around 1970 and included computerized systems and robots in industrial production. (Lee, 2015) And now fourth industrial revolution occurs and computers and automations are integrated. Production systems are able to continuously learning from data from computerized systems and increase the efficiency of production systems.

Industry 4.0 focuses to improve the competitiveness by reducing cost and increasing the flexibility in decentralized production systems to offer customized product which is advantage in satisfying market (Hermann, 2017) The mean of the decentralized system of the author is Production systems became more flexible by divided to the small batch sizes and it increases the complexity. Industry 4.0 is solution to for this complexity and Industry 4.0 decentralized the structures of production.

Key Technologies enabling Industry 4.0

1. Internet of Things(IoT)
2. Big Data
3. Mobile and Augmented Reality
4. Additive Manufacturing
5. Cloud Technologies
6. Cybersecurity

1.1.1 Cyber Physical Systems (CPS)

This system brings the physical and virtual world together that can be explained as integration of the computations, network and physical process (Stochastic Process one of the example). Embedded computers and network monitor and control the physical process. Computers and software embedded in devices. CPS is the Computer Science subject that examples are autonomy cars, Segways, quadcopters, trains without drivers that uses in France and etc.

1.1.2 Supply Chain through the Application of CPS

The planning, control and management of distributed systems (Supply Chain Systems) with CPS is one of the main bringing of Industry 4.0.

The Supply Chain competitiveness is directly related to the physical and information flows (Frazzon, Synchronizing and Improving Supply Chains through the application of Cyber- Physical Systems, 2015) Management of the information into Supply Chain is the basic problem of management of the Supply Chain process such as Inventory Management, Transportation Management, Customer and Supplier Management. One of the main applications of CPS technology is implementation of Data Communication platform. This system allows control the production data, product, inventory etc. and improve the communication. Because of the access to information more quickly in manufacturing environment improve the troubleshooting time.

Frazzon used the simulation method and apply to both Scenarios that Basic scenario is applying the simulation without CPS and second scenario is applying the simulation with CPS. The results of the Frazzon's research, Manufacturer received and produced about 11% more, compared to the first scenario. The Distributor, in turn, showed an increase of, approximately, 14% in the orders delivered. In the Wholesaler entity, there was an increase of almost 10% in the requests served. The Retailer, there was an increase of 5% approximately in the same indicator. CPS technologies can support the improvement of the Supply Chain Performance.

1.1.3 Internet of Things (IoT)

Internet can be considered an initiator of Industry 4.0 (Hermann, 2017) Simple explanation of the Internet of Things will be everything connected to everything. Devices can connect each other by using Cloud computing systems. IoT systems are based on devices which they can make sensing, actuation, control and monitoring activities and importing that Iot devices can connect with other devices and exchange the data. These devices can collect the data for processing the data or sending the centralized servers.

Estimates for the number of connected devices range from 25 to 50 billion by the year 2020 and those connections will facilitate the used data to analyze, preplan, manage, and make intelligent decisions autonomously (Lee, 2015)

The US National Intelligence Council (NIC) has embarked IoT as one of the six ''Disruptive Civil Technologies" (National Intelligence Council, 2008). In this context, we can see that service several sectors, such as: transportation, smart city, smart health, e-

governance, assisted living, e-education, retail, logistics, agriculture, automation, industrial manufacturing, and business/process management etc., are already getting benefited from various architectural forms of IoT.

The hardware components used to connect IoT objects include wireless devices such as portable computers (e.g., laptops or tablet PCs), smartphones, wearable devices (e.g., Apple Watch), Radio Frequency Identification (RFID) (Krotov, 2017)

1.1.4 Supply Chain Management in the Era of the Internet of Things

The identification, traceability, real time tracking of goods in Supply chain is the important and difficult for all Producers, Retailers…etc.

The advent of the Internet of Things and cloud computing brings a new approach, enabling to collect, transfer, store and share information on the logistics flow for better cooperation and interoperability between supply chain partners. (Gnimpieba, 2015) IoT can provide connection of everything in Supply Chain process that flow of information and events are generated by the interconnection of this processes. Management, tracking and control can do in real time.

Market research companies estimate that the number of devices connected to the IoT will grow from 16 billion in 2014 to 50 billion in 2020, creating a global market for IoT products and services measured in trillions of dollars (Weinberg, 2015) When thinking the this potential understanding the importance of the IoT for Supply Chain become more considerable.

1.1.5 Big Data

Big data is defined as the huge or complex sets of data, which has a range of Exabyte and more. It exceeds the space of technical ability of storage system, processing, managing, interpreting and visualizing of a traditional system. (Kaisler, 2013)

Data is generated by several sources like machine controllers, sensors, manufacturing systems, people, among many others.

Data can be collected from different sources into Supply Chain and can be uses different purposes that forecasting, decision making. Big Data has become important thing for organizations.

1.1.6 Importance of Big Data into Supply Chain Management

More Data has been created in the last two years then past years Supply Chain is the one of the sources of Big Data which about Customers, Companies and Operations. Companies are collected the data to gain competitive advantage.

Big data analytics has a big impact to enhance firm performance. By improving big data analytics capability, a firm could create new products and services, provide better customer service, increase sales and revenue, and expand into the new market. (Akter, 2016)

Supply chain management has use statistics and operation research for optimizing the objectives of matching supply and demand. Business analytics using information system support has a strong relationship to supply chain performance (Trkman, 2010)

There is powerful information in their supply chain data and use for

- Improved customer service level
- Lower inventory
- More successful product launches
- Improved product quality
- Shorter order cycle time
- Higher Revenues
- Improving Asset utilization

Also, analyzing data able to understand and identifies the issues and opportunities in advance.

2. Application of the Comparison

Comparison between before Industry 4.0 and after applications of the Industry 4.0 elements is determined by using the Fuzzy Analytical Hierarchy method. Research will be examined three companies into the aspects of the Industry 4.0 Elements. All companies are in the same sector and markets shares are close each other's into current situations. First, Company management perspective totally traditional which not using Industry 4.0 elements. Second company is in the stage of the transition to Industry 4.0. that investments and reengineering their systems to make suitable for Industry 4.0 elements. Last company is new in the market and already applied all Industry 4.0 technologies. Key Performance Indicators are determined by bases of the Industry 4.0 gaining. Evaluation of the these KPIs will be held into Supply Chain Performance Perspective that participants are done their evaluations Supply Chain Performance Perspective and Fuzzy Analytical Hierarchy Process Method is determined to understand which company in the better situations into bases of Industry 4.0.

2.1 Key Performance Indicators

According the literature survey, KPIs are found related to Supply Chain Performance. Determining these KPIs, following 7 KPIs will be used for our performance measurement system. Explanation of the necessity of every KPIS is determined for our system

2.1.1 Failure Rates

Various data sources can provide information regarding different aspects of the factory. In this stage, data utilization to understand the current operating conditions and detect faults and failures is an important issue in an Industry 4.0 factory. In addition to monitoring the condition and providing a fault diagnosis, components and systems are able to gain self-awareness and self- predictiveness, which will provide management with more insight as to the status of the factory Furthermore, peer-to-peer comparison and blending of timely information from various components provides a precise prediction of the components and alerts factory management to trigger required maintenance at the best possible time to reach just-in time maintenance and gain near zero downtime

2.1.2 IT Security Level

One of the most challenge is the IT security risk while implementing Industry 4.0 that require on-line integration among several entities, and this online integration will give room to security breaches and data leaks. Cyber theft would be another dangerous threat. In this case, the problem is not individual, and this will cost manufacturers substantially and might even hurt their reputation. Therefore, security is a crucial issue that should be dealt with seriously.

Privacy is not only the customer's concern, but also the manufacturers. In such an interconnected Industry 4.0 network, manufacturers need to collect and analyze a huge quantity of data. To the customers, this might look like a threat to their privacy. Narrowing the gap between the consumer and the manufacturer will be a huge challenge for both parties.

2.1.3 Investment Cost

The transformation to Industry 4.0 will require large investments in new technology, and the decision for such transformations will have to be taken at the CEO level. Even then, the risks must be calculated and taken seriously.

Transition to Industry 4.0 is not easy and cheap thing for companies. Technological background and education of the Employees while this transition period need to be well defined and economical investments

2.1.4 Forecasting Success Rate

Forecasting is the major problem for companies that consumer requirements change quickly, and Companies need to adopt these quick changes and plan their future production capacity. Customer's demand

The objective of every supply chain should be to maximize the overall value generated (Chopra, 2012) The value (also known as supply chain surplus) a supply chain generates is the difference between what the final product is worth to the customer and the costs the supply chain incurs in filling the customers' requests. These costs may be purely organizational or may include environmental costs as well). Such costs are an increasing function of the uncertainty associated with the demand and thus supply chain forecasting plays a major role in increasing the overall value. (Syntetos, 2016) Companies able to analyze the Big Data and this enables improve the Decision-Making capabilities. Many industries consider big data to be a core component for their strategic decision-making. Capacity Usage Rate (Rajesh, 2016)

2.1.5 Capacity Flexibility Rate

Companies deal with how to increase their productivity and optimize their capacity. Also, customization and new Supply Chain rules force to companies to be flexible use of their capacities. Capacity flexibility means having the capability to provide products/services that meet the individual demands of customers (Gunesakeran, 2004).

The question about the optimal levels of capacity is an important one as many firms and industries suffer from chronic or cyclical overcapacity that can threaten their competitiveness or even survival (Jakubovskis, 2017)

In supply chain management, suppliers usually face stochastic customer demand and increasingly compete on delivery lead times to support the responsiveness of the supply chain (Simchi-Levi, 2008)

Literature on flexible capacity for manufacturing systems merely always includes capacity costs (steady and flexible capacity) which are related to different other performance indicators. Backorder and sometimes inventory costs are treated in discuss the trade-off between inventory, backorder and capacity cost for an MTS production system with steady and flexible capacity. (Tanrısever, 2012)

According to (N. Slack, 1995) of the many aspects of production performance, capacity utilization directly affects the speed of response to customer demand through its impact on flexibility, lead-time and deliverability.

2.1.6 Product Customizations

Products customization by consumers tends to be one more variable in the manufacturing process, and smart factories will have to be able to customize what each customer have into consideration, adapting to the preferences. One of the main characteristics of Industry 4.0 is support the integration and virtualization of manufacturing design and production process using the information and internet to create smart products.

One of the differentials of the companies are the early launch of the products and the ability to the develop them, with the objectives to meet the growing needs and expectations of the customers. The product lifecycle is getting shorter, which encourages the continued flow of new product development projects in the industry. (Kassio, 2017)

2.1.7 On-Time Delivery Rate

Manufacturing right product is not enough into supply Chain, delivery performance also major indicator for Supply Chain performance. Within the hierarchy of supply chain performance metrics delivery performance, as characterized by the timeliness and dependability of product delivery to the final customer in the supply chain, is acknowledged as a key metric for supporting supply chain operations (H. Cirtita, 2012) Delivery performance is classified as a strategic level performance measure by (Gunesakeran, 2004). Another important aspect of delivery performance is on-time delivery. On-time delivery reflects whether perfect delivery has taken place or otherwise and is also a measure of customer service level (Stewart, 1995)

2.2 Operation of the Fuzzy Analytical Hierarchy (Fuzzy AHP)

We have examined the KPI for performance measurement of our system and compare with our competitors in the sector. Decision making hierarchy model is shown in below(Figure 1). Our final goal is determination of our company in market that producing same capacity. Companies' comparisons are determined by using Fuzzy Analytical Hierarchy Process (FAHP) method.

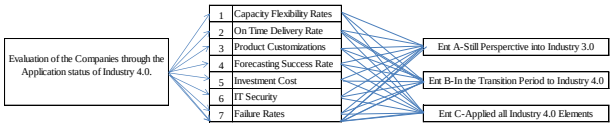

Figure 1: *Decision Making Hierarchy*

2.2.1. Evaluations of KPIs

Understanding the rating of the KPIs are determined by creating three search group that given in Table 1. All group members are working in the same sector. KPI properties are explained them and wanted to determine these KPI by using their experience, knowledge and professions. Group members are evaluated by using Rating table that shown in Table 2. They use 1-9 scale for their evaluations.

Table 1: *Properties of Groups*

Group A	Technical Experts consist of Engineers
Group B	Technical Experts consist of Technicans
Group C	Projecr Managers and Investors

All participant evaluations and consistency analyze are done by excel file. One of the examples is shown in Table 3, Table 4. Consistency Ratios for all participants are calculated and shown in Table 5. Rest of the Group Members evaluations have done by using Excel. Geometric means are calculated by participant's evaluations matrix results. Geometric mean calculation result matrix is given in Table 6. Consistency analyze for Geometric mean table is calculated and results are shown in Table 7, Table 8, Table 9. Consistency analyzes is determined for all evaluations.

Table 2: *Scale for AHP and Fuzzy AHP*

Linguistic Variables	Crisp AHP Scale	Fuzzy AHP Scale TFS	Fuzzy AHP Scale Reciprocal TFS
Equally Preferred (EqP)	1	(1, 1, 1)	(1, 1, 1)
Equally to Moderately Preferred (Eq-MP)	2	(1, 2, 3)	(1/3, 1/2, 1)
Moderately Preferred (MP)	3	(2, 3, 4)	(1/4, 1/3, 1/2)
Moderately to Strongly Preferred (M-SP)	4	(3, 4, 5)	(1/5, 1/4, 1/3)
Strongly Preferred (SP)	5	(4, 5, 6)	(1/6, 1/5, 1/4)
Strongly to Very Strongly Preferred (S-VSP)	6	(5, 6, 7)	(1/7, 1/6, 1/5)
Very Strongly Preferred (VSP)	7	(6, 7, 8)	(1/8, 1/7, 1/6)
Very Strongly to Extremely Preferred (VS-ExP)	8	(7, 8, 9)	(1/9, 1/8, 1/7)
Extremely Preferred (ExP)	9	(8, 9, 9)	(1/9, 1/9, 1/8)

Table 3: *Group Evaluation Example*

Group C 1st Evaluation	Capacity Using Rates	On Time Delivery Rate	Product Customizations	Forecasting Success Rate	Investment Cost	IT Security	Failure Rates
Capacity Using Rates	1	5	1/3	2	2	3	1/3
On Time Delivery Rate	1/5	1	1/3	1/3	1/3	2	1/3
Product Customizations	3	3	1	3	5	5	3
Forecasting Success Rate	1/2	3	1/3	1	2	2	1/3
Investment Cost	1/2	3	1/5	1/2	1	3	1/3
IT Security	1/3	1/2	1/5	1/2	1/3	1	1/5
Failure Rates	3	3	1/3	3	3	5	1
	8.533	18.5	2.73	10.33	13.67	21	5.533 11

Table 4: *Consistency Ratio Calculation*

0.12	0.27	0.12	0.19	0.15	0.14	0.06	0.15034
0.02	0.05	0.12	0.03	0.02	0.10	0.06	0.0588
0.35	0.16	0.37	0.29	0.37	0.24	0.54	0.33086
0.06	0.16	0.12	0.10	0.15	0.10	0.06	0.1059
0.06	0.16	0.07	0.05	0.07	0.14	0.06	0.08837
0.04	0.03	0.07	0.05	0.02	0.05	0.04	0.04226
0.35	0.16	0.12	0.29	0.22	0.24	0.18	0.22348
1.28292	1.08772	0.90435	1.0943	1.20771	0.8874	1.23656	

Eigenvalue	7.70097
Consistency Index	0.11683
Consistency Ratio	0.08851

Table 5: *Consistency Ratio Results for All Participant Evaluations*

	Group A-1st Evaluation	Group A-2nd Evaluation	Group A-3rd Evaluation	Group A-4th Evaluation	Group A-5th Evaluation	Group B-1sth Evaluation	Group B-2nd Evaluation	Group B-3rd Evaluation	Group B-4th Evaluation	Group B-5th Evaluation	Group C-1st Evaluation	Group C-2nd Evaluation	Group C-3rd Evaluation	Group C-4th Evaluation	Group C-5th Evaluation
Eigenvalue	10.2438	8.49376	8.44058	8.03335	7.9011	8.36806	7.92132	8.36472	8.25219	8.45071	7.70097	7.78812	8.43476	8.38672	7.88615
Consistency Index	0.54064	0.24896	0.2401	0.17222	0.15018	0.22801	0.15355	0.22745	0.2087	0.24179	0.11683	0.13135	0.23913	0.23112	0.14769
Consistency Ratio	0.40957	0.18861	0.18189	0.13047	0.11378	0.17274	0.11633	0.17231	0.1581	0.18317	0.08851	0.09951	0.18116	0.17509	0.11189

2.2.2. Calculations of Geometric Mean for All Participants.

Table 6: *Geometric Mean Calculation Result Matrix*

Geometric Mean Results of the Group Evaluations for Seven KPIs	Capacity Using Rates	On Time Delivery Rate	Product Customizations	Forecasting Success Rate	Investment Cost	IT Security	Failure Rates
Capacity Flexibility Rates	1	3 2/3	1/3	2 2/3	3 1/2	3 1/4	1/2
On Time Delivery Rate	1/4	1	2/7	2/7	1/3	1 2/3	1/3
Product Customizations	3	3 3/8	1	3 1/3	3 4/5	4 3/5	3 1/4
Forecasting Success Rate	3/8	3 2/5	1/3	1	2 5/8	2 5/9	1/3
Investment Cost	2/7	3	1/4	3/8	1	2 5/8	1/3
IT Security	1/3	3/5	2/9	2/5	3/8	1	1/4
Failure Rates	2	3	1/3	3 1/7	3 1/7	4	1
	7.39068	18.0515	2.7112	11.178	14.7531	19.772	5.9495

Geometric Mean Fromulation= $b_{ij} = (a_{1ij} \cdot a_{2ij} \cdots a_{kij})^{\frac{1}{k}}$

k=Number of Participant

2.2.3.Calculations of Consistency Ratio.

Table 7 :*Consistency Ratio of Geometric Mean Matrix*

Normalization Matrix $W_i = \frac{\left[\prod_{j=1}^{n} a_{ij}\right]^{\frac{1}{n}}}{\sum_{i=1}^{n}\left[\prod_{j=1}^{n} a_{ij}\right]^{\frac{1}{n}}}$							Eigenvector
0.14	0.20	0.12	0.24	0.23	0.16	0.08	0.16783805
0.04	0.06	0.11	0.03	0.02	0.08	0.06	0.05587717
0.41	0.19	0.37	0.30	0.26	0.23	0.55	0.329339032
0.05	0.19	0.11	0.09	0.18	0.13	0.05	0.114253251
0.04	0.17	0.10	0.03	0.07	0.13	0.05	0.084286686
0.04	0.03	0.08	0.04	0.03	0.05	0.04	0.043940196
0.28	0.17	0.11	0.28	0.21	0.21	0.17	0.204465615
							1

Table 8: *Consistency Index Calculation*

Lamda	1.24044	1.00866	0.89289	1.27713	1.24349	0.86879	1.21647
n=	7						

Random Consistency Index Table									
n	1	2	3	4	5	6	7	8	9
RI	0.00	0.00	0.58	0.90	1.12	1.24	1.32	1.41	1.45

Table 9: *Consistency Ratio Calculation and Result*

Eigenvalue	**7.74787**	$\lambda_{max} = \sum_{j=1}^{n} a_{ij} \frac{W_j}{W_i} \quad i = 1, 2, \ldots, n$
Consistency Index	**0.12464**	$CI = \frac{\lambda_{max} - n}{n-1}$
Consistency Ratio	**0.09443**	$CR = \frac{CI}{RI}$

Result of the Geometric mean matrix is consistence that result of the Consistency Ratio is smaller than 0.1. These mean evaluations of the participants are trustable.

2.3 Application of the Fuzzy Analytical Hierarchy Method

Evaluation of the KPIs for all participant are prepared and result are calculated by using Geometric mean and consistencey ratios are checked for all evaluations. According the Geometric mean matrix, Fuzzy AHP matrix for KPIs is determined by using Fuzzy AHP Scales that shown in Table 2. Fuzzy AHP matrix evaluation is shown in Table 10.

Table 10*:Fuzzy AHP Matrix for KPIs*

	FAHP KPIs Evaluation	Capacity Using Rates			On Time Delivery Rate			Product Customizations			Forecasting Success Rate			Investment Cost			IT Security			Failure Rates		
a1	Capacity Using Rates	1	1	1	3	4	5	1/4	1/3	1/2	2	3	4	2	3	4	3	4	5	1/3	1/2	1
a2	On Time Delivery Rate	1/5	1/4	1/3	1	1	1	1/4	1/3	1/2	1/4	1/3	1/2	1/4	1/3	1/2	1	2	3	1/4	1/3	1/2
a3	Product Customizations	2	3	4	2	3	4	1	1	1	2	3	4	3	4	5	3	4	5	1	2	3
a4	Forecasting Success Rat	1/4	1/3	1/2	2	3	4	1/4	1/3	1/2	1	1	1	2	3	4	2	3	4	1/4	1/3	1/2
a5	Investment Cost	1/4	1/3	1/2	2	3	4	1/5	1/4	1/3	1/4	1/3	1/2	1	1	1	2	3	4	1/4	1/3	1/2
a6	IT Security	1/5	1/4	1/3	1/3	1/2	1	1/5	1/4	1/3	1/4	1/3	1/2	1/4	1/3	1/2	1	1	1	1/5	1/4	1/3
a7	Failure Rates	1	2	3	2	3	4	1/3	1/2	1	2	3	4	2	3	4	3	4	5	1	1	1
		4.9	7.17	9.67	12.3	17.5	23	2.48	3	4.17	7.75	11	14.5	10.5	14.7	19	15	21	27	3.28	4.75	6.83

2.3.1. Calculation of Consistency Ratios and Weights for KPI Evaluations

According the KPI Fuzzy AHP matrix Consistency ratio is calculated and calculation table is shown in Table 11. Result of the CR≤0.1 So Evaluation can be acceptable.

Table 11: *Consistency Calculation Table for KPI Fuzzy AHP Matrix*

Consistency Calculation of Fuzzy AHP Matrix for KPIs								
0.13953	0.22857	0.11	0.12	0.26	0.27	0.28		0.20084
0.03488	0.05714	0.11	0.12	0.03	0.03	0.03		0.06003
0.4186	0.17143	0.33	0.24	0.26	0.27	0.28		0.28143
0.04651	0.17143	0.11	0.12	0.13	0.09	0.07		0.10542
0.04651	0.17143	0.08	0.08	0.03	0.03	0.03		0.06833
0.03488	0.02857	0.08	0.08	0.03	0.03	0.03		0.04626
0.27907	0.17143	0.17	0.24	0.26	0.27	0.28		0.23769
1.43934	1.05045	0.84	1.15965	1.15965	1.00219	1.12902		7.7846
					Consistency Index			**0.13077**
					Consistency Ratio			**0.09907**

After determination of the Consistency, Weighting calculation is prepared for Fuzzy AHP for KPIs matrix. Calculation is made in Excel files and Calculation tables are shown in Table 12, Table 13.

Table 12: *First Iteration of Weight Vector Calculations*

$$\sum_{j=1}^{m} \tilde{M}_{gi}^{j} = \left(\sum_{j=1}^{m} l_j, \sum_{j=1}^{m} m_j, \sum_{j=1}^{m} u_j \right)$$

l	m	u
11.58	15.83	20.50
3.20	4.58	6.33
14.00	20.00	26.00
7.75	11.00	14.50
5.95	8.25	10.83
2.43	2.92	4.00
11.33	16.50	22.00
56.25	**79.08**	**104.17**

$$S_i \approx \sum_{j=1}^{m} \tilde{M}_{gi}^{j} \otimes \left[\sum_{i=1}^{n} \sum_{j=1}^{m} \tilde{M}_{gi}^{j} \right]^{-1}$$

$$\left[\sum_{i=1}^{n} \sum_{j=1}^{m} \tilde{M}_{gi}^{j} \right]^{-1} = \left(\frac{1}{\sum_{i=1}^{n} u_i}, \frac{1}{\sum_{i=1}^{n} m_i}, \frac{1}{\sum_{i=1}^{n} l_i} \right)$$

l	m	u
0.1112	0.20021075	0.36444444
0.03072	0.05795574	0.11259259
0.1344	0.25289779	0.46222222
0.0744	0.13909378	0.25777778
0.05712	0.10432034	0.19259259
0.02336	0.03688093	0.07111111
0.1088	0.20864067	0.39111111

Table 13: *Weight of the KPIs calculation result Table*

$$V(\tilde{M}_2 \geq \tilde{M}_1) = \begin{cases} 1, \text{eğer } m_2 \geq m_1 \\ 0, \text{eğer } l_1 \geq u_2 \\ \dfrac{l_1 - u_2}{(m_2 - u_2) - (m_1 - l_1)} \text{diğer durumlarda} \end{cases}$$

W'(Weight Vector Calculations)	Sa1	Sa2	Sa3	Sa4	Sa5	Sa6	Sa7	
	1	0.0097	1	0.5181	0.4591	0	1	
	0.8136	*	1	1	1	0.6571	1	
	1	0	*	0.3761	0.2814	0	0.8529509	
	1	0.3201	1	*	0.7727	0	1	
	1	0.5447	1	1	*	0.1718	1	
	0.9681	1	1	1	1	*	1	
	*	0.0246	1	0.4947	0.4454	0	*	
MinV(M≥Mi)	0.8136	0	1	0.3761	0.2814	0	0.8529509	3.3241792
Normalization of W	**0.2448**	**0**	**0.3008**	**0.1132**	**0.0847**	**0**	**0.2565899**	**1**

2.3.2. Calculations of Consistency Ratios and Weights for Company Evaluations.

After calculation of the Fuzzy AHP evaluation for KPIs, Company comparison evaluations are determined that Fuzzy AHP matrixes are prepared for all KPIs. Consistency Ratios are calculated for all Company evaluations and results is shown in Table 14. Calculations are done by Excel.

Table 14: *Company Evaluation Consistency Calculations Results*

	CI Consistency Index	**CR Consistency Ratio**
Capacity Using Rates	0.068253968	0.117679256
On Time Delivery Rate	0.029401154	0.050691646
Product Customizations	0.048362902	0.083384313
Forecasting Success Rate	0.055731851	0.096089398
Investment Cost	0.055731851	0.096089398
IT Security	0.026420339	0.045552308
Failure Rates	0.039364231	0.067869363

Weights are calculated for Company evaluation for each KPIs. Calculation example is given in Table 15. Result of the Weight Calculation is given in **Грешка! Източникът на препратката не е намерен.**, Table 17. Example is Company Evaluation for Capacity Using Rate. And rest of the Evaluations is calculated by Excel.

Table 15: *Company Evaluation Matrix for Capacity Usage Rate*

Capacity Using Rates	Ent A			Ent B			Ent C		
Ent A	1	1	1	1/6	1/5	1/4	1/7	1/6	1/5
Ent B	4	5	6	1	1	1	1/4	1/3	1/2
Ent C	5	6	7	2	3	4	1	1	1
	10	12	14	3.167	4.2	5.25	1.393	1.5	1.7

2.4 Results of the Fuzzy AHP Calculations

Company Evaluation calculation are prepared for all KPIs and result of the Weights and Results of Fuzzy AHP method is shown in Table 18. Calculations and results for all Company evaluations are done by Excel.

Table 16: First Iteration of the Weight Calculation of Company Evaluation Matrix

$$\sum_{j=1}^{m} \tilde{M}_{gi}^{j} = \left(\sum_{j=1}^{m} l_j, \sum_{j=1}^{m} m_j, \sum_{j=1}^{m} u_j \right)$$

1,31	1,37	1,45
5,25	6,33	7,50
8,00	10,00	12,00
14,56	17,70	20,95

$$S_i = \sum_{j=1}^{m} \tilde{M}_{gi}^{j} \otimes \left[\sum_{i=1}^{n} \sum_{j=1}^{m} \tilde{M}_{gi}^{j} \right]^{-1}$$

0,0625	0,0772	0,0996
0,2506	0,3578	0,5151
0,3819	0,565	0,8242

Table 17: *Second Iteration of the Weight Calculation of Company Evaluation Matrix*

$ Ent A	$ EntB	$ EntC	
0	1	1	
0	*	1	
*	0,39	*	
0	0,39	1	1,4
0	**0,28**	**0,719**	1

$$V(\tilde{M}_2 \geq \tilde{M}_1) = \begin{cases} 1, \text{eğer } m_2 \geq m_1 \\ 0, \text{eğer } l_1 \geq u_2 \\ \dfrac{l_1 - u_2}{(m_2 - u_2) - (m_1 - l_1)} \text{diğer durumlarda} \end{cases}$$

2.5 Results of the Fuzzy AHP Calculations

Company Evaluation calculation are prepared for all KPIs and result of the Weights and Results of Fuzzy AHP method is shown in Table 18.

Table 18: *Weights Comparison Table*

Fuzzy AHP Evalauation Matrix	Capacity Using Rates	On Time Delivery Rate	Product Customizations	Forecasting Success Rate	Investment Cost	IT Security	Failure Rates	Results
KPI	**0.24**	**0**	**0.3**	**0.11**	**0.08**	**0**	**0.26**	
Ent A-Still Perspercive into Industry 3.0	0	0	0	0	1	1	0	**0.08466339**
Ent B- In the Transition Period to Industry 4.0	0.281	0	0.183	0	0	0	0.5	**0.25211269**
Ent C- Applied all Industry 4.0 Elements	0.719	1.00	0.817	1	0	0	0.5	**0.66322392**
								1

According the Results prove us that Enterprise C which is the Applied all Industry 4.0 Elements values is bigger than Enterprise A and Enterprise B. Enterprise B value is bigger than Enterprise A. Final calculation formulation is comparison of the alternatives and KPIs table. According the final result, Enterprise C is better situation in the sector. By using FAHP evaluation, our performance requirement are determined and compared with the competitors. Excel files are used during the calculation and it helps us to easily update the evaluation values and our company situaiton with competitors can easiliy determine in future decision making and management bottlenacks.

Conclusion

In this research, Industry 4.0 and explanation of the combinations of the existing manufacturing and large technological innovations are explained. Industry 4.0 main elements are determined for how make change into Supply Chain. Second part of the research, Fuzzy AHP is applied for understanding the evaluation of interaction between the Industry 4.0 and Supply Chain Performance and results show us that Industry 4.0 elements gain advantage for Companies competitive advantage. Industry 4.0 is current trend which include mainly automation and data exchange in manufacturing technologies, cyber-physical systems, the Internet of Things. Industry 4.0 refers to create a "smart factory". Application of the Industry 4.0 element is not enough for companies that markets will became larger and larger following days. These elements must be used for all Supply Chain levels and Governments must adapt their policies to new changing markets and Industry 4.0 obligation if they want to accommodate to new world manufacturing system. This research can be extended in two directions. First Suggestion for future study for Application of Industry 4.0 for all Supply Chain levels that can be examined for Retailers, Manufacturers and also how the consumer behavior change after digitization The other one, what kind of indicators will be created for using Performance measurement and decision making in Supply Chain by Industry 4.0.

References

Akter, S. (2016). How to improve the Company Performance using big data analytics. *Internation Journal of Produciton Economics*, 113-131.

Chopra, S. (2012). Supply chain management: strategy, planning and operation. *Pearson(5th Edition)*.

Frazzon, E. M. (2015). Improving Supply Chain through the application of Cyber Physical Systems.*IFAC*,2059-2064.

Frazzon, E. M. (2015). Synchronizing and Improving Supply Chains through the application of Cyber- Physical Systems. *IFAC*, 2059-2064.

Gnimpieba, D. R. (2015). Using Internet of Things technologies for a collaborative supply chain. *Procedia Computer Source*, 550-557.

Gunesakeran, A. (2004). A framework for supply chain performance measurement. *International Journal of Production Economics*, 333-347.

H. Cirtita, D. G.-S. (2012). Measuring downstream supply chain performance. *J. Manuf. Technol. Manag*, 299-314.

Hermann, M. (2017). Analysis of control architectures in the context of Industry 4.0. *Procedia CIRP*, 165-169.

Jakubovskis, A. (2017). Flexible production resources and capacity utilization rates: A robust optimization perspective. *International Journal of Produduciton Economics*, 77-85.

Kaisler, S. (2013). Big data: Issues and challenges. *IEEE*, 995-1004.

Kassio, S. (2017). Opportunities Assessment of Product Development Process in . *Procedia Manufacturing* , 1358-1365.

Krotov, V. (2017). The Internet of Things and new business opportunities. *Business Horizon*, 831-841.

Lee, K. (2015). The internet of things (IoT): Applications, investments, and challenges for enterprises. *Business Horizon*, 431-440.

N. Slack, S. C. (1995). In *Operations Management.* Pitman Publish

Rajesh. (2016). Forecasting supply chain resilience performance using grey prediction. *Electronic Commerce Resarch and Applications*, 42-58.

Simchi-Levi, D. (2008). Designing and Managing the Supply Chain. Concepts, Strategies, and Case Studies. *McGraw Hill*.

Singh, A. (2017). Application of Big Data in Supply Chain Management. *Materials Today*, 1106-1115.

Stewart, G. (1995). Supply chain performance benchmarking study reveals keys to supply chain excellence. *Logistics Information Management*, 38-44.

Syntetos, A. A. (2016). Supply chain forecasting:Theory, practice, their gap and the future. *European Journal of Operational Resarch*, 1-26.

Tanrısever, F. (2012). Managing capacity flexibility in make-to-order production environments. *European Journal of Operation Resarch*, 334-345.

Trkman, P. M. (2010). The impact of business analytics on supply chain performance. *Decision Support System*, 318-327.

Weinberg. (2015). Internet of Things: Convenience vs. privacy and secrecy. *Business Horizon*, 615-624.

ESSENCE AND APPLICATION OF THE SPATIAL DATA INFRASTRUCTURE

Assos. Prof. Milen Ivanov PhD,
NMU „Vassil Levski" Veliko Tarnovo, Bulgaria
e-mail milen_i1970@abv.bg

Abstract: *Spatial data infrastructure (SDI) is the infrastructure that facilitates the discovery, access, management, distribution, reuse, and preservation of digital geospatial resources. The aim of this paper is to present the nature and concept of spatial data infrastructures, which have helped to build understanding about the importance of the relationships within different levels of SDIs to support the interactions and partnerships of the spatial data communities.*

Key words: *GEOINFORMATION TECHNOLOGY, GEOGRAPHIC INFORMATION SYSTEM, DIGITAL ELEVATION MODEL, LIDAR TECHNOLOGY.*

1. Introduction

The emergence of spatial data infrastructures (SDIs) is closely associated with the efforts of collecting and producing geospatial data, as well as the advancement of surveying and computer technologies. In the past decades, a large amount of geospatial data, such as remote sensing images and GPS locations, have been collected by government agencies. Meanwhile, the fast development of geographic information systems facilitates the derivation of various data products from the collected data, such as topographic maps, land cover data, transportation networks, and hydrographic features.

Spatial Data Infrastructure (SDI) is an initiative intended to create an environment in which all stakeholders can co-operate with each other and interact with technology, to better achieve their objectives at different political/administrative levels. SDIs have become very important in determining the way in which spatial data are used throughout an organisation, a nation, different regions and the world.

Spatial Data Infrastructure is a strategically important issue for the countries of the European Union. Spatial Data Infrastructure (SDI) includes the following elements: technology, standards, policies and human resources.

The integration of information from satellite imagery with various other information layers allows:

• syncing a variety of data;

• verifiability check;

• updating and creating the opportunity to provide the basis for effective and sustainable governance.

The co-location of data from space and land-based sources, as well as permanent land-based monitoring (land cover and land use), enables information to be secure and reliable, end-to-end services and effective results from the accompanying analyzes, forecasting models and estimates.

2. Bulgarian spatial data infrastructure

The Bulgarian Spatial Data Infrastructure (BIPD) is a prototype geoportal as a free public benefit service. One of the main goals of BIPD is to present databases, services and operational capacity to Bulgarian organizations with priority:

• sustainable development strategy Europe 2020;

• Danube strategy;

• Earth Observation Program - Global Monitoring for Environment and Security; in integration with the development of the GALILEO satellite navigation system;

• European directives and regulations for the harmonization of spatial data, data quality assurance, land monitoring, risk management and security.

The initiative is part of a framework agreement between the Executive Agency "Electronic Communications Networks and Information Systems" (ESMIS), now State Agency for Electronic Governance (EAU) to the Council of Ministers and the Agency for Sustainable Development and Eurointegration (ASDE) as well as in the execution of tasks under an agreement between ASRE and the Joint Research Center (JRC) Commission. An experimental data geography [4], an element of applied research and development projects, including the 7th Framework Program of the European Union, has been developed. One of the objectives is to facilitate and accelerate the implementation of the requirements of European Parliament Directive 02/07 / EC establishing an Infrastructure for Spatial Information in the European Community (INSPIRE).

The experimental geoportal is user-oriented. The user can open and observe different thematic maps as well as digital satellite images attached to the map of the Republic of Bulgaria. Apart from the thematic card material, attribute data tables are also included, and for more and more diverse information, a link to other websites (Wikipedia) is provided.

The database is continuously complemented by new layers of information coming from different state, scientific and municipal structures. They are presented in a timely manner electronically with the appropriate degree of accuracy.

The first phase of the pilot project - a spatial database for the trans-European transport corridors passing through Bulgaria - is based on satellite images with a 15 m and 30 m satellite resolution from the LANDSAT satellite.

To improve image accuracy, it is also necessary to take into account various types of interference. "The effect of disturbance impacts on the quality of the information processed, resulting in its destruction or aging, which increases the degree of uncertainty in the decision-making process" [1].

Currently finished layers of land cover from satellite images with 5 m resolution SPOT satellite, as well as very high resolution 0.70 m and 1 m from satellites Ikonos and Quickbird for cities, ports and other important sites.

3. SmartSDI Information System.

The SmartSDI system creates and maintains a database of geospatial data and services available in government, as well as information about their administrators. The system offers input, editing and intelligent search tools in the database, these functionalities being implemented in separate modules. The web-based professional implementation of the system, as well as its functional scope, allow use and development within the national geoportal. The main activities include:

• Performing quality control of the accuracy and reliability of spatial data;

• Validation of terrestrial and distance methods for measurement of areas according to ISO standards;

• modeling of requirements and business processes (administrative and system level) through UML;

• inventory of databases and creation of metadata using XML schemas;

• object-oriented analysis, classification and retrieval of geo-objects from satellite and airplane images;

• processing and interpretation of data from satellite and aerospace imaging, in visible, infrared, radar and radiometric spectra. To date maps of land cover have been prepared on different scales for the needs of the most important trans-European corridors with a 10 km buffer and functional urban areas;

• Performing ground observations with radiometric instruments for the assessment of soil moisture for the early diagnosis and reduction of the effects of soil over-wetting, dredging and flooding;

[1] Lazarov L.I., The basics of the electronic war, Veliko Varnovo, 2018, p. 37

• Voice technology for monitoring, control, control and security.

The user can open and observe thematic digital maps [3] as well as digital satellite imagery from any point along the routes of the trans-European transport corridors attached to the map of the Republic of Bulgaria. The integration of information from satellite imagery with various other information layers allows the synchronization of various databases, verifying their authenticity, updating and enabling the basis for effective and sustainable management.

4. *Web SmartCover GIS.*

The SmartCover Information System and its accompanying architecture provides spatial data services in the web GIS environment. SmartCover is unique to Bulgaria and the European Union because it contains cross-border spatial data and services harmonized under the INSPIRE directive. On the other hand, SmartCover is based on a terrestrial layer (land use) layer developed under the global ISO 19144-2 (LCML) [8] standard, thus maintaining coordination and updating of different layers of spatial data and integrating thematic databases into a common harmonized information package. One of the main tasks of SmartCover Architecture is to be an information platform for integrated risk management, territory and citizens' protection as well as regular monitoring of changes and effective absorption of European, regional and national funds.

ASURE and ReSAC are involved in the development of comprehensive spatial planning resources in the border administrative districts between Bulgaria and Romania, covering a large part of the lower Danube region. The co-operation is under the cross-border cooperation program and under the project "General Strategy for Sustainable Territorial Development of the Romania-Bulgaria Region (SPATIAL)".

More detailed technical activities include creating and building systems and information services. The developed services allow the integration of new harmonized spatial databases and other services to be the basis for the creation of information systems at the state / local level. The database will provide the necessary information for a complete set of indicators at the statistical level - Fig. 1.

A specific result of the project is the creation of a comprehensive common land cover database for the cross-border area, based on the philosophy of Land Cover Meta Language - LCML (ISO 19144-2) and fully in line with the principles of the INSPIRE Directive. The Common Specification will provide more effective cross-border analysis and reporting.

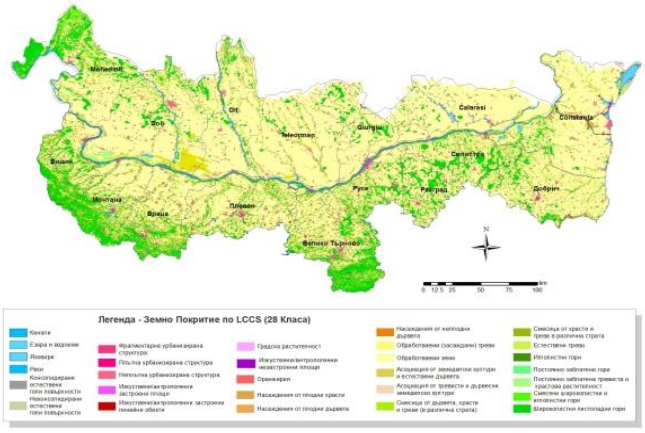

Fig. 1. *Ground cover database.*

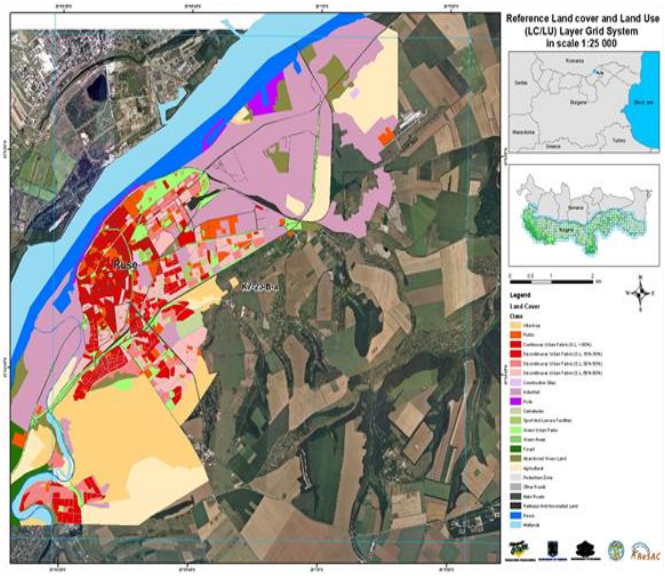

Fig. 2. *Extract from land cover / land use (based on LCCS / FAO) for the city of Rousse.*

5. *Ground cover "reference layer - Bulgaria"*

The Bulgarian initiative for the development of a national land cover database, using the FAO-LCCS methodology, is an example of applying good world practices in assisting in local (national) decision-making. The reference database - a layer of terrestrial coverage on the territory of the Republic of Bulgaria is entirely prepared by specialists from the Agency for Sustainable Development and Eurointegration (ASDE) and the application center for satellite imagery - ReSAC.

The Earth Cover Reference Layer is based on satellite images from Landsat satellite (USA) from 2011, with a resolution of 30 m. Information on the altitude and the slope of the area is provided on each spatial object (Figure 3.9). The authenticity of the interpreted data has been verified and an accuracy of 85% has been achieved.

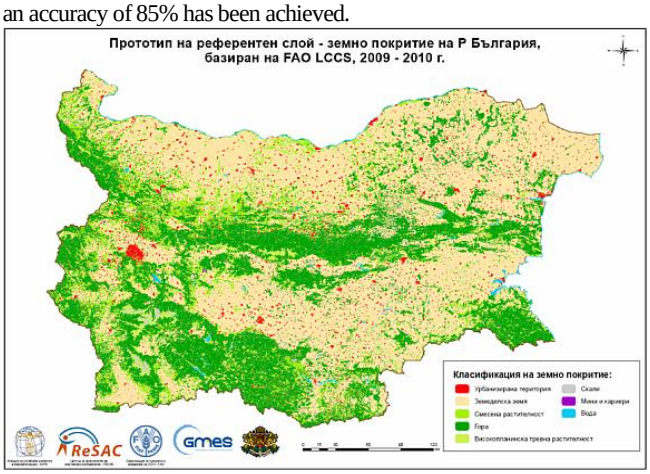

Fig. 3. *Land cover "reference layer - Bulgaria".*

Bulgaria is the first Member State of the European Union to launch a land cover database based on the world-wide accepted LCCS methodology for the territory of the whole country, updated for the period 2009-2013.

The LCCS-based reference database for Bulgaria is one of the first attempts to be combined with a similar approach at local and national level to the global approach to land management and monitoring and land use.

This database is in line with the GLOBCOVER international project, in which, apart from the European Union, the United States, Russia, Canada, etc. (Figure 3.10) participate. The reference layer includes updated information on the relief (SRTM v.4, by DG JRC) and the main types of land cover, thus creating an appropriate product for planning and managing the site.

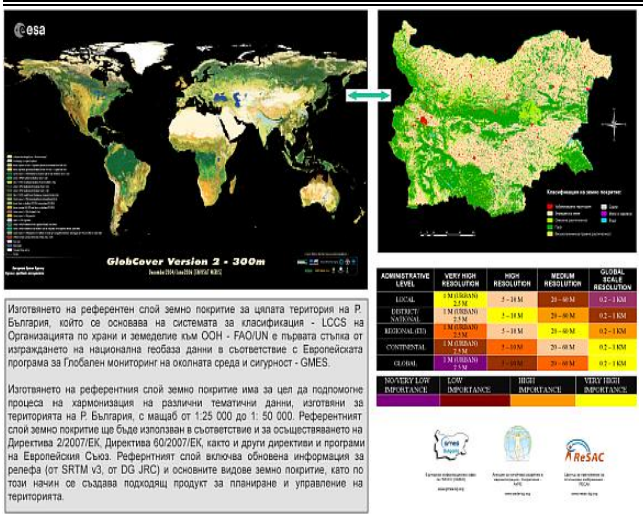

Fig. 4. The reference database for Bulgaria as part of the GLOBCOVER international project.

In partnership with the state administration, municipalities, civic associations, scientifically-applied organizations, universities and scientific institutes from the Bulgarian Academy of Sciences, ASURO participates in the progressive building of operational capacity to fulfill the requirements under Directive 2007/02 / EC and under the Global Monitoring for Environment and Security (GMES).

Global monitoring is also used in the field of intelligence. "Coordination is needed when planning and conducting intelligence in remote areas"[2].

One of the results is the preparation of maps of the terrestrial coverage of the regional cities in Bulgaria based on high resolution satellite imagery. The maps are 1: 5000 scale, using images with a spatial resolution of 0.5 to 1 m from different satellites - "Ikonos", "Quickbird" and "Eros".

Work on the preparation of more detailed maps of the land cover for the district towns, which will enable the map of the town, the regulation map, the thematic maps of the infrastructure, as well as the maps of the lands, the natural environment and the agricultural properties around the cities.

[2] Yankov Y.I., Human intelligence - essence, advantages and limits of info gathering, Collection of reports from the Annual University Scientific Conference, V. Varnovo, 2010, p.2

Conclusion

1. Spatial data infrastructure presents a solution to the problems of resource discovery and data redundancy. It provides a unified platform where people can go and search geospatial data, maps, services, and other digital resources. As multiple government agencies are sharing their data on one platform, SDI reduces data redundancy and the extra efforts in collecting duplicated geospatial data.

2. Spatial data infrastructures heavily rely on computer and information technologies, and are continuously evolving with the technological advancements.

Similarly, we may see the emergence of new technologies that can improve SDIs in various aspects, and some of these technologies are already being tested in research labs.

Literature

1. Lazarov L.I., The basics of the electronic war, NMU "V. Levski", Veliko Varnovo, 2018, p. 37, ISBN 978-954-753-270-0
2. Yankov Y.I., Human intelligence - essence, advantages and limits of info gathering, Collection of reports from the Annual University Scientific Conference NMU "V. Levski", vol. 9, V. Varnovo, 2010, pp. 98-103, *ISSN 1314-1937*
3. Vulchinov V., Geoinformatics, UACEG, Sofia, 2003
4. Minkov P., Use of Space Systems for Geoinformation Security, Yearbook of BA, Sofia, 2007
5. Disaster Risk Reduction Strategy 2014-2020, Sofia, 2014
6. Tepeliev Y. et al., Geographic Information Systems, Sofia, 2003
7. Hoffman-Velenhov B., H. Liechtener, Collins, Global Positioning System, Sofia, 2002 Keenan P. B. Spatial Decision Support Systems: A coming of age, Control and Cybernetics, vol. 35, No. 1, 2006
8. MC 296/1 NATO Geospatial Policy, 2006.
9. STANAG 7016 IGEO – Maintenance of geographic materials, edition 4, 2002
10. http://www.esri.com/arcgisdefensemapping, Defense Solution, Accessed 14.04.2018
11. http://www.nwgis.com, Spatial Analysis, Accessed 15.05.2018

INNOVATIVE APPROACH TO CONTAMINATED SOIL PHYTOREMEDIATION: HEAVY METAL PHYTOEXTRACTION USING ENERGY CROPS

Professor Dr. Valdas Paulauskas
Aleksandras Stulginskis University, Lithuania
valdas.paulauskas@asu.lt

Abstract:
Land contamination is now recognised as a problem capable to affect ecosystems and human health in a range of different ways. Perception of soil as a vital natural element as well as an essential resource for human survival and development raises public awareness of soil contamination as an important environmental issue worldwide. It is reported that more than 10 million contaminated sites exist on our planet, with half of the sites contaminated with heavy metals (Khalid et al., 2017). If most of organic contaminants are easily biodegradable, heavy metals are highly resistant to either biologically or chemically induced degradation. Successful phytoextraction technology development as well as implementation requires comprehensive understanding about heavy metal mobility influencing factors, metal behaviour in soil-plant system and their transfer peculiarities from substrate to different plant parts.

One of the most abundant sources for alternative energy is biomass. However, due to the shortage of arable lands energy cropping is enforced to compete with traditional agriculture. But exists another problem, that upper soil layer in many regions is contaminated with trace elements (e.g. Cd, Cu) as a consequence of intensive farming. Soils with exceeding threshold values for heavy metals are no longer proper for food and feedstock production. Combining traditional phytoextraction with energy cropping could help not only to reduce contamination incorporating plants, and also to use biomass for energy recovery. An interdisciplinary approach on phytoremediation of heavy metal contaminated land could extend the accessibility of arable land for energy cropping, also reveal new possibilities to reuse rest products of phytoremediation process.

In this study heavy metal accumulation potential in the biomass and different plant parts of the selected species of energy crops cultivated on contaminated soil was evaluated. Phytoextraction potential, biomass yield and qualitative parameters of bioenergy plants grown on heavy metal contaminated soil has been measured. Finally heavy metal influence on biomass utilization possibilities, energy recovery and further safe use of the rest products has been evaluated. Demonstrated possibilities to grow bioenergy plants on moderately contaminated soil could increase the use of marginal lands, decrease land use competition between food and liquid biofuels and provide options for a gentle and cost-effective remediation.

ENVIRONMENTAL AIR QUALITY MONITORING SYSTEM AS A SUPPORT FOR PRECISION AGRICULTURE

M-r Elena M.Jovanovska, Prof.Danco Davcev PhD, Prof. Kosta Mitreski PhD
Faculty of Computer Science and Engineering – Skopje, University "Ss. Cyril and Methodius" – Skopje
{elenamitreska@gmail.com,danco.davcev@finki.ukim.mk,kosta.mitreski@finki.ukim.mk}

Abstract. In order to make better decisions in the precision agriculture the measurement of air pollution parameters such as PM10, NOx, SO2, CO, O3 and agriculture parameters such as air temperature, humidity, soil moisture and leaf wetness are of crucial importance. Making analysis using different AI technics based on these parameters can bring better yield and quality in the food production process. In this paper we present our approach in building an environmental air quality monitoring system as a support for precision agriculture.
KEYWORDS: AIR POLLUTION, WIRELESS SENSOR NETWORK, PRECISION AGRICULTURE, IOT

IMPROVING LOGISTIC PROCESSES IN THE PRINTING HOUSE IN THE CONTEXT OF THE "INDUSTRY 4.0" CONCEPT

Marta Hurka (Master of Science)[1], Magdalena K. Wyrwicka (PhD DSc Eng., Associate Prof.)[2*]
[1] Poznan University of Technology, Poland, [2]Poznan University of Technology, Poland
marta.hurka@doctorate.put.poznan.pl, magdalena.wyrwicka@put.poznan.pl

Abstract: *The research in the field of logistic processes in the printing house will be focused on defined the improvement in the context of the „Industry 4.0" concept. In the industry, the growing complexity of production makes logistic processes more and more important. In every printing house industry certain processes which are implemented in the sphere of production can be systematized. The study will focus on the importance and goals of logistics processes; distribution; logistic chain; analysis of the efficiency of processes; selection of suppliers and organization of deliveries, creating networks of cooperators in the enterprise; computer support of processes at production; designing logistic systems. The study will present logistic processes in the printing house based on the „Industry 4.0" concept. "Industry 4.0" is often identified in the first place with the digital transformation of production systems - their digitalization. The production sphere is also moving towards increasing digitalization, first and foremost by using wider applications: data management (Big Data), and above all effective acquisition (via various types of sensors) and analysis of data; automation, e.g. the combination of traditional manufacturing methods with artificial intelligence, allowing to reduce errors and costs; communication using broadband links to connect the whole value chain; digital communication with clients. The conclusion of the research will be providing improvements of processes in chosen printing industry analyzing the solutions of the "Industry 4.0" concept.*
KEYWORDS: *LOGISTICS; LOGISTIC PROCESSES, PRINTING HOUSE; INDUSTRY; INDUSTRY 4.0*

Introduction

The importance of the industry for global economies is enormous therefore companies are still looking for new solutions that simplify production processes and reduce costs and minimize the terms of order deadlines. For companies located in Europe where labor is a high cost, shortening the production cycle is very important from the perspective of the company's competitiveness.

Therefore, each of the world's distinctive economies runs its own industrialization strategy. In China, in accordance with the government FYP program (Five-Year Plan / 11-16) each "western" investment should result in a research and development center serving the development of the transferred technology. In turn, in the United States innovation is the main development strategy. In this country exists an efficient system supporting research and development based on cooperation between academic centers and business. Whereas in Europe, especially in Germany appeared the concept of creating a "smart factory" (digital factory), the assumptions which describe the concept of "Industry 4.0" which aims to connect industrial processes and digital technologies.[1]
In the logistic sense, this means moving away from the value chains and preferring temporarily created virtual physical cyber networks.[2]
The production sphere in printing houses is heading towards digitization, using the following facilities: Big Data efficient data acquisition and analysis; automation is the integration of artificial intelligence into traditional production in the printing industry, will be discussed in greater detail later in the article; digital communication with clients.
The quintessential concept of "Industry 4.0" is the Internet of Things, which is to integrate people, products and machines into one unit in order to deliver the packaging which is final product expected by the customer and with satisfaction for the printing house in terms of production and cost.
Currently, it is estimated that the implementation of the "Industry 4.0" concept will achieve by 2025 an additional total profit of 260 billion euros.[3]
The table shows the Industry section from 1.0 to 4.0 with assigned duration, technology, production system and different markets.

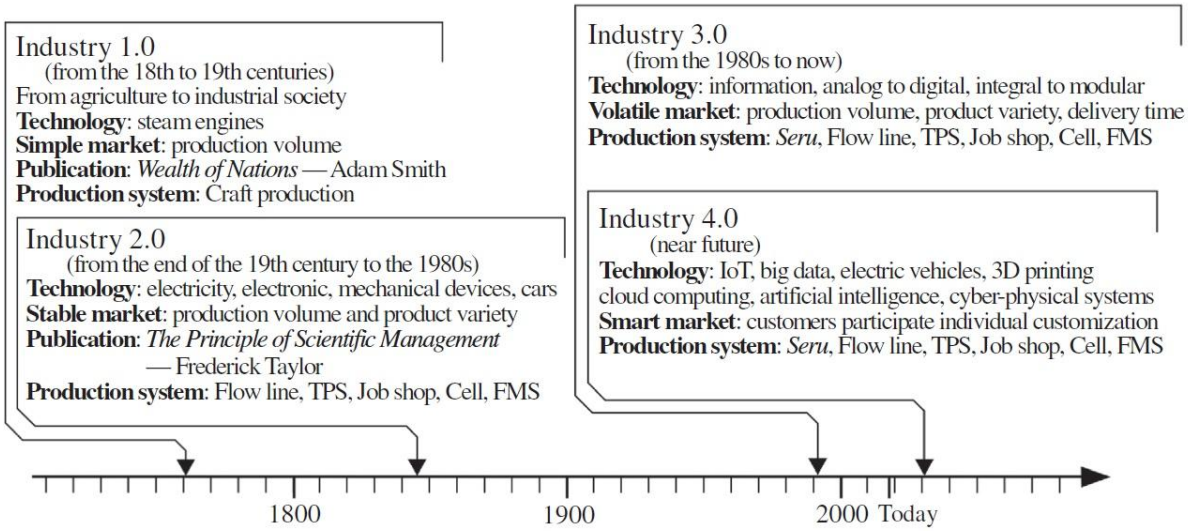

Figure 1. *Time line of Industry 1.0-4.0*[4]

[1] B. Woliński, The concept of "Industry 4.0" as a strategy for reindustrialisation and implementation of next generation production processes
[2] M. Wyrwicka, Revolution or evolution in logistics?
[3] Consultants R.B.S. (2015) The Digital Transformation of Industry, Roland Berger Strategy Consultants, Berlin
[4] Yong Yin, Kathryn E. Stecke& Dongni Li, The evolution of production systems from Industry 2.0 through Industry 4.0

Logistics processes in printing industry

In order to meet the demands placed on the market, new technologies are being created to increase efficiency, decrease the price and improve quality. Most of data in printing house is sent via Internet. A modern printing house is one that is equipped with a modern machine park but is it only that? What is also important is a tightened relationship with the customer, flexibility to meet client's requirements and environmental protection including lower energy consumption. In doing so, it is necessary to improve the logistic processes existing in the enterprise, on the most important ones we will focus below.

Distribution of ready-made packaging in the packaging printing house is delivered directly to the final customer or to the buffer warehouse. Often, deliveries are defined, for example, 2x a week under customer demand. Once a week, the customer sends an EDI call to the current call off which often changes the day before the planned delivery. Therefore it is essential role to be in close contact with the customer and change the demand depending on the customer's planned production and analyze data EDI and compare it with packaging which are on stock. The analysis of the EDI sent by the customer with the planned collection of packaging plays a significant role and decrease inventory levels secured in the event of sudden changes in production plans.

Analysis of the efficiency of processes using the ERP Print Manager System which is one of the most implemented system in printing houses in Poland, it is possible to analyze the profitability of each production orders and the efficiency of individual machines. Every station in each process in the printing house: printing machines, die-cutting and gluing machines are equipped with a computer with Print Manager system where all the data are collected and is associated with the entire system. Therefore, customer service have current access to data in the system and can check in what production process the order is located at the moment. Additionally, when the production order is completed, it is possible to analyze the reason in case the production costs were too high.

Selection of suppliers and organization of deliveries The company needs to have a systematized group of suppliers. The main suppliers for the packaging printing houses are paper manufacturers and wholesalers. Depending on the order and the date of its implementation, the technologist or person from the customer service department decides where the raw material will be delivered from. Inks, varnishes and other articles directly related to printing are ordered on a regular basis within 24 hours delivery. Providers of industrial services (die-cut, matrix etc.) must establish partnerships with cloud solution providers and data analysis so that processes can proceed smoothly.

Creating networks of cooperators in the enterprise there is a common system in the enterprise which allows the employees to have access to the different modes of system depending on their permission. The communication within the company is conducted using instant messaging. Calculations in the system regardless of the person from customer service are made on the same formula previously created and constantly improved by the specialists. Technology cards for each product with access to technology, type and method of packaging, inventory of individual clients that interact and synchronize with system files from customers make it easier to check the position on the production for both side customer and customer service in the printing house. There is a platform available for customers to check stock levels, a list of structure drawings, each client has access to it after log in at any time.

Computer support of processes at production in the case of uncertainty regarding any of the processes, e.g. packaging, the knowledge can be copied from the existing product cards. In the case of the printing process and resumed work, all parameters are already in the system. In the case of new works, the knowledge of the printer as well as the measurement of the color intensity of the densitometer are necessary. In the case of die-cutting and gluing machines the knowledge of the operators of machines is required, machines do not automatically adjust themselves.

Designing logistic systems Creating a system database and then adding data and streamlining processes by analyzing these data is essential to start improve communication and processes. The printing process is always preceded by checking and processing the artwork by graphics in Prepress department. With the help of solution- PREFLIGHT artworks are distributed to individual graphic due to the level of difficulty. However, the printing process is closely related to the data on the printing machine in the case of printing resumption this process is more efficient and the data is collected from the system. Automatization may apply to this sphere but only in theory. While printing the entire printout, optimizing the ink- color, type of different varnishes checking the sheets every 10-15 minutes is compulsory. Each of printing stages has a lot of inflammatory elements which may occur errors. The printing process for packaging is the most important process because of the raw material (cardboard) often accounts for more than 50% of the whole package price. Therefore, incorrect printing and significant color difference which may be visible on the shop shelves cannot take place during production process. Example is to check all the files prepared by the customers. Early detection of any errors can secure at the initial stage before further consequences: waste of time, material and money. To achieve that is essential to know the realities of the printing house in order to optimize the entire production process.[5] Of course, there are existing printing houses where the transfer of graphic files takes place directly to the printing machine without work of people, on the responsibility of the customer.

Other solutions that streamline processes include placing sensors on gluing machine to verify barcodes and packaging identical assortments. This is used to eliminate errors in manual packaging when the graphics are similar, therefore the bar code is the only determinant that the packages differ from each other.

After sending packaging from the warehouse the invoices are automatically issued in the system, the worker must only check them. Then, some clients have platforms on which they want to have invoices attached. In the future, there will be probably possibility to combine these systems and invoices will automatically pop on the client's platform.

As stated, in advanced technology, we are dealing with technological improvements in Research and Development Industry such as **3D Printing**, usage of **codes** from **GS1** standards to help to unify and streamline processes within the company or implement technological solutions to **automate production processes** such as inserter or conveyors and industrial trucks.

3D Printing is the process to create three dimensional object with material. Is used on a logistics system for spare parts to avoid stocking and is useful in Research and development industry to create e.g. appropriate packaging model.

Under the new regulation of the counterfeit prescription directive, from February 2019, the labeling of the packaging of these products will change. The bar code symbol will change from linear to two-dimensional and the individual serial number of the packaging will be added. The use of this solution in the supply chain will guarantee greater transparency of all stages of the supply chain and will give the opportunity to verify the origin of a particular product and will protect the patient. Inconsistent identification systems increase the operating costs, reduce the effectiveness of activities aimed at protecting European borders against counterfeits. GS1 standards are compliant with ISO and communicate with other standards in the field of health and e-health and are in line with trends in the European Union.[6] The use of

[5] https://www.printnews.pl/znaczy-nowoczesna-drukarnia/

[6] A. Gawrońska-Błaszczyk, How to effectively and effectively implement the requirements of the so-called false directive in the field of a unique identifier.

coneyors and industrial trucks, inserters helps in shortening production processes, eliminating errors and reducing costs.

In doing so, we cannot ignore the essential role of technology, which allows the consumers received information very easily and fast to reduce errors. On the demand side, customers will increase their awareness through easy access to information from the printing house. The solution for further improvement of logistic processes may be applied neural networks, which will map recorded data in order to repeat process activities.

References:

1. Consultants R.B.S. (2015) The Digital Transformation of Industry, Roland Berger Strategy Consultants, Germany
2. L. Santos Dalenogare, G.Brittes Benitez, N. Fabian Ayala, A. German Frank, The expected contribution of Industry 4.0 technologies for industrial performance, Brazil, France
3. A. Gawrońska-Błaszczyk, How to effectively and effectively implement the requirements of the so-called false directive in the field of a unique identifier, Poland
4. E. Hofmann, M. Ruesch, Industry 4.0 and the current status as well as future prospects on logistics, Switzerland
5. V. Roblek, M. Mesko, A. Krapez, A Complex view of Industry 4.0, Slovenia
6. B. Woliński, The concept of "Industry 4.0" as a strategy for reindustrialisation and implementation of next generation production processes, Poland
7. M. Wyrwicka, Revolution or evolution in logistics?, Poland
8. Yong Yin, Kathryn E. Stecke& Dongni Li, The evolution of production systems from Industry 2.0 through Industry 4.0, China
9. https://www.printnews.pl/znaczy-nowoczesna-drukarnia/

CRITERIA FOR WIND ENERGY PROJECTS' LOCATION ASSESMENT

КРИТЕРИИ ЗА ПОДБОР НА ЛОКАЦИЯ НА ВЕТРОЕНЕРИЙНИ ПРОЕКТИ

PhD student Eng. Stankova T.[1], assoc. prof. Toneva D.[2], PhD student Dimova D.[3]
Technical University of Varna, Bulgaria
Stankova.todorka@gmail.com; dtoneva@abv.bg; ddimova5@abv.bg

Abstract: *Insuring a sustainable development of wind energy production and consumption is challenging and highly important for /achieving of EU 20/20/20 goals for Bulgaria. Wind energy has been seen as a clean and environmentally friendly in comparison with conventional energy sources, but there are still some conflicts between wind energy project development and environmental protection goals that should be enlighten and solved. One possible way is to enhance the process of wind energy projects' location identification. The current research is focused on identification and classification of criterion that could be used in this process. The legal requirements regarding wind energy projects' location are analyzed and presented. Additional requirements regarding environmental protection and biodiversity conservation are identified and defined as criterion. A set of measurable indicators related to each criteria is established and proposed in this paper.*

Keywords: WIND ENERY PROJETCS, LOCATION, CRITERIA, ENVIRONMENT

1. Introduction

The increasing renewable energy share in energy production and gross final energy consumption is a global sustainable trend. The Worldwide installed wind energy capacity shows 4.47-fold rise for the period from 2008 to 2017. The installed wind energy capacity in the European Union (EU28) increased from 63 865 MW in 2007 to 171 244 MW in 2018 year, which is nearly 2-fold rise. The same trend is observed in Bulgaria: the installed energy capacity in 2007 was estimated to 114 MW while in 2018 reaches 699 MW [7,17]. This impressive 6.13-fold growth is in line with the achievement of EU20/20/20 targets pointed out by the 2009/28EC Directive of the European Parliament on promotion of use of energy from renewable sources [6]. In the conditions of rapid and dynamic development of wind energy in our country appears the objective need of detailed review of the process of wind energy projects' disposition determination. Creation of methodology for potential wind energy projects' location assessment is an opportunity for sector's optimization and avoidance of conflicts in the "energetics-environment" interaction. The wind turbines' lifetime, estimated to 20-25 years, together with the eager of the investors to insure a definite internal rate of return, lead to the need of the WEPs location selection, based on long-term environmental alterations assessment [10]. Obviously the potential land use conflicts should be taken into consideration.

The present research aims to fill in some of the existing gabs in WEPs' disposition determination by proposing set of criteria applicable to WEP location assessment. The efforts are focused on criteria identification and classification, to support practitioners in WEP sector as well as decision makers.

2. Criteria for Wind energy projects potential location assesment

To achieve and maintain sustainable development of wind energy in Bulgaria is essential to balance the economic efficiency with social and environmental goals. In order to ensure long –term sustainability of WEP a set of criteria that fully covers the process of potential WEP location assessment and exact WEP disposition determination is required. The understanding of interaction and interdependence of economic, technical and environmental factors is a key precondition for WEP location assessment optimization.

The reassurance of renewable energy production with the purpose of insuring energy independence, deduction of greenhouse gas emissions and climate change combating is transposed by Directive 2009/28EC of the European Parliament on promotion of use of energy from renewable sources. This interaction already has a legal performance. The EU legislation related to wind energy as apart of renewable energy was transposed in the Bulgarian law for energy by renewable sources at the end of 2011. Other regulations inforce correlate to environmental protection and agricultural territories' protection, urbanization and urban territories. Numerous restrictions regarding WEP development have been introduced in Bulgaria, such as:

- Prohibition of WEP construction closer than 500 meters from regulated territories under the law for servitudes;
- 35 meters minimum distance to forests;
- 200 meters minimum distance to protected forests;
- 100 meters minimum distance to lakes/rivers;
- Maximum 600sq.m of agricultural land for foundation construction and adjoined infrastructure.

The already existing restriction and prohibition by the Bulgarian law are out of the context of the present research. The existing regulation has an imperative character and only WEP territories with building permit are a subject of evaluation of proposed criteria.

To highlight the main proper conditions for WEP development on certain territory a set of criteria is propose. It includes three main groups of criteria: economic, technical and environmental. In Bulgarian practice many of the problems with WEPs' territorial disposition selection originate from the fact that the assessment process lay down only on economic analysis. A social-economic evaluation and assessment of the value of ecological assets is not performed at all. Thus, we adopt an analytical approach with defragmentation of criteria, so they specifically cover the economic, technical and environmental aspects. At the same time the practice requires more detailed and precise overview and assessments of the conditions under which the WEPs will be developed during the whole life-cycle of the project. That leads us to the detailysation of the proposed groups of criteria requirement. Thus, further decomposition of the main criteria is conducted and classification of criteria is presented on Fig.1. The proposed criteria are out of the specifically prohibited by the Bulgarian legislation restrictions. Three groups of interconnected criterion are definitively underlined: i) economic ii) technical and iii) environmental. The WEPs' location assessment requires analyses at least on the above-mentioned criteria and further synthesis. The evaluation of each criteria fulfillment demands observation, monitoring and analyzation of number of parameters.

The group of economic criteria, as proposed, includes: Wind potential; Initial cost; Maintenance cost; Preferential prices/feed in tariffs.

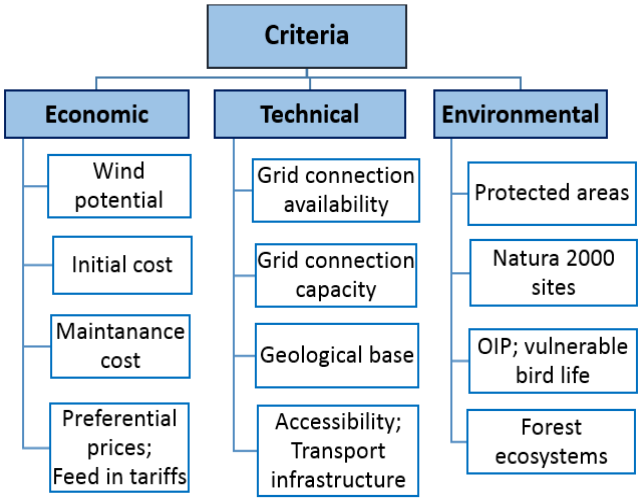

***Fig. 1** Criteria for WEP location assesment and selection*

Beneath "Wind potential" criterion achievement we recognize the presence of wind potential, meeting the qualitatively and quantitatively requirement. It is a predominant condition for WEP' development on certain location. So, the vector realizations of the variables wind speed, velocity and density, compared to the defined minimum requirements for WEP development, manifests the level of criterion's completeness.

"Initial cost" criterion accomplishment suppose that the initial investment, including project purchase fee, project development cost and equipment and construction price, is acceptable and admissible from the investor's perspective. In order to assess the initial expenses on the project additional factors such as project grid connection fee should be evaluated too.

"Maintenance cost" comprises the annual wind project's maintenance. The parameters of interests are operational costs, scheduled and unscheduled fees for reconstruction. The administrative burdens are considered in the frames of "Initial cost" and "Maintenance cost" criterion.

"Preferential prices or feed in tariffs" aims to feed the evaluate expecting internal rate of return (IRR) calculation. Another parameter with significant importance is the state guaranteed period for purchase of the produced energy.

The group of technical criteria is broken down to: Grid connection availability; Grid connection capacity; Geological base; Accessibility and transport infrastructure.

"Grid connection availability" stays to manifest the presence of electrical grid in the area of interest. This criterion alone is not equal to wind energy projects' grid connectivity because the presence of grid does not guarantee the availability of capacity for connection and transfer of energy to the end consumer.

The "Grid connection capacity" is set as a criterion, comprising the presence of free grid capacity and connectivity allowance. The fulfilment of each of those criterion is necessary condition, but only simultaneously jointly achievement of both insure the grid connection of wind projects.

"Geological base" includes the possibility for foundation and installation of wind turbines which weight and base have to be precisely planned on appropriate Earth layers. The parameters of interests are stability of the base and predetermined ease of construction work.

"Accessibility and transport infrastructure" has a multiple means. From one side the WEP's accessibility is crucial for its construction and is highly important for the project maintenance. The wind turbine elements are over-dimensions and require roads via which special vehicles can pass through. On the other side all year round accessibility is needed for the annual maintenance which insures the WEP proper operation.

More parameters could be added to the proposed one but these are considered as the minimum required for the purpose of initial selection of wind project location.

Due to the fact that the economic and technical criteria are well known in practice the interest in the article turns upon the environmental one. The assessment of ecosystem services is an expensive, time taking and challenging task. That's how easy the environmental protection goals and environmental responsibility of organizations drop back as criterion of WEP location determination process. The objective need of simple, clearly defined environmental criterion revealing the interconnection and interdependence between WEPs' development and environmental protection is obvious.

The group of environmental criterion, as proposed, includes: Protected areas; Natura 2000 sites; OIP/vulnerable bird life; Forest ecosystems. The concerns regarding wildlife and natural habitats preservation are taken into consideration. While the economic and technical criteria simply a presence and preference, the environmental suggests absence or avoidance.

For the purposes of current classification the "Protected areas" criterion is fulfilled when the potential WEP location stays off-protected areas and buffer zones.

"Natura 2000 sites" require avoidance of NATURA protected areas as well as buffer zones around them. In accordance to Bulgarian practice we accept the minimal buffering range of 900 meters.

The Ornithology important places (OIP) spread over the marked and overlapped with Natura 2000 areas, the migration routes, especially the one with narrow migration front. No matters that OIP aren't necessarily special protected areas, from investor's perspective, those sites are risky especially when vulnerable bird species are in high abundance.

The high ecologic importance of the "Forest ecosystems" imposes their presence among the environmental criteria, no matter of their legislative status.

Environmental criteria cover the field of direct and indirect interaction between wind energy and environment.

3. Interaction between wind energy projects and environment in Bulgaria

No matter that wind energy is considered as relatively clean energy, with low water consumption [16], saving green gas house emissions there still are some conflicts between wind energy projects' development and environmental protection goals that shouldn't be neglected. Despite that Bulgaria takes less than 1% of European territory, the country is one of the EU member states with richness preserved biodiversity. Proclaimed sites for nature protection and preservation, excluding NATURA 2000 zones, are over 1000. The number of reservs with conservational significance counts to 90. General ban on WEP construction is imposed on-reserves..

Bulgaria obtains the second richest ornithological biodiversity in Europe [14]. It's confirmed by the fact that 78% of the European common bird life including 12 globally endangered by extinction species are presented in Bulgaria [12, 13]. In this context our country is internationally responsible for the protection of vulnerable and threaten of extinction bird species.

In Bulgaria the number of wintering birds of European conservation concern exceeds 200 species [12, 11]. Among them is the Red- breasted goose (*Branta ruficollis*). Almost the whole world population winters in Kraymorska Dobrudzha. 114 ornithology important places (OIP) are appointed by Birth Life International in Bulgaria. In addition 118 Bulgarian sites (22.6% of the national

territory) are a part of the largest network of protected areas - Natura 2000. The map of NATURA 2000 protected zones is presented on Fig.2. These zones are established to ensure the long-term survival of Europe's most valuable and threatened species and habitats, listed under both the Birds Directive and the Habitats Directive. In Bulgaria the OIP and Natura 2000 sites generally are overlapping territories.

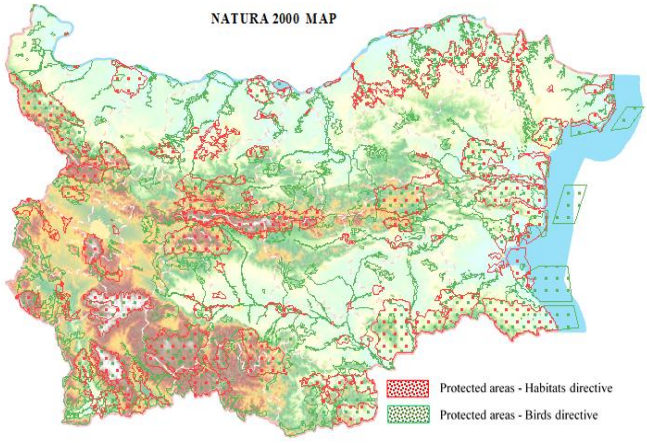

Fig. 2 *Protected sites by NATURA 2000 in Bulgaria*

The main birds' migration routes in Bulgaria are: *Via Balcanica*, *Via Aristotelis* and *Via Pontica*, which is the second largest migration route in Europe. *Via Pontica*, crosses the western Black Sea region via Bulgarian Black Sea coastline, entering up to 100km inland. Over 620 000 soaring birds traverse to South Africa via Bulgaria. Annually 78 % of the world population of white stork /*Ciconia ciconia*/, the whole Europe population of pink pelican */Pelecanus onocrotalus/* as well as 24 species threatened with extinction [12, 11]. The geographical migration regions division are presented on Fig. 3.

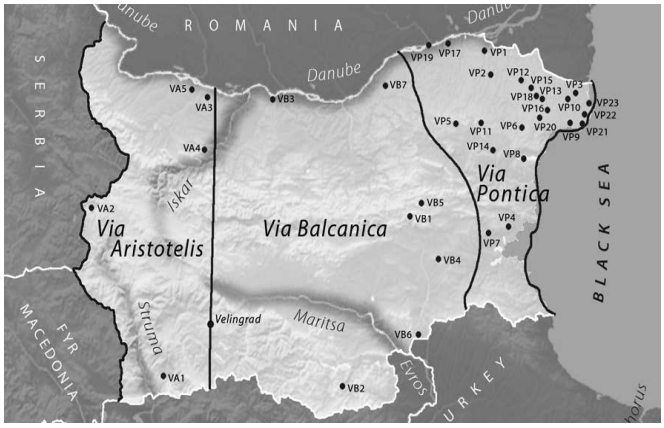

Fig.3 *Migration regions on the territory of Bulgaria with studied sites [10]*

In practice the interaction between WEP development and environment often results in land-use conflicts. The main reason is the territorial overlap between regions with high wind potential and high birds abundance.

For the period of 2003-2009 in Bulgaria 2840 applications for wind energy installations are presented in the Regional inspections of environment. 83 % of them are realized without evaluation of the environmental impact (EEI). [9, 2] Most of the applications are for single wind generators or for less than 7 wind generators in a farm which is used EEI to be avoided. This is one of the flaws which the Ministry of environment found in the procedures. Using this disadvantage some investors administratively "transforms" their large- scale project into small- scale projects [11, 10].

Till August 2015, 3233 are the applied wind generator investor intends only on the territory of Regional inspection for protection the environment – Varna. The realized intends are 401, 245 of which are located in protected zones [15]. Despite the EU court practice for not allowing disturbance of habitat or anxiety in OIP, in Bulgaria after its acceptance as a EU member state, construction of wind farms in IOP and in Kaliakra /Dobrudzha/ was allowed [11, 20].

The Ministry of Environment and Water already accepted some legislative prohibition and provisional restriction due to WEP permition for construction in some areas as Dobrudzha, East Rodophy maintain and Bourgas region purposing protection and minimizing the risk for sensitive to wind generators bird species. Temporal and permanent restrictions regarding WEPs construction are inforce for numerous individual NATURA sites, showed on figure 4 in purple. The blue markings corresponding to the areas with mean wind speed over 4m/s.

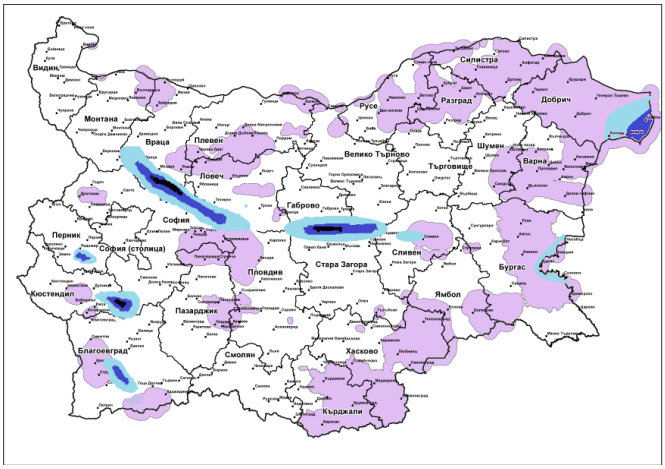

Fig. 4 *Map of restrictions on WEP construction terittories and wind potential map[11]*

The WEPs development is put in disadvantaged situation in Bulgaria by the legislative acts of this kind. At the same time the world practice without doubt proves that encouraging investors to introduce and implement environmentally responsible approach in WEP development is a step in the right direction.

4. Conclusion

The prosed set of criterion and classification does not claim to be exhaustive. It represents an open flexible system, applicable to wind energy projects development, supporting the decision makers in the initial phase of WEPs' potential location assessment and disposition selection. The differences of national legislative requirements regarding WEP development easily can be introduced to the proposed classification.

The implementation of so classified criterion offers to the practitioners a wider perspective allowing them to take into account the full scale of aspects regarding WEPs' disposition and to balance economic and environmental demands and sustainability of the project. The complex achievement of the set of criteria could be evaluated properly only as a dynamic equilibrium, taking into account the use and non-use value of the nature, vulnerability of the assets and the overall added value of project.

The creation of methodology for WEPs' location assessment, based on proposed set of criteria is a subject of team future work.

5. Literature

[1]. BirdLife International, 2003; SEO/BirdLife, 1995; BioSystems Analysis Inc. 1990, Orloff & Flannery 1992.

[2]. Bulgarian organization for birds protection, ornithological important place in Bulgaria (OIP), www.old.bspb.org/print_page.php?id=435&menu_id, 2001-2018;

[3]. BUNARCO, BirdLife International, 2009, p.35-36;

[4]. Damianov D, at all, "Fourth Industrial revolution – essence and problems", KNIG1, 2019;

[5]. Deshalm, 2002, Kahler, Komulative auswirtungen von Offshore windkraftnutzung und schiffsverkehr am beispiel der seetaucher in der deutchen bucht, pp 18-20;

[6]. Euro Lex- European Union laws, Directive 2009/28 EC at all, https://eur-lex.europa.eu/legal-content/EN/ALL/?uri=celex%3A32009L0028

[7]. International renewable energy agency. Renewable capacity statistic 2018, p24, https://www.irena.org/-/media/Files/IRENA/Agency/Publication/2018/Mar/IRENA_RE_Capacity_Statistics_2018.pdf

[8]. Madders, 2004, Chamberlian, Band collision risk model, p.221;

[9]. Michev, T., L. Profirov, K. Nyagolov, M. Dimitrov. 2011. Autumn Migration of Soaring Birds at Bourgas Bay, Bulgaria 1979-2003,British Birds, London, 1, pp 16-37;

[10]. Minchev T, at all., "Migration of soaring birds via Bulgaria", Acta Zooloica Bulgaria, March 2012,

[11]. Ministry of environment and water, 2013 Report of the sensitive birds zone". http://natura2000.moew.government.bg/PublicDownloads/Auto/OtherDoc/276299/276299_Birds_120.pdf

[12]. Ministry of environment and water, Regional inspection of environment and water, Appendix 1 to the law of protecting the environment;

[13]. Ministry of regional development, Regulation 14;

[14]. Newton, A. 2012, The coastal syndromes and hotspots on the coast, p 225;

[15]. Regional inspection of environment and water, data under the law for access to information „Processed wind generators on the territory of RIEW Varna for the period 2003-2015г.

[16]. Toneva D, Stankova T, 2017 Wind energy projects' environmental impact. Sustainable development 3/2017, pp.31-35

[17]. Toneva D, Stankova T., Development of wind energy projects in Bulgaria- challenges and opportunities. In proceedings International conference Applied Computer Technologies. Macedonia, proceeding 1-2018, pp.60-63

[18]. Von Heijnis 1980, Effects on find farm on birds, p.26

[19]. Yankov P. at all, 2007. Atlas of the nesting birds in Bulgaria

[20]. Zehnde, S.& Karllson, L. 2001, Denmark, Remote techniques for counting and estimating the number of birds-wind turbine collisions,p.11;

CERAMIC BEEHIVE - CONCEPTUAL PAPER

eng.ec. Lepkova, T., eng.Martinova, I., Martinova G., Marinova, I., eng.Pincheva, B.
INOVATIONTECH LtD, Bulgaria
rosbul@abv.bg

Abstract: *The present article is a conceptual paper which aims to be a foundation for future experimental work. The conceptual work discusses different aspects of a new utility model – a ceramic beehive. The evidences are based on theoretical models based on the optimal living conditions of the bee family and the specifics of the changing external environment. Along with these factors are considered the ceramic properties and the relevance of the ceramic material as a construction material for the brood (the beehive body). In order to reach the aim of the paper are used the following empiric and non-empiric methods: literature review, expert evaluation, experiment. The results from the study confirm the conceptual model and reason the hypnotized properties of the experimental model for optimization of the living conditions of the bee family. This is supported by evidences in increasing of the honey production in the ceramic beehive.*
Keywords: *CERAMIC, BEEHIVE, CERAMIC BEEHIVE*

Introduction

The importance of the honey bees for the nature of our planet is indisputable- their presence is vital as pollinators (Aslan, Liang, Galindo, Kimberly, & Topete, 2016) of the agro ecosystems, ensuring the productivity and stability in nature (Rogers, Tarpy, & Burrack, 2014), having great importance for national and world economy (Rucker, Thurman, & Burgett, 2012; Southwick & Southwick, 1992) as whole industries benefit and exist due to the bees and their products- agriculture, beekeepers economic sector, the market of honeybee products, cosmetics, pharmacy, etc.

During the last 10 years an alarming event is observed and reported in many North American and European countries- colony loses and the so called "Colony Disease Disorder" (CDD). CDD is associated with complete absence of the colony with no dead bees in/around the colony; presence of capped brood; presence of food stores that are not robbed by other bees or typical colony pets (Ellis, Evans, & Pettis, 2010). The collapsing (weakening) of the colonies can be due to 1. An insufficient number of bees to maintain the amount of brood in the hive; 2. The workforce is composed largely of younger adult bees; the queen is present; 3. The cluster of bees is reluctant to consume food provided to them by the beekeeper. Although the event is not new in the nature, recently its size is going much beyond the normal. Other disturbing facts are concerning increased loses and lethality which can be caused by different factors most commonly connected to bee pathogens and parasites (Genersch, 2010; McMenamin & Genersch, 2015), chemical usage (Gashout, Goodwin, & Guzman-Novoa, 2018), chronic sublethal stress (Bryden, Gill, Mitton, Raine, & Jansen, 2013), etc.

In order to be ready to face the problem, countries like the USA are allocating huge amounts of money for forming ”consortium of investigators working in a coordinated manner to reduce institutional redundancy and optimize the discovery and delivery of sustainable bee management practices”. (Pettis & Delaplane, 2010). This common world problem should attract the attention not only of the academic society but also to the industries and policy makers to join efforts towards finding solution of this problem which is of global importance.

The present paper aims to offer a possible solution matching the reasons for the managed bees loss and the CCD with some specific properties of the baked clay materials. We find it reasonable to explore the potential for a beehive constructed dominantly from ceramic to be a technical solution for improving the living conditions of the managed honey bees. The motivations behind the present study are multidimensional.

The idea for using clay as construction material for beehive is not a new one and we assume that its applicability is already historically proven. There are existing evidences dated back to 2450 BCE when the Egyptians had developed sophisticated apiculture for beekeeping in clay hives which later had spread throughout the Mediterranean (Kritsky, 2017) The continued usage of the clay beehives is evidenced from remainings from the Iron age at the lands of Jordan Valley (Mazar, Namdar, Panitz-Cohen, Neumann, & Weiner, 2008) to different periods from the human history (Francis, 2009) (Harissis & Mavrofridis, 2012; Taxel, 2006).

Combining the example of our ancestors with the trends and development of the technologies in clay processing, theoretically justifies the idea of producing an advanced model of contemporary ceramic beehive. The main reasons for this are in the specific advantages of the ceramic in comparison with the traditionally used for beehive production wooden material. Here we will highlight some of these advantages which we consider as most important.

RH, %	Wood MC (Weight %)	Face Brick MC (Weight %)
50	~9	0.02
80	16	0.09
90	20	0.19
95	24	0.38
100	29+	4.3
100	n/a	5–7

Table 1 Table 1 Correlation of Relative Humidity, Wood Moisture Content, and Brick Moisture Content

Firstly, from technical point of view, one of the most important properties of clay is that when it is baked at high temperatures (over 950 ° C), it is irreversibly transformed into a solid stone-like body that has high strength, fire resistance and low water absorption. What is more, the backed clay is a pore "breathing" structure with high frost durability(Hansen & Kung, 1988) and is performing better in terms of water retain (table 1) which is important when considering the fact that the increased humidity and moisture content of the material are predispositions for bacteria and other microorganisms occurrence in the beehive. This would make the conceptualized ceramic beehive model especially useful for geographical regions characterized with extreme temperatures, high temperature amplitudes between the seasons as well as places with higher risk of fires or windy areas (the relative higher weight of the ceramic lowers the risk of sweeping) which cause serious material damages to the beekeepers. Because of the properties of the baked clay and its relatively higher endurance in terms of physico-mechanical and operational properties, a ceramic beehive is expected to be able to provide an optimal solution for unfavorable environmental conditions both for the bees and the beekeepers.

Additionally, the endurance of the ceramic materials in their solid baked form does not require any successive treatment as it is in the case of the wood materials. The wooden beehives require regular treatment with wood preservatives which affect the quality

of living of the bees as well as the quality of the bee products. Authors who worked on the topic argue that the wood preservatives such as chromated copper arsenate, tributyltin oxide, pentachlorophenol are associated with winter losses of colonies (Johnson, 2015; Kalnins & Detroy, 1984) and increased arsenic content in the products. Wood materials have relatively short life cycle in comparison with the bricks. With the time, the wear resistance of the wooden materials decrease and wood declay process takes place due to the wood-inhabiting bacteria and the actinomycetes (Clausen, 1996; Johnston, Boddy, & Weightman, 2016). The process causes effects on the level of hygiene within the beehives well. In this respect, the ceramic beehive is a more hygienic material which does not favor the development of bacteria, it is rot–proof, impermeable, non–absorbent, insulating and easy to clean and disinfect. Usage of ceramic material has also an environmental advantage as the production of ceramic beehives is not connected with cutting trees.

Considering all the above mentioned we assume that there are enough evidences to hypotize that a ceramic beehive would find a good application in the beekeeping industry providing better conditions for the bees and assuring better quality of the bee products.

Methods

In order to reach the aim of the study, is used a complex of non-empirical and empirical methods such as theoretical analysis, expert evaluation, experiment. The expert evaluation has been conducted in two stages - before and after construction design of a model of the conceptualized beehive. The expert evaluation aimed to gather experts who work in different fields connected to beekeeping (beehive production, beekeepers experts, academicians and researchers, constructors) in order to critically evaluate the idea and generate guidelines for the production of the first experimental model. The first experts' evaluation meeting took place in the spring of 2012. Following the production of the first experimental model, another experts evaluation took place in order to discuss practical aspects of the design, construction and production process. In 2014 starts the consequent process of inhabitation of the experimental model with bee families. The beehives are constantly observed and improvements of the construction of the beehive has been done in timely manner. The last upgraded version of the model has been inhabited in 2017.

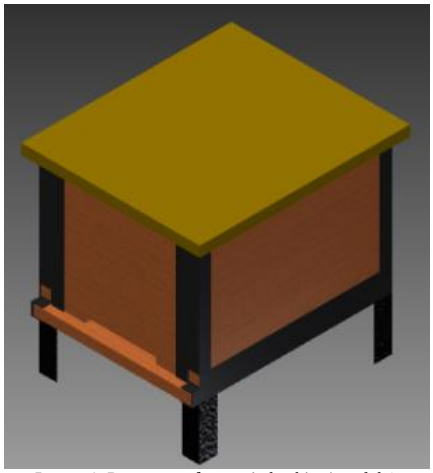

Image 1 *Prototype of ceramic beehive/ model 1*

Results and discussion

The first experts' analysis of the idea gives ground for development of the first utility model. The assumed benefits and advantages of the ceramic beehive have been confirmed by the experts. It was agreed that at this stage of the model development it is most appropriate to be designed and produced only the body (brood) and the top cap as it is the place where the queen lives and where the bees are during the winter season. The construction of the hive consists of ceramic plates and supporting metal structure as it is shown on image 1. The sizes of the design of the prototype is in full compliance with the standard for Langstroth hives enabling the usage of the standard wooden boxes above. The choice of Langstroth standard is not done randomly but because it is the most common used beehive in Bulgaria.

The realization and implementation of the idea has been discussed at the second expert evaluation meeting when advantages and disadvantages of the result has been analyzed. It was concluded that the main disadvantage is the weight of the body so lightening of the construction has been recommended. This led to research and development of new technological solutions ending up with design and production technology of ceramic plates with 66,66 % cavity (image 2). Apart from lightening the construction, the new single plates provide better isolation within the box because of the airbags (the inner part of the plate is filled with air) which ensures better living conditions and optimal temperature, significantly reducing the work of the bees in providing better living conditions.

Image 2 *Ceramic plate with increased cavity*

Along with the utility model has been developed the technology for production of the plates as currently there are model equipment for producing of different types of plates as show in table 2.

Table 2 Specification of the models for production of plates

Size [mm]	**Cavity [%]**	**Water saturation [%]**	**Compressive strength [MPa/ kg/cm^2]**	**Weight [kg]**
310 x 375 x 25	66.66	<10%	28 / 2800	2.900
310 x 500 x 25	66.66	<10%	28 / 2800	3.800
260 x 500 x 25	66.66	<10%	28 / 2800	3.000
260 x 375 x 25	66.66	<10%	28 / 2800	2.600

Image 3 *Ceramic beehives, improved experimental model*

Following the recommended modifications, 14 beehives have been produced and put in natural conditions with bees inhabited in apiaries in different geographical regions. The beekeepers who participated in the experiment were asked to observe the bees' behavior and to report problems and impressions they have from the exploitation of the experimental model. From all the beekeepers feedback has been collected. During the experiment, in summer periods in two of the apiaries occurred fire. In both places the only remaining hive from the burning beehives is the experimental ceramic one. The last report on the results of the usage of the ceramic beehive is from the autumn of 2018 when the beekeepers report 30% increase in the honey production in comparison with the production in the wooden hives. For none of the ceramic hives is reported bee loss or CDD.

Conclusions

The results obtained from the research confirm the conceptual model and reasons the hypnotized properties of the experimental model for optimization of the conditions for life of the bee's family. The idea has been registered as utility model in the Patent Office of Republic of Bulgaria with application number 2412/14.05.2013. Further experimental work is recommended in order to be laboratory tested the qualities of the honey produced in the ceramic beehive as it is assumed that the optimized internal conditions may also have effect not only to the quantity but also to the quality of the bee products.

References

Aslan, C. E., Liang, C. T., Galindo, B., Kimberly, H., & Topete, W. (2016). The Role of Honey Bees as Pollinators in Natural Areas. *Natural Areas Journal*, *36*(4), 478–488. https://doi.org/10.3375/043.036.0413

Bryden, J., Gill, R. J., Mitton, R. A. A., Raine, N. E., & Jansen, V. A. A. (2013). Chronic sublethal stress causes bee colony failure. *Ecology Letters*, *16*(12), 1463–1469. https://doi.org/10.1111/ele.12188

Clausen, C. A. (1996). Bacterial associations with decaying wood: a review. *International Biodeterioration & Biodegradation*, *37*(1), 101–107. https://doi.org/10.1016/0964-8305(95)00109-3

Ellis, J. D., Evans, J. D., & Pettis, J. (2010). Colony losses, managed colony population decline, and Colony Collapse Disorder in the United States. *Journal of Apicultural Research*, *49*(1), 134–136. https://doi.org/10.3896/IBRA.1.49.1.30

Francis, J. (2009). Ancient Ceramic Beekeeping Equipment at the University of Ottawa. *Mouseion: Journal of the Classical Association of Canada*, *9*(2), 159–170. https://doi.org/10.1353/mou.2009.0004

Gashout, H. A., Goodwin, P. H., & Guzman-Novoa, E. (2018). Lethality of synthetic and natural acaricides to worker honey bees (Apis mellifera) and their impact on the expression of health and detoxification-related genes. *Environmental Science and Pollution Research International*, *25*(34), 34730–34739. https://doi.org/10.1007/s11356-018-3205-6

Genersch, E. (2010). Honey bee pathology: current threats to honey bees and beekeeping. *Applied Microbiology and Biotechnology*, *87*(1), 87–97. https://doi.org/10.1007/s00253-010-2573-8

Hansen, W., & Kung, J. H. (1988). Pore structure and frost durability of clay bricks. *Materials and Structures*, *21*(6), 443–447. https://doi.org/10.1007/BF02472325

Harissis, H. V., & Mavrofridis, G. (2012). A 17th Century Testimony On The Use Of Ceramic Top-bar Hives. *Bee World*, *89*(3), 56–58. https://doi.org/10.1080/0005772X.2012.11417481

Johnson, R. M. (2015). Honey Bee Toxicology. *Annual Review of Entomology*, *60*(1), 415–434. https://doi.org/10.1146/annurev-ento-011613-162005

Johnston, S. R., Boddy, L., & Weightman, A. J. (2016). Bacteria in decomposing wood and their interactions with wood-decay fungi. *FEMS Microbiology Ecology*, *92*(11). https://doi.org/10.1093/femsec/fiw179

Kalnins, M. A., & Detroy, B. F. (1984). The effect of wood preservative treatment of beehives on honey bees and hive products. *Journal of Agricultural and Food Chemistry*, *32*(5), 1176–1180. https://doi.org/10.1021/jf00125a060

Kritsky, G. (2017). Beekeeping from Antiquity Through the Middle Ages. *Annual Review of Entomology*, *62*(1), 249–264. https://doi.org/10.1146/annurev-ento-031616-035115

Mazar, A., Namdar, D., Panitz-Cohen, N., Neumann, R., & Weiner, S. (2008). Iron Age beehives at Tel Reḥov in the Jordan valley. *Antiquity*, *82*(317), 629–639. https://doi.org/10.1017/S0003598X00097271

McMenamin, A. J., & Genersch, E. (2015). Honey bee colony losses and associated viruses. *Current Opinion in Insect Science*, *8*, 121–129. https://doi.org/10.1016/j.cois.2015.01.015

Pettis, J. S., & Delaplane, K. S. (2010). Coordinated responses to honey bee decline in the USA. *Apidologie*, *41*(3), 256–263. https://doi.org/10.1051/apido/2010013

Rucker, R. R., Thurman, W. N., & Burgett, M. (2012). Honey Bee Pollination Markets and the Internalization of Reciprocal Benefits. *American Journal of Agricultural Economics*, *94*(4), 956–977. https://doi.org/10.1093/ajae/aas031

Southwick, E. E., & Southwick, L. (1992). Estimating the Economic Value of Honey Bees (Hymenoptera: Apidae) as Agricultural Pollinators in the United States. *Journal of Economic Entomology*, *85*(3), 621–633. https://doi.org/10.1093/jee/85.3.621

Taxel, I. (2006). Ceramic Evidence for Beekeeping in Palestine in the Mamluk and Ottoman Periods. *Levant*, *38*(1), 203–212. https://doi.org/10.1179/lev.2006.38.1.203

Ueno, Kohta & Straube, John & VanStraaten, Randy. (2013). Field Monitoring and Simulation of a Historic Mass Masonry Building Retrofitted with Interior Insulation.

SOME OF THE INOVATIONS APPROCHES IN PLASTIC INJECTION MOULDING TECHNOLOGY

НЯКОИ ИНОВАТИВНИ ПОДХОДИ В ТЕХНОЛОГИЯТА ЗА ЛЕЕНЕ ПОД НАЛЯГАНЕ

Kichukov I. I*; Assos. Prof. Atanasov A. L. PhD.**
National Military University „VasilLevski", Faculty of „Artillery, air defense and CIS", Shumen, Republic of Bulgaria
*iliankichukov@gmail.com

Abstract*: In today's fast changing world it is crucial for businesses to stay in touch with the latest developments in the processing technologies in order to remain competitive on the market. The paper reviews the most recent innovations in plastic injection molding technologies. Their pros and cons and their possible impact on manufactured materials. And how these processes improve the design, function of products, automatically, and cost effectively.Furthermore, the paper researches the application of the injection-moulded products in our everyday lives.*

KEYWORDS: PLASTIC INJECTION MOULDING,INJECTION MOULDING INNOVATIONS, INJECTION MOULDING TECHNOLOGY.

1. Introduction

The injection molding industry is always changing as new technology, materials, and techniques are introduced. There are a number of new changing technologies that are reshaping injection moulding as a whole. While some of these technologies may still be unproven long due to the fact that they are new and unproven they all have the potential to become standardas operating procedures in the future. In modern world, daily, a lot of companies and users communicate and exchange generally accessible and confidential information via the Internet [7].

Injection moulding is one of the chief processes for producing plastic items. It is a fast process that can deliver a large numbers of identical items - from high precision engineering components to small disposable consumer goods.

The use of this process has enabled the extension of boundaries of design in plastics, and also helped in the substitution of conventional materials, thereby reducing the weight of the end product and providing immense design freedom.

Here are a few plastic injection molding industry trends to keep an eye on:

2. Exposure

2.1.Companies involved in injection moulding

Ferromatik Milacron GmbH, Malterdingen, Germany develops, manufactures, and sells injection molding machines. The latest creation is the modular F-Series, which can be configured as an all-electric, hydraulic, or hybrid machine. The company is a part of the American Milacron group;

KraussMaffei is one of the world's leading manufacturers of injection moulding machinery. The injection moulding machine ranges provided by the German company are AX series, CX series, CX-ClassiX, EX series, GX series, MX series, and C3 series;

Sumitomo (SHI) Demag Plastics Machinery GmbH, Schwaig/Germany, is a Japanese-German company dealing with the manufacturing of injection moulding machines. They provide all-electric, hydraulic and hybrid injection moulding machines with clamping forces of between 180 and 20,000 kN;

German company, Arburg is one of the world's leading manufacturers of high-end injection moulding machines for plastics processing. They cater to industries such as electronics, packaging, automotive, medical/optical, and many others as well;

AIM Plastics caters to the wide range of sectors including healthcare/medical, electrical / electronic, automotive/auto aftermarket , commercial/consumer, aerospace/defense, and action sports. They are located in Michigan, USA.

SUSTAINABILITY

Protecting the environment has gone from an individual goal to a big business mission. Companies that can show they use eco-friendly practices and materials are likely to get business over those that don't. During 2018, the injection molding industry is expected to move more towards environmental-friendly approaches. For example, new equipment uses as much as 50% less power than devices introduced less than ten years ago. The amount of scrap plastic has been reduced or has been recycled, decreasing the amount of waste.

Another eco-friendly option that is becoming more and more popular is bio-plastics. This type of plastic is created from biodegradable plants such as corn, soybeans, and flax. This decreases the need to use fossil fuels and creates plastics that without taking years to break down.

METAL TO PLASTIC CONVERSION

More manufacturers are considered changing metal parts and products to plastic, leading to growth in the injection molding industry. While the idea of metal to plastic conversion has been around for quite some time, some companies have never considered it as a viable solution. They often will have the idea that metal is superior to plastic, but that's not always the case thanks to new materials and mixing processes. Today's plastic can be stronger, lighter in weight, and more flexible in design.

While some items may always need to be made from metal, the excuse of "it's always been made this way" is becoming less and less of a reason to put off switching to plastic parts.

AUTOMATION

Many industries have begun moving towards automation. The ability to bring in a machine that can work around the clock and always perform repeatable actions is invaluable. The injection molding industry is expected to greatly ramp up its deployment of automated systems in 2018 now that the accuracy, speed, and flexibility of these machines have increased. Additionally, automation used to have a hefty price tag but with new advancements, deploying an automation solution is now more affordable than ever.

By allowing human employees to focus on tasks that require creativity or personal touch, automated machines will let companies better allocate their resources. The need for skilled employees is still present; in fact, new employees will likely need to be hired to help program and maintain these automated systems.

NEARSHORING

Nearshoring is the concept of outsourcing work to within the United States. Outsourcing to companies in Asia is understood to

help lower costs in production, materials, and labor, but it can have many hidden costs. It also dramatically impacts the timetable, potentially adding weeks to the schedule. Companies that require fast turnaround simply can't afford that.

Faster turnaround times also makes it easier to have a tighter reign on production and quality. If a production run contains a defect, the steps needed to fix the mistake are within reach and can be caught early on. Nearshoring reduces the amount of time it takes to receive the product while still letting companies take advantage of lower costs.

DESIGN FOR MANUFACTURABILITY

The concept of design for manufacturability is another solution that has been around for some time but is becoming increasingly popular across the industry. Designing parts for manufacturability includes:

- Material consideration;
- Gate location;
- Material shrinkage;
- Part rigidness;
- Draft.

Utilizing a successful DFM strategy makes it possible to reduce the amount of time needed for testing and the number of overall errors. By working closely with customers during this phase, companies can improve their processing time and their relations with clients as well as engineer out cost and potential failure modes.

PRECISION MOLDING

Precision molding is the current trend used to address manufacturing challenges. It allows engineers to quickly address production issues using advanced tools that can:

- Simulate mold flow;
- Monitor the injection process;
- Make changes to the process in real-time;
- Send alerts during a malfunction;
- Program machines to alarm when operation outside tolerances.

MOVING FORWARD

While some industry trends die off as quickly as they catch on, many anticipate that concepts are here to stay. As outlined earlier, advancements such as automation, nearshoring, and sustainability, aren't limited to the injection molding industry. They're growing trends seen in many areas and are expected to continue to grow. Those that are more focused on injection molding, including precision molding, design for manufacturing, and moving from metal to plastic, are less popular pieces of technology and more strong concepts that are likely to become the industry norm.

In need of an injection molding partner that understands trends and is quick to adopt those that have proven themselves? New Berlin Plastics makes use of today's most effective injection molding trends to provide customers with high quality, affordable plastic parts. Contact us today to learn more about how we can help you meet your needs.

2.2. Innovations in injection moulding technology

Multi-component injection moulding combines different materials or dyes to produce high-quality plastic parts [1]. This process improves the design and function of products, automatically and cost effectively [1]. Multiple component injection technologies - Under the spectrum of multiple component injection technologies are the sandwich technologies. Sandwich technologies comprise co-injection, mono-sandwich, gas injection technique (GIT) and water injection technique (WIT)[2]. In the co-injection method, two melts are injected into the machine's cavity through one gate [3], one after the other. In mono-sandwich method, two materials are injected with one injection unit via one passage into the cavity. In GIT, the gas used is mostly nitrogen, which is injected into the part to replace the melt in the core and create a hollow space. GIT enables production of parts with high wall-thicknesses and/or material accumulations. It provides increased strength and stiffness at lower or equal part weight. It enables reduction of weight up to 50% [3] and decreasing of the material costs. Likewise it enables reduction of the cooling/cycle time up to 50%,[3] lowers clamp force and machine costs. GIT enables less sink marks, parts with less distortion, and improved part quality. In WIT, there are two processes - the short-shot process and the full shot process. In the short shot process, high speed shooting is required during the filling process in a transparent tool. Many consider WIT to have relatively more advantages than the GIT. WIT provides lesser cycle times, smaller and constant wall thickness with less warpage, large part diameters, and smoother inner surfaces. Additionally, water is cheaper than gas and is incompressible.

Micro injection moulding - To produce very small components using the injection moulding process requires maximum possible accuracy and precision. The core of the processing of plastics of minimal size is the micro injection unit. Sumitomo (SHI) Demage is one such company that caters to the field of miniaturisation by providing customized plastification systems for shot weights of 5 to 0.1 g. their micro injection unit can be integrated in any standard machine for a clamping force up to 500 kN [4].In order for very small components to be produced in the injection moulding process maximum possible accuracy and precision are requiered. From the material and machine to the mould, everything must be streamlined to this objective. Especially in the field of miniaturisation, many interesting developments are gaining ground [4]. Be it minimal connectors for use in automobile engineering, ball bearing retainers for use in nano-mechanics or micro pipettes in medical technology or biotechnology [4].

Modern day injection moulding machines are controlled by a built-in computer. The computer controls all the actions of the machine based on sensor fed information, thereby ensuring consistent output and shot to shot quality. Most of these machines also imply sophisticated smart microcontrollers and sensors to ensure high quality products.

Dual-Shot Injection Moulding.'Two-Shot' injection moulding or dual-shot injection moulding is a method to produce simple to complex parts comprising two different polymers even with two different colours during one machine cycle.

The 'Two-Shot' mould consists of two separate cavities that are used for making a single part. The first step in the process is to create a substrate in the first cavity, which receives material from one of the two injection units. The tool then opens to allow for a 180° rotation to a secondary position after the finished part is removed from the second stage cavity [5]. As the tool closes, the second step commences by positioning the previously molded substrate into the second cavity. The second cavity receives the material from the second injection unit completing a finished part, this occurs simultaneously as the substrate for another part is being molded.When the tool opens again, the finished part is ejected, and another substrate is ready to receive its over-mold. Therefore, by applying alternating rotary motion of the tool, this simultaneous process enables continuous manufacturing operation.

The key benefits of the 'Two-Shot' injection moulding are as follows:

- Soft touch features and multi-color on handles, grips, devices, enclosures, and other components
- Back-lit buttons, dials and other instrumentation products
- Noise/vibration dampening and isolation
- Air/water seal
- Shock absorption and protection
- Movable segments or components such as living hinges and spring type mechanisms

Precision injection molding.Precision injection molding utilizes internal pressure sensors and state-of-the-art BDE and MDE technology produces high quality models with our one or two-component precision injection molded parts.

3. Conclusion

In conclusion, this paper explored different innovations in injection moulding technology. Innovations such as Multi-component injection moulding, Micro injection moulding , Modern day injection moulding machines and Dual-Shot Injection mouldingprocesesresultsinbetterquality detailsat a lowercost. With the facilities having the expertisenecessary to produce highlysophisticated systems and materials. The use of robotics for production of high volume swith automation-friendlya ssemblies drastically lowers the cost of manufactured products. These innovation prove to be very helpful and are improving the quality and cost of the injection moulding process which therefore attract new investors.

4. Sources:

1. https://www.arburg.com/products-and-services/injection-moulding/processes/multi-component-injection-moulding/.
2. https://akro-plastic.com/process-and-technology/fluid-injection-technique-fit/wit/
3. https://www.m-ep.co.jp/en/pdf/product/novaduran/molding.pdf
4. https://uk.sumitomo-shi-demag.eu/processes/micro-injection-moulding.html
5. https://www.ptonline.com/columns/two-shot-molding-and-tool-design
6. http://www.bpf.co.uk/plastipedia/processes/injection_moulding.aspx
7. Stoyanova, V., Steganography System that uses the LSB method of embedding information in images, Defense Technology forum 2015, Shumen, pp.186-193, ISSN 2367-7902, http://www.aadcf.nvu.bg/scientific_events/papers/NS_2015.pdf

СТЕГАНОГРАФСКИ АЛГОРИТЪМ ОТЧИТАЩ РАЗЛИКИТЕ МЕЖДУ ПИКСЕЛИТЕ НА КОМПРЕСИРАНИ ИЗОБРАЖЕНИЯ

STEGANOGRAPHIC ALGORITHM READING THE DIFFERENCES BETWEEN THE PIXELS OF COMPRESSED IMAGES

Стоянова В.[1], Талев Д. [2] , Лилов И.
[1,2] НВУ „Васил Левски“, факултет „А, ПВО и КИС“- Шумен, България

veselka_tr@abv.bg, lfs_13@abv.bg

Abstract: *Steganography can be defined as a method of hiding data within a cover media so that other individuals fail to realize their existence. Steganographic systems play a vital role in covertly transmission of information even in the presence of an arbiter. The difference in the pixel values can be used for hiding the information. To enlarge the capacity of the hidden secret information and to provide an imperceptible stego-image for human vision, a novel steganographic approach using five pixel pair differencing (FPPD) is proposed in this paper. Experimental results shows that the proposed algorithm provides increased capacity of message hiding along with better quality of stego images.*

Keywords: STEGANOGRAPHY, DATA HIDING, HIDDEN CAPACITY, PVD, FPPD, PSNR

1. Въведение.

Благодарение на бързото развитие на съвременната технология за компютри и комуникация, предаването на съобщения става бързо и удобно. За да се предпази тайната информация от кражба по време на предаването, увреждане или друго събитие, широко се използват техниките на стеганографията. Стеганографията реализира скриване на информация, така че да не се забелязва този факт. Съобщението може да бъде скрито в изображения [1], аудио файлове или в текст [2], [3]. Тя дори е начин за предаване на информация между различни групировки с опасни за националната сигурност идеи [8].

Един прост и добре познат подход е директното скриване на тайна информация в най-младшия бит (least-significant bit, LSB) на всеки пиксел в изображението. Алгоритмите използващи този метод обикновено директно вмъкват малка част от тайното съобщение в LSB на всеки пиксел на изображението в пространствената област.

.2. Обзор.

Националната сигурност е важен приоритет и заплахите свързани с бежанската вълна мога да се придадат и с помощта на тайна комуникациПри метода на разликата в стойностите на пикселите се изчислява разликата в стойностите на пикселите между два последователни пиксела. Разликата в стойността се използва за скриване на тайното съобщение. Тя се сравнява с битовете на тайното съобщение, които трябва да бъдат скрити. Ако те са неравномерни, тогава двата последователни пиксела се регулират директно, така че тяхната различна стойност да може да съответства на тайните данни.

Значителното изкривяване на стегоизображението може да се случи, когато методът (pixel value difference, PVD) регулира двата последователни пиксела, за да се скрие тайната информация в стойността на разликата.

При сравнение с LSB метода може да се твърди, че повече данни могат да бъдат скрити чрез използване на PVD метода. Приети са две характеристики за оценка на криенето от стеганографските техники. Първата е капацитетът на скритите данни, а другият е незабележимостта на стегоизображението, наричано още качеството на стегоизображението. Методът за диференциране на пикселите (PVD), предложен от Wu и Tsai, може успешно да осигури, както високо ниво на вграждане, така и изключителна незабележимост за стегоизображенията.

В метода PVD два последователни по хоризонталата пиксела могат да представляват само вертикален стълб, който може да има различни посоки. Това мотивира да се подобри методът PVD, като се разгледат и анализират способностите в [4], [5].

При метода (tri pixel value difference, TPVD) данните могат да бъдат скрити във вертикални и диагонални стълбове от пиксели, заедно с хоризонталните такива. Целият метод е описан както следва в [4] и [7]. Разделя се изображението на блокове от *2x2* пиксела. Промяната на стойностите на пикселите за четвъртата пикселна двойка засяга първата и втората двойки, четвъртата двойка е безполезна и трябва да бъде премахната. Следователно само три двойки могат да бъдат използвани за вграждане на тайните данни.

Всеки *2x2* блок включва четири пиксела от $P_{(x,\ y)}$, $P_{(x+1,\ y)}$, $P_{(x,y+1)}$ и $P_{(x+1,\ y+1)}$, където x и y са местоположението на съответния пиксел в изображението. Ако приемем, че пиксел $P_{(x,y)}$ е начална точка, трите двойки пиксели могат да бъдат образувани чрез групиране на $P_{(x,\ y)}$. Тези три двойки се обозначават с P_0, P_1 и P_2, където съответно $P_0 =(P_{(x,\ y)}, P_{(x\ +\ 1,\ y)})$, $P_1=(P_{(x,\ y),}\ P_{(x,\ y\ +\ 1)})$ и $P_2=(P_{(x,\ y)}, P_{(x+1,y+1)})$.

За всяка двойка се получава стойност на разликата d_i. Блокът с малка стойност на d_i се намира в равномерна област, докато блок с голяма стойност на d_i се разглежда като блок с рязко различие. Според свойствата на човешкото зрение, очите могат да понасят повече промени в рязко различаващия се блок, отколкото в равномерния блок.

Когато се използва този метод за вграждане на тайна информация, стойностите на двата пиксела във всяка двойка се променят и се изчислява новата стойност на разликата за всяка двойка d_i, като за $i = 0,1,2$ [4]. Новите стойности на пикселите във всяка двойка са различни от оригиналните. Това означава, че ще се получават три различни стойности за първоначалния пиксел $P_{(x,\ y)}$, $P_0^{'}$, $P_1^{'}$, $P_2^{'}$, които съответстват на P_0, P_1 и P_2.

Въпреки това, само една стойност за първоначалния пиксел $P_{(x,\ y)}$ може да съществува след приключване на процедурите за вграждане. Следователно, една от P_i двойките е избрана като отправна точка за компенсиране на другите две стойности на пиксела. Това означава, че две пикселни стойности от една двойка се използват за регулиране на другите две двойки за изграждане на нов *2x2* блок. Вградената тайна информация не се променя, тъй като стойностите на разликата за три двойки пиксели са непроменени [4], [7].

В [7] е предложена стеганографска система за сигурност на изображението, използвайки увеличаване на скоростта на вграждане. Системата инициализира някои параметри, които се използват за последваща обработка на данни и области, след което изчислява капацитета на тези избрани области. Ако областите са достатъчно големи, за да скриете дадено тайно съобщение, тогава скриването му се извършва в избраните области. И накрая, се прави последваща обработка, за да се получи стегоизображението. В противен случай схемата трябва да преработи параметрите и след това да повтори избора на област и оценка на капацитета, докато съобщението не се вгради напълно. При извличане на данни схемата първо извлича страничната информация от стегоизображението. Въз основа на страничната информация, се прави предварителна обработка и идентифициране на областите, които са били използвани за скриване на данни. И накрая, се получава тайното съобщение според съответния алгоритъм за извличане. Абсолютната разлика между два съседни пиксела е като критерий за избор на област и LSBMR като алгоритъм за скриване на данни. Текущото състояние и ключовите въпроси, свързани с различни стеганографски техники за изображение в сивата скала/пространствената област, са описани в [6].

3. Предложената система - метод пет пикселни двойки (Five Pixel Pair Differencing, FPPD)

Въз основа на метода TPVD е предложен метод FPPD за увеличаване на капацитета на скриване на информация и поддържане на сходството в прикриващо изображението и стегоизображението.

Това се осъществява чрез разделяне на прикриващото изображение на *3x2* блока от пиксели, като трябва да се отбележи, че то е сиво. Предложено е пет двойки пиксели да бъдат използвани за вграждане на тайната информация. Преди въвеждането на предложения алгоритъм е необходима предварителна обработка, за да се раздели прикриващо изображението на нивото на сивото в оригинала и да е 3*x2* блока с 6 пиксела, както е показано на фигура 1.

PX0	PX1	PX2
$P_{(x,y)}$	$P_{(x+1,\ y)}$	$P_{(x+2,\ y)}$
PX3	PX4	PX5
$P_{(x,y+1)}$	$P_{(x+1,y+1)}$	$P_{(x+2,\ y+1)}$

***Фиг.1. Б**лок от пиксели*

Както е показано на фигура 1, всеки *3x2* блок включва шест пиксела $P_{(x,y)}$, $P_{(x+1,y)}$, $P_{(x+2,y)}$, $P_{(x,y+1)}$, $P_{(x+1,y+1)}$ и $P_{(x+2,y+1)}$, където *x* и *y* са местоположението на пиксела в изображението. Нека $P_{(x,y)}$ е началната точка, след което пет пикселни двойки могат да се образуват като $P_0=(P_{(x,y)}, P_{(x+1,y)})$, $P_1=(P_{(x,y)}, P_{(x+2,y)})$, $P_2=(P_{(x,y)}, P_{(x,y+1)})$, $P_3=(P_{(x,y)}, P_{(x+1,y+1)})$ и $P_4=(P_{(x,y)}, P_{(x+1,y+2)})$.

Когато се използва предложеният FPPD метод за вграждане на тайна информация, всяка двойка пиксели се модифицира като ($P_i^{'}$) и се изчислява нова стойност $d_i^{'}$ за *i=0,1,2,3,4*, където $d_i^{'}$ варира от 0 до 255. Затова е проектирана диапазонна таблица *R*, с *n* съседни обхвата и диапазонът на таблиците е от 0 до 255.

Новите стойности на пикселите във всяка двойка са различни от оригиналните им. Това означава, че пет различни стойности са получени, а именно $P_0^{'}$, $P_1^{'}$, $P_2^{'}$, $P_3^{'}$ и $P_4^{'}$, съответно от P_0, P_1, P_2, P_3, и P_4. Един от $P_i^{'}$, е избран като отправна точка за компенсиране на другите стойности на пикселите. Това означава, че две пикселни стойности от една двойка се използват за регулиране на другите двойки и изграждане на нов *3x2* блок.

Избирането на различни референтни точки води до разнообразно изкривяване на стегоизображението. Да предположим, че $m_i=d_i^{'}- d_i$, където $d_i^{'}$и d_i са стойностите на разликата в пикселната двойка *i* преди и след вграждането. Двойката има минимум $|m|$ и се използва като референтна двойка.

Подробностите за стъпките на скриване на данни са описани както следва.

1. Изчислете различията $d_{i(x,\ y)}$ за петте двойки пиксели във всеки блок, зададен от:

$$d_{0(x,y)} = P_{(x+1,y)} - P_{(x,y)}$$

$$d_{1(x,y)} = P_{(x+2,y)} - P_{(x,y)}$$

$$d_{2(x,y)} = P_{(x,y+1)} - P_{(x,y)}$$

$$d_{3(x,y)} = P_{(x+1,y+1)} - P_{(x,y)}$$

$$d_{4(x,y)} = P_{(x+2,y+1)} - P_{(x,y)}$$

2. Използва се $|d_{i(x,\ y)}|$ където *i=0,1,2,3,4*, за да се намери подходящ диапазон R_k в проектираната таблица с диапазони. Диапазоните в таблиците се приемат като ((0,3), (4,7), (8,15), (16,31), (32,63), (64,127, (128,255))

3. Изчислява се количеството на секретните битове t_i, които могат да бъдат вградени във всяка двойка, като се използва съответния диапазон, даден от $R_{j,k}$. Стойността t_i може да бъде оценена от ширината $w_{i,k}$ на $R_{i,k}$, която се получава като $t_i = \lfloor log_2 w_{i,k} \rfloor$ където ширината $w_{i,k} = u_i - l_i + 1$ и u_i и l_i са горни и долни граници на обхвата R_i. За всяко d_i *(от* d_0-d_4*)* прагът се изчислява като $T_i = u_i - l_i - 1$. За вграждане на бита се прилагат следните правила [6].

   Ако за $d_i \geq T_i$ и $R_i=1$ не се изисква припокриване, но *b* трябва да бъде в диапазона [*0,d-l*], така че големината на новата разлика е по-малка от *d*. Избират се максимален брой тайни битове, така че $b \leq d_i - l_i$, където *b* е десетична стойност. Новата разлика $d_i^{'}$ е $l+b$ [6]. Ако $d_i < T_i$, *b* трябва да бъде в диапазона $[0,u_{i-1} \ldots - l_{i-1}]$, максимален брой тайни битове $b \leq d - l_i$. Ако $b \leq d_i - l_i$, новата разлика за $d_i^{'}$ е $l_{i-1}+b$ [6].

4. Прочитат се t_i битовете от двоичните тайни данни и се трансформират в битова последователност в десетична стойност b_i.

5. Изчислява се нова стойност на разликата $d_{i(x,\ y)}^{'}$,

$$d_i^{'} = l_i + b_i, \text{ ако } d_{i\ (x,\ y)} \geq 0$$

$$d_i^{'} = -(l_i + b_i), \text{ ако } d_{i(x,\ y)} < 0,$$

   като се замества първоначална разлика $d_{i(x,y)}$.

6. Променят се стойностите на пикселите в $P_n^{'}$, като се използва уравнението $(P_n^{'}, P_{n+1}^{'}) = (P_n - |m/2|, P_{n+1} + |m/2|)$, където P_n и P_{n+1} са двата пиксела в двойката P_i и *m* е разликата между d_i и $d_i^{'}$. Това се получава от $m = d_i^{'} - d_i$.

7. Използва се двойката с минимум $|m|$ като оптимална референтна двойка $P_{i\ (x,y)}^{'}$, тогава тази избрана двойка се използва за компенсиране на другите четири пикселни двойки. Така се изчисляват нови стойности за всичките шест пиксела в блока.

8. Проверява се дали всички стойности на пикселите са в диапазона от 0 до 255. Ако една или повече нови стойности на пикселите не са в този диапазон се коригират така, че стойностите на пикселите да бъдат в диапазона от 0 до 255. (*Ако не е възможно да се коригират стойностите на пикселите по този начин, тогава прикриващото изображение не е удачно да се използва за вграждане на тайните данни).

9. Следваща стъпка е да се конструира новият блок от всички двойки пиксели с променени стойности.

10. Повтарят се стъпки от 1 до 9, докато съобщението стане подходящо за прикриващото изображение.

Следният алгоритъм описва как да се извлече вградената информация от стегоизображението:

1. Стегоизображението се разделя на *3x2* пикселни блока, като реда на разделяне е същият като в етапа на вграждане.

2. Изчисляват се стойността на различията поотделно за всеки блок в стегоизображението чрез:

$$d'_{0\,(x,y)} = P_{(x+1,y)} - P_{(x,y)}$$

$$d'_{1\,(x,y)} = P_{(x+2,y)} - P_{(x,y)}$$

$$d'_{2\,(x,y)} = P_{(x,y+1)} - P_{(x,y)}$$

$$d'_{3\,(x,y)} = P_{(x+1,y+1)} - P_{(x,y)}$$

$$d'_{4\,(x,y)} = P_{(x+2,y+1)} - P_{(x,y)}$$

3. Използва се $|d'_{i\,(x,\,y)}|$ където $i=0,1,2,3,4$, за да се намери подходящ $R_{k,i}$ в планираната таблица с области.

4. Изчислява се количеството на тайните битове, които могат да бъдат вградени във всяка двойка. За всяко d_i (от d_0-d_4), прагът се изчислява като $T_i=u_i-l_i-1$. Ако $|d'_{i\,(x,y)}|<T_i$, следва да се намали количеството на тайните битове t_i на 1.

5. След като R_{ki} се намери, l_j се изважда от избрания $|d'_{i\,(x,y)}|$ и b'_i се получава, ако стегоизображението не е променено, b'_i е равно на b_i. Накрая, b'_i се превръща от десетична стойност в двоична последователност с t_i битове, където $t_i=|log_2 w_i|$. Този t_i битов поток е само една част от секретните данни преди вграждането.

6. Повтарят се стъпки от 1 до 5, докато съобщението бъде извлечено от стегоизображението.

Съществуват различни модели с помощта, на които се формират цялостни решения и модели, така на пример в [9] се наблюдава един задълбочен анализ на моделите за формиране на базисни функции.

4. Резултати от изпълнението.

Сравнено с метода TPVD в разгледания метод се формират повече двойки пиксели. Това увеличава капацитета за скриване на информацията. В този алгоритъм се избягва деформации в качеството на стегоизображението.


Прикриващо изображение Стегоизображение

Фиг.2. *Прикриващо и стего изображения за LENA.tiff*

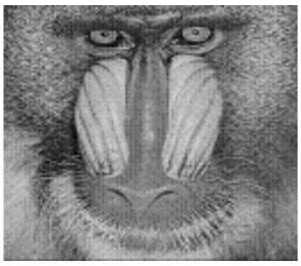
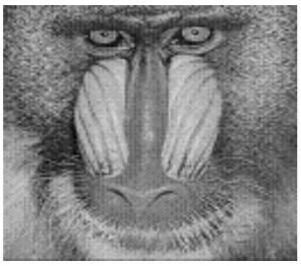

Прикриващо изображение Стегоизображение

Фиг.3. *Прикриващото и стегоизображения за BABOON.TIFF*

Основната му цел е да се направи стегоизображенията сетивно сходни с оригиналното, доколкото е възможно, като заедно с това се увели и количеството за скриваните на данни. На фигура 2 и 3 се показва прикриващото изображение и стегоизображенията, които видимо не се различават.

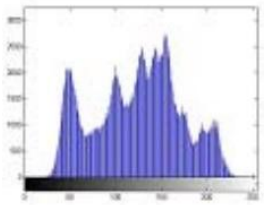
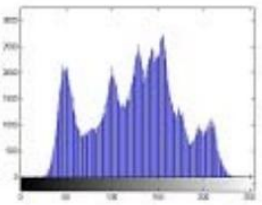

Прикриващо изображение Стегоизображение

Фиг.4. *Хистограма за LENA.tiff*

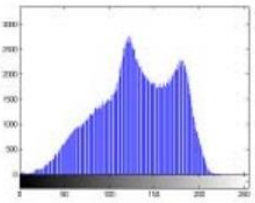
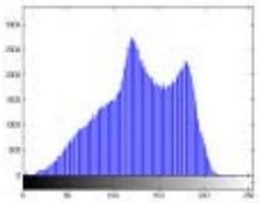

Прикриващо изображение Стегоизображение

Фиг.5. *Хистограма за BABOON.tiff*

Фигури 4 и 5 представят хистограмите на прикриващото изображение и стегоизображението, съответно за lena.tiff и baboon.tiff. Гаусовата форма на хистограмата се запазва в стегоизображенията.

Таблица 1: *Теоретично сравнение*

	TPVD		FPPD	
Размер на блока	2x2		3x2	
Не е възможно блокиране	16384		10880	
Няма двойки пиксели	49152		54400	
Предполагаем минимален брой битове двойки	2	3	2	3
Минимален брой вградени битове	98304	147456	108800	163200

Таблица 1 показва теоретичното сравнение на прикриващия капацитет между метода TPVD и FPPD. За сравнението се приема, че разделителната способност на прикриващото изображение в сивата скала е *256x256*.

Наблюдава се, че по-голям брой двойки пиксели са формирани в FPPD метода. Ако се приеме, че първият диапазон е (*0,3*) в таблицата с диапазони R_i, минимум 2 бита са скрити във всяка двойка. По подобен начин, ако първият диапазон е (0,7), минимум 3 бита са скрити във всяка двойка. Това осигурява по-голям капацитет за скриване в FPPD метода.

За експериментите е използван текстов файл с размер 13Kb (13227 байта). Този текстов файл се използва като тайно съобщение, което трябва да се скрие в прикриващото изображението, което е в сива скала.

Таблица 2 показва стойностите на PSNR (Peak signal-to-noise ratio) за различните изображения. PSNR изчислява пиковото съотношение сигнал/шум между двете сравнявани изображения. Това съотношение често се използва като качествено измерване на разликите между оригиналното и стегоизображението. Колкото по-високо е PSNR, толкова по-добро е качеството на реконструирания образ. Например, при дадено изображение в сиво, за да се скрият тайните данни, е трудно за всеки човек да възприеме разликата между прикриващото изображението и стегоизображението, ако стойността на PNSR на стегоизображението надхвърля 36dB [6].

Таблица 2: *Стойности на PSNR*

Прикриващо изображение	Резолюция	Капацитет (Kb)	PSNR (dB)	MSE
Elaine	512x 512	53.66	50.049	0.6429
Baboon	512x 512	73.37	43.1635	3.1386
Lena	512x 512	53.63	51.0834	0.5067
Tank	512x 512	52.73	50.7922	0.5418
Man	1024 x 1024	222.42	56.1129	0.1591

Резултатите показват, че предложеният подход може да осигури обещаваща производителност при осигуряване на достатъчен капацитет за скриване на данни в изображенията и поддържане на едно качество на незабележимостта едновременно.

5. Заключение

В тази статия се предлага алгоритъм за вграждане на тайни данни в неподвижни изображения, използвайки метод за диференциране на пет пиксела. Този алгоритъм намалява изкривяването на качеството на стегоизображението, което се доказва от резултатите. В горните алгоритми като начален пиксел се използва PX0. Вместо това алгоритъмът може да бъде променен, за да се избере правилно началния пиксел. Това ще позволи да се избере някой от шестте пиксела, които ще се използват като начален пиксел, за да се осигури по-малко изкривяване в стегоизображението и увеличаване на сигурността.

6. Литература:

[1] Antoniya Tasheva, Zhaneta Tasheva, and Plamen Nakov. 2017. Image Based Steganography Using Modified LSB Insertion Method with Contrast Stretching. In Proceedings of the 18th International Conference on Computer Systems and Technologies (CompSysTech'17), Boris Rachev and Angel Smrikarov (Eds.). ACM, New York, NY, USA, 233-240. DOI: https://doi.org/10.1145/3134302.3134325.

[2] Zunera Jalil and Anwar M. Mirza "A Review of Digital Watermarking Techniques for Text Documents", International Conference on Information and Multimedia Technology, 2009

[3] S. Changder ,N.C. Debnath, ,D. Ghosh "A New Approach to Hindi Text Steganography by Shifting Matra", International Conference on Advances in Recent Technologies in Communication and Computing, 2009.

[4] Ko-Chin Chang, Ping S. Huang, Te-Ming Tu, and Chien-Ping Chang, "Adaptive Image Steganographic Scheme Based on Tri-way PixelValue Differencing." 1-4244-0991-8/07/©2007 IEEE pp. 1165-1168.

[5] Han-ling ZHANG , Guang-zhi GENG , "Image Steganography using Pixel-Value Differencing", Second International Symposium on Electronic Commerce and Security, Cai-qiong Xiong 2009 pp.109-112.

[6] Nan-I Wu and Min-Shiang Hwang, "Data Hiding: Current Status and Key Issues", International Journal of Network Security, vol. 4, no. 1, pp. 1-9, Jan. 2007.

[7] Ko-Chin Changa, Chien-Ping Chang, Ping S. Huang, and Te-Ming Tu ,"A Novel Image Steganographic Method Using Tri-way PixelValue Differencing." JOURNAL OF MULTIMEDIA, pp. 37-44 VOL. 3, NO. 2, JUNE 2008.

[8] Atanasov, A., Бежанската вълна от Сирия – заплаха за националната сигурност, II International Scientific Conference ConfSec18, Borovec, Year 2, ISSUE 1(3) ISSN 2603-2945 (print), ISSN 2603-2953 (online) .

[9] Димитров, Д., Използване на полюсни модели за формиране на базисни функции, Сборник научни трудове, Шуменски университет, т 2, с.394 – 397, Шумен, 2009, ISBN:978-954-577-549-6.

СТЕГАНОГРАФИЯ В СЕГМЕНТИТЕ НА ИЗОБРАЖЕНИЕ ЧРЕЗ ГЕНЕТИЧЕН АЛГОРИТЪМ

STEGANOGRAPHY IN IMAGE SEGMENTS USING GENETIC ALGORITHM

Veselka Stoyanova[1] , Stilyana Stoyanova[2]
[1,2] НВУ „Васил Левски“, факултет „Артилерия, ПВО и КИС“, България

veselka_tr@abv.bg

Abstract: *This study offers a heuristic genetic algorithm based method for message hiding in a carrier image. This approach focuses on the "before embedding hiding techniques" by trying to find appropriate places in carrier image to embed the message with the least changes of bits. Due to it, segmentation is done in order to convert the LSBs and message strings to the sets of blocks for participation in genetic algorithm. After finding the right places, secret message blocks are embedded and a key file is created to make the message extraction available by providing the data addresses.*

Keywords: DATA HIDING; GENETIC ALGORITHM (GA); SECURE COMMUNICATIO; STEGANOGRAPHY.

1. Въведение

Сигурната комуникация е една от най-предизвикателните теми в днешния цифров свят. Трудно е да се намери сигурен канал за комуникация през цялото време. Има няколко рамки на ИТ, които могат да бъдат използвани за създаване на модел на заплаха и прилагане на стратегии за смекчаване на последиците [8]. Именно за това се появяват науки и техники като криптографията (преобразуване на обикновена информация в неразбираеми символи [1]), водните знаци [2] и стеганографията.

Стеганографията е наука за криенето на информация в даден цифров носител, така че никой да не може да разбере за съществуването ѝ [3], [2]. Стеганографията е науката за прикриване на съобщения, така че само изпращачът и получателят да знаят съществуването и извличането на съобщения [4], [7]. Тя може да се използва с различни типове дигитални носители, като компютърни файлове, изображения, програми, текстове, мрежи и други методи. Един популярен метод е да се вгражда информацията в изображения. Информацията, която ще бъде скрита се познава като стего съобщение. Обектът, който ще съдържа скритата информация, е познат като прикриващ обект. След като веднъж стего съобщението е вградено в прикриващия обект, полученият обект е известен като стего обект.

В този доклад се разглежда нов метод за скриване на данни в 24-битови RGB изображения. Генетичените алгоритми (GA) ще се използва за осигуряването на стег данни срещу методите на стегоанализа ("стегоанализ" означава откриване на скрити данни в медиите [9], [10], [11]). Най-важният съществуващ метод за стеганализ е анализът на РС [12], който изследва статистическите характеристики на изображението за откриване на дадено съобщение. Статистическият анализ търси различните блокове пиксели в едно изображение, които да не съвпадат с контекста, като по този начин може да се разбере за съществуването на стеганография.

Стеганографията може да се извърши в различни фази, като например по време на изпълнението или чрез предварителна обработка [13]. Процеса на вграждане при прилагането на стеганографски техники се осъществява в два етапа, които водят до увеличаване на устойчивостта:

1. Техники преди вграждане.
2. Техники след вграждане.

Първият етап обикновено включва някои дейности като увеличаване на статистическата несиметричност на изображението. Например, чрез добавяне на шум към прикриващото изображение преди вграждане, което ще доведе резултати от RS анализа, които няма да могат да покажат истината.

GA се използва в голяма степен за увеличаване на устойчивостта на тайните съобщения срещу стеганализа [14] във втория етап. Това означава, че след вграждането на данните в точно определените места на изображението, се използват някои техники за промяна на статистическите характеристики на блоковете от пиксели, така че RS анализа да не може да открие дадено съобщение.

Методът, представен в този доклад се фокусира върху техниките преди вграждане на информация. Той цели да намери подходящи места в прикриващото изображение, които да водят до по-малко промени в оригиналното изображение. По този начин промените в цветовата хистограма са по-малко и откриването на съществуването на стеготекст ще стане по-трудно. Намирането на подходящи места е процес, който може да се реализира чрез генетичен алгоритъм. Системата изцяло взема RGB 24-битово цветово изображение и тайното съобщение като вход, като дава модифицирано изображение, което съдържа вграденото тайното съобщение в най-младшите битове и ключов низ за извличане на съобщение от модифицирано изображение като изход.

1.1 Разновидности на техниките за скриване на данни

Съществуват два вида техники за скриване на данни, използващи изображения: пространствена и честотна област. Първата група се основава на вграждането на съобщение в най-младшия бит (LSB) на пиксела на изображението. Основният LSB метод има проста реализация и висок капацитет [3]. Въпреки това той има ниска устойчивост спрямо някои атаки, като филтриране и компресиране с ниска честота. Моделирането е момент, който обстойно е представен в [6].

Втората група включва съобщенията в честотните коефициенти на изображенията. Тези методи на скриване преодоляват проблема, свързан с устойчивостта и невъзможността да се открият в пространствената област, за които се прилага дискретна вълнова трансформация (Discrete Wavelet Transformations DWT).

1.1.1 Стеганография с голям капацитет, базирана на генетичен алгоритъм и DWT.

Pelham Ghasemi et al. използват GA базирана картографска функция за вграждане на данни в коефициенти на DWT във ***4*4*** блока на дадено прикриващо изображението. Оптималният процес на настройка на пикселите (OPAP) се прилага след вграждане на съобщението. Основната идея за прилагането ѝ е да се сведе до минимум грешката между прикриващото и стегоизображението. След това се използва честотната област за подобряване на стабилността на стеганографията. Следващата стъпка е да се получи оптимална картографска функция за намаляване на разликата между оригинала и стегоизображението, като по този начин се подобрява способността за прикриване на деформациите. Докато сложността на изчисленията е висока, резултатите от симулацията показват, че новата схема надминава адаптивната стеганографска техника, основана на DWT по отношение на Peak Signal to Noise Ratio (PSNR) и капацитет, съответно 39,94 dB и 50% [14].

1.1.2 Техника на вграждане на данни за сивото изображение с помощта на генетичен алгоритъм (DEGGA).

В [5] е представен алгоритъм, базиран на GA наречен DEGGA. Фокусът в този метод е върху голямото количество скрити данни, като резултатите се сравняват с друг метод предложен от Ran-Zan et al. В метода на Мандал, голям обем на съобщение (изображение) се вгражда в пространствена област, използвайки *3x3* маски на изходното изображение. Четири бита на тайното съобщение (изображение) се вграждат за байт на изходното изображение върху най-десния 4-битов пиксел. Мутацията се прилага върху вграденото изображение. Също така се прилага метод за обработка на битовете, за да се поддържа висока точност. При декриптирането следва обратен процес. Генетичният алгоритъм се използва за повишаване на нивото на сигурност. Методът показва, че DEGGA е постигнал по-добри резултати по отношение на PSNR. Предложеният метод използва изображения в сивата скала за сигурно предаване на съобщения. За тайно съобщение е избрано изображение за автентичност с размер $m \times n$. Размерът на прикриващото изображение е $p \times q$.

1.1.3 Метод за сигурна стеганография, основан на генетичен алгоритъм.

За да се гарантира сигурността срещу анализа на PC, Shen Wang et al. представят нов стеганографски метод, основан на генетичният алгоритъм. Няма подход за вграждане на данни в прикриващо изображение с предложения метод. Но осигуряването на стегоизображението се извършва след вграждането на данни. След вграждането на тайно съобщение в LSB на прикриващото изображение, пикселните стойности на стегоизображението се модифицират чрез генетичния алгоритъм, за да се запазят техните статистически стойности. Следователно, наличието на тайното съобщение трудно ще бъде открито от анализа на PC. Междувременно по-добро визуално качество може да се постигне чрез предложения алгоритъм. Експерименталните резултати демонстрират ефективността на предлагания алгоритъм при устойчивост на стеганализа с по-добро визуално качество.

1.1.4. Подобрена адаптивна стенография на LSB, основана на JPEG изображение и генетичен алгоритъм

Lifang Yu et al. представят стеганографски метод в JPEG изображения с висока производителност. Предлаганият метод се състои от 2 части. На първо място е представена подобрена адаптирана стенография на LSB, която може да постигне висок капацитет при запазване на статистиката от първи ред. Второ, за да се сведе до минимум визуалното влошаване на качеството в стегоизображението, се извършва разбъркване на битовете по реда на водещото съобщение, чиито параметри се избират от генетичния алгоритъм. Поради изключителната си чувствителност към началните условия и разпространението в цялото пространство, GA е бил използван за скриване на информация и за повишаване на сигурността. Експерименталните резултати показват, че този метод превъзхожда класическите стеганографски методи в качеството на изображението, като запазва характеристиките на хистограмата и осигурява висок капацитет.

1.2 Предпоставки за реализация:

1.2.1 Най-малко значимият бит (LSB)

В предложения метод се използва LSB техника, защото тя е проста и може да помогне да се предаде смисъла на метода свободно.

Изображението може да бъде представено от група цветни пиксели. Отделните пиксели се представят от техните оптични характеристики като яркост, цветност и т.н. Всяка от тези характеристики може да бъде изразена в цифров вид от 1-ци и 0и. Има различни цветови пространства, които представят различни форми за съхраняване на изображенията. Цветовото пространство е метод, чрез който е възможно да се определи, създаде и визуализира цвят. Най-често срещаното цветово пространство е RGB. Всеки пиксел от 24-битово растерно изображение в това пространство е описан с 3 компоненти от по 8 бита (общо 3 байта), така че всеки набор съдържа стойността на интензитета на RGB. Комбинацията от тези стойности формира характеристиките на пиксела на фигура 1 се илюстрира този въпрос.

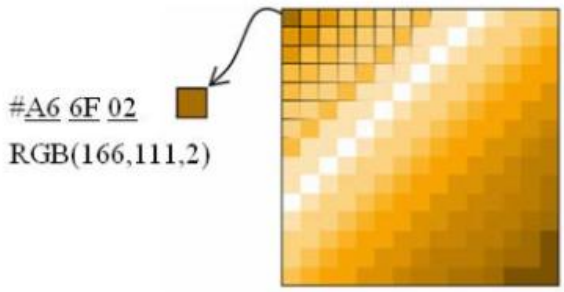

Фиг.1 *Пиксел в RGB цветово пространство*

Кодирането на LSB е една от най-ранните техники, изучавани в скриването на информация от дигиталната медия (включително изображения, аудио и други типове). Най-простите стеганографски техники вграждат битовете на съобщението директно в най-младшия бит на прикриващото изображение в дефинирана последователност. Модулирането на най-малдшия бит не води до възприемане от човека, тъй като амплитудата на промяната е малка. За да се скрие тайно съобщение в изображение е необходимо подходящо прикриващо изображение. Тъй като този метод използва битове на всеки пиксел в изображението, е необходимо да се използва формат за компресиране без загуби, като в противен случай скритата информация ще се загуби в трансформациите от алгоритъма за компресиране. Когато се използва 24-битово цветно изображение, може да се използва малко от всеки основен цвят, така че във всеки пиксел могат да се съхраняват общо 3 бита. Например, следната последователност може да се разглежда като 3 пиксела от 24-битово цветно изображение, като се използва 9 байта памет:

00100111	**11101001**	**11001000**
00100111	11001000	11101001
11001000	00100111	11101001

Когато се вмъкне знак A, чиято двоична стойност е равна на 10000001, се получават следните резултати:

00100111	**11101000**	**11001000**
00100110	11001000	11101000
11001000	00100111	11101001

В този случай само три бита трябва да бъдат променени, за да се вмъкне даден знак успешно. Средно само половината от битовете в изображението ще трябва да бъдат променени, за да се скрие тайно съобщение, използвайки максималния размер на прикриващото изображение. Промените в резултата, които се правят в LSB са твърде малки, за да бъдат разпознати от човешката визуална система (HVS), така че съобщението е ефективно скрито. В изследването може да се види, че най-младшият бит на третия цвят е останал без никакви промени.

1.2.2 Генетични алгоритми

Генетичният алгоритъм е итеративна процедура, поддържаща популация от структури, които са кандидат-решения за специфични предизвикателства в областта. По време на всяко времево нарастване (наречено поколение), структурите в текущата популация се оценяват за тяхната ефективност като домейн решения и въз основа на тези оценки се формира нова популация от кандидатстващи решения, използвайки специфични генетични оператори като възпроизвеждане, кръстосване и мутация .

Те съчетават оцеляването на най-силните сред низовите структури със структуриран, но рандомизиран обмен на информация, за да формират алгоритъм за търсене с някои от иновативните аспекти на човешкото търсене[12].

2. Избор на метод.

Повечето подходи просто вграждат даденото съобщение в прикриващото изображение. След това се опитват да променят другите съседни пиксели по начин, който скрива модифицирането на вградените в пиксела данни. Някои от тези методи променят цялостните характеристики на образа. Докато методът на генетичения алгоритъм се опитва да намери подходящи места в прикриващото изображението, така че те да се нуждаят от по-малко промени. Това означава, че използването на мета-евристични методи като генетичните алгоритми се препоръчва за постигане на по-голяма сигурност.

В първата стъпка от изследването са необходими LSBs на пиксели на изображението, така, че LSBs трябва да бъдат извлечени и поставени в масив във формат на низ от $0^{-и}$ и $1^{-ци}$. Тайното съобщение трябва да се преобразува в подобен формат. Въвеждането на GA е дискретна популация от гени, която не е адаптирана с екстрахирания низ. Сегментирането е решението на този проблем. Всеки низ може да бъде разделен на блокове от L_{block} бита. След сегментирането, блоковете от изображенията правят първоначалната популация на GA. Генетичните алгоритми са алгоритми за търсене, базирани на механиката на естествения процес на селекция (биологична еволюция). След приключване на изпълнението на GA в гените на последното поколение ще се появят подходящи блокове, носители за вграждане на данни. Време е да се модифицират битовете на прикриващото изображение с тайни битове на текстови съобщения. Вграждането ще се осъществи по начин, чрез който ще се променят низовите битове на LSB. Едновременно с това адресът на блока, в който са записани данните се съхранява в масив от ключове. Ключът е необходим за извличане на съобщения.

Извличането на съобщения е много по-лесно. За извличане на секретното съобщение от LSB на стегоизображението, трябва да бъдат извлечени и сегментирани до блокове с дължина L_{block} (като при фазата на вграждане). Адресът на блоковете, които съдържат тайното съобщение се чете от основния файл и данните от тези блокове се извличат и съхраняват.

Стъпките на разглеждания метод са :

Фаза на вграждане:

1. Подготвя се цялото изображение с LSB и тайното съобщение като масиви от $0^{-и}$ и $1^{-ци}$.

- Извличане на цели LSB на изображението на носителя и съхранението им в $\boldsymbol{STR_l}$;
- Конвертиране на тайното съобщение в двоичен низ и съхраняването му в $\boldsymbol{STR_m}$;

2. Трябва да се сегментират STR_l и STR_m на блокове с дължина L_{block}. Броят на блоковете за STR_l и STR_m са N_l=дължина на (STRl) / Lblock и Nm=дължина (STRm) / Lblock;

3. Трябва да се направи първоначална популация на генетичния алгоритъм чрез STRl блокове и след това се изпълнява GA. Това изпълнение на генетичен алгоритъм е до получаване на окончателно състояние и появяване на отговорите;

4. Задължително трябва да се преобразуват битовете на избраните блокове от STR_l с блокове от STR_m и да се вмъкне адреса на блока в масив от ключове;

5. Прилага се STR_l промени към копието на оригиналното изображение и едва след това се съхранява в отделен файл, като се съхранява и масив от ключове;

Етап на извличане:

1. Извличат се LSB на стегоизображението и се съхраняват в STR_l.;

2. Сегментират се STR_l на блокове с дължина L_{block}. Броят на блоковете за STR_l е N_l = дължина от (STR_l) / L_{block};

3. Прочитат се ключовете от файла с ключове;

4. За всеки адрес в ключовете се прави следното: обръщане към адреса на блока, към който ключовите точки сочат и се добавят битовете към масив STR_m.;

5. Конвертират се STRm в нормален формат на символите и накрая се запазват.

3. Експериментални резултати.

Работата на генетичния алгоритъм е изследвана в Matlab 2012. За тайно съобщение за въвеждане на алгоритъма се задава изображение с формат BMP в сивата скала и първата страница на текущата статия. Първоначалният размер на изображението е 1000 * 880. Избрано е L_{block} = 8 (Вж. фигура 2).

а. Оригинално изображение

б. Изображението след вграждане на тайно съобщение

Фиг. 2: *Вграждане на тайно съобщение в изображение*

Вижда се, че няма съществена промяна във формата и целостта на образа. На фигура 3 е показана хистограмата на изображението преди и след вграждането.

А. Хистограма на оригинално изображение

Б. Хистограма на стегоизображение

Фиг 3: *Хистограма на оригинално(А) и стегоизображение(Б)*

Резултатите сочат, че няма промяна в хистограмата на двете изображения. Това означава, че предложеният метод е успешен за вграждане на данни.

Б. Хистограма на изображението след вграждане на тайно съобщение

Съществува тясна връзка между дължината на блоковете и ефективността на този метод. Много голямата дължина на

блоковете (L_{block}=(много голяма)), води до по-малка ефективност. Също така много малкото количество L_{block} води до нарастване на броя на гените в генетичния алгоритъм и увеличава сложността на изпълнение на програмата. Фигура 4 показва общата връзка между ефективност и L_{block}, като е важно е да се отбележи, че правилното L_{block} за различни изображения ще бъде различно.

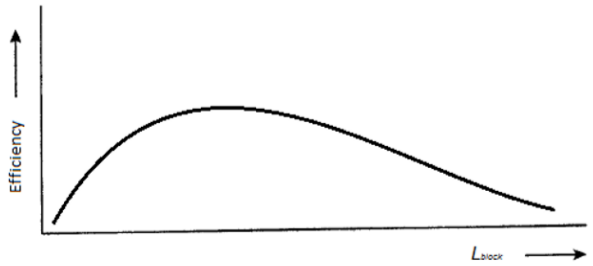

Фиг. 4: *Връзка на ефективността на метода и* L_{block}

Съществува тясна връзка между дължината на блоковете и ефективността на този метод. Eff е избраният критерий за измерване на ефективността на метода, основан на промени в модифицираното изображение, а не на оригиналното изображение. Eff = 1 означава, че няма промяна в оригиналното изображение след вграждането на съобщението и *Eff = 0* показва, че оригиналното изображение е напълно променено.

За изчисляване на Eff входящият оригинален образ е с височина и широчина зададена в пиксели .

Структурата на стойността на всеки пиксел е (*0-255,0-255, 0-255*). Така максималната промяна на всеки пиксел е *255+255+ 255=765.*

Следователно, домейнът на промените в стойностите на всички пиксели на изображенията са следните:

- nP = (височина и широчина) // брой пиксели
- DoC (nP* 765) = // домейн на промените

Eff се изчислява като:

$$Eff = \sum_{Pixel=1}^{nP} ModifiedValue - Original\,Value\,/DoC$$

5. Заключение

В този доклад е разгледан евристичен подход, базиран на GA за стеганографията в прикриващо изображение. Проучени са последните тенденции при използването на генетични алгоритми и се установи, че има два различни вида техники за скриване на информация чрез стеганография: техники преди вграждането и техники след вграждането на тайно съобщение. Разгледаният метод се фокусира върху първия тип, като целта е да се намерят подходящи места в даденото изображението и да се вгради съобщение чрез LSB. Именно затова се прави сегментиране, с цел преобразуване на LSB и низовете на съобщенията в групи от блокове за участие в генетичен алгоритъм. След намирането на правилните места, данните се вграждат и се създава ключов файл, за да направи извличането на съобщението достъпно чрез предоставяне на адресите за данни.

Генетичният алгоритъм се използва за повишаване на нивото на сигурност. Методът показва, че DEGGA е постигнал по-добри резултати по отношение на PSNR. Експерименталните резултати от това проучване показват, че този метод предлага ефективност в тази област. Минималните промени в изображението и хистограмата го потвърждават.

Използвана литература:

[1] Ojha, V., Sharma, A., Lenka, S. K., & Biradar, S. R. (2012). Advantages of Classical Cryptography Over the Quantum Cryptography. World Appl. Program., 2(5), 257-262.

[2] Bagheri Baba Ahmadi, S. (2015). Image Watermarking: Blind Linear Correlation Technique. World Applied Programming. 5(5), 93-100.

[3] Antoniya Tasheva, Zhaneta Tasheva, and Plamen Nakov. 2017. Image Based Steganography Using Modified LSB Insertion Method with Contrast Stretching. In Proceedings of the 18th International Conference on Computer Systems and Technologies (CompSysTech'17), Boris Rachev and Angel Smrikarov (Eds.). ACM, New York, NY, USA, 233-240. DOI: https://doi.org/10.1145/3134302.3134325.

[4] Matt L. Miller, Ingemar J. Cox, Jean-Paul M.G. Linnartz, Ton Kalker. Published in "Digital Signal Processing in Multimedia Systems, Ed. K. K. Parhi and T. Nishitani, Marcell Dekker Inc., 461-485, (1999)

[5] Inoue H, Miyazaki A, Katsura T (2002). An image watermarking method based on the wavelet transform. In: International Conference on Image Processing, IEEE ICIP, Kobe, vol 1, pp 296– 300.

[6] Димитров, Д., Използване на полюсни модели за формиране на базисни функции Сборник научни трудове, Шуменски университет, том 2, стр.394 – 397, Шумен, 2009.

[7] Masoud Nosrati, Ronak Karimi, Mehdi Hariri. Embedding StegoText in Cover Images Using linked List Concepts and LSB Technique. World Applied Programming. Vol (1), No (4), October 2011. 264-268.

[8] Atanasov, А., Бежанската вълна от Сирия – заплаха за националната сигурност, Научна конференция на Факултет „Артилерия, ПВО и КИС", 2013, Шумен

[9] Niels Provos, Peter Honeyman. Hide and Seek: An Introduction to Steganography. IEEE SECURITY & PRIVACY, MAY/JUNE 2003.

[10] Abbas Cheddad, Joan Condell, Kevin Curran, Paul Mc Kevitt, Digital image steganography: Survey and analysis of current methods Signal Processing 90 (2010) 727–752

[11] Zabihi, S., Nasrollahi, P., & Bazmara, M. (2014). Human Activity Recognition Using Accelerometers Values in Different Coordinate Systems. World Appl. Program., 4(12), 237-240.

[12] R. Popa, An Analysis of Steganographic Techniques, The "Politehnica" University of Timisoara, Faculty of Automatics and Computers, Department of Computer Science and Software Engineering, http://ad.informatik.unifreiburg.de/mitarbeiter/will/dlib_bookmarks/digitalwatermarking/popa/popa.pdf, 1998

[13] Reitz, F. B., Demorrow, J. E., & Mock, R. J. (2015). Java/Javascript software for calcium buffer calculations. World Applied Programming. 5(1), 27-30.

[14] Nosrati, M., & Karimi, R. (2012). A Survey on Usage of Genetic Algorithms in Recent Steganography Researches. World Applied Programming. 2(3), 206-210.

[15] Nosrati, M., Karimi, R., & Hasanvand, H. (2012). Spatial and Transform Domains RDH Methods. World Applied Programming. 2(6), 373-376.

СРАВНИТЕЛЕН АНАЛИЗ НА ВЪЗМОЖНОСТИТЕ НА СТЕГАНОГРАФСКИ ПРИЛОЖЕНИЯ

COMPARATIVE ANALYSIS OF THE POTENTIAL OF STEGANOGRAPHY APPS

Талев Д.Д[1], Атанасов А.[2]
[1,2] НВУ „Васил Левски“, факултет „А, ПВО и КИС“- Шумен, България

lfs_13@abv.bg, lenkov@gbg.bg

Abstract: *Steganography can be defined as a method of hiding data within a cover media so that other individuals fail to realize their existence. Steganographic systems play a vital role in covertly transmission of information even in the presence of an arbiter. The article deals with the steganography system which hides text inside images without losing of data (BMP, JPEG). The secret message is hidden in the cover image using Last Significant Bit (LSB) method. Visual and statistical analysis of this algorithms returns good results.*

Keywords: STEGANOGRAPHY, DATA HIDING, HIDDEN CAPACITY, PVD, FPPD, PSNR

1. Въведение

Комуникацията в съвременния свят между компаниите и потребителите се нуждае от един по-защитен и сигурен обмен на конфиденциална информация чрез Интернет. Един от начините, чрез които се реализира това, е стеганографията. Съществуват много определения за стеганография [1], [2], [8], [9], като общото в тях е, че тя е наука, при която с помощта на различни технически средства се извършва скриване на информация в цифрови носители, и се реализира предаването ѝ между две комуникиращи си страни, т.е. тя е науката за скриване на самото съобщение, а не на неговото съдържание.

Методът на най-младшия бит (least-significant bit, LSB) е пример за директното скриване на тайна информация във всеки пиксел на изображението [9]. Алгоритмите използващи този метод обикновено директно вмъкват малка част от тайното съобщение в LSB на всеки пиксел на изображението в пространствената област.

2. Обзор.

2.1. Основни критерии за оценка на стеганографските алгоритми.

Основни критерии, по които могат да бъдат оценени стеганографските методи и алгоритми са:

- Незабележимост;
- Размер на скриваните данни;
- Устойчивост на стеганализ;
- Устойчивост на модификации;
- Файлови формати.

2.2. Основни характеристики за оценка на стеганографски алгоритъм.

При сравнение на две изображения се пресмятат четири основни статистически характеристики, които описват степента на подобие между изображенията: средна квадратична грешка MSE (Mean Squared Error), отношение на пиковия сигнал към шума PSNR (Peak Signal-to-Noise Ratio), индекс за измерване на структурната прилика в изображение SSIM (Structural Similarity Index for Measuring) и ентропията в изображения [3], [4].

Изчисляването на средната квадратична грешка е стандартен статистически подход за обективно измерване на степента на различие между две изображения. Малка стойност на MSE означава, че средното ниво на разликата между тях е малко. В случай на две еднакви изображения, MSE има стойност, равна на нула. За разлика от MSE, по-голяма стойност на PSNR означава по-добро качество на изображението. При еднаквост на две изображения, PSNR има стойност клоняща към безкрайност. Основна цел на всички стеганографски методи е минимизиране на стойността на MSE и съответно максимизиране на стойността на PSNR [3], [5].

Изследваните характеристики са представени съответно чрез формули (1) и (2), като PSNR се базира на стойностите, получени за MSE:

$$(1) \qquad MSE = \frac{1}{mn}\sum_{i=0}^{m-1}\sum_{j=0}^{n-1}[C(i,j) - S(i,j)]^2,$$

където m и n са ширина и височина на изображението; I(i, j) и K(i, j) са съответни пиксели с координати (i, j) в оригиналното и стего-изображение.

$$(2) \qquad PSNR = 10.\log_{10}\left(\frac{max^2}{MSE}\right) = 10.\log_{10}\left(\frac{max}{\sqrt{MSE}}\right),$$

където max = 255 за 8 битови изображения.

Степента на подобие на изображенията преди и след процеса на вграждане на данните, измерена чрез средната квадратична грешка MSE и отношението на пиковия сигнал към шума PSNR, определя качеството на стегоизображението [7]. Когато подобието между изследваните изображение е малко се приема, че качеството на стегоизображението е по-ниско.

Индексът за измерване на структурната прилика в изображение SSIM (Structural Similarity Index for measuring) е подобен на MSE и PSNR, но е създаден с цел да ги подобри. Като показател той измерва промяната в яркостта, контраста и структурата на дадено изображение. За получаването на SSIM се комбинират стойностите, получени за средната интензивност на яркостта, вариациите в контраста и структурата на взаимната корелация между оригиналното и стегоизображението.

3. Анализ на възможностите на специализиран стеганографски софтуер.

Изследваните алгоритми са базирани на LSB метода, приложен и изследван върху BMP и JPEG изображения. Анализирани са резултатите от изследванията на качествените характеристики MSE, SNR, PSNR, SSIM. Визуалният анализ на сравняваните изображения показва липса на визуални разлики при зрителен контрол. Хистограмният анализ и резултатите за качествените характеристики са получени в средата MATLAB 12a.

Изследва се ефективността стеганографските системи при различен размер на скриваните данните в едно и също изображение дава възможност да се анализират очакваните и получени резултати. На база направения анализ, може да се провери ефективността на вграждане на реализираните алгоритми. За целта са избрани две изображения, които са вградени 4 различни по размер съобщения.

4. Резултати от изпълнението.

Избирането на различни референтни стойности е в зависимост от възможностите на софтуера. Основната му цел е да се направи стегоизображенията сетивно сходни с оригиналното, доколкото е възможно, като заедно с това се увели и количеството за скриваните на данни.

На фигура 1 и 2 се показва прикриващото изображение и стегоизображенията, които не се различават.

Прикриващо изображение *Стегоизображение*

Фиг.1. *Прикриващо и стегоизображение на lena. bmp*

Прикриващо изображение *Стегоизображение*

Фиг.2. *Прикриващо и стегоизображение за parrots. bmp*

В таблица 1 и 2 са представени резултатите от изследването на ефективността на вграждане чрез измерване на статистическите характеристики.

Таблица1: Статистически характеристики на Lena.bmp

Програмна реализация	Размер на вградени данни	MSE	Peak-SNR	SSIM
Invisible Secrets 4	10B	0.4996	51.1444	0.9994
	100B	0.5003	51.1388	0.9994
	1кB	0.5003	51.1389	0.9994
	10kB	0.5006	51.1361	0.9994
Master Stego	10B	0.0001	89.8875	1.0000
	100B	0.0007	79.5857	1.0000
	1kb	0.0074	69.4673	1.0000
	10kB	0.0679	59.8148	0.9999
Hide'n' send	10B	16.2716	36.0165	0.9878
	100B	16.3348	35.9997	0.9877
	1kB	16.8900	35.8545	0.9873
	6,1kB	19.9235	35.1371	0.9852

Това сравнение показва промяната в MSE, PSNR и SSIM.

Таблица2: *Статистически характеристики на Parrots.bmp*

Програмна реализация	Размер на вградени данни	MSE	Peak-SNR	SSIM
Invisible Secrets 4	10B	0.5000	51.1415	0.9987
	100B	0.4999	51.1417	0.9987
	1кB	0.4998	51.1424	0.9987
	10kB	0.4999	51.1424	0.9987
Master Stego	10B	0.0000	95.5239	1.0000
	100B	0.0002	85.4837	1.0000
	1kb	0.0019	75.3226	1.0000
	10kB	0.0192	65.2953	0.9999
Hide'n'send	10B	0.8765	48.7031	0.9986
	100B	0.8820	48.6763	0.9986
	1kB	0.9285	48.4530	0.9986
	10kB	1.3952	46.6846	0.9979

За експериментите е използван текстов файл с различна размерност. Този текстов файл се използва като тайно съобщение, което трябва да се скрие в прикриващото изображението.

На фигура 3 и 4 е представен графичен анализ на данните за двете изображения, който съответства с таблици 1 и 2,

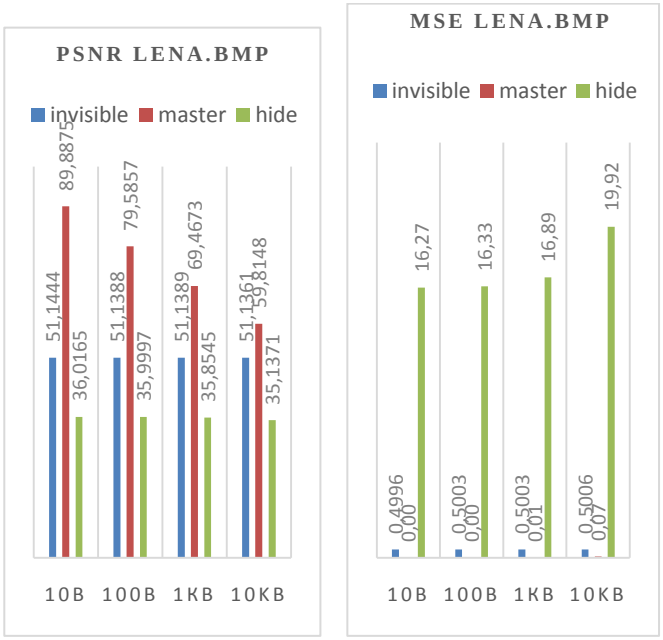

а б

Фиг.3. *PSNR и MSE на lena. bmp*

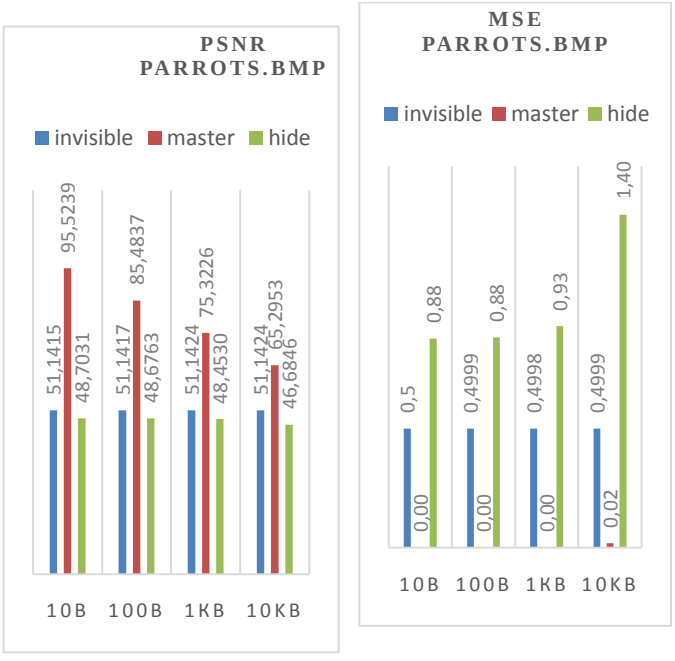

а б

Фиг.4. *PSNR и MSE на parrots. Bmp*

Много важен фактор при сравнения на две изображения се явява хистограмния анализ. Проблемът, който възниква и е основен е , че при реални ситуации, не може да се разполага с оригиналното изображение, за да се сравнят двете изображения и да се докаже наличието на стеганография. На фигура 5 и 6 са представени хистограмите на двойките изображения –стего и оригинал за тестваните Lena.bmp и Parrots.bmp.

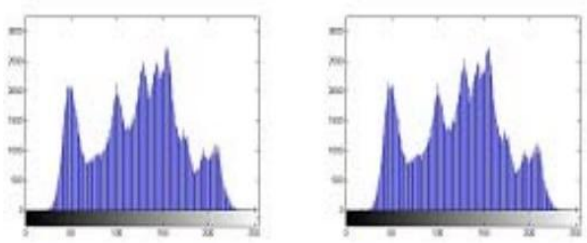

Прикриващо изображение *Стегоизображение*

Фиг.5. *Хистограма за lena. bmp*

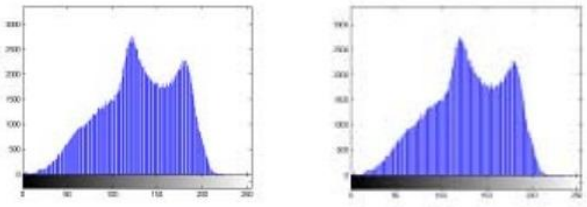

Прикриващо изображение *Стегоизображение*

Фиг.6. *Хистограма за parrots.bmp*

Съотношение сигнал шум, често се използва като качествено измерване на разликите между оригиналното и стегоизображението. Колкото по-високо е PSNR, толкова по-добро е качеството на реконструирания образ. Например, при дадено изображение в сиво, за да се скрият тайните данни, е трудно за всеки човек да възприеме разликата между прикриващото изображението и стегоизображението, ако стойността на PNSR на стегоизображението надхвърля 36dB [6].

Резултатите показват, че предложеният подход може да осигури обещаваща производителност при осигуряване на достатъчен капацитет за скриване на данни в изображенията и поддържане на едно незабележимо качество едновременно.

5. Заключение

В тази статия се предлага сравнение на алгоритми за вграждане на тайни данни в неподвижни изображения, използвайки метод LSB. Те позволяват използването на пароли за осигуряване на допълнителна защита на скриваните данни. Всяко от приложенията притежава своите добри параметри за осигуряване на скритост.

Литература:

[1] Antoniya Tasheva, Zhaneta Tasheva, and Plamen Nakov. 2017. Image Based Steganography Using Modified LSB Insertion Method with Contrast Stretching. In Proceedings of the 18th International Conference on Computer Systems and Technologies (CompSysTech'17), Boris Rachev and Angel Smrikarov (Eds.). ACM, New York, NY, USA, 233-240. DOI: https://doi.org/10.1145/3134302.3134325

[2] Stoyanova V. T. Steganography System Using LSB Methods. In: 2018 ENTRENOVA Conference Proceedings. 2018, Vol. 4, No. 1, pp.381-385, ISSN 1849-7950 https://papers.ssrn.com/sol3/papers.cfm?abstract_id=3283729.

[3] Veselka Stoyanova, Zhaneta Tasheva, Research of the characteristics of a steganography algorithm based on LSB method of embedding information in images, Publication: Trans MotAuto15,https://www.researchgate.net/publication/304579312_Trans_MotAuto15

[4] Ko-Chin Chang, Ping S. Huang, Te-Ming Tu, and Chien-Ping Chang, "Adaptive Image Steganographic Scheme Based on Tri-way PixelValue Differencing." 1-4244-0991-8/07/©2007 IEEE pp. 1165-1168

[5] Han-ling ZHANG , Guang-zhi GENG , "Image Steganography using Pixel-Value Differencing", Second International Symposium on Electronic Commerce and Security, Cai-qiong Xiong 2009 pp.109-112

[6] Nazanin Zaker, Ali Hamzeh, Seraj Dean Katebi, Shadrokh Samavi ,"Improving Security of Pixel Value Differencing Steganographic Method" 978-1-4244-6273-5/09 ©2009 IEEE

[7] Ko-Chin Changa, Chien-Ping Chang, Ping S. Huang, and Te-Ming Tu ,"A Novel Image Steganographic Method Using Tri-way PixelValue Differencing." JOURNAL OF MULTIMEDIA, pp. 37-44 VOL. 3, NO. 2, JUNE 2008.

[8] P. Mohan Kumar and K. L. Shanmuganathan," Developing a Secure Image Steganographic System Using TPVD Adaptive LSB Matching Revisited Algorithm for Maximizing the Embedding Rate", Journal of Telecommunications and Information Technology, 2/2011

[9] Stoyanova, V. , Компютърна реализация на стеганографските методи в изображения, Сборник доклади от Годишна Университетска научна конференция, Изд.комплекс на НВУ "В.Левски" В. Търново,2015, т.12, с.128-135, ISSN 1314-1937.

NUMERICAL ANALYSIS OF REAL OPEN CYCLE GAS TURBINE

PhD. Mrzljak Vedran[1], PhD. Poljak Igor[2], PhD. Orović Josip[2], Prof. PhD. Prpić-Oršić Jasna[1]
[1]Faculty of Engineering, University of Rijeka, Vukovarska 58, 51000 Rijeka, Croatia
[2]University of Zadar, Maritime Department, M. Pavlinovića 1, 23000 Zadar, Croatia
E-mail: vedran.mrzljak@riteh.hr, ipoljak1@unizd.hr, jorovic@unizd.hr, jasna.prpic-orsic@riteh.hr

Abstract: *The paper presents a thermodynamic analysis of gas turbine with real open cycle. Gas turbine operates in combined heat and power (CHP) system. Analysis is provided by using measured operating parameters of operating mediums (air and combustion gases) in all required operating points. Cumulative real turbine developed power amounts 78611.63 kW. In the whole gas turbine process, the highest losses occur in combustion chambers during the heat supply process and amounts 13689.24 kW. Turbine power losses are equal to 7976.22 kW, while the turbo-compressor power losses amounts 4774.24 kW. While taking into account all analyzed gas turbine components, the highest efficiency of 90.79% has turbine, followed by combustion chambers which efficiency is equal to 89.01%. Turbo-compressor efficiency amounts 88.59% and the whole gas turbine cycle has efficiency equal to 33.15%.*

KEYWORDS: GAS TURBINE, REAL OPEN CYCLE, NUMERICAL ANALYSIS, LOSSES, EFFICIENCY

1. Introduction

Gas turbines are today widely used in various power plants or cogeneration plants for simultaneous heat and power production [1], [2]. Investigation and analysis of many gas turbines and its processes are performed in a lot of scientific papers [3].

Energy and exergy analyses are usually used for the investigation of complete power plants or its components in order to obtain efficiencies and losses of the entire plant and each plant component [4], [5]. Such analyses are also very applicable for the gas turbines and all of its components [6].

This paper presents a thermodynamic analysis of gas turbine with real open cycle which operates in combined heat and power system. Real gas turbine cycles involve losses at each analyzed gas turbine component. Power distribution, distribution of delivered and released heat, losses and efficiencies of each constituent component and the entire gas turbine were calculated and discussed.

2. Real open cycle gas turbine process

Main scheme of a gas turbine with real open cycle is presented in Fig. 1, while the temperature-specific entropy diagram of this process is shown in Fig. 2.

Beginning of gas turbine operation from dead-state is ensured with starting electro-motor [7]. In the open gas turbine cycle turbo-compressor takes air from the atmosphere and increases its pressure. Air with increased pressure is then delivered to combustion chambers. In combustion chambers is injected a certain amount of high-quality fuel, fuel is mixed with air after which combustion occurred. Produced combustion gases leave combustion chambers and enter into the turbine. At the combustion chambers outlet (turbine inlet) produced combustion gases has the highest temperature (the highest gas turbine cycle temperature) - point 3, Fig. 1 and Fig. 2. Combustion gases expanded through the turbine and after expansion, they are released from the gas turbine cycle to the atmosphere. One part of produced turbine cumulative power (usually about 50%) is used for a turbo-compressor drive, while with the other part of cumulative produced power is driven any power consumer (usually electric generator).

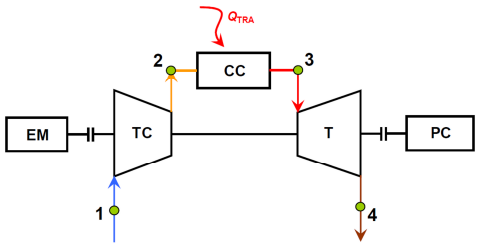

Fig. 1. *Main scheme of the gas turbine with real open cycle (EM = Electro-Motor; TC = Turbo-Compressor; CC = Combustion Chambers; T = Turbine; PC = Power Consumer)*

Real gas turbine cycle includes losses at each gas turbine component [8]. Turbo-compressor compresses air from the atmosphere by polytropic compression, which included compression losses if compared to ideal isentropic compression. Heat supply process in combustion chambers has several heat transfer losses and is characterized with a pressure drop. Real combustion gases expansion process on the turbine is polytropic which included expansion losses if compared to ideal isentropic expansion. Heat release from the real gas turbine process happens at the higher pressure in comparison with atmospheric pressure. For the analyzed gas turbine cycle, mentioned losses are included in measured operating parameters of air and combustion gases in all operating points.

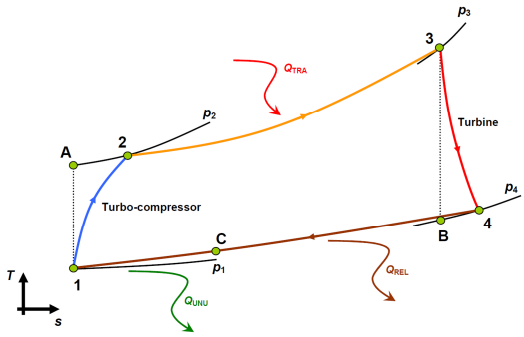

Fig. 2. *T-s diagram of the real open gas turbine cycle with all losses included*

3. Gas turbine with real open cycle numerical analysis – main equations

Most of the equations for the gas turbine with real open cycle analysis were found in [7] and [8]. For each operating point of real open gas turbine cycle, specific enthalpy of operating medium (air or combustion gases) can be calculated as:

$$h = c_p \cdot T \tag{1}$$

where c_p is the specific heat capacity of operating medium at constant pressure and T is current operating medium temperature. For real open cycle gas turbine, specific heat capacity at constant pressure (c_p) is a function of current operating medium temperature.

Specific heat capacity at constant pressure of air is calculated according to [9] by using an equation:

$$c_{p,air}(T) = 1.0484 - 0.0003837 \cdot T + \\ + \frac{9.45378}{10^7} \cdot T^2 - \frac{5.49031}{10^{10}} \cdot T^3 + \frac{7.92981}{10^{14}} \cdot T^4 \tag{2}$$

while for combustion gases (cg), specific heat capacity at constant pressure is also calculated according to [9] by using an equation:

$$c_{p,cg}(T) = 0.936087 + \frac{0.010749}{10^2} \cdot T + \\ + \frac{0.0172103}{10^5} \cdot T^2 - \frac{0.07247}{10^9} \cdot T^3 \quad (3)$$

In equations Eq. 2 and Eq. 3 temperature T must be inserted in (K) to obtain c_p of air or combustion gases in (kJ/kg·K). For the analyzed gas turbine are used measured temperatures in all operating points from Fig. 1 and Fig. 2, therefore specific enthalpies of operating medium can be easily calculated.

By using Fig. 1 and Fig. 2, the operating parameters of the real open cycle gas turbine are:

- Turbo-compressor real power:

$$P_{TC} = \dot{m}_{air} \cdot (h_2 - h_1) = \dot{m}_{air} \cdot (T_2 \cdot c_{p,2} - T_1 \cdot c_{p,1}) \quad (4)$$

Temperature of operating medium (air) after ideal (isentropic) compression is calculated by using an equation:

$$T_A = T_1 \cdot \left(\frac{p_2}{p_1} \right)^{\frac{\kappa_{air}-1}{\kappa_{air}}} \quad (5)$$

where κ_{air} is according to [10] equal to 1.4.

- Turbo-compressor ideal (isentropic) power:

$$P_{TC,IS} = \dot{m}_{air} \cdot (h_A - h_1) = \dot{m}_{air} \cdot (T_A \cdot c_{p,A} - T_1 \cdot c_{p,1}) \quad (6)$$

- Turbo-compressor power losses:

$$P_{TC,PL} = P_{TC} - P_{TC,IS} = \dot{m}_{air} \cdot (h_2 - h_A) \quad (7)$$

- Turbo-compressor efficiency:

$$\eta_{TC} = \frac{P_{TC,IS}}{P_{TC}} = \frac{h_A - h_1}{h_2 - h_1} = \frac{T_A \cdot c_{p,A} - T_1 \cdot c_{p,1}}{T_2 \cdot c_{p,2} - T_1 \cdot c_{p,1}} \quad (8)$$

- Combustion gases mass flow is the sum of air mass flow through a turbo-compressor and fuel mass flow (F) in combustion chambers:

$$\dot{m}_{cg} = \dot{m}_{air} + \dot{m}_F \quad (9)$$

- Turbine real cumulative power:

$$P_T = \dot{m}_{cg} \cdot (h_3 - h_4) = \dot{m}_{cg} \cdot (T_3 \cdot c_{p,3} - T_4 \cdot c_{p,4}) \quad (10)$$

Temperature of combustion gases after ideal (isentropic) expansion is calculated by using the following equation:

$$T_B = T_3 \cdot \left(\frac{p_4}{p_3} \right)^{\frac{\kappa_{cg}-1}{\kappa_{cg}}} \quad (11)$$

where κ_{cg} is equal to 1.3 according to [10] .

- Turbine ideal (isentropic) cumulative power:

$$P_{T,IS} = \dot{m}_{cg} \cdot (h_3 - h_B) = \dot{m}_{cg} \cdot (T_3 \cdot c_{p,3} - T_B \cdot c_{p,B}) \quad (12)$$

- Turbine power losses:

$$P_{T,PL} = P_{T,IS} - P_T = \dot{m}_{cg} \cdot (h_4 - h_B) = \dot{m}_{cg} \cdot (T_4 \cdot c_{p,4} - T_B \cdot c_{p,B}) \quad (13)$$

- Turbine efficiency:

$$\eta_T = \frac{P_T}{P_{T,IS}} = \frac{h_3 - h_4}{h_3 - h_B} = \frac{T_3 \cdot c_{p,3} - T_4 \cdot c_{p,4}}{T_3 \cdot c_{p,3} - T_B \cdot c_{p,B}} \quad (14)$$

- Real useful power (which can be used for power consumer drive):

$$P_{US} = P_T - P_{TC} \quad (15)$$

- Ideal (isentropic) useful power (which can be used for power consumer drive if the compression and expansion processes were ideal ones):

$$P_{US,IS} = P_{T,IS} - P_{TC,IS} \quad (16)$$

- Chemical energy delivered by fuel in the combustion chambers:

$$Q_{CHE} = \dot{m}_F \cdot LHV \quad (17)$$

where LHV is the fuel lower heating value.

- The amount of heat transferred in combustion chambers:

$$Q_{TRA} = \dot{m}_{cg} \cdot (h_3 - h_2) = \dot{m}_{cg} \cdot (T_3 \cdot c_{p,3} - T_2 \cdot c_{p,2}) \quad (18)$$

- Heat supply losses in the combustion chambers:

$$Q_{HSL} = Q_{CHE} - Q_{TRA} \quad (19)$$

- Heat supply (combustion chambers) efficiency:

$$\eta_{HS} = \frac{Q_{TRA}}{Q_{CHE}} = \frac{\dot{m}_{cg} \cdot (h_3 - h_2)}{\dot{m}_F \cdot LHV} = \frac{\dot{m}_{cg} \cdot (T_3 \cdot c_{p,3} - T_2 \cdot c_{p,2})}{\dot{m}_F \cdot LHV} \quad (20)$$

- The cumulative amount of heat released from the process:

$$Q_{REL} = \dot{m}_{cg} \cdot (h_4 - h_1) = \dot{m}_{cg} \cdot (T_4 \cdot c_{p,4} - T_1 \cdot c_{p,1}) \quad (21)$$

- Useful heat released from the process:

$$Q_{REL,US} = \dot{m}_{cg} \cdot (h_4 - h_C) = \dot{m}_{cg} \cdot (T_4 \cdot c_{p,4} - T_C \cdot c_{p,C}) \quad (22)$$

Useful heat released from the process is the amount of heat which can be used for additional heating purposes. Combustion gases which exit gas turbine can be used for additional heating if its temperature exceeds 160 °C (433.15 K). Temperature of combustion gases equal to 160 °C is represented with point C in Fig. 2. Intensive low-temperature corrosion is the main reason why combustion gases with temperature lower than 160 °C cannot be used for additional heating, so one part of heat will always be released from the process as unused heat.

- Unused released heat:

$$Q_{UNU} = \dot{m}_{cg} \cdot (h_C - h_1) = \dot{m}_{cg} \cdot (T_C \cdot c_{p,C} - T_1 \cdot c_{p,1}) \quad (23)$$

- Gas turbine process overall efficiency:

$$\eta_{GT} = \frac{P_{US}}{Q_{TRA}} = \frac{P_T - P_{TC}}{Q_{TRA}} \quad (24)$$

- Specific fuel consumption:

$$SFC = \frac{\dot{m}_F}{P_{US}} = \frac{\dot{m}_F}{P_T - P_{TC}} \quad (25)$$

4. Measured operating parameters of the real open cycle gas turbine

The operating parameters of real open cycle gas turbine process were found in [9], Table 1. The operating points of the gas turbine process in Table 1 are presented in accordance to Fig. 1 and Fig. 2. The real gas turbine process is characterized with real (polytropic) compression and expansion processes with pressure drops during heat transferring in combustion chambers and during heat releasing from the process. Analyzed real open cycle gas turbine operates in combined heat and power (CHP) system, Turkey.

Table 1. *Operating parameters of real open cycle gas turbine [9]*

Operating point*	Temperature (K)	Pressure (bar)
1	298.15	1.0133
2	615.15	10.5030
3	1287.57	9.9779
4	827.15	1.1171
Air mass flow	119.97 kg/s	
Used fuel	Natural gas	
Fuel lower heating value (*LHV*)	44661 kJ/kg	
Fuel mass flow	2.79 kg/s	
Combustion gases mass flow**	122.76 kg/s	

* According to Fig. 1 and Fig. 2
** According to Eq. 9

5. Numerical analysis results of real open cycle gas turbine

After real (polytropic) compression on the turbo-compressor and after real (polytropic) expansion on the turbine, temperatures of operating medium (air or combustion gases) are higher in comparison with ideal (isentropic) processes, Fig. 3. The air temperature after real compression is 33.58 K higher, while combustion gases temperature after real expansion is 50.33 K higher when compared to air and combustion gases temperature after isentropic compression and expansion.

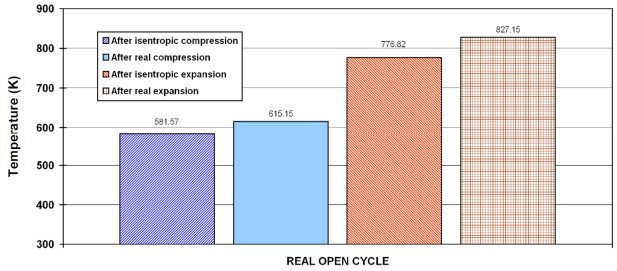

Fig. 3. *The change in real and isentropic temperatures after compression and expansion for the analyzed gas turbine*

A turbo-compressor is power consumer therefore in the real compression process it will use more power (due to losses) than in the ideal process. Real compression process will use 4772.24 kW more power in comparison with the ideal (isentropic) one, Fig. 4.

The turbine is a power producer - in the real expansion process turbine will produce 7976.23 kW less power (due to losses) than in the ideal (isentropic) process.

Real useful power produced by analyzed gas turbine amounts 36768.51 kW and will be used for any power consumer drive. Ideal (isentropic) useful power is calculated according to Eq. 16 and it assumes ideal compression and expansion processes. Isentropic useful power is equal to 49518.98 kW and represents the maximum theoretical power which can be in the ideal situation produced by analyzed gas turbine and delivered to power consumer, Fig. 4.

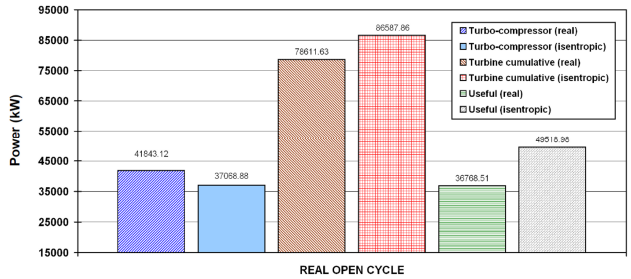

Fig. 4. *The change in real and isentropic power of gas turbine components and the entire gas turbine*

The most expensive element in the analyzed real open cycle gas turbine is used fuel. Chemical energy brought to combustion chambers by fuel represents the highest heat amount delivered in the gas turbine process. Due to several losses in the gas turbine combustion chambers - heat transferred from fuel to operating medium (combustion gases) will be lower in comparison with fuel chemical energy for 13689.24 kW, Fig. 5.

Cumulative heat released from the analyzed gas turbine process amounts 75119.53 kW. This heat amount will be divided on useful released heat (released combustion gases with temperature higher than 160 °C) and unused released heat (released combustion gases with temperature lower than 160 °C). In the analyzed gas turbine process useful released heat, which can be used for any heat consumer drive (or more of heat consumer's drive) amounts 58216.59 kW.

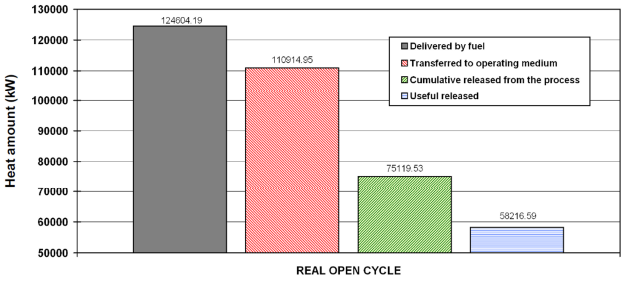

Fig. 5. *Change in heat amounts of the analyzed gas turbine*

Turbo-compressor power losses which amounts 4774.24 kW are represented as a difference between real and ideal (isentropic) power required for turbo-compressor drive. Turbine power losses amounts 7976.22 kW and those turbine losses were calculated as a difference between the ideal (isentropic) and real turbine developed power, Fig. 6.

Heat supply losses are a difference between fuel chemical energy and heat amount transferred to operating medium (combustion gases) in combustion chambers - Eq. 19. Unused released heat from the analyzed gas turbine with real open cycle amounts 16902.94 kW and is calculated by using Eq. 23.

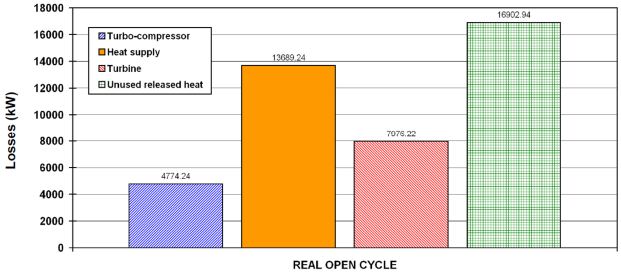

Fig. 6. *Losses of the analyzed gas turbine components*

For the analyzed gas turbine with real open cycle, the highest efficiency has a turbine (90.79%), Fig. 7. The heat supply process has efficiency equal to 89.01%, while the lowest efficiency of analyzed gas turbine components has a turbo-compressor and its efficiency is equal to 88.59%. Real open cycle gas turbine analyzed in this study has an overall efficiency equal to 33.15%, what is usual and expected efficiency for gas turbines used in power plants of any type.

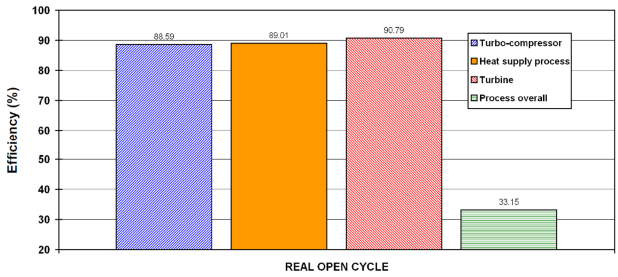

Fig. 7. *Efficiencies of gas turbine components and the entire gas turbine*

In the presented analysis are obtained some additional important operating data of the analyzed real open cycle gas turbine. By using natural gas as a fuel for combustion in combustion chambers, specific fuel consumption, calculated according to Eq. 25, is equal to 273.17 g/kWh. Turbo-compressor power share in the cumulative power developed by the turbine is equal to 53.23%, which leads to a conclusion that a majority of developed cumulative turbine power is used for turbo-compressor drive; only 46.77% of cumulative developed power is used for power consumer driving. Share of unused heat in cumulative released heat is equal to 22.50% therefore the conclusion is that the majority of cumulative released heat from the analyzed gas turbine can be used for the drive of other heat consumers. In the real analyzed gas turbine process turbo-compressor uses 12.88% more power, while the turbine produces 10.15% lower power when compared to ideal (isentropic) compression and expansion processes. Real produced gas turbine useful power which will be used for power consumer drive will be 34.68% higher if the compression and expansion processes are the ideal (isentropic) ones.

6. Conclusions

This paper presents a thermodynamic analysis of gas turbine with real open cycle, which means that all the losses at every gas turbine component were taken into account during analysis. Analyzed gas turbine takes the air from the atmosphere and after expansion process combustion gases were released from the process directly to the atmosphere - two-way atmosphere connection defines gas turbines with open cycle. The main conclusions of the presented analysis are:

- After real compression and expansion processes operating medium temperatures were significantly higher in comparison with the operating medium temperatures after ideal (isentropic) compression or expansion.
- Turbo-compressor power losses amounts 4774.24 kW and its efficiency is equal to 88.59%.
- Turbine power losses amounts 7976.22 kW and its efficiency is equal to 90.79%.
- Heat supply process in combustion chambers resulted with heat losses equal to 13689.24 kW, while the heat supply efficiency (combustion chambers efficiency) is equal to 89.01%.
- Cumulative heat released from the gas turbine process amounts 75119.53 kW. This cumulative heat amount is divided in two parts - first part is useful heat, which can be used for any heat consumer drive and amounts 58216.59 kW, while the second part is unused heat which cannot be used in heat consumers and must be released to the atmosphere. Unused heat amounts 16902.94 kW.
- The whole analyzed gas turbine cycle has an overall efficiency equal to 33.15%.

7. Acknowledgment

This work has been fully supported by the Croatian Science Foundation under the project IP-2018-01-3739.

8. References

[1] Kotowicz, J., Brzęczek, M.: *Analysis of Increasing Efficiency of Modern Combined Cycle Power Plant: A Case Studies*, Energy 153, p. 90-99, 2018. (doi:10.1016/j.energy.2018.04.030)

[2] Yoru, Y., Karakoc, T. H., Hepbasli, A.: *Dynamic energy and exergy analyses of an industrial cogeneration system*, International journal of energy research 34, p. 345–356, 2010. (doi:10.1002/er.1561)

[3] Ibrahim, T. K., Basrawi, F., Awad, O. I., Abdullah, A. N., Najafi, G., Mamat, R., Hagos, F. Y.: *Thermal performance of gas turbine power plant based on exergy analysis*, Applied Thermal Engineering 115, p. 977-985, 2017. (doi:10.1016/j.applthermaleng.2017.01.032)

[4] Adibhatla, S., Kaushik, S. C.: *Energy, exergy, economic and environmental (4E) analyses of a conceptual solar aided coal fired 500 MWe thermal power plant with thermal energy storage option*, Sustainable Energy Technologies and Assessments 21, p. 89–99, 2017. (doi:10.1016/j.seta.2017.05.002)

[5] Mrzljak, V., Poljak, I., Medica-Viola, V.: *Dual fuel consumption and efficiency of marine steam generators for the propulsion of LNG carrier*, Applied Thermal Engineering, 119, p. 331–346, 2017. (doi:10.1016/j.applthermaleng.2017.03.078)

[6] Fallah, M., Siyahi, H., Akbarpour Ghiasi, R., Mahmoudi, S.M.S., Yari, M., Rosen, M.A.: *Comparison of different gas turbine cycles and advanced exergy analysis of the most effective*, Energy 116, p. 701-715, 2016. (doi: 10.1016/j.energy.2016.10.009)

[7] Cengel Y., Boles M.: *Thermodynamics an engineering approach*, Eighth edition, McGraw-Hill Education, 2015.

[8] Moran M., Shapiro H., Boettner, D. D., Bailey, M. B.: *Fundamentals of engineering thermodynamics*, Seventh edition, John Wiley and Sons, Inc., 2011.

[9] Balli, O., Aras, H., Hepbasli, A.: *Exergetic performance evaluation of a combined heat and power (CHP) system in Turkey*, International journal of energy research 31, p. 849–866, 2007. (doi:10.1002/er.1270)

[10] Omar, H., Kamel, A., Alsanousi, M.: *Performance of Regenerative Gas Turbine Power Plant*, Energy and Power Engineering 9, p. 136-146, 2017. (doi:10.4236/epe.2017.92011)

THERMODYNAMICAL ANALYSIS OF HEAT EXCHANGE AND FUEL CONSUMPTION IN MARINE RE-HEAT STEAM GENERATOR

PhD. Mrzljak Vedran[1], PhD. Poljak Igor[2], PhD. Orović Josip[2], Prof. PhD. Prpić-Oršić Jasna[1]
[1]Faculty of Engineering, University of Rijeka, Vukovarska 58, 51000 Rijeka, Croatia
[2]University of Zadar, Maritime Department, M. Pavlinovića 1, 23000 Zadar, Croatia
E-mail: vedran.mrzljak@riteh.hr, ipoljak1@unizd.hr, jorovic@unizd.hr, jasna.prpic-orsic@riteh.hr

Abstract: *The paper presents analysis of heat exchange and fuel consumption in the entire Marine Steam Generator (MSG) with steam re-heating and in all of its components. Analysis is performed by using operating parameters from the steam generator exploitation. The highest heat amount transferred from combustion gases is used in the evaporator (48.17 % of the cumulative heat amount transferred in MSG). Proportionally, evaporator uses the highest fuel mass flow of 0.5172 kg/s when compared to other MSG components. In the high-pressure pipeline heat losses amounts 82.64 kW. Cumulative heat transferred from combustion gases to water/steam in all MSG components amounts 42048.47 kW. Cumulative water/steam specific entropy and temperature increase in the entire MSG is 4.5677 kJ/kg·K and 454.18 K, while the fuel mass flow in the entire MSG is equal to 1.0736 kg/s.*

KEYWORDS: MARINE STEAM GENERATOR, STEAM RE-HEATING, HEAT EXCHANGE, FUEL CONSUMPTION

1. Introduction

Marine propulsion systems are today mainly based on diesel engines, regardless of its type [1], [2]. Marine steam propulsion systems [3] still have a dominant role in the propulsion of LNG carriers. New propulsion systems for LNG carriers, which are at least partially based on steam turbines, are under development [4].

Marine steam propulsion systems have a high level of complexity due to a number of components from which they are assembled [5]. An essential element of such marine steam propulsion systems is steam generator. Older versions of marine steam generators produced superheated steam for all marine steam turbines [6] and for proper operation of other system components, but such steam generators do not posses ability of steam additional re-heating [7], [8]. Newer versions of marine steam generators possess that additional ability of steam re-heating.

In this paper is performed analysis of Marine Steam Generator (MSG) with additional steam re-heating. Analysis is based on the first law of thermodynamics. For each component of MSG with steam re-heating is calculated amount of heat transferred from combustion gases during the superheated steam production. Also, for each component of analyzed MSG is calculated fuel consumption. The analysis takes into account steam specific entropy and temperature increase on each analyzed MSG component along with heat and pressure losses of high-pressure steam pipeline.

2. Description of MSG with steam re-heating and its thermodynamic process

Main scheme of Marine Steam Generator (MSG) with steam re-heating is presented in Fig. 1. Water which enters in MSG (point 1, Fig. 1) is heated in all steam generator components and from that water is produced superheated steam (point 2, Fig. 1). Heating in all MSG components is ensured with fuel burning (with the inevitable presence of air) which is delivered in steam generator furnace.

After production, main superheated steam is led through a high-pressure pipeline into the high-pressure turbine. Due to steam high pressure and temperature, heat and pressure losses in high-pressure pipeline cannot be neglected. Therefore, at the high-pressure turbine inlet (point 3, Fig. 1), superheated steam pressure and temperature are lower in comparison with outlet from the MSG (point 2, Fig. 1).

After expansion in the high-pressure turbine, steam was led back to the MSG for the re-heating process. Due to high-pressure steam turbine extractions, steam mass flow in re-heater is lower in comparison with the main steam mass flow. Re-heating process increases steam temperature (between points 4 and 5, Fig. 1) and after re-heating steam was lead to medium-pressure steam turbine.

Each steam generator consists of three main components in the same housing. Those components are water heater, evaporator and superheater. MSG from this analysis in the housing also has fourth component - steam re-heater. To be able to present heat transfer and fuel consumption of each MSG component, operating points from Fig. 1 are not sufficient, so between operating points 1 and 2 are added two additional operating points which divided MSG on its constituent components. That division is presented in Fig. 2.

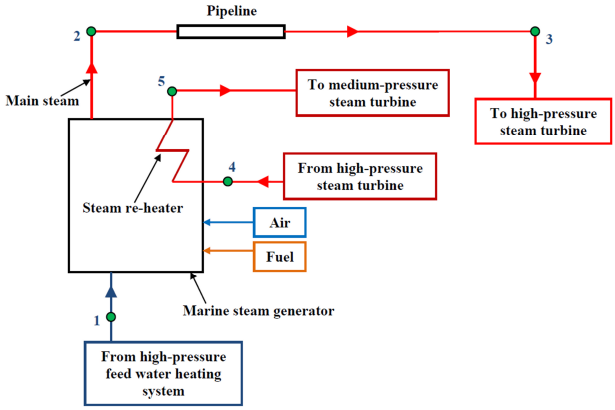

Fig. 1. *Scheme of the MSG with marked operating points for the analysis*

Division of MSG into the components required some assumptions. The first assumption is that the process of water heating, evaporation and superheating is happening at the same pressure (pressure losses at each mentioned component is neglected). The second assumption is that water heating, evaporation and superheating processes begins or ends at the saturation line (for the evaporator process begins and ends at the saturation line), which varies from the real process. Only pressure loss which has taken into account is in re-heater due to high steam volume and speed through re-heater.

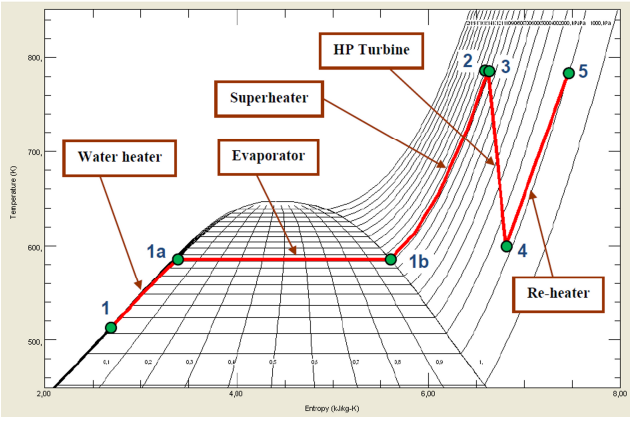

Fig. 2. *T-s diagram of the MSG process with marked operating points necessary for the analysis of each component*

Besides analyzed process at each MSG component, in Fig. 2 can also be seen temperature (and pressure) loss in high-pressure steam

pipeline (between points 2 and 3) as well as the real (polytropic) steam expansion process in a high-pressure steam turbine. The analysis in this paper ends with point 5, after steam exits the steam re-heater and was lead to medium-pressure steam turbine.

3. Equations for the thermodynamic analysis of MSG with steam re-heating

Analysis of MSG is performed according to the first law of thermodynamics [9] which is related to the conservation of energy [10]. Equations for the analysis are defined according to Fig. 1 and Fig. 2:

- Heat transferred from combustion gases to water in the MSG water heater:

$$\dot{Q}_{\mathrm{WH}} = \dot{m}_{1} \cdot \left(h_{1\mathrm{a}} - h_{1}\right) \tag{1}$$

- MSG water heater fuel consumption:

$$\dot{m}_{\mathrm{f,WH}} = \frac{\dot{Q}_{\mathrm{WH}}}{H_{\mathrm{low}} \cdot \eta_{\mathrm{WH}}} = \frac{\dot{m}_{1} \cdot \left(h_{1\mathrm{a}} - h_{1}\right)}{H_{\mathrm{low}} \cdot \eta_{\mathrm{WH}}} \tag{2}$$

- Heat transferred from combustion gases to water/steam in MSG evaporator:

$$\dot{Q}_{\mathrm{EVAP}} = \dot{m}_{1\mathrm{a}} \cdot \left(h_{1\mathrm{b}} - h_{1\mathrm{a}}\right) \tag{3}$$

- MSG evaporator fuel consumption:

$$\dot{m}_{\mathrm{f,EVAP}} = \frac{\dot{Q}_{\mathrm{EVAP}}}{H_{\mathrm{low}} \cdot \eta_{\mathrm{EVAP}}} = \frac{\dot{m}_{1\mathrm{a}} \cdot \left(h_{1\mathrm{b}} - h_{1\mathrm{a}}\right)}{H_{\mathrm{low}} \cdot \eta_{\mathrm{EVAP}}} \tag{4}$$

- Heat transferred from combustion gases to steam in MSG superheater:

$$\dot{Q}_{\mathrm{SH}} = \dot{m}_{1\mathrm{b}} \cdot \left(h_{2} - h_{1\mathrm{b}}\right) \tag{5}$$

- MSG superheater fuel consumption:

$$\dot{m}_{\mathrm{f,SH}} = \frac{\dot{Q}_{\mathrm{SH}}}{H_{\mathrm{low}} \cdot \eta_{\mathrm{SH}}} = \frac{\dot{m}_{1\mathrm{b}} \cdot \left(h_{2} - h_{1\mathrm{b}}\right)}{H_{\mathrm{low}} \cdot \eta_{\mathrm{SH}}} \tag{6}$$

- Heat transferred from combustion gases to steam in MSG re-heater:

$$\dot{Q}_{\mathrm{RH}} = \dot{m}_{4} \cdot \left(h_{5} - h_{4}\right) \tag{7}$$

- MSG re-heater fuel consumption:

$$\dot{m}_{\mathrm{f,RH}} = \frac{\dot{Q}_{\mathrm{RH}}}{H_{\mathrm{low}} \cdot \eta_{\mathrm{RH}}} = \frac{\dot{m}_{4} \cdot \left(h_{5} - h_{4}\right)}{H_{\mathrm{low}} \cdot \eta_{\mathrm{RH}}} \tag{8}$$

- Heat loss in MSG high-pressure pipeline:

$$\dot{Q}_{\mathrm{PL}} = \dot{m}_{2} \cdot \left(h_{2} - h_{3}\right) \tag{9}$$

- Heat transferred from combustion gases to water/steam in the entire MSG:

$$\begin{aligned} \dot{Q}_{\mathrm{MSG}} &= \dot{m}_{1} \cdot \left(h_{2} - h_{1}\right) + \dot{m}_{4} \cdot \left(h_{5} - h_{4}\right) = \\ &= \dot{Q}_{\mathrm{WH}} + \dot{Q}_{\mathrm{EVAP}} + \dot{Q}_{\mathrm{SH}} + \dot{Q}_{\mathrm{RH}} \end{aligned} \tag{10}$$

- Entire MSG fuel consumption:

$$\begin{aligned} \dot{m}_{\mathrm{f,MSG}} &= \frac{\dot{Q}_{\mathrm{MSG}}}{H_{\mathrm{low}} \cdot \eta_{\mathrm{MSG}}} = \frac{\dot{m}_{1} \cdot \left(h_{2} - h_{1}\right) + \dot{m}_{4} \cdot \left(h_{5} - h_{4}\right)}{H_{\mathrm{low}} \cdot \eta_{\mathrm{MSG}}} = \\ &= \frac{\dot{Q}_{\mathrm{WH}} + \dot{Q}_{\mathrm{EVAP}} + \dot{Q}_{\mathrm{SH}} + \dot{Q}_{\mathrm{RH}}}{H_{\mathrm{low}} \cdot \eta_{\mathrm{MSG}}} \end{aligned} \tag{11}$$

Data for the MSG thermodynamic analysis were found in [5]. In this document the authors specified that used fuel have a lower heating value (H_{low}) equal to 43038 kJ/kg and steam generator efficiency (η_{MSG}) is 91 %. In this analysis were taken the same fuel lower heating value, while the efficiency of 91 % is assumed for the entire MSG and each of its components. Water/steam specific enthalpies (h) and specific entropies (s) were calculated with NIST REFPROP 9.0 software [11] from known temperature and pressure at each operating point of Fig. 1 and Fig. 2.

4. Operating parameters at each MSG point necessary for the analysis

Water/steam temperature, pressure and mass flow at each operating point of MSG (Fig. 1) were found in [5] and presented in Table 1. In Table 1 are also presented water/steam specific enthalpies and specific entropies calculated with NIST REFPROP 9.0 software [11] at each observed MSG operating point.

Table 1. *Data for the MSG analysis at each operating point [5]*

Op. point*	Temperature (K)	Pressure (kPa)	Mass flow (kg/s)	Specific enthalpy (kJ/kg)	Specific entropy (kJ/kg·K)
1	514.87	10300	15.593	1046.5	2.7028
2	786.00	10300	15.593	3404.6	6.6247
3	783.00	10100	15.593	3399.3	6.6263
4	599.95	2260	12.859	3079.2	6.8087
5	783.00	2030	12.859	3489.7	7.4545

* Operating point numeration refers to Fig. 1 and Fig. 2

Analysis of heat transfer and fuel consumption at each MSG component requires widening of data between operating points 1 and 2 (Fig. 1). Operating points 1 and 2 has the same pressure (Table 1), so at each main component of the analyzed MSG (re-heater not included) is assumed the same pressure of 10300 kPa. Through each MSG component the water/steam mass flow is equal (15.593 kg/s). Widening of operating data is performed according to Fig. 2 (new added operating points are 1a and 1b) to be able to analyze each MSG component individually. Operation parameters for all added operating points are presented in Table 2.

Table 2. *Expanded data for the MSG analysis between operating points 1 and 2*

Op. point*	Temperature (K)	Pressure (kPa)	Mass flow (kg/s)	Specific enthalpy (kJ/kg)	Specific entropy (kJ/kg·K)
1	514.87	10300	15.593	1046.5	2.7028
1a	586.33	10300	15.593	1420.9	3.3819
1b	586.33	10300	15.593	2719.9	5.5974
2	786.00	10300	15.593	3404.6	6.6247

* Operating point numeration refers to Fig. 2

5. The results of the MSG with steam re-heating thermodynamic analysis

Heat transferred from combustion gasses to operating medium (operating medium is water/steam) at each analyzed MSG component, along with heat losses in the high-pressure pipeline is presented in Fig. 3. In high-pressure pipeline occurs decrease of steam pressure (Table 1) and simultaneous decrease in steam temperature which resulted with heat losses equal to 82.64 kW. Heat losses also occur in all the other steam pipelines, but in high-pressure steam pipeline heat losses are the highest (due to the highest steam pressure and temperature), so it should not be neglected as in other pipelines.

Heat transfer at MSG components shows that the highest heat amount of 20255.31 kW is transferred from combustion gases to operating medium in evaporator during the change in water aggregate state (from water to saturated steam). Superheater is the second heat consumer which increases saturated steam temperature and for that temperature increase uses heat amount of 10676.53 kW. In the analyzed MSG, water heater uses a higher heat amount of

combustion gases than re-heater (5838.02 kW for water heater and 5278.62 kW for re-heater). The main reason for such occurrence is that water mass flow, which passes through water heater, is notably higher when compared with superheated steam mass flow, which passes through the re-heater, Table 1. Heat transferred in the entire analyzed MSG (water heater, evaporator, superheater and re-heater) amounts 42048.47 kW, Fig. 3.

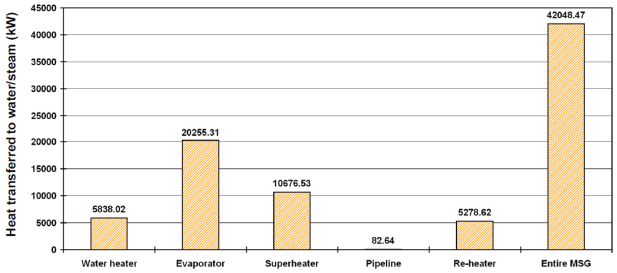

Fig. 3. *Distribution of heat transferred from combustion gases in all analyzed MSG components along with heat loss in the high-pressure pipeline*

From the entire heat amount which is transferred from combustion gases to water/steam in the analyzed MSG, 48.17 % is used by the evaporator, Fig. 4. After evaporator, 25.39 % of the cumulative transferred heat amount uses superheater, water heater uses 13.88 % and the lowest percentage of the cumulative transferred heat amount uses re-heater (12.55 %).

Analyzed MSG acts as many other marine steam generators and steam generators from the land-based steam power plants because the largest heat amount is used for changing the water aggregate state. Change of water aggregate state, according to early adopted assumptions did not result in water/steam temperature increase in evaporator (water/steam temperature in the evaporator can only decrease due to losses).

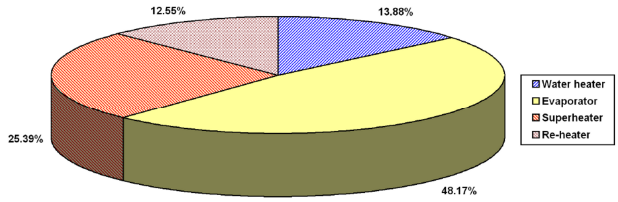

Fig. 4. *Percentage distribution of transferred heat in all MSG components*

Increase of water/steam specific entropy in the analyzed MSG is the highest in the evaporator after which follows the superheater, two components which uses the highest delivered heat amount, Fig. 4 and Fig. 5. Increase in specific entropy of operating medium is higher for water heater than for re-heater, Fig. 5. From this observation can be concluded that heat transferring process in the components of analyzed MSG is directly proportional to operating medium specific entropy increment - increase in delivered heat amount from combustion gases is followed by a proportional increase in specific entropy.

The increase in operating medium temperature of analyzed MSG is not proportional to heat transfer process, Fig. 4 and Fig. 5. Evaporator which gets the highest heat amount of burned fuel does not increase water/steam temperature because of the aggregate state change. The highest operating medium temperature increase can be seen in superheater and re-heater, which both increase temperature of superheated steam (superheater for 199.67 K and re-heater for 183.05 K). MSG water heater increases water temperature for 71.46 K, Fig. 5.

The sum of operating medium specific entropy and temperature increment at each analyzed MSG component resulted with a conclusion that analyzed MSG increases the specific entropy of operating medium for a cumulative value of 4.5677 kJ/kg·K, while the cumulative increase in operating medium temperature in this steam generator is equal to 454.18 K.

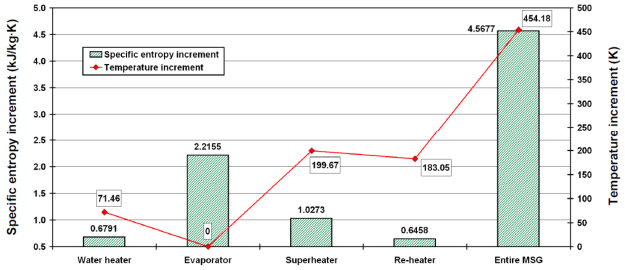

Fig. 5. *Increase in water/steam specific entropy and temperature in each component and in the entire MSG*

Fuel consumption for each MSG component is also directly proportional to heat transferred on each component, Fig. 6. The highest fuel consumer (and proportionally the highest heat consumer) is evaporator which uses fuel mass flow of 0.5172 kg/s. After the evaporator follows superheater and water heater which uses fuel mass flow of 0.2726 kg/s and 0.1491 kg/s. The lowest fuel mass flow (and proportionally the lowest heat amount) of all analyzed MSG components can be seen at re-heater which uses fuel mass flow of 0.1348 kg/s. All the MSG components use the same fuel, which lower heating value amounts 43038 kJ/kg.

Cumulative fuel mass flow used in the entire analyzed MSG is the sum of fuel mass flows used in each component. Fuel mass flow in the entire MSG is 1.0736 kg/s, Fig. 6.

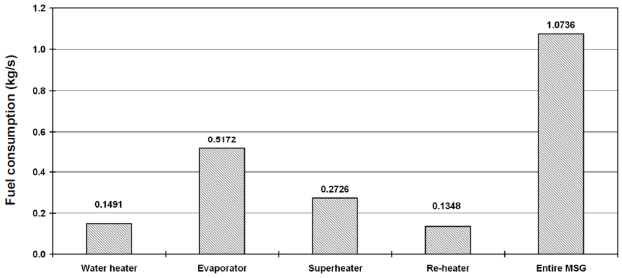

Fig. 6. *Fuel consumption for each component and in the entire MSG*

NIST REFPROP 9.0 software [11] allows calculation of many water/steam operating parameters (besides specific enthalpies and specific entropies) at each observed operating point of the analyzed MSG. Some of important water/steam operating parameters necessary for detail calculation of MSG operation is presented in Fig. 7. Those operating parameters are presented in each operating point of MSG according to Fig. 2.

Water/steam specific volume, which is directly proportional to operating medium volume, is one of the indicators for losses at each MSG component (especially pressure losses). In MSG water heater (points from 1 to 1a) increase in water specific volume is low, so pressure losses in that component can be neglected. In evaporator (points from 1a to 1b) and in superheater (points from 1b to 2) increase in operating medium specific volume is significant and in that MSG components can be expected a notable operating medium pressure decrease during MSG operation, which are neglected in this analysis (according to used operating parameters from [5]). So, in the real exploitation of analyzed MSG will be important precise measurements of steam pressure and temperature at the evaporator and superheater inlets and outlets, if possible. Temperature and pressure decrease in high-pressure pipeline (points from 2 to 3) resulted with an increase in superheated steam specific volume from 0.03250 m^3/kg to 0.03302 m^3/kg. The most significant increase in superheated steam specific volume can be seen during the steam expansion in the high-pressure turbine (points from 3 to 4) and in steam re-heater (points from 4 to 5). Such significant increase in superheated steam specific volume through the MSG re-heater resulted in steam pressure decrease between re-heater inlet

(operating point 4) and outlet (operating point 5), which can be seen in Table 1.

Compressibility factor denotes the difference between the real and ideal gas. Compressibility factor value equal to 1 denotes an ideal gas, while its value lower than or greater than 1 represents the real gas. Compressibility factor is usually used to observe how much the current operating medium characteristics deviate from the ideal gas. For the analyzed MSG in the water heater (points from 1 to 1a) operating medium characteristics significantly deviates from ideal gas because in water heater operating medium is water, so compressibility factor is 0.05299 at the water heater inlet and 0.05569 at the water heater outlet. Saturated steam at the evaporator outlet (operating point 1b) has compressibility factor 0.66152 which means that saturated steam characteristics getting closer to an ideal gas (in comparison with water in water heater). At the superheater outlet (operating point 2) superheated steam has a compressibility factor equal to 0.92266, what indicates that superheated steam has a characteristics very close to ideal gas. After the expansion in high-pressure steam turbine (at the re-heater inlet-operating point 4) superheated steam has a compressibility factor of 0.95199, while at the re-heater outlet (operating point 5) superheated steam has a compressibility factor of 0.98525.

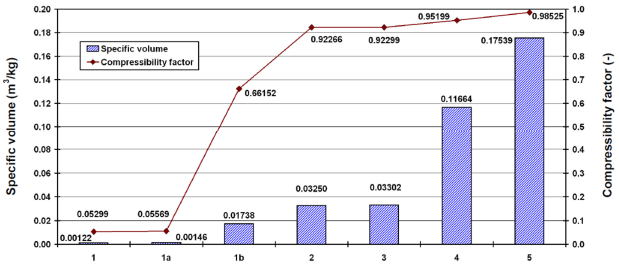

Fig. 7. *Change in water/steam specific volume and compressibility factor at each analyzed MSG operating point*

6. Conclusions

This paper presents analysis of heat exchange and fuel consumption in Marine Steam Generator (MSG) with steam re-heating and in all of its constituent components. The presented analysis provides insight into the operation of each MSG component and presented the most important temperature and pressure losses during the superheated steam production. The most important conclusions of this analysis are:

- The highest transferred heat amount of the entire analyzed MSG is used in the evaporator and amounts 20255.31 kW (48.17 % of the cumulative heat amount transferred in MSG).
- The lowest transferred heat amount of the entire analyzed MSG is used in steam re-heater and amounts 5278.62 kW (12.55 % of the cumulative heat amount transferred in MSG) due to lower operating medium mass flow through re-heater when compared to other MSG components.
- Due to the highest transferred heat amount, evaporator uses the highest fuel mass flow, which amounts 0.5172 kg/s and causes the highest specific entropy increase of operating medium (2.2155 kJ/kg·K), when compared to other MSG components.
- The highest operating medium temperature increase occurs in superheater and re-heater (superheater for 199.67 K and re-heater for 183.05 K), while the evaporator uses the highest heat amount but did not increase operating medium temperature (in evaporator operating medium change its aggregate state).
- Superheated steam, after it leaves MSG superheater, has characteristics very similar to ideal gases.
- Cumulative heat transferred from combustion gases to water/steam in all MSG components (in the entire MSG) amounts 42048.47 kW. Cumulative water/steam specific entropy and temperature increase in the entire analyzed MSG is 4.5677 kJ/kg·K and 454.18 K, while the fuel mass flow in the entire MSG is 1.0736 kg/s.

7. Acknowledgments

This work has been fully supported by the Croatian Science Foundation under the project IP-2018-01-3739.

8. Nomenclature

Abbreviations:		**Greek symbols:**	
MSG	Marine Steam Generator	η	efficiency, %
Latin symbols:		**Subscripts:**	
h	specific enthalpy, kJ/kg	EVAP	Evaporator
H_{low}	fuel lower heating value, kJ/kg	f	fuel
$\dot{m}$	mass flow, kg/s	PL	Pipeline Loss
p	pressure, kPa	RH	Re-Heater
$\dot{Q}$	heat transfer, kW	SH	Super Heater
s	specific entropy, kJ/kg·K	WH	Water Heater
T	temperature, K		

9. References

[1] Sakellaridis, N. F., Raptotasios, S. I., Antonopoulos, A. K., Mavropoulos, G. C., Hountalas, D. T.: *Development and validation of a new turbocharger simulation methodology for marine two stroke diesel engine modelling and diagnostic applications*, Energy 91, p. 952-966, 2015. (doi:10.1016/j.energy.2015.08.049)

[2] Mrzljak, V., Medica, V., Bukovac, O.: *Volume agglomeration process in quasi-dimensional direct injection diesel engine numerical model*, Energy 115, p. 658-667, 2016. (doi:10.1016/j.energy.2016.09.055)

[3] Mrzljak, V., Poljak, I., Mrakovčić, T.: *Energy and exergy analysis of the turbo-generators and steam turbine for the main feed water pump drive on LNG carrier*, Energy Conversion and Management 140, p. 307–323, 2017. (doi:10.1016/j.enconman.2017.03.007)

[4] Fernández, I. A., Gómez, M. R., Gómez, J. R., Insua, A. A. B.: *Review of propulsion systems on LNG carriers*, Renewable and Sustainable Energy Reviews 67, p. 1395–1411, 2017. (doi:10.1016/j.rser.2016.09.095)

[5] Koroglu, T., Sogut, O. S.: *Conventional and Advanced Exergy Analyses of a Marine Steam Power Plant*, Energy 163, p. 392-403, 2018. (doi:10.1016/j.energy.2018.08.119)

[6] Mrzljak, V., Senčić, T., Žarković, B.: *Turbogenerator Steam Turbine Variation in Developed Power: Analysis of Exergy Efficiency and Exergy Destruction Change*, Modelling and Simulation in Engineering 2018. (doi:10.1155/2018/2945325)

[7] Mrzljak, V., Prpić-Oršić, J., Senčić, T.: *Change in Steam Generators Main and Auxiliary Energy Flow Streams During the Load Increase of LNG Carrier Steam Propulsion System*, Scientific Journal of Maritime Research 32, p. 121-131, 2018. (doi:10.31217/p.32.1.15)

[8] Mrzljak, V., Poljak, I., Medica-Viola, V.: *Dual fuel consumption and efficiency of marine steam generators for the propulsion of LNG carrier*, Applied Thermal Engineering 119, p. 331–346, 2017. (doi:10.1016/j.applthermaleng.2017.03.078)

[9] Mrzljak, V., Poljak, I., Medica-Viola, V.: *Energy and Exergy Efficiency Analysis of Sealing Steam Condenser in Propulsion System of LNG Carrier*, International Journal of Maritime Science & Technology "Our Sea" 64 (1), p. 20-25, 2017. (doi:10.17818/NM/2017/1.4)

[10] Orović, J., Mrzljak, V., Poljak, I.: *Efficiency and Losses Analysis of Steam Air Heater from Marine Steam Propulsion Plant*, Energies 2018, 11 (11), 3019; (doi:10.3390/en11113019)

[11] Lemmon, E.W., Huber, M.L., McLinden, M.O.: *NIST reference fluid thermodynamic and transport properties-REFPROP*, version 9.0, User's guide, Colorado, 2010.

AUTOMATED MULTISTAGE FILTRATION DEVICE FOR ON-LINE LIQUID ANALYZERS

Stavros Hadjiyiannis, Eftychios Christoforou, Atanas Terziev
CyRIC - Cyprus Research & Innovation Center Ltd

stavros@cyric.eu

Abstract: *A multistage filtration system has been conceptualized, designed, and prototyped. The system is suitable for various types of on-line liquid analyzers. The developed technology resulted to a low-cost, compact, flexible and reliable automatic system that is based on the use of common, low-cost filters combined with a novel, automatic filters replacement mechanism. A general overview of the device is provided and the design procedure that was followed is discussed.*

KEYWORDS*: LIQUID FILTERS, MULTI-STAGE FILTERING, ON-LINE LIQUID ANALYZERS*

1. Introduction

There is a large number of industries that rely on water or other fluids periodic quality analysis for meeting regulatory requirements or for ensuring safety and security for the population. One of the most typical examples is the drinking-water supply industry. Water analysis has become mandatory in residential, commercial, and industrial sectors, and thus water analysis instruments are used for determining the biological, physical, and chemical properties of water. Typically, water quality is assessed only in the laboratory. Samples of water are taken at certain intervals based on diverse regulations in different countries. Lab-based analysis methods of water quality are usually more reliable, but they cannot provide continuous information depicting the real-time data associated with water quality parameters. To safeguard public health, it is necessary to employ a system that can detect and respond to the changes instantaneously. This need has led to the development of real-time monitoring and on-line analysis of water quality, which has become a major trend in today's water analysis instrumentation market [1]. Likewise, the need for on-line analysis of water quality exists in the food industry and the aquaculture industry. The pharmaceuticals industry has similar needs and, in this case, not only for water quality analysis, but also for the analysis of other fluids used for pharmaceuticals production, such as various solvents.

One of the major problems when dealing with on-line fluid analysers is sample filtration. In fact, in the aforementioned examples, the sample cannot be used directly for the analysis. Pre-treatment is required, including a filtration step. Especially for field samples, this is critical since field samples are usually more contaminated than laboratory samples. It is not surprising that contaminants in field samples are reported to be the most frequent cause of problems with on-line analysers [2]. Furthermore, for on-line analysers, sample contamination is also a problem due to the frequency of the analysis. While a laboratory analyser might perform 100 tests a month, an on-line plant analyser could do 100 tests a day. Some technical solutions have been developed and used for overcoming this issue, including self-cleaning filters. Nevertheless, these solutions are very expensive and large in terms of size, thus useful only to specific application fields where cost and size might not be an issue. Most importantly, the lifetime of such solutions is still limited, while in many cases such filters cannot guarantee high retention rates.

Our project answers the need of the on-line analysers industry for a low-cost, compact, flexible and reliable automatic liquid sample filtering device. The overall objective of the project has been to design, develop and verify an automated multistage filtration concept to be used in various types of on-line liquid analysers. The developed prototype device is based on the use of common, commercial filters combined with a novel, automatic filters replacement mechanism and a smart, modular design for combining multiple filtration steps in a single process.

Herein, a brief description of the device is provided considering the limitations due to patenting issues. A systematic engineering procedure was followed for the design of the system, which is also discussed.

2. Design procedure

The system was designed, and detailed engineering drawings were produced using computer-aided-design (CAD) tools. The dimensional compatibility of the individual parts was confirmed using 3D assembly models of the overall device. The CAD drawings were used for manufacturing the prototype through accurate computer-numeric-control (CNC) machining.

For the system development a systematic engineering design procedure was followed, as shown in Figure 1. The procedure starts with the definition of the problem followed by an extensive background research. A thorough market search was carried out and the results revealed that such a device does not exist in the market. It also became apparent that commercially available, filtration systems installed with on-line analysers need constant maintenance and filter changing intervention, which causes significant delays to the overall filtration process. Additionally, some of these on-line analysers, especially when filter changing has to be done in harsh conditions, are prone to error. Furthermore, frequent opening of the device for filter replacement may result to sample contamination.

The next design step was to identify the requirements for the system and prepare a list of specifications which served as a basis for the design (see more details below). Based on the design specifications alternative solutions were generated and systematically evaluated before selecting the most appropriate one, which was developed in detail. Engineering drawings were prepared using CAD software. The prototype was manufactured and then tested following a systematic evaluation procedure (see Section 3). Along the design procedure it was required to return to previous steps and iterate through the process until a satisfactory outcome was achieved.

Design specifications

In general, the system is required to be customizable and adaptable to various application scenarios. The design process includes both the mechanical/electrical parts of the system, as well as the control system. The requirements/specifications also provided a basis for the testing and evaluation of the developed prototype. The requirements were grouped into certain categories:

(1) Functional (multistage filtering operation, use of commercially available continuous filter paper, operation independent of paper porosity / thickness / manufacturer, compactness and transportability of device, high reliability.

(2) Operational (reliable filter paper feeding, cutting, and disposal operations).

(3) Usability (easy/quick installation of the device, intuitive and user-friendly interface, customizable).

(4) Safety (safety-by-design, electrical and mechanical hazards both considered).

(5) General (material selection to meet application requirements and manufacturability, minimize filter paper waste, labelling of cables and components for easy reference).

(6) Control/actuation system (use reliable industrial control electronics and hardware, design to support integration with external devices and expandability).

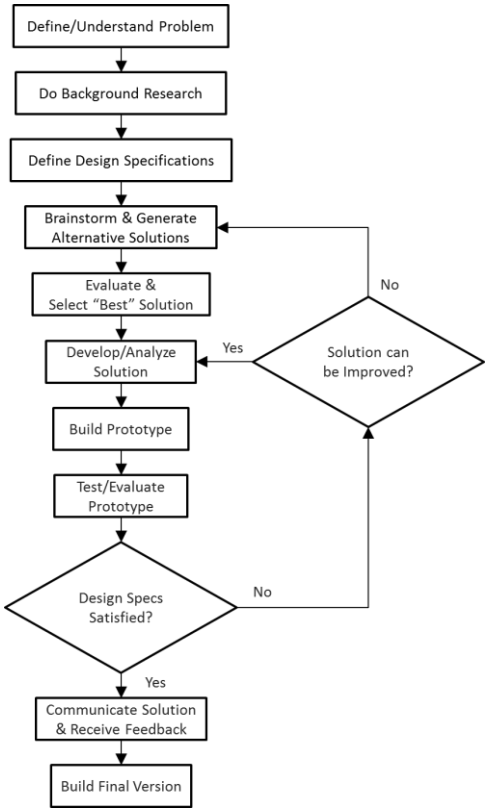

Fig. 1 *General Design Procedure used for the design of the automatic filtering system.*

Materials Selection

The materials were selected based on functional criteria (liquid handling applications), structural requirements, cost and manufacturability. The main materials that were selected were both metallic (aluminum and stainless steel), as well as plastic (POM).

3. Description of the device

Mechanical system

The mechanical system is composed of various subsystems that were integrated together: (i) Structural system (ii) Central multistage filtering module; (iii) Filter cutting; (iv) Filter advance and disposal; (vi) Liquids system. The individual parts are connected together using screws so that the system can be easily assembled and disassembled. Three motors are required for the operation of the device and correspond to the new filter supply system, the filter cutting mechanism, and the filter disposal. Stepper motors were selected for this purpose. The filter paper cutting is performed using a blade that is rolled over a cutting board. On the system it was also included an automated cleaning procedure, which can be performed between filtering cycles by passing water or other cleaning liquids through the system. The overall structure of the system is shown in Figure 2 that includes the mechanical, liquids, and control subsystems.

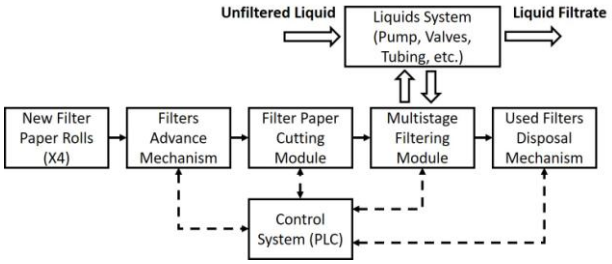

Fig. 2 *Structure of the designed automatic filtering system.*

Control system

Control of the system is based on a programmable logic controller (PLC) which is a reliable and robust industrial option. User interface is implemented through a dedicated touch screen and a user-friendly, intuitive graphics environment. The user can change the functional settings, select between manual and automatic operation, and also test all individual functions of the device. The use of a PLC allows for flexibility and direct integration with other devices. The same PLC can also be used for controlling the pumps that direct the liquid through the filtering system, as well as any valves that may be involved depending on the application.

The general structure of the PLC-based control system is shown in Figure 3. The power supply unit provides the required 24V DC supply to the system. The PLC system comprises the central processing unit (CPU), the memory (where programs and data are stored), and the input/output modules. The latter receive sensory input and send control signals to the actuators (stepper motors), respectively. Communication with the user is via a touch screen and the screen menus that were designed for this purpose.

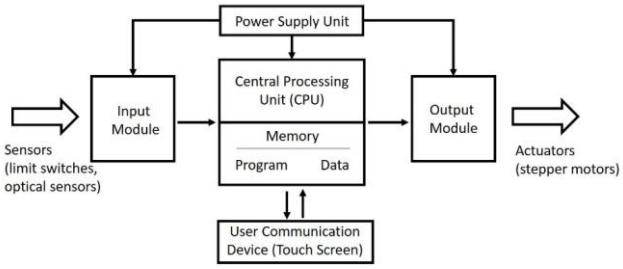

Fig. 3 *Structure of the PLC-based control system of the automatic filtering system.*

3. Testing procedure

Filtration performance is characterized by the pressure drop across a filter and the filtration efficiency. Given that the specific device uses commercial filters from reputable manufacturers, filtration efficiency is ensured. Testing focused on the overall operation of the device itself under realistic conditions.

Initially, various aspects of the device were assessed including the safety and the usability of the device (filter replacement and disposal process, user-friendliness and effectiveness of user interface). The operation robustness was verified by performing repeated cycles in automatic mode. Liquid was pumped through the system using a peristaltic pump, which can supply the required pressure. It was shown that the device can handle different liquid samples including sea water.

4. Conclusions

A multistage filtering system was designed, and the prototype has been developed and tested. A systematic engineering procedure was followed for the design. It is suitable for various types of on-line liquid analyzers and it allows automatic filter changes as well as an automated cleaning procedure. The operation of the system is user-friendly, and integration with other systems is straightforward.

Acknowledgments: The automated multistage filtration device is the result of a co-funded project from Research Promotion Foundation of the Republic of Cyprus, European Regional Development Fund and Structural Funds of the European Union in Cyprus; Acronym: On-FiSy, CONCEPT/0617/0004.

References

1. Global Water Analysis Instrumentation Market, Forecast to 2022, Ramprasad Manishankar, 2016 (http://www.frost.com/sublib/display-report.do?id=P8F0-01-00-00-00).
2. Filtering samples to on-line analyzers, Ken Perrotta et al., Parker Balston, 2013 (https://www.parker.com/literature/Balston%20Filter/IND/IND%20Technical%20Articles/PDFs/Filtering_Samples_Online_Analyzers.pdf).

MODEL BASED ROBUST ENGINEERING APPROACH FOR PARAMETER OPTIMIZATION OF ELECTRON BEAM INDUCED GRAFTING PROCESSES

Asist. Prof. M.Sc. Eng. Koleva L.[1], Assoc. Prof. M.Sc. Eng. Koleva E. PhD.[1,2], M.Sc. Eng. Nemțanu M.R. PhD.[3], M.Sc. Brașoveanu M. PhD.[3]

University of Chemical Technology and Metallurgy, Bulgaria [1]
Institute of Electronics, Bulgarian Academy of Sciences, Bulgaria [2]
National Institute for Lasers, Plasma and Radiation Physics, Electron Accelerators Laboratory, Romania [3]

sura@abv.bg, eligeorg@abv.bg

Abstract: *Electron beam irradiation has the ability to modify polymer substrates by the process of graft copolymerization in order to synthesize water-soluble copolymers having flocculating properties. The influence of the variation of the process parameters acrylamide/starch (AMD/St) weight ratio, electron beam irradiation dose and dose rate is investigated. Models of the means and variances for the dependencies of the quality characteristics (monomer conversion coefficient, residual monomer concentration and apparent viscosity) from the described process parameters are estimated by implementation of the robust engineering methodology for quality improvement. Multi-criteria optimization involving requirements for economic efficiency, assurance of low toxicity and high copolymer efficiency in flocculation process is also presented.*

Keywords: GRAFT COPOLYMERIZATION, ELECTRON BEAM IRRADIATION, WATER-SOLUBLE COPOLYMERS, STARCH, ACRYLAMIDE, FLOCCULATION PROPERTIES, RESPONSE SURFACE METHODOLOGY, MULTI-CRITERIA OPTIMIZATION.

1. Introduction

Electron beam (EB) grafting process involves the modification of the polymer substrates by implementing radiation-induced graft copolymerization in order to yield water-soluble copolymers for flocculation processes [1-3]. The advantages of EB induced grafting process are connected with the ability of the electron beam to ionize polymers with limited reactivity in chemical processes. The generation of polymer radicals is performed by clean non-chemical method, which can be precisely controlled, modified and integrated into complete process lines and uses low energy. During the EB graft process the depth of EB energy deposition into materials can be controlled by the accelerating potential of the equipment, the composition and the density of the material being irradiated. EB irradiation grafting is used to develop a wide variety of ion exchangers, polymer-ligand exchangers, chelating copolymers, hydrogels, affinity graft copolymers and polymer electrolytes, having various applications in water treatment, chemical industry, biotechnology, biomedicine, etc. [4, 5].

Robust (not sensitive to noises and errors) engineering approach can be implemented when analyzing experiments during which the variance is non-homogeneous over the factor (process parameters') space and when the noise factors cannot be identified nor an experiment to study them can be conducted [6, 7]. The observations in this case are called heteroscedastic (variance varies with the factor levels). On the other hand, many performance characteristics depend on both quantitative and qualitative factors. In this case models for the mean and the variance of the quality characteristics of the product, based on repeated observations and taking into account the influence of the qualitative factors, can be estimated. Parameter optimization in terms of obtaining repeatability of the product parameters and quality improvement by minimization of variations in the quality characteristics can be performed.

Response surface methodology for the case in presence of both quantitative and qualitative process parameters should be applied after some generalizations. The model selection problem is an important task, because it is associated with the choice of an experimental design, prediction accuracy of the mean value and the variance of the performance characteristic in production conditions or product's usage, the complexity of the optimization procedures, etc.

In this paper multi-criteria optimization involving requirements for economic efficiency, assurance of low toxicity and high efficiency of the synthesized copolymers in flocculation processes is presented. Models, describing the dependencies of the means and the variances of the quality characteristics: y_1 - monomer conversion coefficient (%), y_2 - residual monomer concentration (%) and y_3 - apparent viscosity (mPa•s) on the variation of the process parameters: EB irradiation dose, dose rate and acrylamide/starch (AMD/St) weight ratio are estimated.

2. Experimental conditions

Experimental investigation of the modification of starch by grafting acrylamide using electron beam irradiation in order to synthesize water-soluble copolymers having flocculation properties is performed. The synthesis of graft copolymers was carried out into two stages:

Stage 1: Preparation of solutions based on starch and monomer, resulting in various acrylamide/starch (AMD/St weight ratios) homogenous aqueous solutions - Starch aqueous solutions were prepared by dissolving corn starch in distilled water. Acrylamide was added to starch aqueous solution with further stirring and different acrylamide/starch (AMD/St weight ratios) homogenous aqueous solutions were obtained.

Stage 2: Electron beam irradiation of the prepared solutions – the homogenous aqueous solutions, prepared in *Stage 1*, were exposed to electron beam irradiation. The irradiations were carried out at ambient temperature and pressure by using a linear electron accelerator of mean energy of 6.23 MeV with different irradiation doses and dose rates.

The synthesized graft copolymers were characterized by the following performance quality parameters: y_1 [%] - residual monomer concentration, y_2 [%] - monomer conversion coefficient and y_3 [mPa•s] - apparent viscosity.

The variation regions [z_{min} - z_{max}] of the process parameters for each experiment set are presented in Table 1.

Table 1: *Experimental design with one dummy variable*

Parameter	$z_{i,\,min}$	$z_{i,\,max}$
EB irradiation dose [kGy]	0.65	5.50
Dose rate [kGy/min]	0.41	1.50
AMD/St weight ratio	2.00	11.00

There were 30 process parameter experimental sets and for each set three replicated measurements are used for estimation of the means $\bar{y}_{ui}$ and the variances s_{ui}^2 of each quality characteristic of the graft copolymers:

$$(1) \quad \bar{y}_u = \frac{1}{n}\sum_{i=1}^{n} y_{ui} \qquad s_u^2 = \frac{1}{n-1}\sum_{i=1}^{n}(y_{ui} - \bar{y}_u)^2 \qquad u = 1, 2, ..., N,$$

where n is the number of replications (n = 3), N is the number of experimental sets (N = 30).

The observed variations are due to unmeasured and uncontrolled factors and internal and external noises, as well as errors in the controlled process parameters, and depend on the values of the process parameters.

3. Models for the mean and variance of the quality characteristics

The estimated mean value $\bar{y}_{ui}$ and s_{ui}^2 variance can be considered as two responses at the design points, and ordinary least squares method can be used to fit the regression models of the mean value and the variance for the quality characteristic [7, 8]:

$$(2) \quad \tilde{\bar{y}}(\vec{x}) = \sum_{i=1}^{k_y} \hat{\theta}_{yi} f_{yi}(\vec{x})$$

$$(3) \quad \ln\left(\tilde{s}^2(\vec{x})\right) = \sum_{i=1}^{k_\sigma} \hat{\theta}_{\sigma i} f_{\sigma i}(\vec{x}),$$

where $\hat{\theta}_{yi}$ and $\hat{\theta}_{\sigma i}$ are estimates of the regression coefficients, and f_{yi} and $f_{\sigma i}$ are known functions of the process parameters x_i.

The variance of normally distributed observations has a χ^2-distribution. The use of the logarithm transformation of the variance function makes it approximately normally distributed, which improves the efficiency of the estimates of the regression coefficients.

The models are estimated for the coded in the region [-1÷1] values of the process parameters, using the following equation:

$$(4) \quad x_i = (2z_i - z_{i,\max} - z_{i,\min})/(z_{i,\max} - z_{i,\min})$$

where x_i and z_i are the coded and the natural values of the process parameter, correspondingly, $z_{i,min}$ and $z_{i,max}$ are the minimal and the maximal values of the parameter experimental variation region.

The dependencies of the means and the variances of the product quality characteristics: y_1 – residual monomer concentration (%), y_2 – monomer conversion coefficient (%) and y_3 – apparent viscosity (mPa•s) on the variation of the process parameters: x_1 – electron beam irradiation dose, x_2 – electron beam irradiation dose rate and x_3 – AMD/St weight ratio are estimated.

Table 2: *Models for the means of the product quality characteristics*

	Models for the means of the product quality characteristics	R
$\tilde{\bar{y}}_1(\vec{x})$	$-4.3456957x_1 + 5.3915161x_1^2 - 1.5283048x_2^2 - 1.3886159x_1x_2 - 5.0568769x_1x_3$	0.8913
$\tilde{\bar{y}}_2(\vec{x})$	$86.89582 + 34.751905x_1 - 7.1056848x_2 - 34.141859x_1^2 + 34.945289x_3^2 + 33.500225x_1x_3$	0.9097
$\tilde{\bar{y}}_3(\vec{x})$	$1.8341046 - 1.4972781x_1 + 1.5368173x_1^2 + 1.401751x_3^2 - 1.3446153x_1x_2 + 1.1090262x_2x_3 - 3.1125045x_1x_3$	0.8470

Table 3: *Models for the variance of the product quality characteristics*

	Models for the variance of the product quality characteristics	R
$\ln\left(\tilde{s}_1^2(\vec{x})\right)$	$-8.1907995 - 2.4376459x_1 - 2.0808965x_2 + 1.2422924x_3 + 3.3800892x_1^2 + 3.0435881x_3^2 - 3.064369x_1x_2$	0.8520
$\ln\left(\tilde{s}_2^2(\vec{x})\right)$	$-2.0505708x_2 + 1.1227946x_3 + 1.3503166x_1x_2^2 + 2.2543255x_2x_3^2 - 2.8020033x_1x_3^2$	0.8670
$\ln\left(\tilde{s}_3^2(\vec{x})\right)$	$-5.3591952 + 1.6879963x_1^2 + 1.7422987x_3^2 - 2.1837351x_1^3 - 1.6195118x_1x_3 + 2.7501263x_1x_2^2$	0.6779

The obtained regression models are presented in Table 2 and Table 3, together with the values of the corresponding multiple correlation coefficients R.

These coefficients are tested for significance and their values are measures of the accuracy of the estimated models. The closer to 1 the value of R is, the better the model describes the variations of the quality characteristics as a function of the process parameters. All models have enough high and significant values of their multiple correlation coefficients and consequently the models are good for prediction and optimization of the considered quality characteristics.

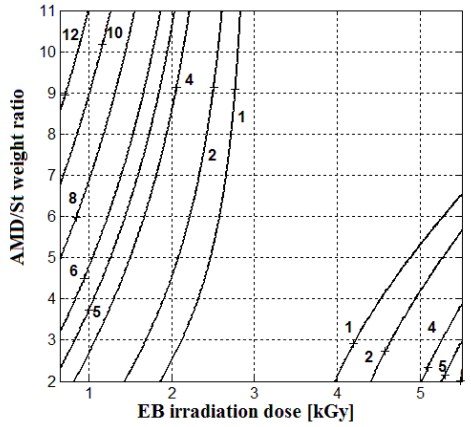

a) $\tilde{\bar{y}}_1(\vec{x})$

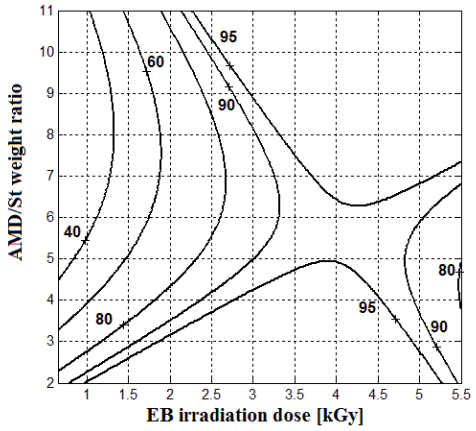

b) $\tilde{\bar{y}}_2(\vec{x})$

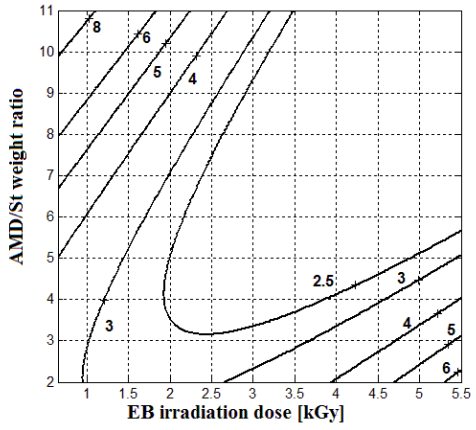

c) $\tilde{\bar{y}}_3(\vec{x})$

Fig. 1 *Contour plots of the mean values of the product quality characteristics, depending on the variation of EB irradiation dose (z_1) and*

the AMD/St ratios (z_3) for constant EB irradiation doses z_2= 0.955 kGy/min: a) monomer conversion coefficient - $\tilde{\tilde{y}}_1(\vec{x})$; b) residual monomer concentration - $\tilde{\tilde{y}}_2(\vec{x})$ and c) apparent viscosity - $\tilde{\tilde{y}}_3(\vec{x})$.

In Fig. 1 contour plots of the mean values of the product quality characteristics, depending on the variation of EB irradiation dose (z_1) and the AMD/St ratios (z_3) for constant EB irradiation dose rate z_2 = 0.955 kGy/min are presented.

The standard deviations of the product characteristics are calculated by the equation:

$$\tilde{s}_i(x) = \sqrt{e^{\ln(\tilde{s}_i^2)}} \quad (5)$$

Contour plots of the standard deviations $\tilde{s}_i(x)$ of the product characteristics, depending on the EB irradiation dose (z_1) and the AMD/St ratios (z_3) for constant EB irradiation dose rate z_2= 0.955 kGy/min is shown in Fig. 2. It can be seen that the standard deviation $\tilde{s}_2(x)$ of the process parameter monomer conversion coefficient ($\tilde{\tilde{y}}_2(\vec{x})$, %) has the highest values within the experimental region.

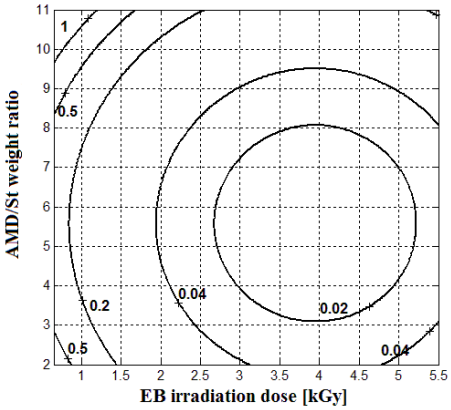

a)

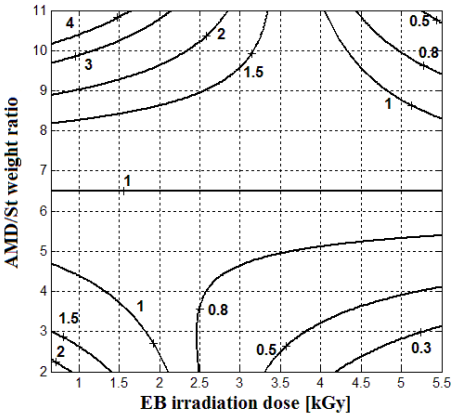

b)

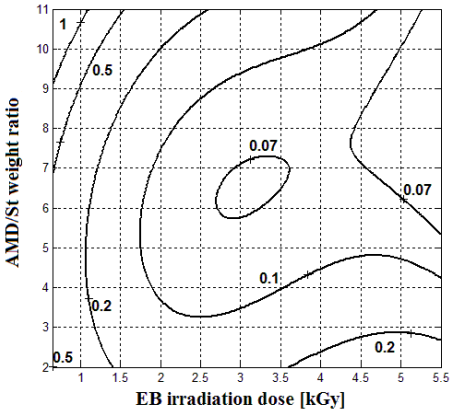

c)

Fig. 2 *Contour plots of the standard deviation of the variance of the product quality characteristics, depending on EB irradiation dose (z_1) and the AMD/St ratio (z_3) for EB irradiation dose rate z_2= 0.955 kGy/min for a) $\tilde{s}_1(x)$; b) $\tilde{s}_2(x)$; c) $\tilde{s}_3(x)$.*

4. Optimization

Multi-criteria graphical optimization unifying requirements for economic efficiency, assurance of low toxicity and high copolymer efficiency in flocculation process is performed. The set of all performance characteristics' requirements is the following:

- $\tilde{\tilde{y}}_1(\vec{x}) < 5\%$ - residual monomer concentration in this region ensures low toxicity;
- $\tilde{\tilde{y}}_2(\vec{x}) > 90\%$ - monomer conversion coefficient values are related to the economic efficiency;
- $\tilde{\tilde{y}}_3(x) > 3$ mPa·s - apparent viscosity copolymer values are related to the efficiency in the flocculation process.

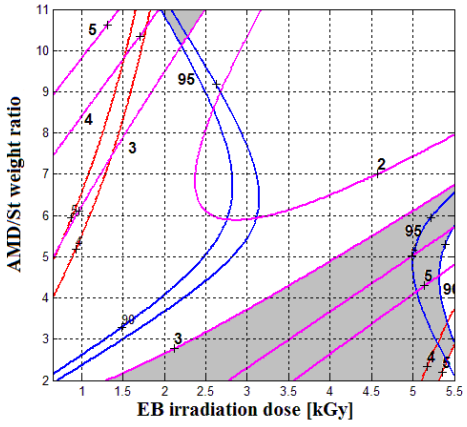

a) z_2= 0.41 kGy/min

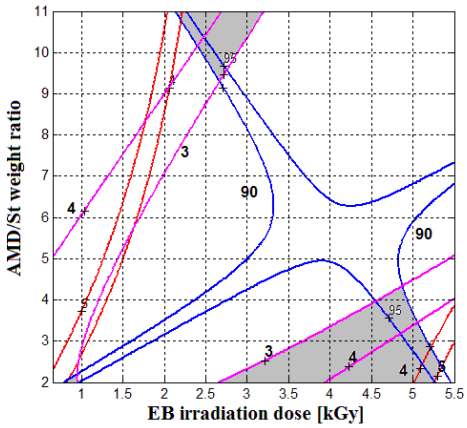

b) z_2 = 0.955 kGy/min

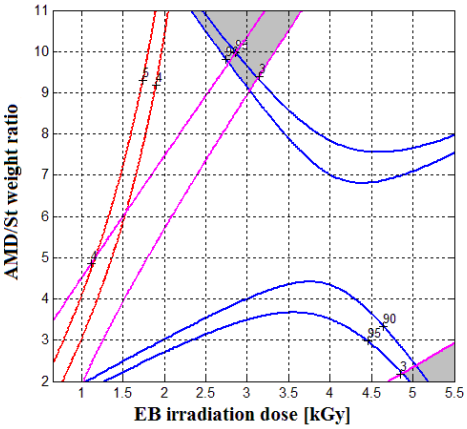

c) z_2=1.50 kGy/min

Fig. 3 *Graphical optimization – optimal regions of EB irradiation dose (z_1) and the AMD/St ratios (z_3) where: $\tilde{\bar{y}}_1(\vec{x})$ is red; $\tilde{\bar{y}}_2(\vec{x})$ - blue and $\tilde{\bar{y}}_3(\vec{x})$ - violet.*

Table 4: *Pareto-optimization – optimal process parameters, values of the means $\tilde{\bar{y}}_i(x)$ and the standard deviation $\tilde{s}_i(x)$ of the product characteristics*

№	z_1	z_2	z_3	$\tilde{\bar{y}}_1$	$\tilde{\bar{y}}_2$	$\tilde{\bar{y}}_3$	$\tilde{s}_1$	$\tilde{s}_2$	$\tilde{s}_3$
1	5.3458	1.0832	2.0041	4.9985	91.3731	5.5340	0.0321	0.1633	0.3206
2	5.0177	0.9880	2.6926	3.3337	94.7047	4.6124	0.0284	0.2753	0.2181
3	5.1486	1.0500	2.4059	3.9071	93.2699	4.8829	0.0269	0.2229	0.2570
4	5.0814	1.0879	2.4617	3.4793	93.8116	4.5735	0.0215	0.2386	0.2593
5	4.7856	0.5546	4.5061	1.0922	96.0325	3.8484	0.0795	1.4995	0.1836
6	4.8009	0.6463	4.1560	1.5822	95.4245	3.9507	0.0602	0.9987	0.1661

Graphical optimization is conducted in order to find the regions of the process parameters where the requirements for the quality characteristics are fulfilled simultaneously. The optimal regions are obtained by superimposing the contour plots of the calculated limit values of the characteristics, thus finding the section of all the admissible values of the process parameters. Fig. 5 presents the optimal values' regions of the EB irradiation dose (z_1) and AMD/St weight ratios (z_3) for EB irradiation dose rate (z_2) of 0.41 kGy/min, 0.955 kGy/min and 1.50 kGy/min, i.e. for the lower, middle and the upper limits of the experimental region.

It can be seen that at middle and highest values of the EB irradiation dose rate the working region is small and is obtained for big values of the EB irradiation dose and AMD/St ratios less than 3 or middle values of the EB irradiation dose and AMD/St ratios more than 9.

From the Fig. 3a it can be seen that the decrease of the EB irradiation dose rate to z_2 = 0.41 kGy/min increases the working area for the EB irradiation dose and AMD/St ratio. There are many possible process parameter sets, fulfilling the defined requirements. The choice between them can be done by adding supplementary requirements or criteria. Such criteria can be, for example, the minimization of the standard deviations of the product characteristics.

For improving the reproducibility of the obtained results the variations of the product quality characteristics should be minimized. This puts additional requirements for the solutions that are obtained through graphical optimization. In order to minimize the variances of the product parameters, multi-criterion optimization is performed and compromise Pareto-optimal solutions are obtained. Some of the estimated results are presented in Table 4. If these compromise solutions are compared two by two, one can note the property of these solutions – some of the obtained optimal product characteristic values are better but at least one value is worse than the one in another compromise solution. The compromise choice should be made according additional criteria or requirements or estimated weight coefficients, giving the relative importance of the optimized performance characteristics.

5. Conclusions

Investigation of the modification of starch by grafting acrylamide using electron beam irradiation in order to synthesize water-soluble copolymers having flocculation properties is performed. Models for the mean values and the variances of the investigated product quality characteristics depending on the variations of the process parameters were estimated.

Optimal regions of the process parameters that satisfy the specified optimization criteria based on the estimated models for the mean values of the product parameters are obtained by implementation of graphical optimization.

In order to meet simultaneously the requirements for economic efficiency, assurance of low toxicity and high copolymer efficiency in flocculation process the EB irradiation doses (z_1) should be higher than 2.0 kGy, AMD/St weight ratio (z_3) should be lower than 5 and EB irradiation dose (z_2) should be 0.41 kGy/min.

Parameter optimization in terms of obtaining repeatability of the product parameters and quality improvement by minimization of variations in the quality characteristics is performed. Compromise Pareto-optimal solutions within the investigated experimental region of the process parameters are obtained.

Acknowledgements

This research was conducted under the contracts: bilateral joint project between the Bulgarian Academy of Sciences and The Romanian Academy, and KP-06-N27/18, funded by the National Fund "Scientific Investigations".

References

[1]. Suman D., Optimization in Chemical Engineering, Cambridge: Cambridge University Press, 2016, 1-11.
[2]. Nemţanu M. R., Braşoveanu M., Polymer science: research advances, practical applications and educational aspects, ed. A Méndez-Vilas and A. Solano-Martín, Badajoz: Formatex Research Center, 2016, 270-277.
[3]. Craciun G., Manaila E., Niculescu M., Ighigeanu D., Obtaining a new type of polyelectrolyte based on acrylamide and hydrolyzed collagen by electron beam irradiation, Polymer Bulletin, 74(4), 2017, 1299 – 1326.
[4]. Stephen C. Lapin, Modification of Polymer Substrates using Electron Beam Induced Graft Copolymerization, UV+EB Technology • Issue 1, 2015, 44-49.
[5]. M.M. Nasef, Radiation-grafted copolymers for separation and purification purposes: Status, challenges and future directions, Progress in Polymer Science, 37, 2012, 1597– 1656.
[6]. Koleva E., Vuchkov I., Model-based approach for quality improvement of EBW applications in mass production, Vacuum, 77, 2005, 423-428
[7]. Vuchkov I. N, Boyadjieva L. N., Quality improvement with design of experiments, The Netherlands, Kluwer Academic Publishers, 2001.
[8]. Najafi S., Salmasnia A., Kazemzadeh R. B., Optimization of robust design for multiple response problem, AJBAS, 5/9, 2011, 1566-1577.

NETWORK TECHNOLOGIES FOR E-LEARNING

M.Sc. Petrova V. PhD Student
Department of Computer Systems &
Technologies - University of Veliko Turnovo, Bulgaria

vmb75bg@gmail.com

Abstract: *In this paper are presented some conclusions on the selection of the LMS to be used. The results of this study give readers information to make their own decisions when choosing an LMS platform based on the needs of their institution. The process of LMS selection is a multi-criteria decision-making problem and an Analytical Hierarchy Process (AHP) was used to assist in building the model and draw decisions. The paper presents an environment "Network technologies for e-learning"(NTEL) using the offered Model for describing, structuring, and organizing the ontological representation of learning objects through providing a semantic infrastructure. Strategies and methodologies in ontology development and implementation are also discussed.*

Keywords: LMS, LEARNING OBJECTS, ONTOLOGY, AHP

1. Introduction

The main goal of the research is to describe and structure ontology based learning objects and use for developing a uniform learning support environment considered with the requirements of the existing Learning Object Metadata (LOM) of IEEE Learning Technology Standards Committee (LTSC) [7] and the specification suggested by the Instructional Management System (IMS) [8].

The most serious problems are caused by the semantic evaluation process. There is a great variety of LMS. As far as evaluation is concerned, current platforms may be helpful to acquire tacit knowledge in organizations, but they do not solve the problematic of doing automatic semantic information. Thus, cooperative cognitive processes are not efficient and not found matching between LOs and student information. This makes the learning process to be impersonal, and not many users can keep track properly of their students' progress [1].

A possible solution might include a component model for network technologies for e-learning and its applications in NTEL to deal with this issue.

2. A Component Model for Network Technologies for e-Learning

The Component model for network technologies for e-learning was developed on the grounds of the existing standards, specifications and ontologies for creation, management, development, and interchange of learning objects and means and the existing instructional design theory. The key aspects of the learning support environment "Network technologies for e-learning" (NTEL) have been presented in the following components of the model:

2.1. A model for describing, structuring, and organizing the ontological representation of learning objects

Figure 1 depicts the composition of the model and the relationships between its modules. At the top of the figure, the Learning object is connected to the Metadata and Knowledge. The Standard Learning Object Metadata (LOM) contains various metadata describing the learning object. The LOM categories are connected with module Categories. A learning activity could be published (using LOM) and integrated in a learning object instructional sequence. A learning object can be created to be used in different courses, and its content can be created on many ways (e.g. using text editor, slide presentation creator, HTML editors, graphical tool, domain applications, etc.). Once created a learning object with its ontology-based content can be included in different courses [3]. We use LOs when a new instructional design is being constructed.

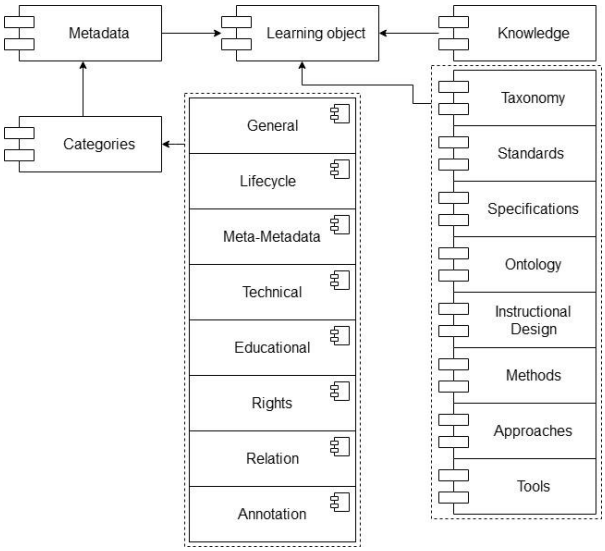

Fig. 1 *A model for describing, structuring, and organizing the ontological representation of learning objects*

2.2. Standards in Learning Object Ontology

In conformity with the IMS specification the environment content package includes two components – an XML file describing the course structure, called imsmanifest.xml and the physical files forming the course structure.

The XML manifest file consists of the following components: meta-data, organizations, resources, and a sub-manifest of each separate environment course. The meta-data are used for describing the content package and its characteristics in particular. The characteristics suggested by the Learning Object Metadata Standard are used in the environment grouped in the following order: general, lifecycle, meta-metadata, technical, educational, rights, relation, annotation, and classification categories. The learning objects stored in the Learning Repository can be found using the metadata. The organizations component shows the systematization of the course content. It includes several subcomponents describing the separate elements of the course. It does not include a description of the physical files but ensures an information work frame guiding the user in the consecutive implementation of particular actions.

The resources component describes the physical files used in the learning course and the relations between them. It shows features different from the organizations component.

The physical files include the following content: a course information, a theoretical material, tests, simulations, games, an interactive editor, and a glossary.

The IMS specification [8] allows placing the content package in the Package Interchange File. It is a single compressed file which can be used in different learning systems. By packaging the separate courses of the learning support environment presented in the

research they can be used independently in learning management systems.

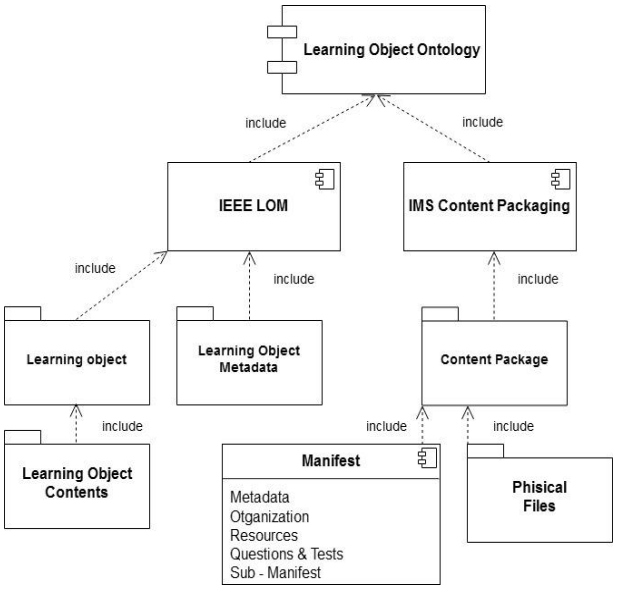

Fig. 2 *Standards in Learning Object Ontology*

We have designed and implemented a LOM ontology that establishes an intermediate layer offering a shared vocabulary that allows specifying restrictions and gives a common semantics for any application which uses Learning Objects Metadata. LOM aims at the abstract description of learning objects by providing an interoperable form and vocabulary for semantic learning objects description and discovery in repositories. Some of the technical aspects in the domain and instruction model provide input for the transformation to LOM. An ontology of a specific domain for a learning objects repository serves as a map and suggests paths for retrieving candidate learning objects to reach a certain objective of learning or teaching [1].

2.3. Application of Instructional Design for ontological organization of e-learning

The IMS Learning Design specification (IMS-LD) provides a model of semantic notation to describe both the content and processes of units of study. This specification is based on: a well-founded conceptual model that defines the vocabulary and the functional relations between the concepts of the LD; an information model that describes in an informal (natural language) way the semantics of every concept and relation introduced in the conceptual model; a behavioral model that specifies the constraints imposed to the software system when a given LD is executed in runtime [8].

The Learning Design has a number of components used to describe the learning process: the execution entities to be carried out, which can be *Activity* or *Activity Structure* (groups of activities that will be executed in sequence); the *Role* that participate in the execution of those activities as instances of the *Learner* and *Staff* concepts; and the *Environment* that describe the educational resources to be used in the activities (Fig. 3). These concepts constitute an exhaustive and disjoint partition, because an instance of a component must necessarily be an instance of one of its subclasses.

The Learning Design is related to the *Method* concept, which describes the dynamics of the learning process (Fig. 3): a method is composed of a number of instances of the *Play* concept that could be interpreted as the *runscript* for the execution of the unit of learning. All the play instances have to be executed in parallel, and each one consists of *Act* instances, which could be understood as a *stage* of a course or module. The *Act* instances must be executed in sequence (according to the values of the execution order attribute), and they are composed by a number of Role Part instances that will be executed concurrently. A *Role* Part associates a *Role*(s) with an execution entity to be carried out in the context of the *act*. Every execution entity requires an *Environment*, which manages Learning Objects as resources The execution of an act consists on the simultaneous participation of roles in an activity or group of activities, and once the activities are completed, the associated roles could participate in the execution of any other activity through different role part instances. The Activity has two subclasses: the Learning Activity and the Support Activity. A Learning Activity includes an educational activity that uses a relation with the Prerequisite and the Learning Objective. The Support Activity is introduced to facilitate a learning activity [6].

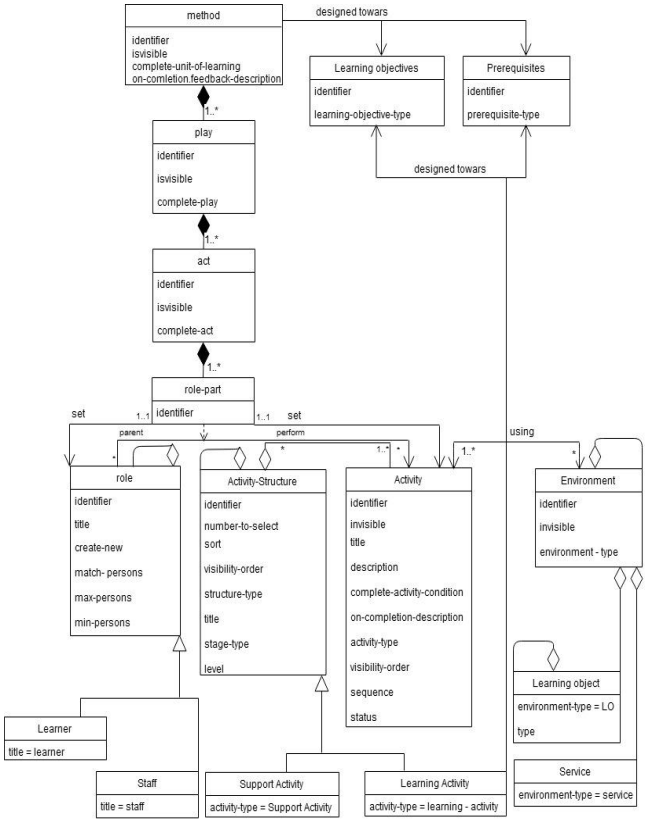

Fig. 3 *Application of Instructional Design for ontological organization of e-learning*

2.4. Web based learning support framework with scaffolding

The processes of supporting e-learning are presented on the fig.4.

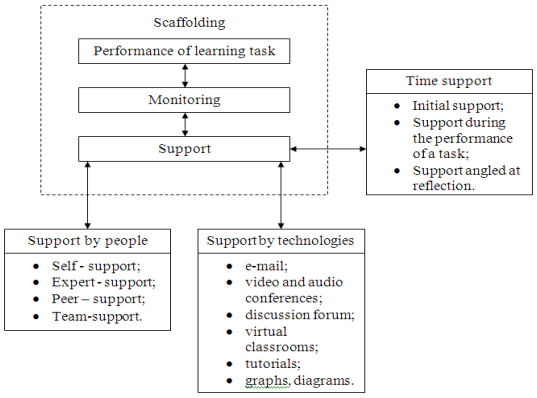

Fig. 4 *Web based learning support framework with scaffolding*

The support has been an effective and intensive way for individuals on users group to learn about the consequences of his behavior, for users group to improves its effectiveness, and for organization to monitor learner progress. Users receive on-going support from their personal tutor. When problems in task performance are expected and known beforehand, place support for these problems in the learning environment, so that the NTEL instead of the mentor becoming the main source of just-in-time support.

These decision aspects, provide a model for the categorization of learning support used in this research.

2.5. A model for E-Learning Network Technologies

The LMS must be guided by instructional design approach. This model (fig. 5) is theoretically motivated by socio-cultural approach and cognitive apprenticeship model for each element of the learning environment. While each form of scaffolding provides support, each differs in the level of social support, collaboration with peers and type of feedback offered. These forms of scaffolding with technology researchers are now developing more principled and innovative forms of instructional design to guide the process.

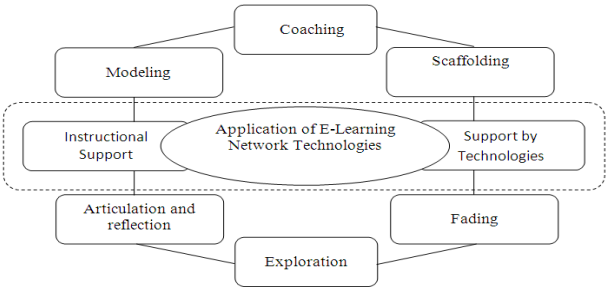

Fig. 5 *A model for E-Learning Network Technologies*

3. A multi-criteria decision-making approach

In recent years, most educational organization have preferred to use open source LMSs. They have to decide which LMS is suitable for them. Problems have been experienced when determining the features to be considered in selecting the most suitable LMS for their institutions due to the high number of LMSs available with different specifications. This has created a multi-criteria problem, which can be solved using a multi-criteria decision making approach (MCDM) [5].

Table 1 *Summary of applications of the DM techniques [4]*

Метод	Честота на приложение	Процент
AHP	128	32,57%
ELECTRE	34	8,65%
DEMATEL	7	1,78%
PROMETHEE	26	6,62%
TOPSIS	45	11,40%
ANP	29	7,38%
Aggregation DM methods	46	11,70%
Hybrid MCDM	64	16,28%
VIKOR	14	3,56%

The selection process is based on a literature review and classification of international journal articles from 2000 to 2014 [4]. MCDM provides strong decision making (DM) in domains where selection of the best alternative is highly complex. MCDM method has been applied to many domains to choose the best alternatives. Where many criteria have come into existence, the best one can be obtained by analysing different scopes of the criteria, weights of the criteria, and the selection of the optimum ones using any MCDM techniques. Table 1 shows frequency of MCDM techniques and approaches. Based on the results presented in this table, a total of 393 studies have employed DM techniques and approaches. Table 1 and fig. 6 shows that AHP method (32.57%), and its applications have been used more than other tools and approaches.

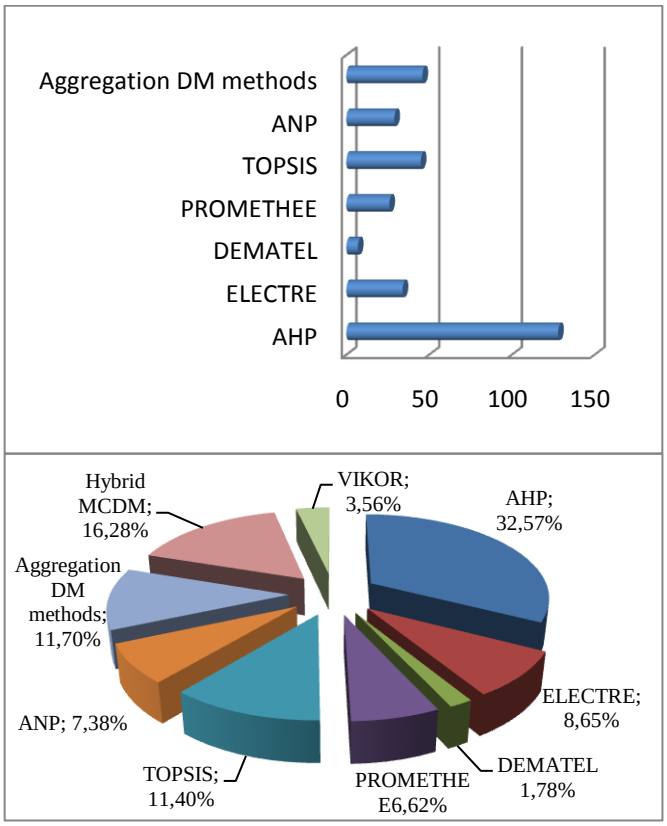

Fig. 6 *Frequency of MCDM techniques and approaches*

Steps of LMS selection process of effective system are [2]: determination of the affecting criteria,questionnaire collection and statistical analysis, weighting these criteria, evaluation of the entire performance according to these weighted criteria. We compare three LMS (Sakai, Moodle, NTEL) with AHP Process. The evaluation criteria used in this study are: usability, accessibility, compatibility, evaluation tools, portability, reliability, sustainability, and user satisfaction. Reveal that which LMS is best, when altered the weight of evaluation criteria values for main object. According to giving priority to criteria weight, the application allow to find best choice (NTEL) and worst choice (Sakai) from all results shown in fig. 7.

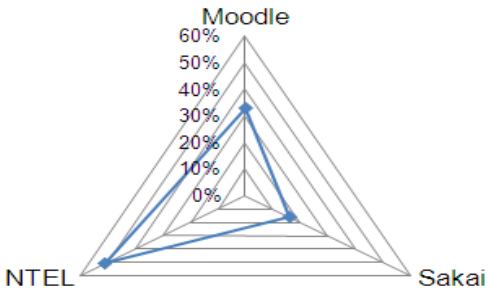

Fig. 7 *Comparison of LMSs*

NTEL provide instructors with support for activities, such as preparation of learning content, structuring and organization of the content in accordance with the chosen teaching strategy, interactions with coordination of users' activities using online communication tools, that allows

learners to collaboratively create and share knowledge. The information coming from users, for instance, how other users have tagged or commented a piece of learning content is an important factor in increasing learner interest.

4. Conclusion

In this paper, we present a learning design ontology based on the IMS LD specification and the LOM standard for metadata. In ontology, the IMS LD elements are modeled in a concept taxonomy in which the relations between the concepts are explicitly represented. The model suggested for structuring the learning objects can be applied as a whole or in separate parts of the learning assistance media which can be set by the teachers themselves without the intervention of the development teams.

The structures obtained as a result of the model application can be very useful at the development of learning management systems through developing a uniform "frame" of the system and its including in a particular semantics can be done later.

It is so important to carry out all types of comparisons, presenting the strengths and weaknesses of the different LMS. According to the AHP method the best solution seems to be the NTEL system.

5. References

1. Ahmed A., A. Ali, S. Talab, Matching User Preferences with Learning Objects in Model Based on Semantic Web Ontologies. International Journal of Engineering Inventions e-ISSN: 2278-7461, p-ISSN: 2319-6491 Volume 4, Issue 3 (August 2014) PP: 00-00.

2. Chao R., Y. Chen, Evaluation of the criteria and effectiveness of distance elearning with consistent fuzzy preference relations, Expert Systems with Applications, 36, no. 7, 10657–10662, 2009.

3. Gaševi D., J. Jovanovi, V. Devedži, Enhancing Learning Object Content on the Semantic Web, Proceedings of the IEEE International Conference on Advanced Learning Technologies (ICALT'04), 2004.

4. Mardani A., A. Jusoh, K. Nor, Z. Khalifah, N. Zakwan, A. Valipour, Multiple criteria decision-making techniques and their applications – a review of the literature from 2000 to 2014, Economic Research-Ekonomska Istraživanja, 2015.

5. Muhammad N., N. Cavus. Fuzzy DEMATEL method for identifying LMS evaluation criteria. 9th International Conference on Theory and application of Soft Computing, Computing with Words and Perception, 2017.

6. Amorim R., M. Lama, E. Sánchez, A. Riera, X. Vila, A Learning Design Ontology based on the IMS Specification, IEEE Journal of Educational Technology Society (Special Issue) , January, 2006.

7. http://ltsc.ieee.org/wg12/files/LOM_1484_12_1_v1_Final_Draft.pdf

8. http://www.imsglobal.org

PERSPECTIVE DEVELOPMENT TENDENCIES OF ELECTRON BEAM TECHNOLOGY IN PRECISION INSTRUMENTS INDUSTRY

ПЕРСПЕКТИВНІ НАПРЯМКИ РОЗВИТКУ ЕЛЕКТРОННО-ПРОМЕНЕВОЇ ТЕХНОЛОГІЇ У ТОЧНОМУ ПРИЛАДОБУДУВАННІ

D. Eng. Sc. Yatsenko I. V.[1], d. Eng. Sc. Kyrychenko O. V.[2] , d. Eng. Sc. , Professor Vashchenko V. A. [1], Dibrova O.S.[2], Mel′nyk V.P.[2]
Cherkasy State Technological University[1] , Ukraine; Cherkassy Institute of Fire Safety named after Heroes of Chornobyl[2] , Ukraine
E-mail: irina.yatsenko.79@ukr.net

Abstract: *Perspective development tendencies of electron-beam technology in precise instruments industry were introduced and after them the following results were obtained: 1. Capacity expansion of electron-beam technology in the optical-electronic instruments industry for obtaining high-quality curved surfaces and the creation of functional microprofiles on them of different geometric forms. A new method of more accurate and reliable processing of curved surfaces of optical elements (concave, buckled, spherical, cylindrical, etc.) was developed for this purpose. 2. Electron-beam surfaces processing of elements from piezoelectric ceramics. Modern production technologies of piezoelectric products are based on the known methods of mechanical, chemical and chemical-mechanical processing of the surfaces of piezoelectric materials, in particular ceramics. The main drawback of these methods is the impossibility of getting high electromechanical and strength characteristics of products from piezoelectric ceramics, which requires additional processing of these products. Electron-radiation technology was used to exclude the mentioned negative defects on the surface of elements from piezoelectric ceramics. 3. Electron-beam processing of nanosized oxide coatings on optical elements. Nanosized oxide coating, which represent the composition of oxides SnO_2, Bi_2O_3, TiO_2, ZnO, SiO_2, Al_2O_3, are applied for improvement of wear resistance, reduction of radiation and convective components of thermal losses on optical elements of precision instruments industry. Thus, the resulting coatings are heterogeneous, contain hidden microdefects (cracks, chips, etc.), the surface contains significant microroughnesses and low microhardness, etc. All this reduces the performance characteristics of these coatings. Their electron beam processing was used for elimination of the mentioned shortcomings and improvement of the quality of these coatings.*

Keywords: ELECTRON-BEAM TECHNOLOGY, PRECISION INSTRUMENTS INDUSTRY, PIEZOELECTRIC CERAMICS, NANOSIZED OXIDE COATINGS ON OPTICAL ELEMENTS

1. Introduction

The modern level of development of precision instrument industry claims increased requirements to the performance characteristics of their elements: microhardness of the surface; spectral transmission coefficient; resistance to external thermal and mechanical shocks, etc., which influence technical and performance characteristics of devices (pulse laser devices of sighting complexes, laser medical devices, infrared devices, etc.) [1-5].

Wide use of traditional methods concerning preparation and processing of surfaces of elements (mechanical, chemical, chemical-mechanical) showed that it is impossible to get simultaneously clean and flawless surface, and also flawless surface layers, which leads to deterioration of technical and performance characteristics of optoelectronic devices [1, 10-12].

As the practice has shown, the most convenient, ecologically friendly and easily controlled method of elements processing is the electron-beam method. Application possibilities of moving electron beam of tape form were shown for polishing elements from optical glass and receiving high purity surfaces with minimal roughness, as well as for strengthening elements from optical ceramics and obtaining surfaces with increased microhardness and thickness of strengthened layers by tens of microns [1, 6-9].

Thereat, the lack of research in the following perspective directions prevents further expansion of application of electron-beam technology in precision instrument making. These directions are:

- electron-beam processing of curvelineal surfaces and creation of functional microprofiles of different geometric forms;
- electron-beam processing of surfaces of elements from piezoelectric ceramics;
- electron beam surface processing of oxide coatings on the elements from optical materials.

Therefore the purpose of this work is to present the preliminary results of researches on the specified directions, confirming their development prospects for precision instrument-making.

2. Results and discussion

Expansion of the possibility of electron-beam technology in the precision instrument industry for obtaining high-quality curvelineal surfaces and creation of functional microprofiles of different geometric forms.

For this purpose a new method of more accurate and reliable processing of curvelineal surfaces of optical elements (concave, convex, spherical, cylindrical, etc.) was developed (Fig. 1, 2) [13].

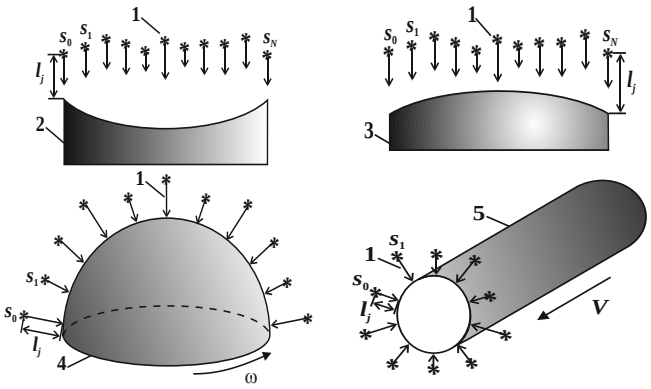

Fig. 1. *Scheme of processing method of curvelineal surfaces of optical elements with the help of the system of discretely placed fixed electron beams (1): concave (2) and convex (3) surfaces; semi-spherical (4) and cylindrical (5) surfaces; s_0, s_1,… – the system of electronic beams, which are located at different distances l_j (j = 0, 1, …) from the processed surface; ω, V – angular velocity of circulation of the half-spherical element and the advance rate of the cylindrical element in the processing area, which provide the distributed thermal influences on their surfaces.*

The point of this method is the following (fig. 3): the curvelineal surfaces of optical elements are placed at distances l_j ($j = \overline{1, N}$, N – the number of beams) from the system of discretely placed occasional electron beams (s_0, s_1,…, s_N), which provide the specified distributions of thermal influences on the surfaces of

optical elements: concave and convex surfaces; spherical and cylindrical surfaces. Semi-spherical elements, for example, can move in the processing area with angular speed of rotation of ω, cylindrical – with the feed velocity of V.

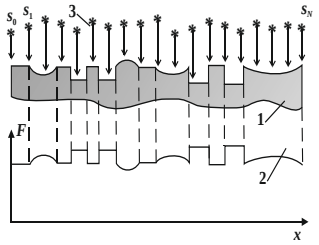

Fig. 2. *The scheme of creation method of functional microprofiles on the surface of optical elements of complex geometric shape with the help of the system of discretely placed fixed electron beams: 1 – specified microprofile on the surface of the element that is obtained through its processing by the system of occasional electron beams s_0, s_1,... s_n with different parameters; 2 – complex spread thermal influence along the surface of the element $F(x)$, which must be realized by optimizing the parameters of beams and their quantity.*

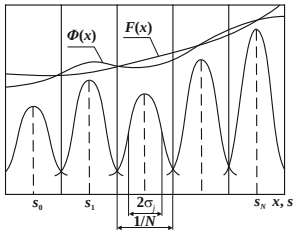

Fig. 3. *Schematic representation of approximation to the given distributed thermal influence $F(x)$ along the surface of the optical element of the totality of discretely placed stationary sources S_j $(j=\overline{1,N})$ of thermal influence of Gaussian type $\Phi(x)$.*

According to the probing results the distribution of the density of thermal influence of j-($j=\overline{1,N}$) of electron beam along x coordinate of the processed surface of the element is described by Gaussin law:

$$F_{nj}(x)=\frac{1}{B\cdot\sqrt{\pi}}\cdot\sum_{j=1}^{N}\frac{I_{\pi j}\cdot V_{yj}}{erf(a_{rj})}\cdot\sqrt{k_{0j}(I_{\pi j},l_j)}\cdot e^{-k_{0j}(I_{\pi j},l_j)(x-s_j)^2} \quad (1)$$

$$erf(a_{rj})=\frac{2}{\sqrt{\pi}}\cdot\int_0^{a_{rj}}e^{-t^2}dt \quad (2)$$

where B is the width of electron beams ($B = 6\cdot10^{-2}\ldots8\cdot10^{-2}$ m); $I_{\pi j}$, V_{yj}, k_{0j} are currents, accelerating voltages and beam concentration coefficients; $k_{0j}=\frac{1}{2\sigma_j^2}=a_{0j}+a_{1j}\cdot l_j+a_{2j}\cdot I_{\pi j}+a_{3j}\cdot I_{\pi j}\cdot l_j$; a_{rj} $(r=\overline{0,4})$ are empirical constants.

The amount of discrete sources N and parameters $I_{\pi j}$, V_{yj} та l_j ($j=\overline{1,N}$) are chosen such, that the approach to a specified distributed thermal influence $F(x)$ along the surface of the optical element by the totality of discretely placed fixed sources s_j ($j=\overline{1,N}$) of thermal influence of Gaussian type $\Phi(x)$ would be minimal:

$$S=\sum_{i=1}^{M}\left[\frac{1}{B\cdot\sqrt{\pi}}\cdot\sum_{j=1}^{N}\frac{I_{\pi j}\cdot V_{yj}}{erf(a_{rj})}\cdot\sqrt{k_{0j}(I_{\pi j},l_j)}\cdot e^{-k_{0j}(I_{\pi j},l_j)(x_i-s_j)^2}-F(x_i)\right]^2\rightarrow\min_{\substack{N,I_{\pi j},\\V_{yj},l_j}} \quad (3)$$

As a result of the conducted numerous experiments for the defined distributions of $F(x)$ (uniform, parabolic, hyperbolic, etc.) it is found that, for example, for $N = 5\ldots7$ the approximation of the total $\Phi(x)$ from the occasional beams to the specified $F(x)$ is reached within 3...5 % in real-time. It is also shown that by increasing the number of sources of electron beams (up to 50... 70) high accuracy can be achieved (relative error to $10^{-4}\ldots10^{-5}$) and compliance with the specified distributed thermal influences along the processed curvilinear optical elements of the specified geometric shape.

Using the obtained dependencies (1) – (3) one can technically implement the developed method in the form of automated control system of technological process of electron-beam processing of surfaces in optical elements of different geometric forms and creation of functional microprofiles on them.

Electron beam processing of elements surfaces from piezoelectric ceramics.

Modern production technologies of piezoelectric products are based on the known methods of mechanical, chemical and chemical processing of the surfaces from piezoelectric materials, in particular ceramics.

The main drawback of these methods is the impossibility of getting high electromechanical and power characteristics of products from piezoelectric ceramics, which requires additional processing of these products. Thus, the imperfection of surfaces and the presence of micro and nanodefects in piezoceramic imposes restrictions on the effectiveness of the whole element base of piezoelectric elements of microtechnics. Above mentioned electron-beam technology was used to exclude the mentioned negative defects on the surface of elements from piezoelectric ceramics.

In the result of the conducted researches on the samples from piezoelectric ceramics ЦТС-19 brand (disks with the diameter of $3{,}5\cdot10^{-3}$ m, 10^{-3} m thick) it was established, that microroughness of the surface decreases from 120…160 nm (fig. 4 a, b) to 95…105 nm (fig. 5 a, b) by electron beam processing.

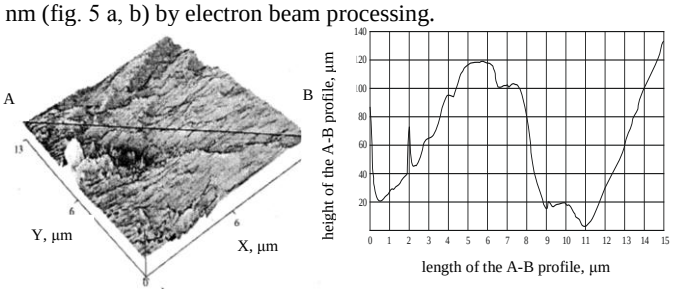

a) b)

Fig. 4. *Topogram (a) and the profile along A – B line of the scanned area (13×13 μm) (b) of the piezoceramic element, which is not processed by electron beam.*

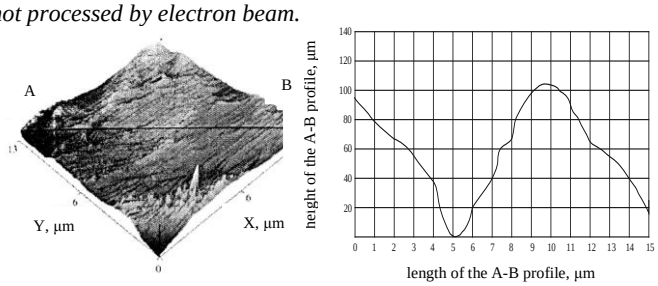

a) b)

Fig. 5. *Topogram (a) and the profile along A – B line of the scanned area (13×13 μm) (b) of the piezoceramic element, which is processed by electron beam.*

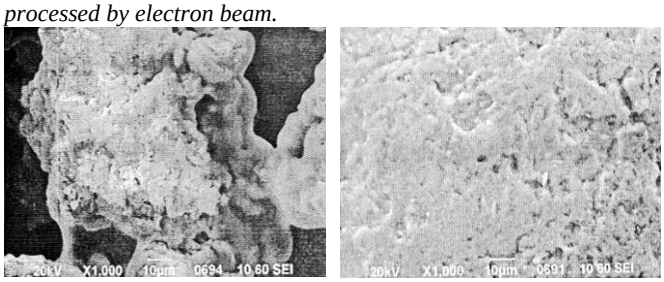

a) b)

Fig.6. *Surface of piezoceramic element before (a) and after (b) electron beam processing.*

It is shown, that after electron-beam processing there is a reduction of surface voidage of the piezoceramic element (Fig. 6): the average size of the voids of the output element is 15... 20 μm

and after electron-beam processing it decreases by 5... 8 μm. At the same time there occurs a removal of individual micro-and nanodefects on the surface of elements (up to 5... 10% microcracks with width to 5...7 μm and up to 50... 60% of voids), its microhardness increases by 0,5… 0,8 MPa. This results, finally, to the increase of their exploitation term, the increase of the electromechanical connection coefficient, the increase of the piezoelectric module and other operational characteristics.

Electron beam treatment of nanosized oxide coatings on the optical elements.

Nanosized oxide coatings, which represent the composition of oxides SnO_2, Bi_2O_3, TiO_2, ZnO, SiO_2, Al_2O_3, are applied on the optical elements of precision instrument industry to improve wear resistance, reduction of radiation and convective components of thermal losses.

One of the methods of obtaining such coatings, which is widely used, is the method of thermal-vacuum deposition of materials, which allows to get nanosized (< 100 nm) coatings in the form of separate layers. The resulting coatings are heterogeneous, contain hidden microdefects (cracks, chips, etc.), the surface contains significant microroughnesses and low microhardness, etc. All this leads to a decrease in the performance of these coatings: their wear desistance decreases; the reflection coefficient in low temperature infra-red area and in the area of visible radiation reduces as well, etc.

For elimination of the mentioned drawbacks and improvement of the quality of these coatings, their electron beam processing was used.

As a result of conducted researches on the samples from optical glass K8 (the plates $6 \cdot 10^{-2}$ m long, $3 \cdot 10^{-2}$ m wide and $4 \cdot 10^{-3}$ m thick were used) it was found that after electron-beam processing of oxide coatings negative microdefects are not observed, and microroughnesses decrease from 30... 35 nm to 9... 15 nm (fig. 7, 8).

Conducted researches of the microhardness of the surface of optical elements with oxide coatings have shown its increase after electron beam processing: from 21,5…17,5 GPa to 24,9…23,7 GPa for Al_2O_3 coating; from 13,1…9,3 GPa to 15,9…14,7 GPa for ZnO coating; from 3,5…2,3 GPa to 7,1…6,3 GPa for TiO_2 coating (fig. 9). Thus for coatings, processed by electron beam, the influence of their thickness on to value of the microhardness surface diminishes by 30…40 %.

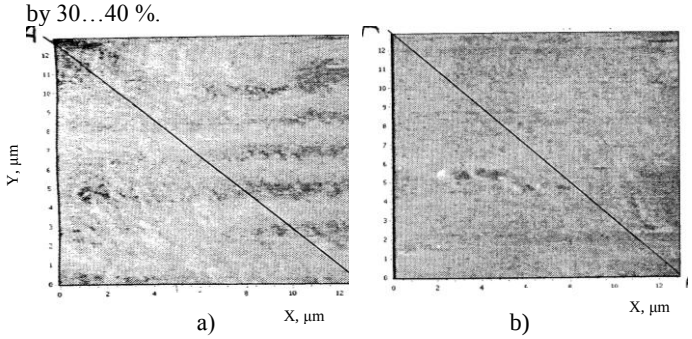

Fig. 7. *Topogram of the surface area (13×13 μm) of the optical element with TiO_2 coating before (a) and after (b) electron beam processing.*

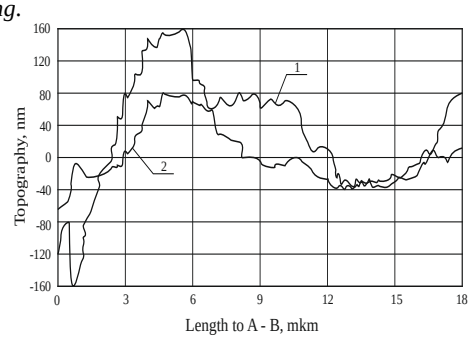

Fig. 8. *Topogram along A – B line of the surface area 13×13 μm) of the optical element with TiO_2 coating before (1) and after (2) electron beam processing.*

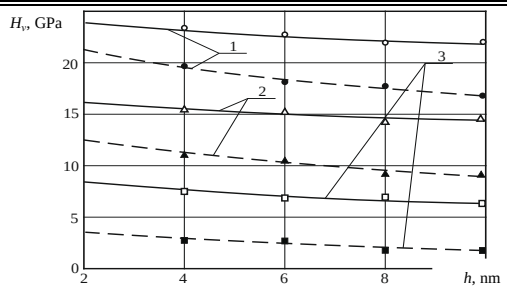

Fig. 9. *Dependencies of surface microhardness of optical elements with oxide coatings Al_2O_3 (1), ZrO_2 (2) and TiO_2 (3) from their thickness: ——— – after electron beam processing; – – – – before electron beam processing; Δ, ○, □, ▲, ■, ● – experimental data.*

It is also found that after electron-beam processing of oxide coatings on the optical elements the term of their exploitation increases by 20... 30%. At the same time voidage of surface decreases by 5... 10% and their wear resistance rises up to 7... 12%.

3. Conclusions

Thus, in the spotlight of modern new technologies used in the optical-electronic instrument-making, electron-beam processing of elements from optical glass and ceramics, elements from piezoceramics, as well as optical elements with nanosized coatings from metal oxides is defined as potentially capable for quality processing of flat and curvelineal elements, obtaining functional microprofiles on their surfaces with the help of electronic beam system, which can be used as element base in microoptics, integrated and fiber optics, optoelectronics, functional electronics and other areas of precision instrument industry.

4. References

1. Vashchenko V. A. Osnovy elektronnoi pbrobky vyrobiv z optychnych materialiv [The basics of electronic processing of optical materials] / V. A. Vashchenko, I. V. Yatsenko, Y. G. Lega, O. V. Kirichenko // Kiev: Naukova Dumka, 2011. – 562 p.

2. H. V. Kanashevych, M. O. Bondarenko, Y. U. Bondarenko, I. V. Yatsenko ta V. A. Vashchenko, "Vyvchennya vplyvu vysokykh temperatur na mikroheometriyu poverkhni optychnoho skla ta p″yezoelektrychnykh keramik" [Investigation of the influence of high temperatures on microgeometry of the surface of optical glass and piezoelectric ceramics] // Materialy II mizhnarodnoyi naukovo-praktychnoyi konferentsiyi "Pryrodnychi nauky ta yikh zastosuvannya v diyal′nosti sluzhby tsyvil′noho zakhystu"(APB im. Heroyiv Chornobylya MNS Ukrayiny, Cherkasy, 2008) [Materials of the II International Scientific and Practical Conference "Natural sciences and their application in the activity of the civil protection service" (APB Heroes of Chernobyl, Ministry of Emergencies, Cherkasy, 2008)] – P.P. 132 – 134.

3. Lycholit, M. I. KP SPB "Arsenal". Osnovni dosyagnennya ta perspektyvy u galuzi spetsialnogo pryladobuduvannya [Main achievements and prospects in the field of special instrument manufacture] // Zbirnyk tez dopovidei 2-i Ukrainskoi naukovo-technichnoi konferentsii "Spetsialne pryladobuduvannya: stan ta perspektivy " [Collection of abstracts of the 2nd Ukrainian Scientific and Technical conference "Special instrument making: Status and Prospects", Desember 6 -7, 2016, Kyiv] – P.P. 11 -15.

4. Yatsenko I. V. Poperedzhennya mozhlyvych ruinuvan optychnych elementiv tochnogo pryladobuduvannya v umovach zovnishnich termodii [A warning of possible destruction of the optical elements of precision engineering in terms of external thermo-influences] / I. V. Yatsenko, V. S. Antonyuk, V. A. Vashchenko, V. V. Tsybulin // Zhurnal nano ta elektronnoi fizyky [Journal of nano- and electronic physics]. 8 (1), 01027 (6 pp) (2016), DOI: 10.21272/jnep.8(1).01027.

5. Yatsenko I.V. Vyznachennya krytychnykh znachen′ parametriv elektronnoho promenyu pry poverkhnevomu oplavlenni optychnykh

elementiv tochnoho pryladobuduvannya [Determination of the critical values of the parameters of an electron beam at the surface melting of optical elements of precision instrumentation] / I. V. Yatsenko, V. S. Antonyuk, V. I. Gordienko, V. A. Vashchenko, O. V. Kirichenko // Zhurnal nano ta elektronnoi fizyky [Journal of nano- and electronic physics]. 9 (1), 01010 (5 pp) (2017), DOI: 10.21272/jnep.9(1).01010.

6. V. A. Vashchenko, I. V. Yatsenko, YU. I. Kovalenko, I. A. Reva ta V. P. Boyko, "Osobennosti opredeleniya mikrogeometricheskikh kharakteristik nanorazmernykh oksidnykh pokrytiy na poverkhnostyakh opticheskikh dielektrikov metodom atomno-silovoy mikroskopii" [Features of the determination of the microgeometric characteristics of nanoscale oxide coatings on the surfaces of optical dielectrics by atomic force microscopy] // Materialy XIX Mezhdunarodnoy konferentsii "Sovremennyye metody i sredstva nerazrushayushchego kontrolya i tekhnicheskoy diagnostiki"(g. Gurzuf, 2011) [Materials of the XIX International Conference "Modern methods and means of non-destructive testing and technical diagnostics" (Gurzuf, 2011)] – P.P. 193 – 195.

7. I. V. Yatsenko, "Influence Patterns of the Finishing Electron Beam Treatment of the Surface of Optical Parts on their Physical-mechanical Properties", Journal of Multidisciplinary Engineering Science Studies (JMESS). Germany. 3 (5), 1764 – 1770 (2017).

8. I. V. Yatsenko Zbil′shennya virohidnosti bezvidmovnoyi roboty ICH-pryladiv samonavedennya ta sposterezhennya shlyakhom elektronno-promenevoyi obrobky optychnykh obtichnykiv [Increased probability of non-failure operation of infrared homing devices and observation by electron beam processing of optical rays] / I. V. Yatsenko, V. S. Antonyuk, V.I. Gordienko, V. A. Vashchenko, O. V. Kirichenko // Zhurnal nano ta elektronnoi fizyky [Journal of nano- and electronic physics]. 10 (4), 04028 (7pp) (2018), DOI: 10.21272/jnep.10(4).04028.

9. M. A. Bondarenko, YU. I. Kovalenko, YU. YU. Bondarenko, S. A. Bilokon' ta I. V. Yatsenko, "Izucheniye mekhanizma formirovaniya ul'tra tonkikh funktsional'nykh pokrytiy na opticheskom stekle pri kombinirovannoy elektronno-luchevoy mikroobrabotke" [Study of the mechanism of formation of ultra thin functional coatings on optical glass with combined electron-beam micro-processing] // Sbornik trudov III mezhdunarodnoy nauchnoy konferentsii "Sovremennyye problemy fiziki kondensirovannogo sostoyaniya, nanotekhnologiy i nanomaterialov" (g. Almaty, Kazakhstan, 2014) [Collection of Works of the 3rd International Scientific Conference "Modern problems of condensed matter physics, nanotechnology and nanomaterials" (Almaty, Kazakhstan, 2014)] – P.P. 64 – 65.

10. Okatov, M. A. Spravochnik optika-technologa [Handbook of optics technologist] / M. A. Okatov, E. A. Antonov, A. B. Baigozhin // Sankt-Petersburg.: Polytechnica, 2004. – 679 p.

11. Zverev, V. A. Opticheskie materialy. Uchebnoe posobie dlya konstruktorov opticheskich sistem i priborov [Optical materials. Textbook for designers of optical systems and devices] / V. A. Zverev, E. V. Krivopustova, T. B. Tochilina // Sankt-Petersburgh: SP NIUITMO, 2009. – 243 p.

12. Vilchinskya, S. S. Opticheskie materialy i technologii [Optical materials and technologies] / S. S. Vilchinskya, V. M. Lisitsyn // Tomsk: Ed. Tomsk Polytechnic University, 2011. – 107 p.

13. I. V. Yatsenko, V. S. Antonyuk, V. A. Vashchenko "Sposib obrobky kryvoliniynykh poverkhon"" [Method of processing of curvilinear surfaces], Patent Ukrayiny na korysnu model′ №119627 (25 Veresen′, 2017) [Patent of Ukraine for Utility Model №116262 (September 25, 2017)].

ТЕНДЕНЦИИ В СВЕТОВНИЯ ДОБИВ И ПОТРЕБЛЕНИЕ НА МОЛИБДЕН

TRENDS IN MOLYBDENUM GLOBAL PRODUCTION AND CONSUMPTION

Eng. Georgi Savov[1], Assoc. Prof. PhD Valeriya Kovacheva-Ninova[2], Assoc. Prof. PhD Vania Vassileva[3], Prof. DSc. PhD Katia Vutova[3]

[1]Premiatec Ltd., Sofia, Bulgaria
e-mail: premiatec@yahoo.com

[2]University of Mining and Geology "St. Ivan Rilski", Sofia, Bulgaria
e-mail: valeria.kovacheva@mgu.bg

[3]Institute of electronics, Bulgarian Academy of Sciences;
1784 Sofia, Bulgaria
e-mail: vvvania@abv.bg ; katia@van-computers.com

Abstract: *An analysis of the historical and current state of global production, processing and consumption of molybdenum ores and their products is presented. The trend of running low of global molybdenum ores will generate a high investment prospects in search, investigation of new productive deposits and construction of new production and processing facilities and the search and development of new technological approaches for recycling and processing of raw materials. New possibilities for production of molybdenum with low content of gases and other impurities are also presented both by refining of enriched and separated natural concentrate and by processing of metal waste from metallurgical production and mechanical treatment.*

Keywords: MOLYBDENUM, RAW MATERIALS, PRODUCTION, PROCESSING, HIGH PURITY MATAL, ELECTRON BEAM

1. Увод

Преходният елемент молибден (Mo) принадлежи към групата на трудно топимите и легиращи редки елементи (B, Ti, Zr, Hf, W, Mo, Ta, Nb и V), които в промишлеността се използват, основно както като чисти метали, така и като легиращи компоненти, в сплавите на черните и цветните метали [1]. Металът притежава редица специфични физико-механични свойства, които определят широкото му приложение преди всичко за инженерни цели, по-важните от които са: висока температура на топене (2623 ^{o}C), нисък коефициент на термично разширение ($4.8.10^{-6}$/K при 25 ^{o}C), висока термична проводимост (138 W/m.K при 20 ^{o}C), незначително налягане на неговите пари (1900-2000 ^{o}C), висока якост на опън и стойност на модула на еластичността (329 GPa), сравнително висока електропроводимост (2.107 S/m при 20 ^{o}C) и др. Характерни за молибдена свойства са и високата корозионна устойчивост, съвместимост със съставките на стъклото, инертност по отношение на азота, въглеродния диоксид и дисоцииран амоняк (до 1100 ^{o}C), устойчивост на сярна, солна и флуороводородна киселина, алкални разтвори и течни алкални метали, магнезий, живак, бисмут и др. Тези свойства определят широкото приложение на метала в различни области на индустрията: черна и цветна металургия, електроника, електротехника, химическа промишленост, стъклопроизводство, приборостроене, самолето- и ракетостроене, медицина и др. [2-7]. Като легиращ метал молибденът придобива все по-значима роля в съвременната индустриална технология, изискваща материали, издържащи на работа при високи напрежения, налягане, температури и силно корозионна среда. Широко разпространената употреба на молибдена в металургичните приложения се дължи на неговата ефективност като легиращ елемент, който не е чувствителен към окисляване, той също повишава механичните свойства на сплавите, укрепва твърдите разтвори и подобрява тяхната издръжливост. Приблизително две трети от произведения молибден се използва за производството на сплави, легирани стомани и суперсплави. Неръждаемите молибденови стомани с необходимата якост и корозионна устойчивост намират приложение във водоразпределителните системи, оборудване за производство на храни и химикали, както и за битово, мединцинско и лабораторно оборудване. Молибденовите легирани стомани с висока якост и твърдост се използват за производството на автомобилни части, тежко строително оборудване и констукции, газопреносни тръби и др. Други значителни приложения на молибдена са в производството на огнеупорни материали и оборудване и в множество химични приложения, включително катализатори, смазочни материали и пигменти. Най-важните приложения на молибдена за крайна употреба в индустрията са в нефто/газова, химическа/ нефтохимическа, автомобилна, преработвателна и енергийна промишлености и машиностроене.

Структурата на световното потребление на първичен молибден (от руда) и приложението на крайните молибденови продукти в индустрията е представена в таблица 1 [8,9].

Таблица 1: *Структура на световното потребление на първичен молибден и приложението му в индустрията за 2016 г.*

Потребление на първичен молибден	**%**	**Приложение на молибден в индустрията**	**%**
Общо сплави	22	Добив и производство на нефт и газ	17
Неръждаеми стомани	19	Химическа и нефтохимическа промишленост	15
Инструментални стомани	9	Автомобилна промишленост	13
Въглеродни стомани	8	Машиностроене	13
Чугун	8	Преработвателна промишленост	9
Катализатори	8	Енергийна промишленост	8
Mo метал/сплави	7	Друг транспорт	8
Суперсплави	4	Строителство/конструкции	6
Смазочни материали/пигменти	3	Космическа промишленост и отбрана	3
Др. химикали	1	Електроника/медицина	2
Други	11	Други	6

Потреблението на молибден се увеличава и според Roskill Information Services Ltd. нарастването ще продължи [10]. Според International Molybdenum Association (IMOA) световното молибденово потребление за 2015 г. е 231.4 хил. t, а за 2016 г. нараства до 232.5 хил. t (International Molybdenum Association, 2017). В световен мащаб по потребление на

молибден Китай заема първо място, следван от Европа. Само за първото тримесечие на 2018 г. те са консумирали съответно 21772.43 t Mo и 16645.84 t Mo [11]. Понастоящем Китай оказва най-голямо влияние върху пазара на молибден, тъй като разполага със значителни мощности за преработка на молибденовите концентрати и експортен потенциал на молибденови продукти.

Според оценките на British Geological Survey [12] на химическите елементи или групи елементи с икономическа значимост, молибденът е определен със сравнително висок индекс за рискова доставка със стойност 8.1 при скала от едно до десет.

2. Суровинна база, ресурси и запаси, минно производство

Доказаните молибденови ресурси за 2017г. са оценени на около 25.4 млн.t Mo, а общите запаси [13] на около 17 млн.t Mo. За двадесет годишен период запасите са се увеличили 3.1 пъти, което показва че е извършена обемна търсеща, проучвателна и оценъчна дейност (фиг.1). Според използвана класификация, определяща скоростта на изтощаване на минните запаси [14,15], молибденовите запаси се характеризират с умерена до висока скорост на изтощаване, при който индексът на използване на запасите (ИИЗ, %) е по-голям от 1.7 %. За двадесет годишния период ИИЗ намалява 1.3 пъти, но е със стойност 1.7 % за 2017г. и 2.3 % за 1997г. Минерално-суровинната база на молибдена се характеризира с висока степен на концентрация на запасите. Сравнението на запасите по страни за 1996г. и 2017г. дадени на фиг.2 показва, че има мащабно преразпределение в световните молибденови запаси. За 2017г. около 95 % от световните запаси са съсредоточени в пет страни с дялово участие 49.1 % за Китай, 16 % за САЩ, 13 % за Перу, 10.6 % за Чили и 5.9 % за Русия, докато за 1996г. около 95.5 % са съсредоточени в 7 страни - САЩ 49 %, Чили 20 %, Китай 9.1 %, Канада 8.2 %, Русия 4.4 %, Перу 2.5 %, Казахстан 2.4 %. Най-голямо увеличение на запасите за периода се наблюдава в четири от страните – Китай 16.6 пъти, Перу 15.7 пъти, Чили 1.6 пъти и Русия 4.2 пъти.

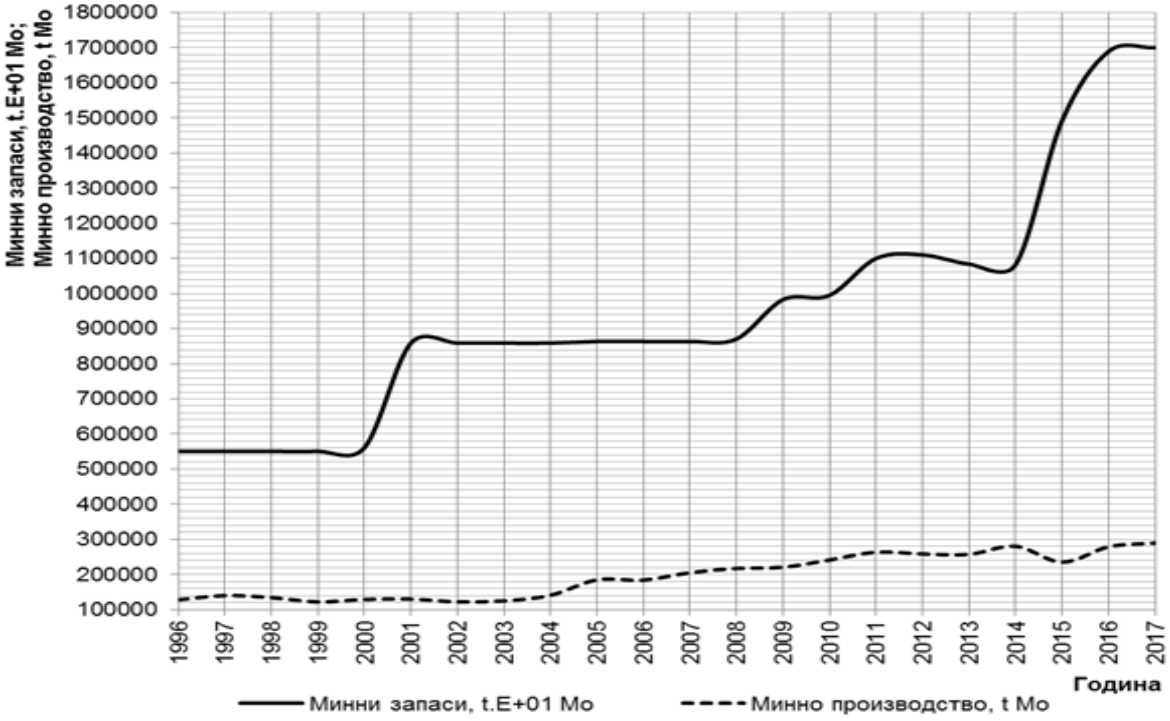

Фиг. 1 *Световни минни запаси и производство на молибден.*

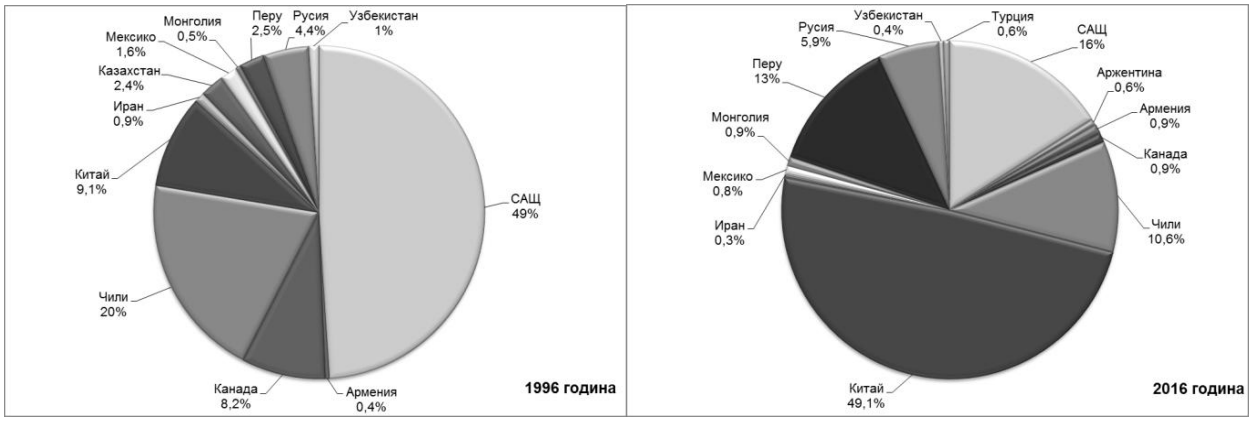

Фиг. 2 *Разпределение на световните минни запаси на молибден за 1996г. и 2016г.*

Към основните геолого-промишлени типове молибденови находища се отнасят плутоногенно хидротермалните (щокверкови молибден-порфирни и медно-молибден-порфирни), скарновите, и грейзеновите (грейзеново щокверкови, грейзеново жилни и кварцово жилни). Основа на минерално-суровинната база на молибденовите руди са плутоногенно хидротермалните находища, в които е съсредоточено 96.4% от световните молибденови запаси (над

70 % в щтокверкови медно-молибденови порфирни и над 20 % в щтокверкови молибден-порфирни) и са с най-голямо икономическо значение. Скарновите находища заемат 2.9 %, а грейзеновите 0.7 % от световните молибденови запаси. Скарновият тип обединява комплексни находища с молибден-волфрамови и по-рядко молибден-медни руди. Грейзеновите също са комплексни находища с волфрам-молибденови и волфрам-калаени (с Mo, Bi и редки метали) руди. В таблица 2 са представени главните промишлени молибденови находища [16].

Таблица 2: *Основни промишлени молибденови находища.*

Тип находище	Рудни минерали		Находища
	Основни	**Второстепенни**	
Плутоногенни хидротермални:			
Кварц-молибденитова формация	MoS_2, (Mn,Fe) $[WO_4]$	SnO_2, $Ca[WO_4]$, FeS_2, FeAsS, $CuFeS_2$, PbS, ZnS и др.	Белуха, Бом-Горхон, Букука, Давенда, Джида, Жирекен, Шахтама, Умалта (Русия); Верхнее Кайракты, Шалгия (Казахстан); Ред-Роуз, Босс-Маунтин (Канада); Квеста-I и Квеста-II (САЩ); Тумен-Цокто (Монголия); Ляндушан, Щанпин (Китай) и др.
Кварц-молибденит-серицитова и кварц-молибденит-халкопирит-серицитова формация	MoS_2, $CuFeS_2$, FeS_2	Fe_3O_4, Fe_2O_3, Cu_5FeS_4, PbS, ZnS и др.	Клаймакс, Хендерсън, Бингем (САЩ); Коунрад, Бозшаколь (Казахстан); Калмакыр (Узбекистан); Каджаран, Агарак (Армения); Сора (Русия); Токанема (Перу); Чукикамата, Ел Тениенте (Чили); Ерденет (Монголия) и др.
Скарнови	MoS_2, $Ca[WO_4]$, FeS_2, $Ca(W,Mo)O_4$, $CuFeS_2$, Fe_3O_4	PbS, ZnS и др.	Тырныаузск, Киялых-Узень, Ингичке и др. (Русия); Санг-Донг (РКорея); Азгур (Мароко); Пайн-Крик (САЩ); Каратас-I и Каратас-IV (Казахстан); Янцзъ-Чжандзъ (Китай); Байтца (Румъния); Тахталъдаг (Турция); Чорух-Дайрон (Таджиксистан); Койташ, Лянгар (Узбекистан)
Грейзенови	MoS_2, (Mn,Fe)$[WO_4]$	SnO_2, Bi_2S_3, Fe_3O_4, FeS_2, $CuFeS_2$, PbS, ZnS	Первомай, Булуктай (Русия); Акчатау, Коунрад, Жанет (Казахстан); Югодзър (Монголия); Серро-Асперо (Аржентина); Сихуа-шан (Китай) и др.

Известни са около 20 молибденови минерала, но с основно промишлено значение е молибденита MoS_2 (Mo 59.9 %), от който се извлича над 95 % от добивания в света молибден. Типично за молибденита е наличието на изоморфни примеси от рений (Re), чието съдържание достига до 0.3 (0.33) %. Минералът с второстепенна икономическа роля е молибдошеелита $Ca(Mo,W)O_4$ (0.5-15 % Mo), а минералите повелит $Ca[MoO_4]$ (48 % Mo), феримолибдит $Fe_2[MoO_4]_3.7H_2O$ (40.5 % Mo) и вулфенит $Pb[MoO_4]$ (25.7 % Mo) са с незначително икономическо значение. Съдържанието на молибден в рудите на молибден-порфирните находища е от 0.05 до 0.5 %, а в медно-молибден-порфирните от 0.005 до 0.025 %.

Световното минно производство на молибден и разпределението му по страни са показани на фиг.1 и фиг.3. Световното минно производство от 1996 до 2017г. се е увеличило 2.3 пъти (през 1996г.- 128460 t Mo; през 2017г.- 290000 t Mo). При поддържане на глобалното минно производство на нивото на 2017г., запасите ще гарантират световна осигуреност с молибден за не повече от 60 години. Сравнението на минното производство за 1996г. и 2016г. показва отново мащабно преразпределение на производството по страни. За двете години около 98 % от световното минно производство е концентрирано в девет страни. Дяловото участие за 1996г. е както следва - САЩ 42.7 %, Китай 19.5 %, Чили 14 %, Канада 7 %, Русия 6.6 %, Мексико 3.0 %, Перу 2.9 %, Монголия 1.7 % и Иран 0.9 %, докато за 2016г. – Китай 46.6 %, Чили 19.9 %, САЩ 12.8 %, Перу 9.2 %, Мексико 4.2 %, Армения 2.3 %, Иран 1.2 %, Русия 1.1 % и Канада 1.0 %. Световното минно производство на молибден е нараснало с 4 % през 2017г. (290 хил.t Mo) в сравнение с 2016г. (279 хил.t Mo).

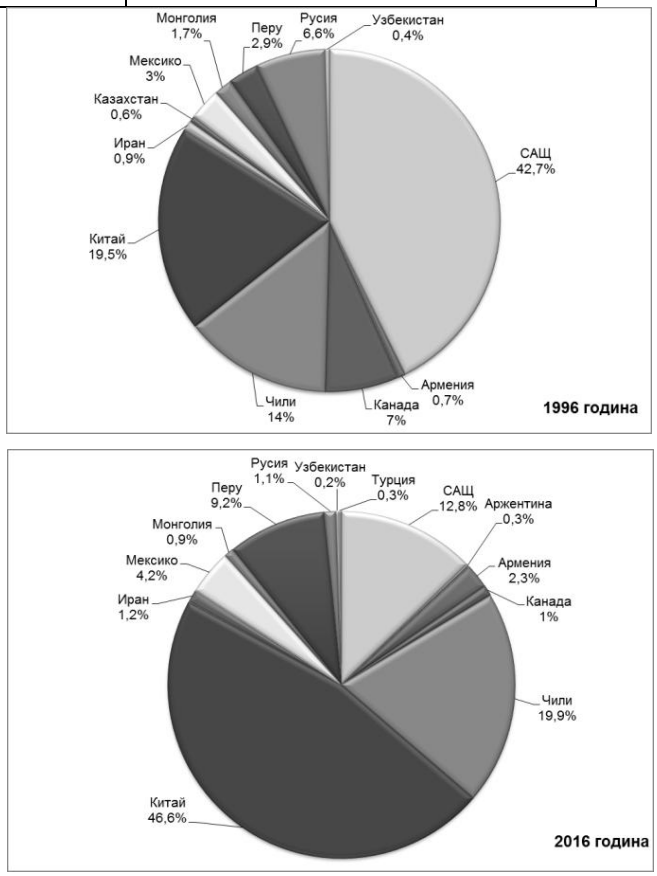

Фиг. 3 *Разпределение на световното минно производство на молибден за 1996г. и 2016г.*

От началото на 2010г. новият и разширен капацитет на минните производители на мед от медно-молибденови руди доведе до свръх предлагане на молибден до 2015г. Въпреки усилията на много минни производители да намалят производството от молибденови руди, редица мини бяха затворени през 2014г. и 2015г., включително Thompson Creek Mine, Endako Mine (TCMC) и Mineral Park Mine (Mercator). Това намали доставките на молибден с повече от 10 000 t, но те бяха компенсирани от увеличаване на производството в медно-молибденовите мини и най-вече в Sierra Gorda (Чили) и в молибденовата мина "Yichun Luming" (Китай). Очаква се съществуващите производители на молибден да формират по-голямата част от допълнителните доставки до 2020г., особено от мините в Китай и САЩ [10].

3. Производство на молибден, основни процеси за извличане и преработване

Първични източници

Въпреки че молибденът се съдържа в различни минерали, само молибденитът (MoS2) е подходящ за промишлено производство на продукти от молибден. Молибденът се извлича от първични молибденови рудници или като съпътстващ продукт при други – основно медни рудници. Където молибден е първичен продукт, той обикновено се извлича под формата на сулфиден концентрат, който се подлага на пържене за да се превърне в молибденов оксид.

От руди, където молибденът е съпътстващ, обикновено молибденовият концентрат се подлага на излужване за намаляване на съдържанието на мед до приемливи нива, преди те да бъдат изпратени за по-нататъшна обработка за производството на Феромолибден, амониев молибдат или молибден метал. На схемата на фиг.4 са илюстрирани основните производствени процеси [17].

Приблизително 50 % от производството на молибден в света идва от медно-молибденова руда. В Европа такива медни мини са Herzogenhügel (Белгия), Елаците (България), Kimmeria (Гърция), Recsk (Унгария), Polkowice, Sieroszowice, Rudna, Gaworzyce, Lubin-Malomice, Niecka Retkow и Wartowice (Полша), Аитик и Лаверня (Швеция), Майданпек, Борска река и Велики (Сърбия).

След като се получи концентрат, една малка част от него се прилага директно за производство на чисти молибден съдържащи химикали, а останалата по-голяма част се преработва до молибденов оксид, важно изходно съединение за праховата металургия и производството на феромолибден.

По-голямата част от концентрата се пържи и след това се използва директно в стоманодобивната и желязната промишленост, докато останалата част претърпява допълнителна преработка, за да се получи висококачествен молибденов оксид, подходящ за използване в катализатори, фармацевтични продукти, торове, пигменти и др.

Има няколко хидрометалургични техники, които могат да се използват за извличане на молибден от обогатителни концентрати. В много случаи се извършват етапи на предварителна обработка за намаляване на примесите преди пържене. Обикновено, натриев цианид се използва за отстраняване на мед и злато, железен хлорид за отстраняване на мед, олово и калций и солна киселина за отстраняване на олово и бисмут [18,19].

Извличането чрез автоклавно окислително излужване се превръща в най-популярната хидрометалургична техника, поради неговата екологичност и гъвкавост при третиране на високо/нискокачествени концентрати [18]. Процесът включва автоклавна оксидация, пречистване на разтворите и кристализация, сушене на крайния продукт, калциниране и опаковане.

Фиг. 4 *Типична технологична схема за преработка на молибденови руди.*

Вторични източници

Някои отпадъци, съдържащи молибден, използвани като вторични ресурси, са показани в таблица 3.

Таблица 3: *Mo Вторични ресурси.*

Наименование на източника	Индустрия	Съдържание на Mo
Отработени киселини	Производство на осветителни тела	40-70 г/л
Прахове от индустриални филтри	Електроцентрали на тежки горива	~0.35%
Димни прахове	Стоманодобив	0.02 до 1.2%
Утайки	Стомано-преработка	0.02 до 1.2%
Медни шлаки	Медно-преработвателна	0.3%
Промишлени отпадъчни води	Медно-молибденов и урано-добив и преработка	10-900 мг/л
Радиоактивни отпадъци	Mo/Tc генератори в медицината	-
Прах от пържилни пещи	Пържене на молибденови концентрати	-

Молибденът е напълно рециклируем метал. Около 60 % от скрапа от молибден се използват за производството на неръждаема стомана и стоманени конструкции. Останалата част се използва за производство на легирана инструментална стомана, супер-сплави, високоскоростна стомана, чугун и химикали.

Що се отнася до рециклирането на стоманен скрап, съдържащ Mo, общият подход е повторно топене на стоманения скрап, например, в електрическа дъгова пещ. Преди да бъде подложен на повторно топене обаче, скрапът обикновено трябва да бъде предварително обработен, за да: 1) се гарантира, че скрапът е с подходящ размер, който да се зарежда в пещта; 2) се осигури хомогенен състав на скрапа; 3) се отстранят примесите от скрапа.

В случай на отработени катализатори, те обикновено се рециклират чрез изпичане, за да се елиминира съдържанието на C и S (обезмасляване и декоксуване) и/или да се улесни превръщането на огнеупорния метален оксид в други форми. След това се извършва раздробяване/смилане, след което се подлагат на процес на излужване [17].

4. Получаване на метали и сплави с висока чистота

За специалните приложения на молибдена изискванията към механичните му свойства са все по-големи. Чрез легиращи добавки е възможно получаване на молибденови сплави с висока температура на рекристализация, добра корозионоустойчивост и якост при повишени температури.

Анализът на българския и световен опит за получаване на чисти труднотопими и химически активни метали показва, че от съвременните металургични методи, като достатъчно ефективни за рафинирането на молибден са се наложили "праховата металургия", електролизата на соли, металотермичното йодидно рафиниране и някои от методите на специалната електрометалургия като плазмено-дъгово топене (ПДТ), вакуумно индукционно топене (ВИТ), електроннолъчево топене (ЕЛТ), кристалофизически (зонно) топене, които се прилагат успешно в металургичната практика по света поотделно или комбинирани в различна последователност на металургичния процес.

Основни промишлени методи за получаването на чист молибден са редукционните – молибденови оксиди, хлориди или амониеви соли се редуцират чрез водород до молибден на прах или метална гъба, която се преработва до плътни метални слитъци чрез спичане или топене. Класически методи за получаване на молибден са праховата металургия и електродъговото топене. За някои приложения, чистотата, респективно технологичните свойства на молибдена, получен по тези методи, са недостатъчни.

Тези технологии за преработка на молибден не осигуряват на метала достатъчно добра пластичност и способност да се заварява. Физико-механичните свойства на молибден, получен чрез спичане, са твърде анизотропни и зависят от изходното състояние, чистотата и структурата на праховете преди спичане [20]. Металът, получен след редукцията, е с висок процент от метални и газови примеси. Необходимо е той да бъде подложен на допълнително рафиниране. При промишленото производство на чист молибден и на молибденови сплави, в страни като САЩ, Украйна, Русия и др., за допълнително рафиниране са се наложили методи като вакуумно-дъгово топене (ВДТ) и електроннолъчево топене (ЕЛТ).

За получаване на чист молибден (> 99.99 %) все по-често се използва съчетаването на различни химични, електрохимични и физико-химични металургични методи. Като заключителен етап на металургичния процес обикновено се прилагат вакуумните електрофизични методи, при които в резултат от съвместното протичане на изпарение, кондензация, дифузия и кристализация на метала се осъществява отстраняване и/или равномерно разпределение на останалите примеси (метални, неметални и газове) в обема на рафинирания чист молибден. Подходящи методи за доброто рафиниране на металите (в частност на молибдена) са вакуумните методи като дистилация, високовакуумно отгряване, електроннолъчево топене, зонно топене и прекристализация и др. При вакуумните методи, лимитиращи за рафинирането на метала са главно газовите и газообразуващи примеси като азот, водород, кислород и въглерод. Крайната степен на рафиниране се постига чрез ускоряването и пълното протичане на газоотделянето от течната метална повърхност, контактуваща с вакуумната среда.

Така при рафиниране на молибден в плазмено-дъгови пещи, съдържанието на въглерод в рафинирания метал може да бъде намалено до 0.01 %, а съдържанието на кислород – до 1 ppm. Още по-добро рафиниране се постига чрез зонно топене на молибден. Съдържанието на въглерода от 0.01 % в изходния метал може да бъде намалено до концентрации по-ниски от 0.002 % след зонно рафиниране, при което рафинираният молибден запазва своите пластични свойства до температури (-140 0C). Молибден с такова съдържание на газове може лесно и бездефектно да се валцова и щампова без нагряване.

Получаването на нови конструкционни материали, чисти метали и сплави със специфични физико-химични свойства е неразривно свързано с усъвършенстване на съществуващите и разработване на нови технологични процеси. Най-големи са възможностите на методите, протичащи при високи температури и висок и свръх висок вакуум. Практическата реализация на тези процеси изисква мощни източници на нагряване с висока плътност на енергия. Най-перспективни методи за осъществяване на тези процеси са плазмените и електроннолъчевите методи на нагряване.

Между изброените методи като безспорен лидер се е доказал електроннолъчевият метод за топене и рафиниране във вакуум. В сравнение с други методи от специалната електрометалургия, методът има някои предимства, като например: чистота на вакуумната среда, в която протичат процесите, възможност да се прегрява течния метал до високи температури, липса на допълнително замърсяване от контакт на материала с керамични тигли, поради използването на водноохладен меден кристализатор, в който се отлива получавания блок. Тези предимства, комбинирани с възможността да се поддържа течния метал в прегрято състояние достатъчно дълго време, правят метода предпочитан пред останалите конвенционални, а и пред

другите методи на специалната електрометалургия (вакуумно-дъгово, вакуумно-индукционно и електрошлаково топене) при получаването на метали и сплави с ниско съдържание на газове и други примеси.

Основните особености на електронния лъч, като източник за нагряване са: възможност за плавно изменение на температурата на метала в широки граници (от стайна до 5000–6000 ^{0}C), изключителна гъвкавост, позволяваща създаване на различни лесно регулиращи се зони на нагряване, които осигуряват стабилност на автоматизацията и програмирането на процеса на нагряване, висок к.п.д. на електроннолъчевия източник. При електроннолъчевия метод за претопяване и рафиниране на метали тези предимства на лъча са съчетани с висок вакуум. Използването на вакуума в металургията дава възможност за изместване на равновесието на реакции и процеси, протичащи с участието на газова фаза. При понижаване на налягането протичат реакции, които са невъзможни при атмасферно налягане: редукция, дегазация, изпарение на летливи компоненти и др. Тези хетерогенни реакции протичат на границата на две или три фази и сумарната им скорост зависи от скороста на движение на веществата към граничната повърхност, от химичните реакции, които протичат на тази повърхност, от скоростта на отделяне от повърхността, от условията на топлопредаване и др.

При ЕЛТ на труднотопими метали (молибден, волфрам, тантал) течната вана е плитка. По-подходящо за постигане на ефективен рафиниращ ефект е многократното последователно претопяване вместо еднократно продължително задържане на метала в прегрято състояние. Чрез многократно краткотрайно рафиниране и непрекъсната осцилация на лъча по време на рафинирането се осъществява сегрегация на генерираните от химични реакции оксидни включения във вид на равномерно разпределени частици.

Наличието на кислород в състава на молибден повишава неговата трошливост. При концентрация на кислород 0.01 %, молибденът губи пластичните си свойства при 300 0C, докато при концентрация на кислород 0.002 %, температурата на трошливост е 25 ^{0}C, а при концентрация на кислород 0.0001 % е -196 ^{0}C. Кислородът се съсредоточава в свързано състояние като оксиди по границите на зърната в структурата на твърдия метал. Доказан рафиниращ ефект и понижаване вредното влияние на кислорода върху пластичните качества на молибдена се постига чрез зонно електроннолъчево топене и израстване на монокристални слитъци с дължина от порядъка на 500 мм и сечение до 80 мм [21]. В тези монокристали концентрацията на кислород е 4 ppm, а молибденът запазва своите пластични свойства до температурата на течен Не. Фолио от молибден с такава чистота може да бъде подложено на студено щамповане и да се получат бездефектни детайли с отговорно предназначение в електровакуумни прибори.

Отпадъците, съдържащи ценни труднотопими и химически активни при висока температура метали, се считат за важна вторична суровина при производството на тези метали. Проучване за наличните количества на отпадъци от труднотопими и химически активни метали показва, че най-големите количества отпадъци, съдържащи молибден и негови сплави са: скрап от металургични производства; отработени катализатори, съдържащи молибден и кобалт; стружки и малки парчета метал. Има данни и резултати за електроннолъчево претопяване и рециклиране на молибденов скрап до получаване на слитъци или полуфабрикати от чист молибден [22]. След двукратно електроннолъчево рафиниране на молибденов скрап с мощност 1200 kW и производителност 50 кг/ч са получени слитъци с размери 1570x470x150 мм. Съдържанието на кислород намалява от 600 ppm в молибденовия скрап преди ЕЛТ до 20 ppm в Мо след рафинирането. Съдържанието на С при същите условия за ЕЛТ намалява от 260 ppm до 50 ppm. От рафинирания Мо е изтеглен проводник с химичен състав и свойства, подходящи за изработване на електроди в газоразрядни лампи и други електровакуумни прибори.

Отработените катализатори – отпадък от нефтохимическата промишленост също са суровина, подходяща като изходен материал за производство на редки труднотопими метали чрез ЕЛ рециклиране. Срокът на употреба на съдържащите Мо катализатори обикновено е от 5 до 7 години, след което те се изхвърлят от употреба и се натрупват в депа. Съдържанието на Мо в тях е от 7 % до 13 %. Обикновено за рециклирането на тази суровина се прилагат пирометалургични (отгряване, спичане) и хидрометалургични (алкализиране, химическо отлагане, екстракция, йонообменна сорбция) технологии. Тези технологии са ефективни за извличането на Мо и други метали, присъстващи в тези катализатори. Чрез тях успешно се извлича до 95 - 98 % Мо [23]. Проблем е, че при тези технологии (особено при хидрометалургичните) се използват неекологични алкални и киселинни реактиви, които са вредни за обслужващите работници и за околната среда.

5. Развитие на пазара и цени

Европа е произвела през 2012г. четири метрични тона (като метално съдържание) на молибден и осем тона през 2013г., всички в Норвегия. Потреблението на молибден в Европа през 2013г. е 63 500 t. Европа е вторият най-голям потребител на молибден в света със средно годишно потребление от 63 500 тона през 2011 и 2012г., което представлява 25 % от годишното световно производство.

През 2015г. общото световно производство на молибден е приблизително 267 000 тона. Що се отнася до вноса в ЕС, молибденовите отпадъци и скрап представляват най-големите количества от внесени продукти с 3 221 019 тона, последвани от молибденови пръти (830 667 тона), необработен молибден (59 1937 тона), молибден прах (231 320 тона) и Молибден тел (163 663 тона), главно от САЩ, Китай и Армения. Основният износ на продукти от молибден в ЕС са отпадъци и скрап (336 738 тона изнесени), следвани от молибден прах (229 751 тона) и необработен молибден, включително пръти (136,367 тона), обикновено в САЩ, Бразилия и Мексико.

Феромолибден (FeMo) е една от най-важните молибденови сплави, със съдържание на молибден 60-75 % и е основният ресурс използван в легирането с молибден на високоякостни нисколегирани стомани. В ЕС Австрия е единствената страна, която произвежда малки количества FeMo. Белгия е най-големият износител на FeMo, следвана от Великобритания и Холандия, докато Германия е най-големият вносител, следвана от Италия, Белгия, Испания и Швеция. Очаква се желязната и стоманодобивната промишленост да продължи да стимулира потреблението на молибден в Европа и по света. Молибденът се използва предимно като легиращ елемент в стомана, чугун и цветни метали. ЕС е вторият най-голям производител на стомана в света след Китай, с продукция от над 177 милиона тона стомана годишно (11 % от световното производство), което означава, че ЕС ще трябва да продължи да внася молибден.

Голямо количество молибден идва от рециклирането. Според проучване, проведено от изследването на пазара на стомана и метал през 2011г., почти 80 000 тона (26 %) от всичкия произведен молибден идва от рециклирани материали, което означава, че скрапът е много важен за веригата на доставки. Европа е регионът с най-високата първоначална употреба на молибден скрап, с темп от около 3 000 тона годишно.

IMOA [11] изчислява, че търсенето на молибден от краен потребител може да нарасне средно с 3.6 % в периода до 2024г. и подобна стойност на растеж от 4.6 % е публикувана в „Molybdenum Market Outlook" [24]. Roskill също анализира еволюцията на този метал и прогнозира увеличение за Европа с около 105 kt/година между сега и 2025г., и че сегашният капацитет е недостатъчен, за да отговори на този ръст в търсенето [25]. Тъй като пазарът за основните приложения на молибден

нараства и няма потенциални заместители на молибден по отношение на неговите приложения в машиностроенето и в автомобилостроенето, нефта и газа, енергетиката, химическата / нефтохимическата, преработвателната, космическата, отбранителната промишлености, електрониката търсенето на молибден се очаква да нарасне съответно. Молибденът също е бил предложен като потенциален заместител на волфрам и ниобий, разглеждани като CRM [17].

Като се имат предвид добрите търговски отношения, които ЕС има със страните производителки, неговата силна промишлена база и относително ниските разходи и голямото количество молибден, балансът между търсенето и предлагането не би трябвало да предизвиква голяма загриженост за Европа в средносрочен план. Ресурсите на молибден са достатъчни, за да осигурят световните нужди в обозримо бъдеще [17].

6. Заключение

Изложеното по-горе позволява да бъдат направени следните основни изводи за състоянието и бъдещото развитие на добива, преработката и производството на молибден и молибденови продукти:

- Тенденцията за продължаващо нарастване на световното потребление на молибден ще се запази и през следващите едно-две десетилетия в условията на прекратяване на дейността на редица от мащабните действащи минни обекти;
- Независимо от увеличаващия се дял в използването на молибденов скрап и факта, че към момента ресурсите на молибден са достатъчни, е необходимо да се продължат проучването и въвеждането в експлоатация на нови находища;
- Новите приложения на молибдена и неговите сплави в съвременни технологии и направления предполагат повисоки изисквания към състава, структурата и технологичните й свойства, които могат да бъдат постигнати единствено чрез прилагането на съвременни металургични методи. Добра възможност е електроннолъчевият метод за топене и рафиниране, който съчетава предимствата на вакуумната металургия и високоенергийната специална електрометалургия. Опитът и оборудването за прилагането на метода при получаване на чисти метали и сплави със специални изисквания към състава и свойствата им могат да бъдат приложени и при производството на чист безкислороден молибден;
- Инвестирането в нови и развитието на съществуващите минни мощности за добив и преработка на молибденсъдържащи руди е перспективно с ниска компонента на пазарния риск.

Благодарности

Авторите Г.Савов, В.Ковачева-Нинова, В.Василева и К.Вутова изказват благодарност за подкрепата на Националния Фонд „Научни изследвания" по договор ДН17/9.

Литература

[1] Филянд М.А., Е.И. Семенова. 1964. Свойства редких элементов, изд. Металургия, Москва.
[2] IMOA. 2007. Molybdenum - an extraordinary metal in high demand, via https://www.imoa.info/download_files/molybdenum/Molybdenum.pdf
[3] IMOA. 2013. Applications of Molybdenum and its Alloys, via https://www.imoa.info/download_files/molybdenum/Applications_Mo_Metal.pdf
[4] IMOA. 2015. Lighting the way to a greener future, via https://www.imoa.info/download_files/molyreview/excerpts/15-1/LED.pdf
[5] Ковачева В., В. Велев, И. Нишков, Т. Колева. 2009. Молибденът-метал с удивителни свойства и широко приложение, Минно дело и геология, бр.8-9, стр.39-42.
[6] Ковачева-Нинова В., В. Велев. 2010. Тенденции в производството и потреблението на молибден- металът на съвременния живот, Геология и минерални ресурси, бр.7-8, стр.17-23.
[7] IMOA. 2018. MoRe® unique implants, via https://www.imoa.info/download_files/molyreview/excerpts/18-1/MoRe_implants.pdf
[8] International Molybdenum Association, "Uses of new Molybdenum", via http://www.imoa.info/molybdenum-uses/molybdenum-uses.php
[9] www.statista.com
[10] Roskill Information Services Ltd. 2017. Global industry markets and outlook to 2026, London, United Kingdom
[11] www.imoa.info
[12] www.bgs.ac.uk/mineralsuk/statistics/risklist/html
[13] U.S. Geological Survey, Mineral Commodity Summaries, January 2018
[14] Сластунов С.В., В.Н. Королева, К.С. Коликов, Е.Ю. Куликова, А.Е. Воробьев, В.В. Качак, В.И. Бабков-Эстеркин, А.Т. Айруни, А.С. Батугин, А.А. Шилов, Горное дело и окружающая среда, Москва, Логос, 2001, с.192.
[15] Ковачева В., В. Велев, Съвременни аспекти за устойчиво развитие на минералните ресурси, Минно дело и геология, 2018, бр.3, стр.35-41.
[16] Ермолов В.А., Г.Б. Попова, В.В. Мосейкин, Л.Н. Ларичев, Г.Н. Харитонинко. 2009. Месторождения полезных ископаемых, М., Горная книга, ММГУ.
[17] Deliverables of EU-H2020-MSP-REFRAM project (Multi-Stakeholder Platform for a Secure Supply of Refractory Metals in Europe). http://prometia.eu/deliverables/
[18] A.G. Kholmogorov, O.N. Kononova, G.L. Pashkov,S.V. Kachin, O.N. Panchenko, O.P. Kalyakina 2002. Molybdenum Recovery from Mineral Raw Materials by Hydrometallurgical Methods, The European Journal of Mineral Processing and Environmental Protection,Vol. 2, No. 2, 1303-0868, 2002, pp. 82-93
[19] M.L.C.M. Henckens⋆ , P.P.J. Driessen, E. Worrell 2018, Molybdenum resources: Their depletion and safeguarding for future generations, ELSEVIER, Resources, Conservation & Recycling 134 (2018) 61–69
[20] Мушегян В.О., Электроннолучевая плавка восстановленного концентрата молибдена, сп. Современная Электрометаллургия, 4(97), (2009), 26-28.
[21] Пат. 2349657 Российская Федерация, МПК С 22 В 34/34, С 22 В 9/20. Способ производства молибдена высокой чистоты [Текст] / В. Г. Глебовский, Е. Д. Штинов, А. И. Пашков, О. С. Кочетов; патентообладатель В. Г. Глебовский. – № 2007140538/02; заявл. 02.11.2007; опубл. 20.03.2009, Бюл. № 8.
[22] Колобов Г.А., К.А. Печерица, А.В. Карпенко, Ю.В. Мосейко, В.Н. Очинский, "Рафинирование вольфрама и молибдена", Металургія, 1 (33), (2015) , 45-51.
[23] Колобов Г.А., А.С.Медведев, Л.П. Колмакова, А.В. Карпенков, "Новые технологии извлечения молибдена из отработанных катализаторов", Металургія, 2 (32), (2014), 86-93.
[24] Bascur P., 2010 "Molybdenum Market Outlook". www.Molyexp.com.
[25] https://roskill.com/product/molybdenum/

CONCEPT FOR DETERMINING DRIVING FACTOR OF GEARBOX SPEED REDUCER

Prof. Dr. Sc. Hristovska E. mech. eng.[*], Assoc. Prof. Dr. Sc. Sovreski Z[*], Assoc. Prof. Dr. Sc. Stavreva S. [*], Prof. Dr. Sc. Jovanovska V. [**], Curcievska D. [***], Aziri Z. [***], Zekiri Z. [***]
[*] Faculty of Technical Sciences – Bitola, University St. Kliment Ohridski, Republic of Macedonia
[**] Faculty of Biotechnical Science – Bitola, University St. Kliment Ohridski, Republic of Macedonia
[***] Ph.D. students at Faculty of Technical Sciences – Bitola

elizabeta.hristovska@uklo.edu.mk

Abstract: *The driving factor is an important technical feature of dynamical loaded working machines. It is especially important to know its value for the working wheel speed reducer of the rotating excavators. In this paper is presented a concept for determining the driving factor of a concrete gearbox speed reducer. To calculate the value of the driving factor according to the specified concept, knowledge of the load regime and the carrying capacity of the gearbox is necessary. The load regime is known from the load function, which is given in the paper, and is determined on the basis of the experimental measurements carried out for this purpose. The carrying capacity of the speed reducer is calculated by theoretical analysis according to the established methodology in this paper, for the characteristic pairs of gears determined in this analysis. As the most important gear pair, from the aspect of determining the driving factor, the most loaded gear pair is taken, in which during the exploitation of the speed reducer the most interventions are made, compared to the other gear pairs of the gearbox.*

Keywords: DRIVING FACTOR, GEARBOX REDUCER, ROTATING EXCAVATOR, COALMINE

1. Introduction

The load regime of the gearbox speed reducer of the working wheel of rotating excavator for normal and specific exploitation conditions is defined by the torque distribution function of the output shaft, depending on the number of load changes in the expected working life of the speed reducer.

The load regime of the speed reducer of the working wheel of the rotating excavator SRs-630 which is used in the coalmine Suvodol-Bitola in Macedonia, is determined on the basis of conducted experimental measurements and extensive theoretical analysis. The load function of this speed reducer is shown in this paper.

The carrying capacity of the gearbox speed reducer of the working wheel of rotating excavator is determined for its most loaded gear pair, i.e. for the gear pair that has certain operational weaknesses.

The carrying capacity for all gear pairs from the working wheel speed reducer of the rotating excavator SRs-630 has been obtained theoretically, with a set methodology for this purpose, presented in the continuation of the paper. The practice of maintaining the speed reducer showed that certain weaknesses during the exploitation were observed in the first, second and last (the fifth) gear pair, but most was intervened at the last gear pair which is the most loaded in the speed reducer, that is, the following gear of this gear pair which is mounted on the output shaft of the speed reducer.

The driving factor is a technical feature of dynamical loaded working machines. The driving factor is an important indicator of the dynamic load of the speed reducers in the rotating excavators, in particular for the working wheel speed reducer of the excavator.

In this paper, the concept for determining the driving factor of the working wheel speed reducer of the rotating excavator SRs-630 is presented and a numerical value for the driving factor based on such a methodology has been obtained.

2. Load regime of the speed reducer

The loading of the speed reducer is a change in the torque T_2 of the following shaft depending on the time t in the total exploitation life of the speed reducer.

The load function of the speed reducer of the excavator SRs-630 (shown in Figure 1) was obtained by processing the deformations of the output shaft of the speed reducer under the characteristic working regimes for the excavator, which deformations were obtained by experimental measurements.

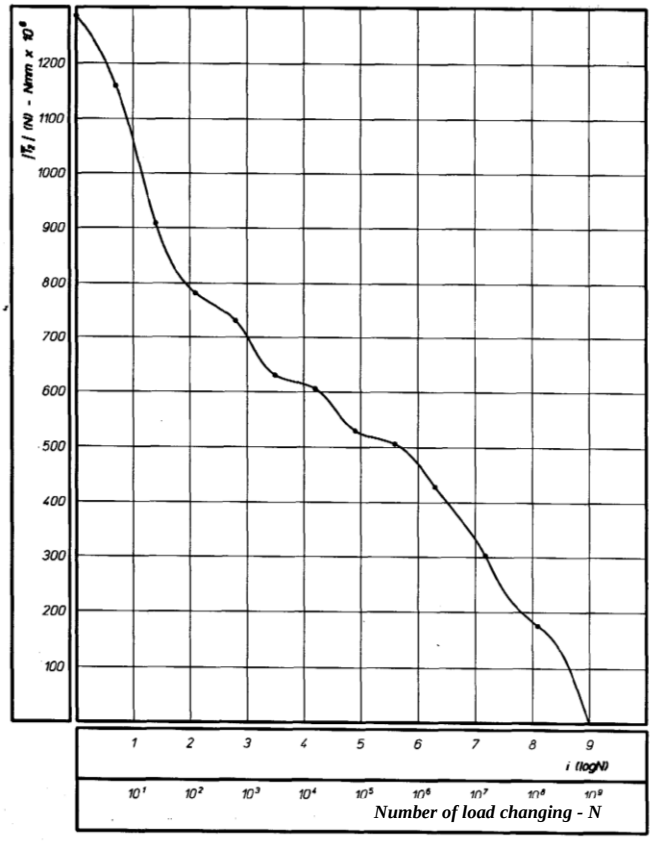

Fig. 1 *Load function of the working wheel speed reducer of the rotating excavator SRs-630 under working conditions at the coalmine Suvodol-Bitola*

3. Carrying capacity of the speed reducer

3.1. Generally for the carrying capacity and characteristics of the speed reducer

The carrying capacity is the ability of the speed reducer to receive certain types of maximum loads with a certain number of changes, under certain working conditions. The carrying capacity of the speed reducer can be associated with the Veler's curves of fatigue of the material for the gears in the speed reducer, obtained by examining the gears (in particular on the surface pressure of the tooth side, and in particular the flexion in the root of the tooth). This is necessary for theoretically obtaining the curve of the load function, while for practical use it is sufficient to find only two points of the curve and to determine the value of the driving factor for those two points.

The initial basis for this calculation is the knowledge of the materials characteristics from which the gears are made:
- Fatigue strength for Hertz surface pressure σ_{Hlim}
- Static strength for Hertz surface pressure σ_{H0}
- Fatigue strength for strain at the root of the tooth σ_{Flim}
- Static strength for strain at the root of the tooth σ_{F0}

Since this is a speed reducer that is in exploitation, whose scheme is shown in Figure 2, in addition to these data are also known the type of stresses, working conditions, shape and dimensions of the gears, etc., which can determine the value of the static and fatigue capacity.

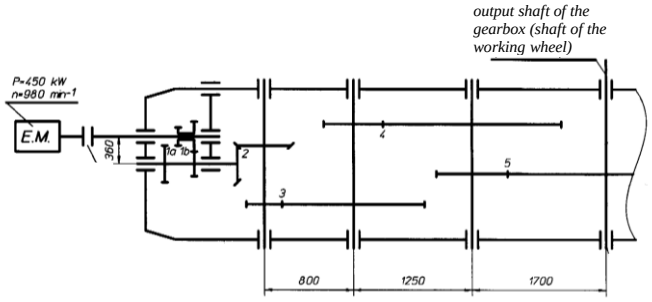

***Fig. 2** Sheme of the gearbox speed reducer with the working wheel of the excavator SRs-630*

The practice showed that in the work of the speed reducer, the weakness of the first, second and last gear pair was observed (the gear pair 1, the gear pair 2 and the gear pair 5, marked in Figure 2). For the third and fourth gear pair, no problems were encountered in the speed reducer's current exploitation life, so they are practically working as delivered by the manufacturer. Because of the above, only the first, second and last gear pair will be treated.

The first gear pair is double, its driving gear is made of two cylindrical gears with slanted teeth made on a common carrier that fit together with two following gears respectively, whereof the following gears are mounted on the same shaft. Depending on which part of the pair is coupled, two speeds can be achieved by rotating the output shaft for one speed at the input shaft and thus two gear ratio of the speed reducer. In practice, the excavator operates with the higher speed, so for this reason only the right part of the gear pair is analyzed in the paper (gear pair 1b).

The second gear pair is conical with curved teeth (conical helical gear pair), and the last gear pair is a cylindrical with a arrow teeth (herring-bone gear pair).

Data on the characteristics of the materials from which the gear pairs are made are used by the theoretical data from the excavator manufacturer, TAKRAF-Germany.

3.2. Nominal loading of the speed reducer

The nominal loading of the speed reducer defines the average load during a lasting drive.

The nominal load is calculated as the average load for all working regimes of the excavator (for which measurements were made), with the exception of the extreme values achieved during the experimental measurements. The indicator of the load is taken showing of the ammeter during the measurement (the measurement methodology is not subject to analysis in this paper). The average value of the electric current during the experimental measurements was:

$$I_{sr} = \frac{40+48+30+40+24+32+30+60}{8} = 38 \text{ A}$$

The power corresponding to this load is rated (nominal) power, so on the output shaft of the speed reducer has a value

$$P_R = (\sqrt{3}\cdot 6\cdot 38\cdot 0{,}86)\cdot 0{,}97\cdot 0{,}92 = 303{,}08 \quad \text{kW}$$

and the nominal torque of the output shaft is:

$$T_{20} = 159155\cdot \frac{P_R}{n} = 159155\cdot \frac{303{,}08}{0{,}11885} = 405858445{,}3 \text{ Nmm}$$

3.3. Calculation of the carrying capacity of the gear pairs 1b and 5

3.3.1. Carrying capacity of surface pressure

a) Fatigue carrying capacity

- Maximum peripheral force on the tooth side

$$F_{tH\infty} = \frac{b\cdot d}{S_{H\lim}}\cdot\frac{u}{u+1}\cdot\frac{(Z_x\cdot Z_L\cdot Z_R\cdot Z_v\cdot Z_N\cdot Z_w\cdot Z_{Eht})^2}{K_v\cdot K_{H\alpha}\cdot K_{H\beta}\cdot Z_\varepsilon{}^2\cdot Z_E{}^2\cdot Z_{H\beta}{}^2}\cdot\sigma_{H\lim}{}^2$$

- Maximum peripheral torque from the peripheral force

$$T_{H\infty} = \frac{F_{tH\infty}\cdot d}{2}$$

b) Static carrying capacity

- Maximum peripheral force on the tooth side

$$F_{tH0} = \frac{b\cdot d}{S_{H\lim}}\cdot\frac{u}{u+1}\cdot\frac{(Z_x\cdot Z_L\cdot Z_R\cdot Z_v\cdot Z_N\cdot Z_w\cdot Z_{Eht})^2}{K_v\cdot K_{H\alpha}\cdot K_{H\beta}\cdot Z_\varepsilon{}^2\cdot Z_E{}^2\cdot Z_{H\beta}{}^2}\cdot\sigma_{H0}{}^2$$

- Maximum peripheral torque from the peripheral force

$$T_{H0} = \frac{F_{tH0}\cdot d}{2}$$

c) Carrying capacity at N = 10^4 load changes

$$T_{H(10^4)} = \sqrt{T_{H\infty}\cdot T_{H0}}$$

3.3.2. Carrying capacity of flexion in the root of the tooth

a) Fatigue carrying capacity

- Maximum peripheral force at the root of the tooth

$$F_{tH\infty} = \frac{b\cdot d\cdot\cos\beta}{z}\cdot\frac{\sigma_{F\lim}}{S_{F\lim}}\cdot\frac{Y_x\cdot Y_{ST}\cdot Y_N\cdot Y_\delta\cdot Y_R\cdot Y_{Eht}}{K_v\cdot K_{F\alpha}\cdot K_{F\beta}\cdot Y_{FS}\cdot Y_\varepsilon\cdot Y_\beta}$$

- Maximum peripheral torque from the peripheral force

$$T_{F\infty} = \frac{F_{tF\infty}\cdot d}{2}$$

b) Static carrying capacity

- Maximum peripheral force at the root of the tooth

$$F_{tF0} = \frac{b \cdot d \cdot \cos\beta}{z} \cdot \frac{\sigma_{F0}}{S_{F\lim}} \cdot \frac{Y_x \cdot Y_{ST} \cdot Y_N \cdot Y_\delta \cdot Y_R \cdot Y_{Eht}}{K_v \cdot K_{F\alpha} \cdot K_{F\beta} \cdot Y_{FS} \cdot Y_\varepsilon \cdot Y_\beta}$$

- Maximum peripheral torque from the peripheral force

$$T_{F0} = \frac{F_{tF0} \cdot d}{2}$$

c) Carrying capacity at N = 10^4 load changes

$$T_{F(10^4)} = \sqrt{T_{F\infty} \cdot T_{F0}}$$

The influential factors in the preceding formulas are determined by an appropriate methodology for this purpose, for gears of the gear pairs 1b and 5.

In order to cover the remaining impacts on the work of gears, which are not yet covered by their own factor, the factor of safety is still being used. Because the maximum potential for loadings on the gears (maximum carrying capacity) should be determined here, its minimum values are taken for the factors of safety: $S_{H\lim} = 1$ and $S_{F\lim} = 1.2$.

According to the known data for the gears and the formulas of items 3.3.1. and 3.3.2. the carrying capacity of the gear pairs 1b and 5 are calculated and given in Table 1 for the gear pair 1b and table 2 for the gear pair 5.

Table1

carrying capacity		gear pair 1 b	
		$z_1 = 56$	$z_2 = 45$
$F_{tH\sim}$	[N]	127164.2	103166.1
$T_{H\sim}$	[Nmm]	25390875.81	16553000.74
F_{tH0}	[N]	5208646.8	3337790.79
T_{H0}	[Nmm]	1040010506	535548533.5
$T_{H(10^4)}$	[Nmm]	162501623.3	94153785.21
$F_{tF\sim}$	[N]	127918.8	135094.1
$T_{F\sim}$	[Nmm]	25542546.8	21675848.3
F_{tF0}	[N]	447715.7	472829.2
T_{F0}	[Nmm]	89395392.8	75865443.1
$T_{F(10^4)}$	[Nmm]	47783853	40551791.9

3.4. Calculation of the carrying capacity of the gear pair 2

3.4.1. Carrying capacity of surface pressure

a) Fatigue carrying capacity

- Maximum peripheral force on the tooth side

$$F_{tH\infty} = \frac{b \cdot d_m}{S_{H\lim}} \cdot \frac{u}{\sqrt{u^2+1}} \cdot \frac{(Z_X \cdot Z_L \cdot Z_R \cdot Z_V \cdot Z_W \cdot Z_N \cdot Z_{Eht})^2}{K_V \cdot K_{H\alpha} \cdot K_{H\beta} \cdot Z_{H\beta}{}^2} \cdot \sigma_{H\lim}{}^2$$

where $d_m = d - b\sin\varphi$ and it is a diameter of the pitch circle

- Maximum peripheral torque from the peripheral force

$$T_{H\infty} = \frac{F_{tH\infty} \cdot d_m}{2}$$

Table 2

carrying capacity		gear pair 5	
		x 2 $z_1 = 23$	x 2 $z_2 = 98$
$F_{tH\sim}$	[N]	447077.43	2198172.23
$T_{H\sim}$	[Nmm]	143210077.3	3000186363
F_{tH0}	[N]	16094788.15	54954306.2
T_{H0}	[Nmm]	5155563010	75004659000
$T_{H(10^4)}$	[Nmm]	859260482.6	15000931000
$F_{tF\sim}$	[N]	892999.97	819305.64
$T_{F\sim}$	[Nmm]	286050216.6	1118233401
F_{tF0}	[N]	3162708.6	3098378.6
T_{F0}	[Nmm]	1013094644	4228837513
$T_{F(10^4)}$	[Nmm]	5383226984.5	21745867708

Note for Table 2: The listed carrying capacity for gear pair 5 in the table refers for half gear. For whole herring-bone gear the given values are multiplied by 2 and the carrying capacity is obtained with respect to surface pressure and flexion.

b) Static carrying capacity

- Maximum peripheral force on the tooth side

$$F_{tH0} = \frac{b \cdot d_m}{S_{H\lim}} \cdot \frac{u}{\sqrt{u^2+1}} \cdot \frac{(Z_X \cdot Z_L \cdot Z_R \cdot Z_V \cdot Z_W \cdot Z_N \cdot Z_{Eht})^2}{K_V \cdot K_{H\alpha} \cdot K_{H\beta} \cdot Z_{H\beta}{}^2} \cdot \sigma_{H0}{}^2$$

- Maximum peripheral torque from the peripheral force

$$T_{H0} = \frac{F_{tH0} \cdot d_m}{2}$$

c) Carrying capacity at N = 10^4 load changes

$$T_{H(10^4)} = \sqrt{T_{H\infty} \cdot T_{H0}}$$

3.4.2. Carrying capacity of flexion in the root of the tooth

a) Fatigue carrying capacity

- Maximum peripheral force at the root of the tooth

$$F_{tF\infty} = \frac{b \cdot d_m \cdot \cos\beta_m}{z} \cdot \frac{\sigma_{F\lim}}{S_{F\lim}} \cdot \frac{Y_X \cdot Y_N \cdot Y_R \cdot Y_\delta \cdot Y_{Eht}}{K_V \cdot K_{F\alpha} \cdot K_{F\beta} \cdot Y_{FS} \cdot Y_\varepsilon \cdot Y_K \cdot Y_{LS}}$$

- Maximum peripheral torque from the peripheral force

$$T_{F\infty} = \frac{F_{tF\infty} \cdot d_m}{2}$$

b) Static carrying capacity

- Maximum peripheral force at the root of the tooth

$$F_{tF0} = \frac{b \cdot d_m \cdot \cos\beta_m}{z} \cdot \frac{\sigma_{F0}}{S_{F\lim}} \cdot \frac{Y_X \cdot Y_N \cdot Y_R \cdot Y_\delta \cdot Y_{Eht}}{K_V \cdot K_{F\alpha} \cdot K_{F\beta} \cdot Y_{FS} \cdot Y_\varepsilon \cdot Y_K \cdot Y_{LS}}$$

- Maximum peripheral torque from the peripheral force

$$T_{F0} = \frac{F_{tF0} \cdot d_m}{2}$$

c) Carrying capacity at N = 10^4 changes

$$T_{F(10^4)} = \sqrt{T_{F\infty} \cdot T_{F0}}$$

The influential factors listed in the preceding formulas are determined for the gears of the gear pair 2. For the factors of safety, it is taken: $S_{H\lim} = 1.2$ and $S_{F\lim} = 1.4$.

According to the specified data for the gears and the formulas of items 3.4.1. and 3.4.2. the carrying capacity of the gear pair 2 is calculated and given in Table 3.

Table 3

carrying capacity		gear pair 2	
		$z_1 = 29$	$z_2 = 38$
$F_{tH\sim}$	[N]	2667868701	3354330573
$T_{H\sim}$	[Nmm]	375996070000	619460990000
F_{tH0}	[N]	58100247000	64939839000
T_{H0}	[Nmm]	9422117200000	13799715000000
$T_{H(10^4)}$	[Nmm]	1882200500000	2923762000000
$F_{tF\sim}$	[N]	41943.4	42162.1
$T_{F\sim}$	[Nmm]	5911293.1	7786285.8
F_{tF0}	[N]	114924.9	115524.1
T_{F0}	[Nmm]	18637382.9	24548855.1
$T_{F(10^4)}$	[Nmm]	10496239	13825498.3

4. Driving factor

4.1. Standardized load numbers

$$a_{(10^0)} = \frac{T_{2(10^0)}}{T_{20}} = \frac{1286377308}{405858445{,}3} = 3{,}17$$

$$a_{(10^4)} = \frac{T_{2(10^4)}}{T_{20}} = \frac{624750000}{405858445{,}3} = 1{,}54$$

$$a_{(10^7)} = \frac{T_{2(10^7)}}{T_{20}} = \frac{333200000}{405858445{,}3} = 0{,}82$$

$A_1 = 4$ $A_2 = 1.6$ $A_3 = 1$

The magnitudes $T_{2(10^0)}$, $T_{2(10^4)}$, $T_{2(10^7)}$ are read from the diagram in Figure 1 and the magnitudes T_{20} is from item 3.2.

4.2. Standardized carrying capacity numbers

$$b_{(10^0)} = \frac{T_{(10^0)}}{T_{F\infty}} = \frac{4228837513}{1118233401} = 3{,}78$$

$$b_{(10^4)} = \sqrt{b_{(10^0)}} = 1{,}94$$

$$b_{(10^7)} = 1$$

$B_1 = 3.15$ $B_2 = 1.8$ $B_3 = 1$

$T_{(10^0)} = T_{F0}$, the magnitudes T_{F0} и $T_{F\infty}$ are from Table 2 for the following gear of the gear pair 5.

Because the carrying capacity of flexion in the root of the tooth is less favorable (smaller), it is considered the most relevant when defining the standardized carrying capacity numbers.

4.3. Value of the driving factor

$K_A = \max [A_1/B_1, A_2/B_2, A_3/B_3] = \max [4/3.15; 1.6/1.8; 1/1] = \max [1.27; 0.89; 1] = 1.27$

It is adopted $K_A = 1.25$ for the value of the driving factor of the speed reducer, which is the number from the standard array R20.

5. Conclusion

In this paper is shown the load function of the working wheel speed reducer for a real excavator and known working regimes, which is a function derived from the experimental measurements carried out for that purpose. The load function gives a description of the speed reducer's load regime in its total lifetime.

The paper presents a methodology for theoretical calculation of the carrying capacity of the speed reducers, that is, for its gears, both fatigue and static carrying capacity, for surface pressure on the tooth side and flexion in the root of the tooth. The presented methodology is confirmed by analysis of the specific reducer. Also this paper presents a concept for determining the value of the driving factor of the speed reducer as an important characteristic of its dynamic load, and defines the value of that factor on the basis of this concept for the mentioned speed reducer.

The gain value for the driving factor can serve as a benchmark for the driving factors of the rotating excavators with similar technical characteristics operating in approximate working conditions.

6. References

Hristovska E.: Own papers with this topic and data from experimental measurement

Manual handling for the excavator SRs-630 and other technical documentation from the manufacturer TAKRAF-Germany

Numerous documentation for modifications and repairs of gearboxes from the coalmine Suvodol-Bitola.

ENVIRONMENTAL ASPECTS OF PORT INFRASTRUCTURE DEVELOPMENT IN VARNA LAKE

ЕКОЛОГИЧНИ АСПЕКТИ НА РАЗВИТИЕТО НА ПРИСТАНИЩНАТА ИНФРАСТРУКТУРА ВЪВ ВАРНЕНСКО ЕЗЕРО

Assoc. Prof. Dr. Toneva D.[1], PhD student Dimova D.[1], PhD student Stankova T.[1]
Technical University of Varna, Bulgaria, dept. Ecology and Environmental Protection[1]
dtoneva@abv.bg

Abstract: *The development of sustainable maritime industry is declared to be a national priority for Bulgaria. The marine ports' infrastructure development is a key element (aspect) in the process of obtaining sustainability and safety and security insuring. In this context environmental issues should to be tackled with regards to economical, social and environmental perspectives. The main Bulgarian Black Sea port is the port of Varna, located in Beloslav lake (Varna-West) and Varna bay (Varna-East). At the same time in Varna and Beloslav lakes alone 14 ports operate. In the last 2 decades the international importance of Varna port is decreasing dramatically because of multiple factors among which the most important are: lack of real investments in port infrastructure development and modernization; increased competitiveness of other port operators mainly Romanian and Turkish; controversial port management policy; limited objective capacity of Varna- Beloslav lake complex and Varna bay to sustain continues enlargement of ports infrastructure. From ecological point of view continues coast modification and development of new engineer port infrastructure especially in lakes is hazardous. It contains multiple environmental risks that are observed and analyzed in this research regarding Varna lake ecological status.*

Keywords*: ENVIRONMENT, ENVIRONMENTAL PROTECTION, PLANING, PORTS, PORT INFRASTRUCTURE*

1. Въведение

Необходимостта от опазване на околната среда и превенцията на екологичния риск при развитието на пристанищна инфраструктура нарастват непрекъснато. За постигане на ефективно управление на екологичния риск е необходимо идентифициране на конкретните измерения на екологичния риск за дадено водно тяло във всичките му аспекти. Варненското езеро е важен пристанищен център и зона с интензивно антропогенно натоварване, водещо до съществени негативни ефекти. Движещите сили, обуславящи натиска основно са индустрията, водния транспорт, и урбанизация. Замърсяването на водите, трайната еутрофикация, нарушенията в кислородния режим на води и подтиснатото състояние на водните екосистеми са характерни за Варненското езеро. [1, 2] Управлението на езерната екосистема изисква оценка на антропогенния натиск и предприемане на активни мерки за подобряване на екологичното й състояние. В настоящото изследване се разглеждат екологичните аспекти на изграждането и разширяването на пристанищна инфраструктура във Варненското езеро, касаещи рецепторите води, дънни седименти и биоразнообразие.

2.Транспортно значение на Варненско езеро

Варненският залив и свързаният с него Варненско-Белославски езерен комплекс оформят район с ключово значение за развитието на българското морско корабоплаване. На Варненския залив се разполага едно от двете главни морски пристанища на България – пристанище Варна (Изток) с 14 корабни места (в това число 1 корабно място за пътници) за генерални и насипни товари, наливни торове, Ро-Ро товари и контейнери. При Варненско-Белославския езерен комплекс и свързващите го с Черно море канали функционират 14 товарни и 1 яхтено пристанище [16].

Варненското езеро е обект с високо транспортно значение. На езерото и каналите, свързващи го с Черно море (стар и нов канал) са ситуирани 2 пристанища с национално значение, 4 с регионално значение, и 6 пристанища със специално предназначение. Към 2018г. са регистрираните 6 действащи пристанища с национално и регионално значение [16], които са представени в таблица 1. Регистрираните към 2018г. пристанища със специално предназначение, в едно с основните услуги, които те предоставят са представени в таблица 2.

Таблица 1: Регистрирани пристанища с национално и регионално значение във Варненско езеро към 2018г.

№	Пристанище/ терминал	Типове обработвани товари	Брой места
I. Пристанища за обществен транспорт с национално значение			
I.1.	Терминал Леспорт	Генерални, насипни, „Ро-Ро“, наливни товари, празни 20-футови контейнери - стиф	3
I.2.	Терминал „Петрол“	Опасни наливни товари от клас 3 по класификацията на ИМО*	3
II. Пристанища за обществен транспорт с регионално значение			
II.1.	ПЧМВ - Варна	Генерални, насипни и опасни (клас 4.2 и клас 5.1); контейнери	2
II.2.	Одесос ПБМ - Варна	Генерални и насипни; контейнери	3
II.3.	ПЧМВ – Варна Терминал за базови масла	Нефтоналивни	1
II.4.	ТЕЦ Езерово	Насипни, генерални, контейнери и поща	3

Таблица 2: Регистрирани пристанища със специално предназначение във Варненско езеро към 2018г.

№	Пристанище	Предлагани пристанищни услуги	Брой места
1.	Строителен и технически флот	Приставане, домуване, престой и ремонт на драгажна, крановоподемна, водолазна, буксирана и друга плаваща техника на СТФ	1
2.	ПЧМВ	Приемане, съхраняване и преработка на течни и твърди отпадъци	1
3.	КРЗ Одесос	Приставане и престой на кораби и други технически средства за кораборемонт; швартоване	6
4.	МТГ Делфин	Дейности, технологично свързани с производствения процес	1
5.	БУЛЯРД	Дейности, технологично свързани с производствения процес; морско-технически пристанищни дейности и услуги; швартоване; приемане и обработване на отпадъци от корабоплаване	8
6.	ТЕРЕМ – КРЗ Флотски арсенал-Варна	Дейности, технологично свързани с производствения процес; морско-технически пристанищни дейности и услуги; швартоване; приемане и обработване на отпадъци от корабоплавателне	6

Разположението на функциониращите пристанища е представено на фигура 1.

Fig. 1. *Разположение на функциониращите пристанища във Варненско езеро към 2018г.*

1 – Терминал Леспорт; 2 – Терминал „Петрол“; 3 – ПЧМВ-Варна (терминал генерални товари); 4 – Пристанище Одесос ПМБ-Варна; 5 – ПЧМВ- Варна (терминал базови масла); 6 – ТЕЦ Езерово; 7 - Material technical base of the Civil Engineering and Technical Fleet JSC; 8 –ПЧМВ (специално предназначение); 9 – Кораборемонтен завод „Одесос“; 10 - MTG Делфин; 11 - Булярд; 12 – Терем Флотски арсенал- Варна

Пристанищната инфраструктура е съсредоточена при двата канала, като най-висока е гъстотата на разположените съоръжения на стария канал, свързващ езерото с Варненски залив. Висока е концентрацията на пристанищата и на северния бряг на езерото (4 пристанища), докато на южния бряг е разположено само едно пристанище със специално предназначение. През последното десетилетие интересът към разрастване на пристанищата и модернизация на пристанищната инфраструктура се засилва[8]. За това свидетелстват процесираните инвестиционни предложения за изграждане на нови пристанища и разширяване на съществуващите в акваторията на Варненското езеро.

Към настоящия момент 4 инвестиционни предложения са преминали процедури по Оценка на въздействието върху околната среда (ОВОС): разширение на Пристанищен терминал „Леспорт”– Варна [12]; разширение на пристанище за обществен транспорт с регионално значение „Одесос ПБМ”, [11]; изграждане на „Интермодален терминал Варна”[10]; изграждане на пристанище за обществен транспорт с регионално значение „Езерово” в района на съществуващата материално-техническа база в землището на с. Езерово, общ. Белослав, обл. Варна [9].

Три от инвестиционните предложения се предвижда да бъдат реализирани на северния бряг на Варненското езеро, а едно - на плавателен канал №3 („стария канал”) от страната на град Варна. Разположението на процесираните инвестиционни предложения е представено на фигура 2.

Fig. 2. *Разположение на процесираните инвестиционни предложения във Варненско езеро*

1 - Терминал „Леспорт“- Варна; 2 – Интермодален терминал Варна; 3 – Пристанище „Езерово“ ; 4 – Одесос ПМБ

3. Състояние на Варненско езеро

Варненското езеро е подложено на голямо антропогенно натоварване, включително от пристанищната дейност и корабоплаването. Самото езеро представлява крайбрежен лиман с естествен произход с площ 19км^2, максимална дълбочина 19м и воден обем 166млн.м^3. До 1909г. Варненското езеро е сладководен езеро с незначителна връзка с Белославското езеро на запад и със слаб отток към Черно море на изток.

През 1909г., с прокопаването на първия канал (стар канал), Варненско езеро се свързва с Черно море. Връзката на езерото с Варненския залив е интензифицирана с прокопаването на втори канал (нов канал) през 1976г. През 1978г. е установена връзка между Варненското и Белославското езеро чрез покарването на канал, свързващ двете езера. Създадени са предпоставки за интензивфициране на индустриалното развитие на територията и превръщането на Варненското езеро в значим пристанищен район. Тези съществени промени в хидроморфологията на Варненското езеро, както и удълбочаването му, водят до много големи изменения в екологично отношение. Солеността му е нараснала до 15‰ в повърхностните и до 17‰ в придънните водни слоеве, с което екологичните условия са се доближили до тези на морската акватория.

Езерната система се характеризира с трайна еутрофикация, липса на запазени референтни условия, редуцирано видово разнообразие, съпроводено с опростяване на водните екосисетми и силно изразено доминиране на толерантни към замърсяване видове. Водно тяло BG2PR100L001 „Варненското езеро” е класифицирано като силно модифицирано водно тяло (СМВТ), тип L9: „Черноморски средно солени езера и блата” при екорегион 12 „Понтийска провинция” [13]. Водите му са трайно еутрофицирани (преобогатени основно с азот и фосфор) без запазени референтни условия.

Акваторията на Варненското езеро е силно повлияна от интензивната антропогенна дейност и замърсяването на водите при експлоатация на пристанищата от акостиращи и преминаващи кораби, от притока отпадни води от Пречиствателната станция за отпадъчни води „Варна”, от дейностите на Девненските химически заводи посредством канала, свързващ го с Белославско езеро, от ТЕЦ Езерово.

С цел оценка на състоянието на Варненско езеро, прогнозиране на състоянието му и съставяне на предложения за неговото подобряване, езерот е обект на екологичен мониторинг. Наблюдения над водното тяло се извършват в 4 мониторингови пункта, представени в таблица 3.

Таблица 3: Пунктове за мониторинг - Варненско езеро

Пункт	Код на пункт	Код на ВТ
Варненско езеро-запад	BG2PR00155MS013	BG2PR100L001
Варненско езеро-северозапад	BG2PR00155MS014	BG2PR100L001
Варненско езеро-център	BG2PR00155MS015	BG2PR100L001
Варненско езеро-изток	BG2PR00155MS016	BG2PR100L001

Обощените данни за състоянието на Варненското езеро за периода от 2014г. до 2016г., представени в таблица 4, показват известно екологично възстановяване през 2016г, в сравнение с предходните две години.

Table 4: Екологично и химично състояние на СМВТ „Варненско езеро” BG2PR100L001 за периода 2014-2016г.

Година	Екологично състояние			Химично състояние
	БЕК	ФХЕК	Екологичен потенциал	
2014	много лошо	умерено	много лошо	няма данни
2015	много лошо	умерено	много лошо	няма данни
2016	добро	умерено	умерено	непостигащо добро

Данните показват тенденция към намаляване степента на замърсяване на езерните води, дължащо се на снижаване на индустриалния отток в езерото и редуциране на замърсителите, в резултат на спада в промишленото

производство, доизграждане на канализационните системи на населените места и модернизиране на пречиствателните станции за отпадъчни води. Екологичният потенциал на Варненско езеро за посочения период се подобрява от „много лош“ до „умерен“ [4, 5, 6]. По отношение на биологичен елемент за качество (БЕК) също е налице подобрение: от „много лошо” през 2014г. и 2015г., до „добро” през 2016г., като през посочения период оценката се основава на БЕК фитопланктон. По отношение на физикохимичните елементи за качество (ФХЕК) състоянието устойчиво се определя като „умерено“, което се дължи на концентрациите на амониев азот, фосфати и общ фосфор. Същевременно през 2016г. концентрациите на нитритен азот намаляват в сравнение с регистрираните през 2015 и 2014г. Спрямо Плана за управление на речните басейни (ПУРБ) за 2016-2021г., екологичното състояние на Варненско езеро е определено като „много лошо” [7]. Особено притеснително е химично състояние на Варненското езео - „непостигащо добро”, дължащо се на наличие на живак в биота.

Цъфтежите на водораслите се съпътстват от неблагоприятен кислороден режим и временно установяване на аноксични условия и „мъртви зони“, основно през лятно-есенния период след пролетния максимум в развитието на планктона. Видовият състав на макрозообентоса е опростен, а цялата им биомаса се дължи на толерантни видове, с ниска екологична чувсвителност и висока екологична пластичност [15]. Видовото разнообразие на дънните безгрбначни е най-голямо в стария и новия канали, свързващи Варненско езеро с Варненски залив и намалява в посока от Варненски залив към Белославско езеро [14]. Числеността на макрозообентосните видове във Варненското езеро бележи пик през пролетта, но като цяло показва ниска биомаса.

Акваторията на Варненското езеро е загубила ролята си на размножителен ареал за представители на ихтиофауната и безгръбначната дънна фауна. Почти цялата част от рибата намирана тук е от трансфери по водоемите и залива, при периодично настъпваща масова смъртност на съобществата от безгръбначната дънна фауна.

Не може да се пренебрегне фактът, че Варненското езеро попада в защитена зона BG0000191 „Варненско-Белославско езеро” от мрежата НАТУРА 2000, както и в Орнитологично важно място (1997г.). Защитената зона „Варненско-Белославско езеро”, карта на която е представена на фигура 3, е обявена с цел опазване и поддържане на местообитанията на застрашени и мигриращи видове птици, съгласно Директива 2009/147/ЕО. Това налага прилагане на принципа на предпазливостта при вземане на решения, предполагащи усилване на антропогенното въздействие и/или поставяне под заплаха този елемент на европейската екологична мрежа.

Фиг. 3. *Карта на защитена зона Варненско-Белославско езеро BG0000191 [14]*

Като цяло през последните години се наблюдава слабо екологично възстановяване, дължащо се най- вече на намалената интензивност на индустриалното натоварване. Интензифицирането на транспорта, както и разрастването на пристанищните комплекси и развитието на пристанищната инфрструктура са носители на съществен екологичен риск, който не може да бъде пренебрегван.

4. Екологични аспекти на развитието на пристанищата във Варненско езеро

Изграждането на нови пристанища и разширяването на съществуващи са предпоставка за възникване на различни по срочност, обхват и интензивност негативни въздействия върху околната среда. Въздействия се очакват в етапа на изграждане и в дългосрочен план при експлоатацията на пристанищните обекти. Реализацията на инвестиционни предложения за изграждане и разширяване на пристанищната инфраструктура, особено в акваториалната част са носители на значим екологичен риск, изискващ проактивно управление.

От дейностите извършвани на етапите на строителство/ реконструкция, най-значим източник на екологичен риск върху акваторията и водните екосистеми са:

- коригирането на езерното дъно
- изграждане на кейови стени
- модифициране на брегова линия

На етап експлоатация основните дейности, носители на екологичен риск са:

- товар- разтоварните пристанищни дейности
- корабоплаването
- корабостроене и кораборемонт
- поддържането на дълбочината на плавателните пътища.

Коригирането на дънота на езерото се извършва, както при изграждане на нови пристанища, за достигане проектните дълбочини пред кейовите стени, така и за поддържане на плавателните пътища. Така драгажните работи са присъщи на етапита изграждане и експлоатация, както и за поддържане на дълбочината на водните пътища. Изграждането на кейови стени, ограничено в етапа изграждане във Варненско езеро се основава на технологично решение „висок ростверк“. Модифицирането на бреговата линия съпровожда изграждането и реконстукцията на пристанищните зони, в акваторията и на сушата. Отнемането на територия и акватория са пряко следствие от реализиране на проектите и инвестиционните предложения за изграждане на пристанища.

Присъщите за пристанищата дейности като товаро-разтоварни работи, приемане на отпадъци- резултат от корабоплаването, кораборемонт и др. също имат потенциал да причиняват негативни ефекти върху качеството на водите и устойчивостта на екосистемите.

Сред посочените дейности с висока опасност се отличават драгажните работи, като ефектите от тях се изпитват при рецепторите: седименти, биоразнообразие и качество на водите. Драгирането пряко резултира в перманентни промени в структурата на езерното легло, нарушаване на процесите на седиментация и реседиментация и трайни геоморфоложки изменения в зоните на драгиране. Същевременно процесът на изземане на дънен субстрат е съпроводен с отнемане на дънни хабитати и асоциираните биологични видове и съобщества в зоната на въздействие. Необходимият период за възстановяване или реколонизация на дънното съобщество за Варненското езеро е оценяван на две- три години. При това съставът на макрозообентоса в езерото е опростен с ясно доминиране на толерантни видове с висока екологична пластичност.

Качеството на водите в периодите на драгиране рязко се понижава поради многократно увеличената мътност и присъствието и разпространението на мътностния шлейф. Увеличеното присъствие на общо разтворени твърди вещества и „трансферът“ на суспензия на замърсителите от дънните утайки във водната колона в зоната на удълбочаване рефлектира върху кислородния режим. Наличието на мътностен облак (шлейф) от суспендиран

седиментен материал с различна едрина на частиците (преобладаващо от пясъчни разновидности) води до влошаване на кислородния режим в придънните води, т.к. съдържанието на разтворения кислород във водата намалява в резултат на окисляване на дънни органични

Драгажните маси са специфичен проблем за Варненското езеро. Езерната система почти е изчерпила потенциала си за преразпределение на драгираните маси за коригиране на езерното легло. Това предполага необходимост от депониране на драгажните маси. Към 2018г в близост няма депа със свободен капацитет, които могат да приемат съществени обеми драгажни маси. Вариантът депониране в 12-милната зона на Черно море е свързано с геоморфоложки изменения в мястото на депониране, риск от замътване и образуване на облак от диспергиран седиментен материал, изместващ се генерално по посока на теченията. Зоните, в които е разрешено извършването на такава дейност са с изчерпан кааците и БДЧР все още не са определили нови такива.

Спазването на добрите практики при дълбоководно депониране осигурява запазване интегритета на морското дъно, силно ограничаване присъствието на мътностния облак във времето (до часове след депонирането), несъществени промени в химичното състояние на крайбрежните морски води. По-сериозен риск съществува при едновременно депониране на драгажни маси от различни инвестиционни предложения, поради изчерпване на предвиденото депо, повишено замърсяване - мътност от разпространението на по-финни частици.

Внимание изискват и ефектите на замърсяване на водите от постоянната дейност на пристанищата; образуването на отпадъци; повишената запрашеност на въздуха, особено при обработване на насипни товари; нарушаването на акустичния комфорт и шумовото натоварване на околната среда, представляваща защитена зона. Рискът от отнемане на територия и акватория от защитена зона BG0000191 Варненско-Белославско езеро в резултат на реализация на инвестиционни предложения за изграждане и разширяване на пристанища във Варненското езеро следва да бъде постоянно мониториран.

5. Заключение

Настоящото изследване не претендира за изчерпателност по отношение на екологичните аспекти от развитието на пристанищната инфраструктура на Варненското езеро, но дава основание да се заключи, че при процесиране на нови инвестиционни предложения за изграждане на пристанища и разширяване на съществуващи в акваторията на езерото следва да се изискват допълнителни изследвания върху седиментите и дънните тини.

В цялост може да се заключи, че екологичните аспекти са изключително важен елемент от дейностите по изграждане и разширяване на пристанищната инфраструктура, засягащи непосредствената околност на инвестиционните предложения или по-широка географска област. Като една от основните промишлени зони на гр. Варна, Варненското езеро е значително натоварено откъм промишлени обекти и инвестиционни предложения, реализирането на които е свързано с риск от влошаване качеството на езерните води, на състава и баланса на седиментите и дънните утайки, нарушаване на биологичното равновесие, фрагментиране на популациите на отделни хидробионти и водолюбиви птици в защитена зона „Варненско-Белославско езеро” BG0000191.

Предвиждането и оценката на пълната гама потенциални последици от изграждането и развитието на пристанищна инфрастуктура е от съществено значение за ефективното проактивно управление на екологичния риск при Варненско езеро. Тази необходимост се обуславя от една страна от значимостта на езерото като пристанищен център и съществуващият значителен антропогенен натист, и не доброто състояние на СМВ Варненско езеро. От друга страна от природозащитния статус на обекта и необходимостта от гарантираното му опазване.

6. Литература

[1]. Dzhurova, B. Contamination of sediments in Varna Lake and Varna Bay. Water Science & Technology, 50 (5), 2004, 317-320 http://natura2000.moew.government.bg/Home/ProtectedSite?code=BG0000191&siteType=BirdsDirective;

[2]. Report on biological monitoring of coastal marine waters and lakes - benthic invertebrate fauna, IO-BAS, 2009 - https://docplayer.net/21108024-Report-biological-monitoring-of-coastal-marine-waters-and-lakes-benthic-invertebrate-fauna.html;

[3]. Toneva-Zheynova, D. Environmental Impact of Transport and Tendencies for Development of Sustainable Transport in Bulgaria. Journal of Marine Technology and Environment, Constanta Maritime University, 2011, pp.143-150

[4]. БДЧР, Годишен доклад за оценка на актуалното състояние на водите в Черноморски район- 2014г., *https://www.bsbd.org/UserFiles/File/annual%20reports/2014/Doklad_2014.pdf*;

[5]. БДЧР, Годишен доклад за оценка на актуалното състояние на водите в Черноморски район- 2015г., https://www.bsbd.org/UserFiles/File/annual%20reports/Doklad_2015.pdf;

[6]. БДЧР, Годишен доклад за оценка на актуалното състояние на водите в Черноморски район - 2016г., https://www.bsbd.org/UserFiles/File/annual%20reports/Doklad_2016.pdf;

[7]. БДЧР, План за управление на речните басейни в Черноморски район за басейново управление на водите (2016-2021г.), *ttps://www.bsbd.org/bg/index_bg_5493788.html*;

[8]. Дамянов Д. Гешев Т., Чукалов К. Четвърта индустриална революция- същност и проблеми. изд. КНИГ1, 2019

[9]. ДОВОС „Изграждане на пристанище за обществен транспорт с регионално значение „Езерово”, 2018 http://www.riosv-varna.org/Prevantivna%20dejnost/OVOS-EO/VA-9-2018.pdf;

[10]. ДОВОС „Интермодален терминал Варна“, 2015, http://www.riosv-varna.org/Prevantivna%20dejnost/OVOS-EO/VA-3-2015.pdf;

[11]. ДОВОС „Разширение на пристанище за обществен транспорт с регионално значение „Одесос ПБМ”“, 2019 http://www.riosv-varna.org/Prevantivna%20dejnost/OVOS-EO/VA-1-2019.pdf;

[12]. ДОВОС разширение на Пристанищен терминал „Леспорт”– Варна, 2009 https://www.moew.government.bg/static/media/ups/tiny/23-7-2009.pdf;

[13]. Наредба № Н-4 за характеризиране на повърхностните води, ДВ, бр. 22/2013г., изм. и доп., ДВ бр. 79/2014 г.;

[14]. НАТУРА 2000, 2018

[15]. Петрова-Павлова, Е. Биоразнообразие на макрозообентоса на границата море– езеро (Варненски залив – Варненска езерна система) за периода 2009-2010г. - Изв. на Съюз на учените - Варна, Серия „Морски науки”, 2011, 92-96;

[16]. Регистър на пристанищата в районна дирекция Морска администация- Варна, 2018, http://www.marad.bg/upload/docs/Vn_reg_ports_12092018.pdf

USE OF WILD-RAW RAW MATERIALS OF THE KR TO DEVELOP NEW FOOD PRODUCTS WITH INCREASED BIOLOGICAL VALUE

ИСПОЛЬЗОВАНИЕ ДИКОРАСТУЩЕГО СЫРЬЯ КР ДЛЯ РАЗРАБОТКИ НОВЫХ ПРОДУКТОВ ПИТАНИЯ С ПОВЫШЕННОЙ БИОЛОГИЧЕСКОЙ ЦЕННОСТЬЮ

Prof. Dr. Djurupova B.[1], Phd. Samatova G.[2], Phd. Cand. Sheinshenbek kizi N.[3], Aisuluu Duishebaeva. [4] , Junko Ishikawa[5],
Faculty of Technology [1, 3,] - Kyrgyz State Technical University after I. Razzakov, School of Tourism and Hotel Management [2] - Kyrgyz Turkish Manas University, Kyrgyzstan, Project for development of rural business with forest products in the Kyrgyz Republic, HIT Япония.

Abstract: *The article discusses the problems of nutrition, the impact on the human body and the ways of nutrition correction through the development of new products with high biological value from wild-growing raw materials of Kyrgyzstan. The possibilities of using wild fruits and berries and their complex processing are shown.*

***KEYWORDS**: FOOD, A WILD RAW MATERIAL, BIOLOGICALLY ACTIVE SUBSTANCES, EXTRACTS, HAW, GELATINE AND DRINK*

1. Introduction

The past century, especially the second half, was marked by an unprecedented rate of enrichment of a person with new knowledge, which entailed everything that is called scientific and technical progress. The rapidly changing modern civilization, with its colossal possibilities in any field of human activity, has generated and still unprecedented pollution of the human habitat, since human development has taken the anthropogenic and nature-destructive path. Air, water and food are over-saturated with industrial and transport waste (including carcinogenic and mutagenic benzo (a) pyrene, heavy metals, radionuclides, etc.), pesticides, antibiotics, mycotoxins and other numerous xenobiotics. The consequence of this is the deterioration of the so-called "endoecology" of human and the widespread increase in environmentally determined diseases and mortality from them.

In the Kyrgyz Republic, the negative dynamics in the state of health of the population is more pronounced due to the economic, social crisis that continues today, and entails a deficit in the nutritional structure of vital macro and micronutrients that can enhance the adaptive functions of the body.

The emergence and development of many nutritionally-related diseases are associated with the quality of nutrition. The solution to this problem is the large-scale industrial production of so-called “healthy” food products, raised to the rank of a state program. The first step in the implementation of this program should be the development of scientific approaches to the creation of new generation food products containing biologically active substances with protective, regulatory and therapeutic effects.

Food, as it is known, is a complex containing many precursors of biologically active substances, of which New biologically active substances are created in the body: hormones, transmitters, enzymes, biomolecules (DNA, RNA), and other structural elements of the living body.

Being one of the most important factors determining the health of the population, a complete, balanced, rational, age-appropriate, professional activity, living conditions, and state of health largely determines not only the health of children and adults, but is also an important element in the prevention of many common chronic diseases, including cardiovascular, oncological, gastrointestinal, endocrine, increases efficiency and creates the conditions for adequate adaptation of the organism to adverse factors of the environment. Water, air, food raw materials and food products contain an increased number of radionuclides, highly toxic chemical compounds, biological agents, pesticides, industrial and transport waste, nitrates and nitrites, mycotoxins, antibiotics, etc., which contributes to the growth of negative trends in the health of the population, reduce the well-being of people in almost all continents and states.

Food partially or completely ceased to have medicinal properties, to satisfy the human body in the daily required food nutrients in accordance

with physiological needs. According to the WHO, 80-95% of the substances alien to humans come with food, 4-7% with drinking water, 1-2% of the atmospheric air through the skin of the body into the adjacent tissues [1].

Another objective reason for the decline in human health, especially in economically developed countries of the world, is the widespread use of industrial products that have undergone tough technological processing, canning, and refining, which leads to almost complete and partial degradation of natural biologically active compounds - vitamins, minerals, phytosterols, nucleotides and other bioregulators of metabolism. This in turn leads to immunodeficiency, reduced mental and physical performance, exacerbation of chronic diseases [2].

Kyrgyzstan is among the first in terms of incidence and mortality from stroke. Distortions in the nutritional structure of the population of our country, the use of poor-quality and often counterfeit products affect the body's ability to withstand environmental aggression, hence its health, especially the health of children.

2. Background to solve the problem

Indirect evidence of serious problems with food, the quality of food consumed in the Kyrgyz Republic is not only a decline in the physical development and health of children of all age groups, but also the continued growth of diseases of the adult population of the country in such nosology groups as cardiovascular, cancer, and metabolic diseases and etc.

In the Kyrgyz Republic, if in 2015 the energy value of the diet (2212 kcal / day) of the population as a whole and its working part was higher than the minimum consumption rate (2101 kcal / day) (approved by the Government of the Kyrgyz Republic (November 6, 2009 No. 694)), then 2017 there was a decrease by 5.1% and 0.2%, compared with data from 2015 (2097 kcal / day) and the minimum consumption rate (2101 kcal / day), respectively. According to research results, it is clear that almost all these years there has been an insufficient consumption of proteins (meat, dairy products and legumes) and fats (vegetable oils) on average by 23.3% and 16.9%, respectively [2].

Energy demand of the population is filled by flour and confectionery (sugar) products and potatoes, since the majority of people in the Kyrgyz Republic (74% of the total population, 76.7% of men and 71.1% of women) consume less than 5 servings of vegetables and fruits per day (MOH KR, WHO, 2013) with the recommended 5-9 servings (on average at least 400 g / s).

Of great concern is the lack of nutrition among children. So, in the diet of the child population (1-17 years) during 2015-2017. there was a pronounced shortage of not only protein (by 27.5%) and fat (by 22.7%), but also energy value (by 2.5-2.8%). In children aged 1-3 years, the lack of proteins (by 46.8-45.2%), fat (by 44.1-40.7%) is almost half, and the deficit of kilocalories (by 26.1-22, 5%) - one fourth of the minimum need for them per day [3].

According to the Ministry of Health's research, there is a high prevalence of iron deficiency anemia among the population of the Kyrgyz Republic (37.8% of pregnant women and 34.2% of non-pregnant women, 42.6% of children), latent iron deficiency (41% of women), folate deficiency (42% of non-pregnant women), iodine deficiency disorders (61.6% of pregnant women and 43.1% of children of school age), obesity overweight (35.7% of women and 9% of children of the first 5 years of age), underweight (7, 3% of women and 18% of girls 15-19 years) [4].

Another important problem for citizens of the Kyrgyz Republic related to nutritional deficiencies is the high content of transgenic fatty acids and salt in the food products of the population of the Kyrgyz Republic. The development of overweight and obesity, diseases of the heart and blood vessels (high blood pressure, heart attack, stroke, etc.), type 2 diabetes, and some forms of malignant tumors are associated with excess ingestion of transgenic fatty acids into the human body. In the

Kyrgyz Republic, for several years, heart and vascular diseases continue to occupy the first place in the structure of causes of mortality of the population (50.5%, RMRC).

In rural areas in Kyrgyzstan, more than 60% of families are unable to provide the minimum physiological need of children for basic foodstuffs, which is a threat to the preservation of the gene pool of the nation.

In terms of social groups (in terms of income), the most disadvantaged nutritional situation was among the citizens of the first quintile group (1 million 252 442 thousand people), who did not receive kilocalories, proteins and fats in the prescribed amount. Nutrition above the established level in all three estimated indicators is obtained only by citizens from the fifth, most wealthy quintile group (1 million 250 448 thousand people) [5].

Socio-economic shocks, the deterioration of the material well-being of the majority of the population, together with psychosocial and climatic-geographical factors, led to the growth of such diseases as anemia, iodine deficiency, malnutrition, and dystrophy of children and adults. In this case, the first thing need is treatment with proper nutrition.

Accumulated international experience suggests that it is almost impossible, due to economic, social and other factors, to achieve a rapid correction of the nutritional structure due to increasing the production of common types of food, as well as improving its quality and safety in traditional ways [6].

3. Experimental part

In these conditions, the most effective, reasonable and economically acceptable way to solve this problem is the creation and expansion of food products with high biological value.

The use of wild-growing fruits and berries as food with a high biological value makes it possible, on the one hand, to quickly and easily eliminate the deficiency of essential nutrients that have a regulating effect on the organism as a whole or on certain systems, organs or functions, and on the other, to increase non-specific resistance of the organism to the effects of adverse environmental factors, to maintain a beneficial microflora in the human body, to reduce the risk of developing long-term effects of the environment [7].

For the prevention and correction of nutrition, we propose the use of wild-growing raw materials, which are not widely in demand, but at the same time are most important for maintaining human health and developing new foods with high biological value, natural foods made from environmentally friendly wild-growing raw materials, growing on the territory of our republic.

The main advantage of new types of food is 100% use of natural valuable types of raw materials with a high content of biologically active substances and multifunctional therapeutic and prophylactic properties. The basis of the selection of food models with a high biologically active value is the state of public health (reduced immunity, impaired functional activity of the gastrointestinal tract, cardiovascular system, atherosclerosis, arthritis, etc.), as well as the requirements of good flavoring and high biological value, balancing the nutritional value of foods according to the formula of nutrition in a quality set [8].

Blood red hawthorn is an additional raw material resource for the processing industry. When hawthorn fruits are combined with cultural fruits and berries, a product of better taste, aroma, color is obtained than products obtained from some varieties, which allows expanding the assortment of the products. According to the Department of Forestry of the Kyrgyz Republic, 130 species of wild fruits and berries grow in the south part of the country, which occupy 603 hectares of land. The annual collection of wild fruits and berries amounts to 5,000 tons. Among them the great interest is the blood-red hawthorn. Due to varietal characteristics, hawthorn is not used in the food industry.

The main purpose of the work is to develop optimal modes of extracting blood-red hawthorn, with the aim of further using the extract in the production of food with high biological value (drinks and jelly).

Extraction of blood-red hawthorn was carried out in experimental conditions in reactors with a stirrer on the basis of JSC "Bailyk".

Extraction was carried out in two staged direct-flow method, with different margins and water ratios, and different temperature conditions. The obtained extracts were subjected to chemical analysis.

The modes in which the largest amount of biologically active substances passes into the extract and in which no color changes occur, the taste of the extract, and which do not lead to difficulties in carrying out technological processes were chosen as the optimal temperature regimes of extraction.

To extract the fruits, the blood red hawthorn was blanched at a temperature of 80-90 ° C with live steam for 3-5 minutes, then wiped with a single-stage wiping machine. Primary marc after obtaining puree, poured water was extracted at a temperature of 750 ° C for 30 minutes. The ratio of water and marc: 2:1.

The obtained primary extract was reused to extract secondary marc under the same conditions. The chemical composition of the raw material of blood-red hawthorn and secondary extract was studied. The results are listed in table 1.

Table 1

Analysis of the chemical composition of blood-red hawthorn and secondary extract

Name of raw materials Indicators		Blood-red hawthorn	Secondary extract of blood-red hawthorn
Dry matters, %		22,2	7,84
Carbohydrates, %	Total	15,40	6,30
	Mono and disah	12,00	5,54
	Sucrose	3,40	0,76
Organic acids, %		0,60	0.31
Vitamin C mg%		89,00	12,2
Pectic substances, %		3,66	3,08
Cellulose, %		1,78	2,32

In these conditions, the most effective, reasonable and economically acceptable way to solve this problem is the creation and expansion of food products with high biological value.

The chemical composition of the extracts obtained according to the above regimes shows that mono and disaccharides, pectic substances are contained in the greatest quantity.

The content of a large amount of pectic substances in the extract is due to the fact that hawthorn fruits are subjected to heat treatment, which leads to an increase in soluble pectin. Pectic substances are very important matrix polysaccharides. Pectic acids are very easily extracted with water and are capable of forming gels. This ability in this work we use in the production of marmalade from secondary extracts.

A significant decrease in the sucrose content is due to the fact that in the process of extraction, obviously, under the influence of high temperature, sucrose is inverted to monosaccharides.

The mineral composition of the secondary extract of the blood-red hawthorn extract was also studied.

Table 2

The mineral composition of the secondary extract of the blood-red hawthorn

Name of studied raw material		Blood-red hawthorn (second extraction)
The content of macro and micronutrients: mg% per 100 g of product	Na	11,74
	R	178,2
	Ca	10,24
	Mg	8,99
	P	7,79
	Fe	0,74

From table 2 it can be seen that the mineral composition of the secondary extracts is also rich.

Residues from secondary extraction mainly contain fiber. From the recently published WHO data on the relationship between the nutritional status of the population in economically developed countries and mortality from cardiovascular diseases, it follows that there is a clear negative correlation between the latter and

the level of fiber intake and positive - with the total caloric intake and also with the consumption of food of animal origin. Given these properties of dietary fiber, squeezing hawthorn after secondary extraction is used for the production of dietary fiber.

4. Conclusion

Thus, studies on the study of secondary extracts from blood-red hawthorn, as a basis for creating new products with high biological value, show that:

- the obtained extracts contain a sufficiently high amount of biologically active substances;
- due to the biological value, the obtained extracts can be used for the production of diffusion drinks, jelly, marmalade;
- residual squeeze after secondary extraction, mainly contain fiber, and their use for the production of dietary fiber is possible;

From the obtained secondary extracts, a technology and formulation for obtaining diffusion drinks and marmalade have been developed.

Conclusion:

- experimental data obtained confirm the feasibility of using blood-red hawthorn as an object for obtaining food products;
- justified and obtained a number of relationships that allow at the stage of preliminary research and practical implementation of the production of beverages, jellies, the necessary rational parameters of extraction modes.
- the results of various extraction methods were studied and summarized, the optimal ones were chosen.

- blood-red hawthorn husks are a rich source of pectic substances, and can be used to obtain food semi-finished products used in the canning and confectionery industry.

Thus, the blood-red hawthorn is an effective source of biologically active substances, most of which are extracted from the pomace with water, under certain optimal conditions, and can serve as an additional raw material for obtaining new foods with high biological value.

Sources:

[1]. The state of food security and nutrition in the world. Increasing resilience to peace and food security. Food and Agriculture Organization of the United Nations. Rome, 2017.

[2]. Trunova S.E., Bogomolov A.V., Belimova E.A. Management of the enterprise resource potential based on functional products // Bulletin of the Voronezh State University of Engineering Technologies. 2015.33. p 186-193

[3]. Helsing E. The scientific basis for the formulation of nutrition policy // Nutrition issues. - 2006.-№3.-C.-3-8

[4]. Information Bulletin of the Kyrgyz Republic on Food Security and Poverty, 06.12.2018

[5]. Open data - Statistics of Kyrgyzstan, website: http://www.stat.kg/ru/opendata/

[6]. Monitoring the situation of children and women of the Kyrgyz Republic. Multisectoral cluster survey. Final Report, November 2015

[7]. Bulletin of the National Bank of the Kyrgyz Republic 2008-2017 The official website of the National Bank http://www.nbkr.kg./

[8]. Ranaa S, Guptad S, ranaa a, Bhushana S. Funktional properties, phenolic constituens and antioxsidant potential of industrial apple pomace for utilization as active food ingredient// Food Science and Yuman wellness. 2015. V.4. №4. P. 180-187

[9]. Environment and food. Uryupina TV, Dzhurupova B.K. // Food industry. 2004-№7.

CORROSION STABILITY IN SALT MEDIUM OF STAINLESS STEEL AND CARBON STEEL, USING DIFFERENT OXIDE SOL GEL COATINGS

Chief Assist. Prof. Dr. St. Yordanov[1], Assoc. Prof. Dr. I. Stambolova[2], Prof. Dr. L. Lakov[1],
Prof. Dr. S. Vassilev[3], Assoc. Prof. Dr. B. Jivov[1], Chief Assist. Dr. A. Nedelcheva-Bachvarova[2]

[1]Bulgarian Academy of Sciences, Institute of Metal Science, Equipment and Technologies with Hydro- and Aerodynamics Centre "Acad. A. Balevski", Sofia, Bulgaria, e-mail: stancho14@abv.bg.
[2]Bulgarian Academy of Sciences, Institute of General and Inorganic Chemistry, Acad. G. Bonchev St., bl. 11, 1113 Sofia, Bulgaria
[3]Bulgarian Academy of Sciences, Institute of Electrochemistry and Energy Systems, Acad. G. Bonchev St., bl. 10, 1113 Sofia, Bulgaria

Abstract. *Three types of oxide sol gel coatings: TiO_2, CeO_2 and TiO_2/CeO_2 composite were deposited by sol gel method on stainless steel and carbon steel. The morphology was examined by means of Scanning electron microscopy (SEM). X-ray diffraction analyses (XRD) were applied to investigate the phase composition. The corrosion resistances of the coatings were studied by evaluation of the weight loss in NaCl medium for 1200 hours. The surface of the TiO_2 samples were relatively dense with a few surface nanocrystals and after tests does not shown any signs of corrosion. The composite TiO_2/CeO_2 samples possess deep cracks which evidently favor the attacks in corrosion medium. Ceria and titania coatings deposited on stainless steel have zero weight loss in corrosive medium. The TiO_2 coatings could also effective protect carbon steel, while the TiO_2/CeO_2 and CeO_2 coatings exhibited lower corrosion resistance.*

Keywords: SOL-GEL, NANOSIZED FILMS, PROTECTIVE PROPERTIES, FILMS

1. Introduction

The family of stainless steels is widely used in various industires as well as in the biomedical sectors due to its tailorable barrier, mechanical, etc properties and biocompatibility [1]. However, in the presence of halide ions, corrosion proceeds in stainless steels [2]. Carbon steels are the most commonly used pipeline materials in petroleum industry, but they are prone to corrosion in environmental containing CO2 [3]. In order to overcome this problem various oxide films (SiO_2, ZrO_2, Al_2O_3 and TiO_2) can be deposited on the metals to improve their barrier properties [4,5]. Among them titania and ceria coatings are the most widely used the barrier properties of the steels. Pinzon et al have successfully obtained thermally sprayed alumina-titania anticorrosion coatings on carbon steel/DIN 1.0065 USt37-1/ [6]. The preparation and properties of TiO_2-CeO_2 coatings by the sol-gel dip-coating process, using cerium chloride and various titanium alkoxides, and the effect of catalysts were studied. Gelation time of the coating solution became longer with an increase in the molecular weight of titanium alkoxide. The transmittance, thickness, chromaticity and acidic durability of the coating films were measured as a function of aging time of the coating solution. The most transparent and acidic durable coating film was obtained by using a solution just before gelation. In the case of using a solution with a catalyst, the thickness became thinner with increasing pH of the coating solution [7]. Mixed CeO_2-TiO_2 films with different Ce/Ti mole ratios were prepared following an alcohol based sol-gel route via the spin coating technique using mixed inorganic-organic [$CeCl_3.7H_2O$ and $Ti(OPr)_4$] precursors. Ion storage capacity for films obtained from aged sols was studied. Enhanced titanium oxide content improved the insertion capacity of the corresponding films as was evident from inserted charge determined by multiple step chronoamperometric measurements [8]. The aim of this study is to investigate and compare the corrosion behavior of three oxide coatings (CeO_2, TiO_2 and CeO_2-TiO_2) deposited on stainless steel AISI 316 and carbon steel.

2. Experimental procedures

2.1.Deposition procedures

Two types of substrates were used for the deposition of anticorrosion coatings: stainless steel AISI 316 and carbon steel/DIN 1.0065 USt37-1/. The substrates were cleaned ultrasonically in hot ethanol and acetone, after that were dried in air at 100oC.Three types of samples were prepared: cerium oxide, titanium dioxide and titanium –cerium composite oxide. Cerium nitrate ($Ce(NO_3)_3.6H_2O$) dissolved in isopropanol was used as precursor solution. The substrates were immersed in the solution and holding for 10 seconds, after that withdrawn at a speed of 30 mm/min. Then, the samples are dried in air first at 100°C for 1 hour, after which the temperature rises to 300°C for 1 hour. After fifth dipping-drying cycles the samples were treated at 400°C and were denoted as C1 (on stainless steel) and C3 (on carbon steel/DIN 1.0065 USt37-1/). Titanium isopropoxide (TTIP) were used to obtain the TiO2 deposition solution. Acetylacetone (AcAc) is used as a stabilizing agent. Titanium isopropoxide (TTIP); $Ti(OC_3H_7)_4$, 98% purity, (Acros) and AcAc are dissolved in 2-propanol. The resulting solution is transparent and orange in color, which is typical of the chelated complex formed. The complex formation reaction is exothermic. After vigorous stirring at room temperature, a mixed solution of distilled water and i-propanol was added dropwise to the above solution under continuous stirring. The molar ratio of components is TTIP: iPrOH: H_2O:AcAc=1:30:1:1. The resulting solution was denoted as 1. Then the deposition-drying procedures and final treatment followed the scheme described deposition of CeO_2 coatings. The samples were denoted as T1 (on stainless steel) and T3 (on carbon steel). For the composite coatings were used solution mixture of titanium and cerium precursors in atomic ratio 30/70. Then the deposition-drying procedures and final treatment followed the scheme described deposition of CeO_2 coatings. The corresponding samples were denoted as CT1 (on stainless steel) and CT3 (on carbon steel)

2.2 Analyses

The phase compositions of the samples were studied by X-ray diffraction (XRD) with CuKα-radiation (Philips PW 1050 apparatus). A scanning electron microscope (SEM) Philips 515 was used for morphology observations of the films**.**

2.3. Evaluation of the corrosion resistance of the coatings.

The corrosion resistance of the samples was evaluated weight loss method, using salty corrosive solution of 3.5% NaCl at 25°C (EN ISO10289/2006). The corrosion resistance of the investigated samples and uncoated stainless steel (reference sample). The temperature of the solution and the air temperature were controlled by calibrated thermometers. The mass weight loss was determined after 1200 hours of corrosion attack.

3. Results and discussion

From the XRD analyses of the both C and CT samples confirm the presence of pure cubic CeO_2 phase according to JCPDS card 43-1002 with polycrystalline nature. It has to be note that in the composite CT1and CT3 coatings (i) no peaks corresponding to anatase phase were detected; (ii) peak broadening was observed in comparison to the pure ceria coatings (Fig. 1a,b). X-ray diffraction pattern of T1 and T3 coatings revealed pure anatase phase without any peaks of rutile or brookite phase. The average crystalline size of CeO_2 coatings is 7 nm, while the composite materials have lower crystalline size - 4 nm. This may be due to the formation of Ce–O–Ti bonds, which inhibited the crystallite growth of TiO_2. The TiO_2 crystallite size was calculated from the highest intensity plane (101) and found to be around 13 nm.

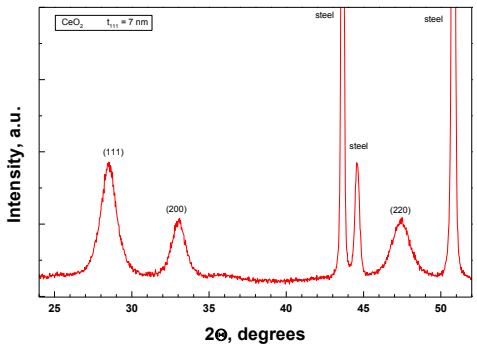

Fig. 1-a

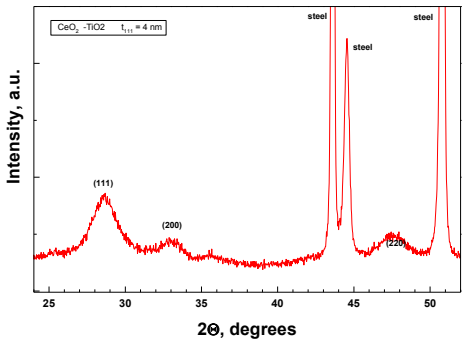

Fig. 1-b

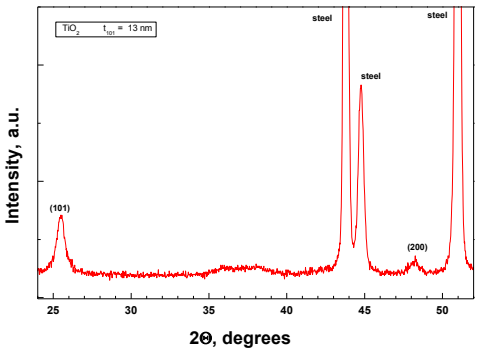

Fig. 1 –c

Fig. 1*. XRD patterns of CeO_2 (a), CeO_2-TiO_2 (b) and TiO_2 (c) coatings on stainless steel AISI 316*

Figure 2 shows the SEM images on the surface of the samples before and after the corrosion test. Sample C2 is relatively dense and smooth. After the corrosion test, the surface retains its characteristics and holes, pits and other characteristic signs of corrosion are not obsevable (Fig 2b).

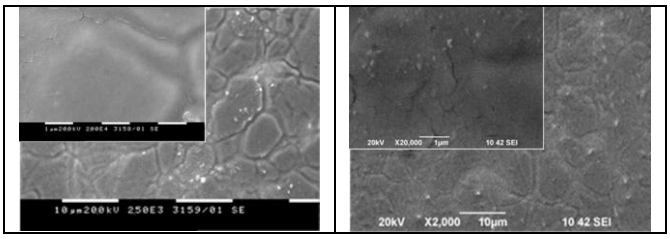

Fig. 2. *Morphology of freshly prepared CeO_2 (C1) - (left) and after corrosion test (right)*

.

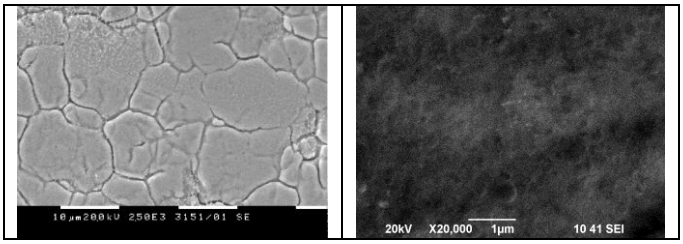

Fig. 3. *Morphology of freshly prepared TiO_2 (T1) - (left) and after corrosion test (right) at higher magnification (20 000).*

Fig. 3 shows the morphology of the TiO_2 coating, obtained from the titanium isopropoxide sol on stainless steel substrates. The surface is continuous, but microcracks are visible, which could be due to the small residual compressive stresses [9]. During the drying, crystallization and densification processes the coatings were subjected to fracture and macro cracking due to the intrinsic film stresses, caused by chemical reactions during drying, difference in thermal expansion coefficients between substrate and the TiO_2 film, grain interaction and grain size of the TiO_2 film [10]. Also the stainless steel substrate has a higher coefficient (17×10^{-6}∘C) of linear thermal expansion than the TiO_2 film ($2.1–2.8\times10^{-6}$∘C) [11]. On cooling, the stainless steel substrate shrinks more than the TiO_2 film leading leading to the formation of small microcracks.

As can be seen the coating C3 has a relatively dense, but rough surface with several microcracks. After the corrosion attack the morphology changes, and visible signs of corrosion are visible (Fig 4-c,d).

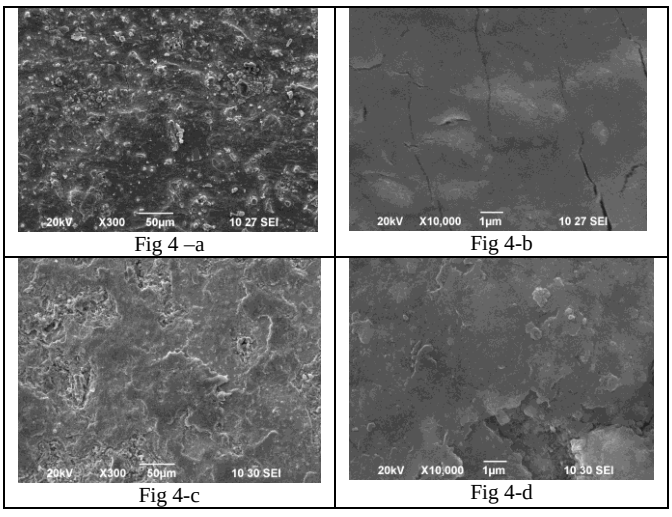

Fig 4 –a Fig 4-b

Fig 4-c Fig 4-d

Fig. 4. *Morphology of freshly prepared CeO_2 on carbon steel/DIN 1.0065 USt37-1/ (C3) - (a,b) and after corrosion test (c,d).*

It has to be note that the surface morphology of TiO_2 coating is a relatively dense without cracks. (Fig. 5) It is obvious numerous small crystallites on the surface. After the immersion in corrosive salt medium the surface of titania coating remains almost unchanged even

such long period of time. This result proves the good barrierproperties of TiO_2 coatings deposited on carbon steel/DIN 1.0065 USt37-1/.

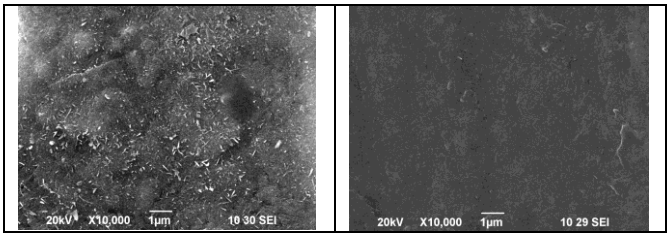

***Fig.5**. Morphology of freshly prepared TiO_2 coatings on carbon steel/DIN 1.0065 USt37-1/ (T3) - (left) and after corrosion test (right).*

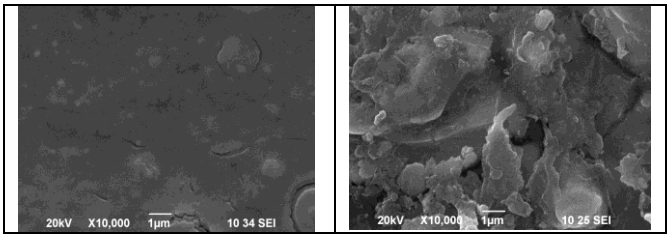

***Fig. 6**. Morphology of freshly prepared CeO_2 –TiO_2 coatings on carbon steel/DIN 1.0065 USt37-1/ (CT3) - (left) and after corrosion test (right).*

It has to note that the corrosion attack influences significantly the surface features of the composite CT coatings. The SEM pictures revealed deep craters and even sections, where the coating has begun to be removed from the substrate.

***Table 1.** Corrosion rate for all tested coatings after 50 and 1200 hours corrosion attack.*

Sample Code	K_{50} [g/m$_2$h]	K_{1200} [g/m$_2$h]
CT 1	0	0.002
CT3	0.030	0.028
C 1	0	0
C 3	0.021	0.032
T 1	0	0
T3	0.002	0.007

The analysis of the results of the corrosive test is as follows. For CT samples the corrosion rate K is the lowest for CT1 (after the first fifty hours it is zero) and the highest for CT3. In the Ce series in the Ce1 sample there is no corrosion process during the first fifty hours, and in the second run (1200 hours) the weight loss is negligible and the value of K is equal to zero. These results refer to both test periods. In the TiO_2 coatings, T1 corrosion rates K are zero for both test periods due to minor weight changes. In T3, the corrosion rate is higher than that of T1 in both periods.

The weight loss of CT coatings deposited on stainless steel after corrosion atack is 7 x10^{-5} g/m^2, while for T1 and C1 zero weight loss was observed (Fig. 7) The corrosion resistance of the all investigated coatings on stainless steel is higher, than those on carbon steel/DIN 1.0065 USt37-1/. The results presented on Figures 6 and 7 confirm that TiO_2 coatings exhibit increased ability to protect both the stainless and carbon steels, in comparison to that of C and CT coatings. This result probably is due to the less pronounced crystallization of titanium dioxide (Fig. 1-c) and suitable surface features.

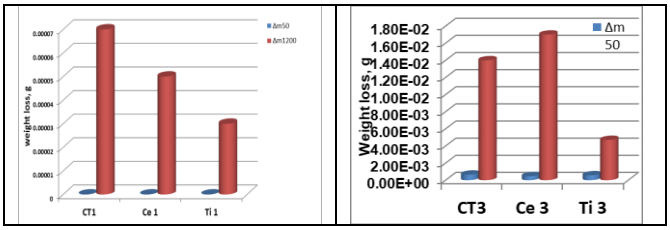

***Fig. 7.** Weight loss for all tested coatings after 50 and 1200 hours corrosion attack.*

4. Conclusion

The anticorrosion resistance of stainless steel and carbon steel coated with several coatings: TiO_2, CeO_2 and TiO_2/CeO_2 by sol gel method were investigated. The coatings on stainless steel are relatively dense. After the corrosion attack the morphology of cerium dioxide coatings changes, and visible signs of corrosion are visible. It is obvious numerous small crystallites on the surface. The composite TiO_2/CeO_2 samples possess deep cracks which evidently favor the attacks in corrosion medium. Titania coatings exhibit good barrier properties both on stainless steel and carbon steel: the surface of titania coating remains almost unchanged even at such long period of corrosion attack. Ceria and titania coatings deposited on stainless steel have zero weight loss in corrosive medium. The TiO_2 coatings could also effective protect carbon steel, while the TiO_2/CeO_2 and CeO_2 coatings exhibited lower corrosion resistance. This results could be due to the less pronounced crystallization and suitable surface morphology of the titania coatings.

Acknowledgement: The authors are grateful to the financial support of Bulgarian National Science Fund at the Ministry of Education and Science, Contract No DN07/2 14.12.2016.

5. Literature

[1] Fini M, Aldini N. N, Torricelli P., Giavaresi G., Borsari V., Lenger, H, Bernauer J., Giardino R., Chiesa R, Cigada A., Biomaterials 24 (2003) 4929.
[2] Durán A., Castro Y., Aparicio M., Conde A., De Damborenea J.J., Protection and surface modification of metals with sol–gel coatings, Intern.Mater.Rev. 52 (2007) 175.
[3] Lopez D.A., Simison S.N., Sanchez SR., The influence of steel microstructure on CO_2 corrosion. EIS studies on the inhibition efficiency of benzimidazole, Electrochim. Acta, 48 (2003) 845-85
[4] Padhy N., Mudali U.K, Chawla V., Chandra R, B. Raj, Mater. Chem. Phys. 130 (2011) 962.
[5] Gallardo J., Duran A., Damborenea J.J., Corros. Sci. 46 (2004) 795.
[6]. Pinzón A. V., K. J. Urrego, A. González-Hernández, M. R Ortiz, F.V. Galvis, Corrosion protection of carbon steel by alumina-titania ceramic coatings used for industrial applications, Ceram. Intern., 44 (2018), 21765.
[7]. Makishima, A., Asami M.,' Wada K, Preparation and properties of TiO_2-CeO_2 coatings by the sol-gel process, J. Non-Crystall. Solids, 121(1990)310.
[8]. Makishima, A., Asami M.,' Wada K., Preparation and properties of TiO_2-CeO_2 coatings by the sol-gel process, Journal of Non-Crystalline Solids, 100 (1988) 321.
[9]. Exarno, G. J., Hess N. J, Spectroscopic measurements of stress relaxation during thermally induced crystallization of amorphous titania films, Thin Solid Films 220 (1992) 254.
[10]. Teeuw D. H. J., De Haas M., De Hosson J. Th. M, Residual stress fields in sol-gel-derived thin TiO_2 layers, J. Mater. Res. 14 (1999) 1896.
[11]. Scott, M. L., Nat. Bur. Stand. (US) Spec. Publ. 688 (1985) 329.

GEOINFORMATION MODELING

Assos. Prof. Milen Ivanov PhD,
NMU „Vassil Levski" Veliko Tarnovo, Bulgaria
e-mail milen_i1970@abv.bg

Abstract: Modeling can be defined in the context of geographic information systems (GIS) as occurring whenever operations of the GIS attempt to emulate processes in the real world, at one point in time or over an extended period. Models are useful and used in a vast array of GIS applications, from simple evaluation to the prediction of future landscapes. Modeling in GIS raises a number of important issues, including the question of validation, the roles of scale and accuracy, and the design of infrastructure to facilitate sharing of models.

Key words: *GEOSPATIAL DATA-MODEL, GEOINFORMATION TECHNOLOGY, GEOGRAPHIC INFORMATION SYSTEM, DATA INTEROPERABILITY*

1. Introduction

In recent years, information has become a growing and vital place in the development of society. Because of its growing importance, the XXI century is increasingly being called a century of information technology. This applies equally to the military field where the preparation and conduct of combat operations is impossible without reliable information.

In the process of development, the modern information society is increasingly experiencing new form and content conflicts and crises caused by different processes. The experience of recent years shows that crises are interdependent with the internal and external socio-economic and political environment and heavily dependent on the information linking of society.

2. The essence of geoinformation modeling.

In order to make a logical description of the subject area, a model of the data is required for its modeling. In an appended embodiment, the data model is such a data organization that, through the types and structures of data processed by a computer, allows logical and physical implementation of the database for any subject area.

Data modeling means a multitude of conceptual data organization solutions and the data structure is a detailed description of the data through lists, arrays, files and their storage in a computer [7].

The basis of most data processing methods in information systems and technologies lies in the concept of an information model representing a formalised representation of existing objects from reality. The information model serves to describe the relationships between real objects and phenomena and can be built for an object, a set of objects, complex systems, information systems, etc.

The information model of the object (process) provides a formalized representation of the studied elements of the system and their interrelations and contains different levels of descriptions: object, system and base [3].

Information modeling is the ability to build information models and their analysis needed to study real-world objects. Information modeling can be seen as a modern information technology. It includes skills for creating, interpreting and modeling different information models.

Modern information modeling requires skills to work with information to make a qualitative transition from descriptive models to resource and resource to intellectual. For this reason, it can be argued that information modeling is the basis for future intellectualization of education, linking the link between information and intellectual society.

To construct an optimal information model that meets the requirement to increase the efficiency and quality of the information system, it is necessary to define the basic concepts and constructions characteristic of the subject area.

The introduction to the spatial object modeling theory provides a basis for defining the information concept of the real world.

3. Information concept for the real world.

According to the information concept [5], space consists of separate objects. Each object is represented by:

- points;
- boundaries defined by lines;
- graphic attributes for the border elements;
- attribute data for the object;
- relationships (links) of one graphic object with the other objects.

At the same time, space consists of continuous areas. Each continuous area has:

- boundaries defined by points or by analytical function;
- graphic attributes for the border elements;
- attribute data for the area;
- relationships (relationships) of one area with other areas.

Objects and continuous areas make up the space without overlaps and without any omissions (no shortage).

Through the information concept, the following stages of modeling are distinguished:

- a conceptual model of space;
- modeling with data (data models);
- computer presentation, visualization, and model usage.

The sequence of modeling of the real world is presented in figure 1.

Informational modeling in general, regardless of the field of application, must correspond to a particular concept and be directed to presenting and studying the surrounding reality.

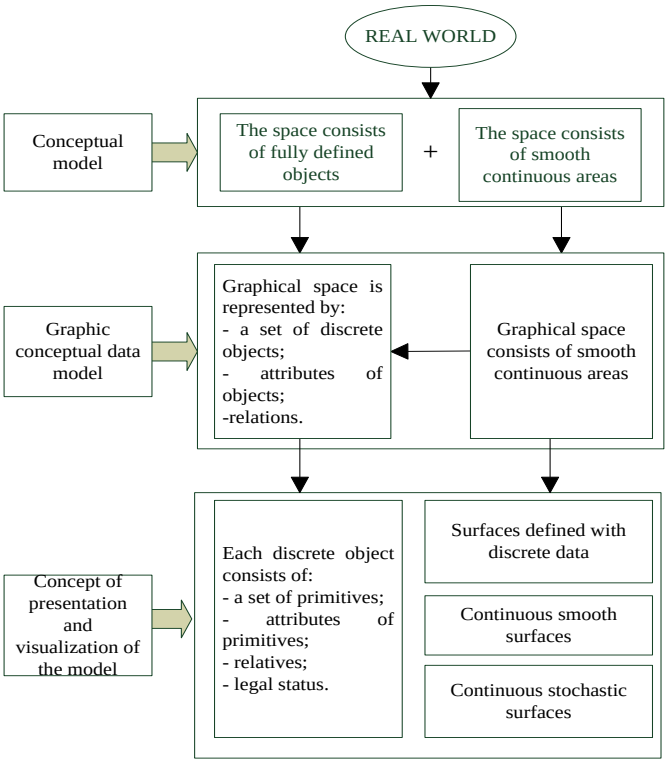

Figure 1. *Information concept for the real world.*

Similar trends are also observed in electronic intelligence systems. For example, by determining the location of an

opposing station, it can be affected[1].

The process of examining objects of real reality can simply be represented by the attitude:

object → content → presentation (1)

Using information modeling, this process is interpreted as follows:

essence → description of properties → referral of properties to a known class → description of relations between properties → abstract description of systems of properties and relations → functional description of properties and relations → selection of sets of information units → modification of input sets of information units → study of the change of the input data sets. (2)

The basis of the data processing process is digital modeling. It allows for vector-topology modeling, object buffering, network analysis, building a digital model of the site, etc.

In the processing of information to create a database, the geo-data grouping units are geo-information models. They serve as the basis for the formation of geoscience for real objects and phenomena.

The data model presents static and dynamic properties of the surrounding world with the desired degree of precision. Modeling means abstraction of reality, and this is the core of any information system. Abstraction simplifies reality, but retains the relevant information for each user and the necessary detail. In geoinformation, modeling is a formalization or representation of reality through a variety of tools and approaches.

Geoinformation modeling is defined [9] as a graphical object modeling model interconnected with databases and includes five basic types of modeling:

1. Conversion of graphical information resulting in modification of graphical and tabular data;
2. Structuring of tabular data, resulting in alteration of graphical and tabular data;
3. Converting graphical objects from one type to another;
4. Building digital phenomena models;
5. Editing, editing or modifying graphical objects based on spatial object relationships (without the use of graphical editors).

The basis of geo-information modeling as a specialized technology are transformations based on the theoretical-multiple relationships, the laws of formal logic, image processing algorithms, computer graphics, DBMS technologies and others [9].

There is no ideal model that is claimed to represent 100% of reality. This is due to the existing stages of modeling and the accepted concepts, definitions and semantics used by different user groups.

Planning operations in military intelligence[2] requires the creation of a well-known battlefield picture, which is basically geo-information modeling.

In geo-information modeling, real objects and phenomena are represented by a formalized description, which becomes the basis for the study of the objects and their interrelation. The following abstraction levels are applied (Figure 2):

- reality - the real world;
- a conceptual model - a user-oriented, partially structured model of the selected objects and processes used in a particular problem area;
- a logical model - is an application-oriented image of reality; is often represented as a diagram showing the selected objects and the relationship between them;
- physical model - describes the files and tables used to store data; specific application.

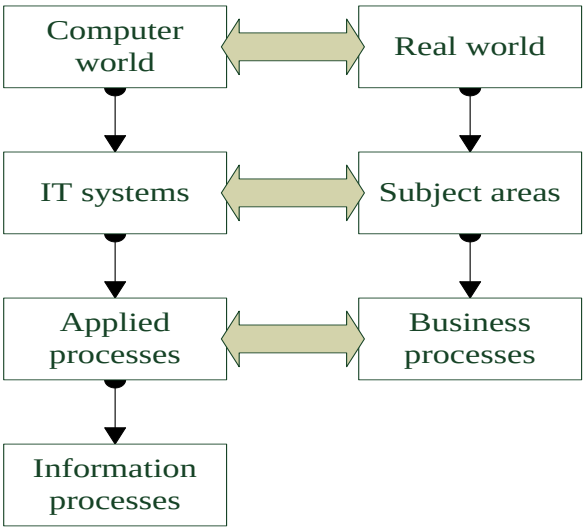

Figure 2. *Abstraction levels in geoinformation modeling.*

The data model M consists of basic rules R and operators O [11]. The basic rules R are implemented by:

- the Rs structure, which includes the type and organization of model data;
- the Ro restrictions, which define boundaries of the model structure.

Operators O include operations and procedures for working with data, with their properties and relationships at any particular point in time.

For defining, formalizing, and solving a given task, a part of the real world, called a subject area, with clearly defined boundaries that can be described by a finite number of objects, actually existing or abstract, is used.

With the development of database theory (DB), various methodological approaches are being developed to design and physically store data. The external level is the initial stage of designing an AB [6], where each user declares his / her interests from the real world, which must be reflected in the DB. This process is accepted to be called the creation of external schemes or external models that are not associated with a particular operating system or computer configuration.

Space can be conceptualized in different ways for geospatial analysis purposes. The conceptual model can be created when external schemes are described with the concepts of a particular data model. It does not depend on the operating system of the computer and its parameters.

CONCLUSION

1. In geoinformatics, the extraction of knowledge about the surrounding world is accomplished by a maximum of sources compared to other sciences. Geoinformatics operates geo-information and geodata, integrating different types of information. This extends the scope for complex analysis to support decision-making and response forces management.

Modern trends in the development of geoinformation technologies that are relevant in terms of maximizing the rapid production and dissemination of geospatial information are an important element for achieving early warning system operability.

[1] Lazarov L.I., The basics of the electronic war, Veliko Varnovo, 2018, p. 88

[2] Yankov Y.I., Human intelligence – planning in operations other than war, Collection of reports from the Annual University Scientific Conference, V. Varnovo, 2011, p.2

LITERATURE

1. Lazarov L.I., The basics of the electronic war, NMU "V. Levski", Veliko Varnovo, 2018, p. 88, ISBN 978-954-753-270-0

2. Yankov Y.I., Human intelligence – planning in operations other than war, Collection of reports from the Annual University Scientific Conference, V. Varnovo, 2011, *vol. 6,pp. 136-140, BT, 2011, ISBN 978-954-753-089-8*

3. Andreev AI, Markov M.M., Geographic Information Systems, Shumen, 2009

4. Bugayevsky L.M., Tsvetkov Y., Geoinformation Systems, School Supplies for Moscow, 2000, 222 p.

5. Valchinov VG, Geoinformatics, UACEG, Sofia, 2003

6. Delieska B., Geographic Information Systems, Lotus IS, Sofia, 2003

7. de Mers M.N., Geographical Information Systems, Moscow, Date +, 1999Bright Osei Twumasi, Modelling spatial object behaviours in object-relational geodata-base, International institute for geo-information science and earth observation, Enschede, Netherland, 2002

8. Cova T.J. Extending geographic representation to include fields of spatial objects, Int. J. geographical inforation science, vol.16, № 6, 509-532 p., 2002

9. Goodchild M.F., Towards a general theory of geographic representation, Wiley, 2002

10. Konechny M. at all, Multimedia textbook of Geoinformatics, First int. conference on cartography and GIS, Боровец, 25-26 януари, 2005

11. Longley P. A., Goodchild M. F., Maguire D. J., Rhind D. W., Geographic Information Systems and Science, WILEY, 2006

12. Smith M. J., Goodchild M. F., Longley P. A., Geospatial Analysis, SE, 2007

13. http://www.nwgis.com, Spatial Analysis, Accessed 15.05.2018

2.

PHYSICAL AND LUMINESCENT PROPERTIES OF GLASSES IN THE SYSTEM WO_3-La_2O_3-B_2O_3-Nb_2O_5

ФИЗИЧНИ И ЛУМИНЕСЦЕНТНИ СВОЙСТВА НА СТЪКЛА ОТ СИСТЕМАТА WO_3-La_2O_3-B_2O_3-Nb_2O_5

Assoc. Prof. Iordanova R. PhD., Aleksandrov L. PhD., Milanova M. PhD,
Institute of General and Inorganic Chemistry, Bulgarian Academy of Sciences, G. Bonchev, str. bld. 11, 1113 Sofia, Bulgaria.
reni@svr.igic.bas.bg, lubomirivov@gmail.com, margi71@abv.bg

Abstract: *New multicomponent glasses in the system WO_3-La_2O_3-B_2O_3-Nb_2O_5 doped with Eu^{3+}, as a transparent active media for optical application were obtained. Physical parameters as density, molar volume, oxygen molar volume and oxygen packing density were determined. The thermal behavior of the obtained glasses was examined by differential thermal analysis (DTA). It was established that glass crystallization temperature is about 750°C. Microstructural characterization was made by Raman and UV-VIS spectroscopies. Based on the obtained spectral data short-range order and connectivity in glass network were determined. High photoluminescence emissions due to the 4f transitions $^5D_0 \rightarrow {}^7F_j$ (j=0-4) of Eu^{3+} ions were observed. Colorless bulk tungstate glass, containing Nb_2O_5 with high transparency and high refractive index were prepared.*

KEYWORDS: GLASS, DENSITY, REFRACTIVE INDEX, RAMAN SPECTROSCOPY

1. Introduction

Glasses belong to advanced functional materials. Their properties (electrical, optical) depend significantly on the local structure of the glass. Thus, the luminescence properties of rare earth elements depend largely from the matrix in which they are doped.

The tungsten and niobium oxide based glasses are suitable for optical applications, as well suitable matrices for doping with active ions possessing characteristic emission in the visible area [1-3].

Eu^{3+} ion is the most popular and important active ion for obtaining intensive red emission. The emission intensity of europium (III) ion embedded in tungstate phases is prominently enhanced (compared with that of Eu^{3+} in the most hosts) because of the non - radiative energy transfer from the WO_4 group in the host matrix to the rare earth ion. Moreover, in Eu^{3+} doped tungstates, pure red color can be obtained due to the distortion of the local symmetry of Eu^{3+} ion in the host. As a result, tungstate glasses can serve as competitive host materials in the optical field. On the other hand Nb_2O_5-based glasses exhibit excellent optical properties exceeding those of commercial optical glasses. These glasses show a wide optical transparency in the visible to IR range and have a high refractive index (over 2.1) in the visible region with low wavelength dispersion.

Our experience in synthesis and structural investigations of tungstate glasses motivates us to examine the possibility of synthesis of tungstate glass with participation of Nb_2O_5 and to establish its influence on physical, structural and luminescent properties of Eu^{3+} added in the glass matrices.

For the initial tungstate glass, $50WO_3 \cdot 25La_2O_3 \cdot 25B_2O_3$ composition was chosen whose structure and physical properties were established in our previous studies [4-6].

2. Experimental

Samples with the compositions: $50WO_3$:$25La_2O_3$:$25B_2O_3$ (WLB); $40WO_3$:$25La_2O_3$:$25B_2O_3$:$10Nb_2O_5$ (WLBN); $50WO_3$:$22La_2O_3$:$25B_2O_3$:$3Eu_2O_3$ (WLBE); and $40WO_3$:$10Nb_2O_5$:$22La_2O_3$:$25B_2O_3$:$3Eu_2O_3$ (WLBNE) (mol%) were prepared using reagent grade Nb_2O_5, H_3BO_3, La_2O_3 WO_3 and Eu_2O_3. The batches (each batch weight: 20 g) were melted at 1250–1280 °C for 30 min in a platinum crucible in air. The glasses were obtained by pouring the melts onto an iron plate and by pressing with another iron plate (cooling rate: ~10^2 K/s). Density of the glasses at room temperature was determined with the Archimedes method using distilled water as an immersion liquid. The glass transition (T_g) and crystallization (T_p) temperatures were established by differential thermal analyses (DTA) (RigakuThermo Plus TG 8120) at a heating rate of 10 K/min (±1 K). Optical transmission spectra were measured in the wavelength (λ) range of 300–1000 nm at room temperature using a spectrometer (Shimadzu U-3120). The uncertainty in the observed wavelength is about ± 1 nm. The optical energy gap (E_{opt}) of glasses was calculated from the transmittance spectrum using Tauc plot road and following equation:

$$\alpha h\nu = A(h\nu - E_{opt})^2 \quad \text{.....(1)}$$

where α is the absorption coefficient, h is the constant of Planck, ν is the frequency of light and A is the energy constant.

Refractive indices at a wavelength (λ) of 632.8 nm (He–Ne laser) were measured at room temperature with a prism coupler (Metricon Model 2010). Raman scattering spectra at room temperature were measured with a laser microscope (Tokyo Instruments Co., Nanofinder) operated at Ar^+ (λ = 488 nm) laser with resolution of ±1 cm^{-1}. The photoluminescence (PL) spectra of $50WO_3$:$22La_2O_3$:$25B_2O_3$:$3Eu_2O_3$ and $40WO_3$:$10Nb_2O_5$:$22La_2O_3$:$25B_2O_3$:$3Eu_2O_3$ glasses in the visible region of Eu^{3+} ions for the glass samples were measured with a PL spectrometer (Hamamatsu Photonics: C9920-20) at room temperature, in which the excitation light with a wavelength of ʎ = 397 nm was used.

3. Results and Discussion

3. 1. Glass formation

Homogeneous transparent glasses were obtained from the all compositions studied. Figure 1 presents pictures of $50WO_3$:$25B_2O_3$:$25La_2O_3$ and $40WO_3$:$25La_2O_3$:$25B_2O_3$:$10Nb_2O_5$ (WLBN) glasses. In order to polish the glass samples, they were heat treated at temperature, which is 10 °C below the glass transition temperature for the relaxation from the internal stresses. Despite this, the Nb_2O_5 - free glass, cracked and broke into small pieces. This result shoes that desirable sized bulk sample can be obtained from the Nb_2O_5 - containing composition only.

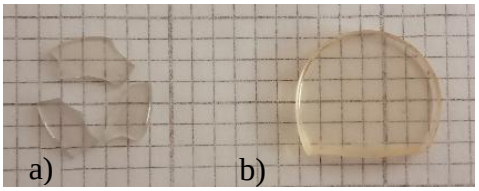

Fig. 1. *Pictures of a) $50WO_3$:$25B_2O_3$:$25La_2O_3$ (WLB) glass; b) $40WO_3$:$25La_2O_3$:$25B_2O_3$:$10Nb_2O_5$ (WLBN) glass*

Obviously, the presence of Nb_2O_5, increases the glass forming ability and stability of the samples which is important from the technological point of view.

3. 2. Physical properties

The simplest way of detecting structural changes in glass network, with compositional variation is by probing its rigidness/flexibility by measuring the glass density and calculating of molar volume, oxygen molar volume and oxygen packing density of the glass system [7, 8]. Having in mind this, we measured the density of the obtained multicomponent glass containing 10 mol% Nb_2O_5 (WBLN) and compared with the density of the $50WO_3.25B_2O_3.25La_2O_3$ (WBL) glass previously reported by us in ref [6] in order to check the effect of the Nb_2O_5 on the physical properties and structure of the ternary tungstate glass.

The density of glasses was estimated according to the Archimedes principle by using the equation:

$$\rho_g = \frac{W_a}{W_a - W_b} \times \rho_o \quad \text{.....(2)}$$

where, W_a is the sample weight in air, W_b is the sample weight in the water, ρ_0 is the density of the water. Theoretical density of glasses was calculated by the following equation

$$\rho_{th} = \frac{\Sigma x_i \rho_i}{\Sigma n_i} \quad \text{.....(3)}$$

where, ρ_i is the density of i^{th} oxide component and x_i is its mole fraction in the composition. From the experimentally evaluated density values the molar volume (V_m), the molar volume of oxygen (V_o) (volume of glass in which 1 mol of oxygen is contained) and the oxygen packing density (OPD) of $50WO_3.25B_2O_3.25La_2O_3$ and $40WO_3{:}25La_2O_3{:}25B_2O_3{:}10Nb_2O_5$ glasses were estimated, using the following relations respectively:

$$V_m = \frac{\Sigma x_i M_i}{\rho_g} \quad \text{.....(4)}$$

$$V_o = V_m \times \left(\frac{1}{\Sigma x_i n_i}\right) \quad \text{.....(5)}$$

$$OPD = 1000 \times C \times \left(\frac{\rho_g}{M}\right) \quad \text{.....(6)}$$

where x_i is the molar fraction of each component i, M_i the molecular weight, ρ_g the glass density and n_i is the number of oxygen atoms in each oxide, C is the number of oxygen per formula units, and M is the total molecular weight of the glass compositions. The values obtained are listed in the Table 1.

Table 1. *Molecular weight* M_w, *theoretical density* ρ_{th}, *measured density* ρ_{exp}, *molar volume* V_m, *oxygen molar volume* V_o, *oxygen packing density OPD*

Sample ID	M_w g/mol	ρ_{th} g/cm^3	ρ_{exp} g/cm^3	V_m cm^3/mol	V_o cm^3/mol	OPD mol/L
WLB	214.78	5.85	5.614	38.26	12.75	78.42
WLBN	218.17	5.59	5.503	39.65	12.39	80.72

As it is seen from the table, the experimentally evaluated density and the density estimated through formula compositions are comparable. It was found that the density decreases, while the molar volume increases with the introduction of Nb_2O_5 into a $50WO_3{:}25La_2O_3{:}25B_2O_3$ glass. These changes could be related to the incorporation of voluminous NbO_6 octahedra in the glass network resulting in its expanding. Compared to the ternary tungstate glass, a slight decrease in oxygen molar volume of Nb_2O_5 - containing glass, is detected due to the substitutions of higher field intensity W^{6+} ions (1.58) with lower field intensity Nb^{6+}ions (1.26) [9]. OPD value of $40WO_3{:}25La_2O_3{:}25B_2O_3{:}10Nb_2O_5$ glass is higher as compared with that of $50WO_3{:}25La_2O_3{:}25B_2O_3$ glass that can be attributed to an increasing network connectivity due to the formation of new linkages between NbO_6 and the other structural units, existing in the amorphous network.

3. 3. Thermal analysis

In order to check the influence of Nb_2O_5 on the thermal behavior and structural features of $50WO_3{:}25La_2O_3{:}25B_2O_3$ glass, we have studied $40WO_3{:}25La_2O_3{:}25B_2O_3{:}10Nb_2O_5$ by DTA. DTA analysis is a useful method in suggesting structural change that take place due to the compositional changes [10]. The glass-transition temperature T_g gives information on both the strenght of inter atomic bonds and the glass network connectivity. The higher T_g corresponds to more rigid structure, whereas the glasses having a loose-packed structure have lower T_g [8, 11]. The difference $\Delta T = T_p - T_x$, between crystallization temperatures of the glasses (T_p) and glass transition temperature (T_g) has been frequently used as a rough measure of the glass thermal stability [12]. The higher ΔT value, the more favored is the glass forming process [13]. Fig. 2 compares DTA curves of $40WO_3{:}25La_2O_3{:}25B_2O_3{:}10Nb_2O_5$ glass investigated in this work and of $50WO_3{:}25La_2O_3{:}25B_2O_3$ glass previously studied by us [6]. The hump, corresponding to the glass transition temperature (T_g) followed by exothermic effects connected with the crystallization temperatures of the glasses (T_p) are clearly observed. Their values and the calculated thermal stability $\Delta T = T_p - T_x$ are listed in Table 2.

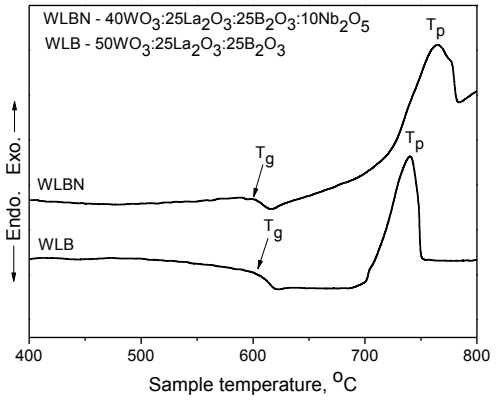

Fig. 2. *DTA curves of $50WO_3{:}25B_2O_3{:}25La_2O_3$ (WLB)and $40WO_3{:}25La_2O_3{:}25B_2O_3{:}10Nb_2O_5$ (WLBN) glasses*

Table 2. *Values of glass transition temperature T_g, crystallization temperatures (T_p), thermal stability ΔT and average single-bond enthalpy E_B of investigated glasses.*

Sample ID	T_g/(ºC)	T_p/(ºC)	ΔT/(ºC)	E_B/kJ mol^{-1}
WLB	598	745	147	727.75
WLBN	594	762	168	737.75

As one can see, both glasses are characterized with high values of the glass transition temperature (T_g), which is an indication of the formation of well packed glass structure. The addition of Nb_2O_5 does not affect significantly the amorphous network of the ternary 50WO3:25La2O3:25B2O3 glass as both glasses possess the same T_g values.

The values of T_g were correlated with average single bond enthalpy of glasses using the following relationship proposed in the ref [14, 15]:

$$E_B = \frac{50E_{w-O} + 25E_{La-O} + 25E_{B-O}}{100} \quad \text{.....(7)}$$

$$E_B = \frac{10E_{Nb-O} + 40E_{w-O} + 25E_{La-O} + 25E_{B-O}}{100} \quad \text{....(8)}$$

where $E_{W\text{-}O}$; $E_{B\text{-}O}$ $E_{La\text{-}O}$ and $E_{Nb\text{-}O}$ are the bond dissociation energies for the single bonds: W-O; B-O, La-O and Nb-O respectively [16].

Having in mind that glass transition temperature is very sensitive to any change in the coordinating number of network forming atoms and to the formation of non-bridging oxygens [17-19] we can explained the equal T_g of both glasses as a result of the

replacement of WO_6 octahedral units by NbO_6 octahedra. The higher E_B value of the Nb_2O_5-containing glass can be connected with the difference in bond dissociation energies of metal oxide. Since Nb-O bond enthalpy is 753 kJ mol^{-1}, which is higher than W-O bond enthalpy (653 kJ mol^{-1}), the average single bond energy increases with the addition of niobium, because of the formation of stronger Nb-O at the expense of weaker W-O bonds.

The thermal stability criterion ΔT of Nb_2O_5-containing glass is larger indicating that Nb_2O_5 contribute to increase the thermal stability and glass forming ability of the composition.

3. 4. Raman analysis

Raman spectroscopy was used to deduce structural features of the obtained multicomponent glass containing 10 mol% Nb_2O_5. A comparison was made with the Raman spectrum of $50WO_3{:}25B_2O_3{:}25La_2O_3$ glass previously studied by us [4]. The deconvoluted Raman spectra of both glasses are shown on Figure 3. It is known that the Nb–O and W–O characteristic vibrations overlap and appear in the same frequency range of the spectra. The strong Raman bands at 850 and 950 cm^{-1} in the spectrum of $50WO_3.25B_2O_3.25La_2O_3$ (WLB) glass have been assigned to isolated $(WO_4)_2$ units. The formation of WO_6 units have been suggested due to the presence of the band at 980 cm^{-1} [4]. In the spectrum of $40WO_3{:}25\ La_2O_3{:}25\ B_2O_3{:}10Nb_2O_5$ (WLBN) glass a new band at 913 cm^{-1} appears, bands at 980 and 760 cm^{-1} disappear and intensity of band at 688 cm^{-1} increases with addition of Nb_2O_5. All bands observed in the spectrum of Nb_2O_5 containing glass can be also related to vibration of Nb-O bonds except those at 954 and 1040 cm^{-1}, which are related with the symmetric stretching vibration (ν_1) of $(WO_4)_2$ and vibrations of BO_3 and BO_4 structural units respectively.

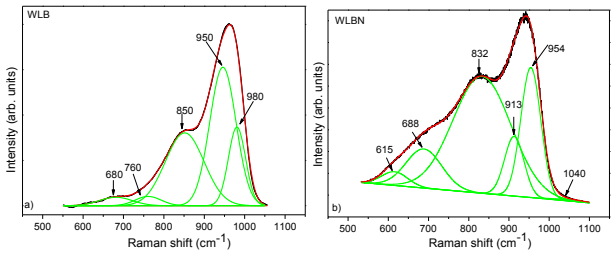

Fig. 3. *Raman spectra of a) $50WO_3{:}25B_2O_3{:}25La_2O_3$ (WLB) and b) $40WO_3{:}25La_2O_3{:}25B_2O_3{:}10Nb_2O_5$ (WLBN) glasses.*

The band at 913 cm^{-1} was attributed to short Nb–O bond in isolated NbO_6 units. The bands at 688 and 832 cm^{-1} can be associated with corner shared octahedra. [20-23]. Disappearance of the band at 980 cm^{-1} is probably a result of destruction of W-O-W linkages between WO_6 units and their transformation to WO_4. Obviously Nb_2O_5 incorporates into amorphous network trough W^{6+} forming new Nb-O-W bonds. NbO_6 polyhedra are mainly connected to each other by corner-sharing with vibrations in 800-600 cm^{-1} range. Further investigations are needed to establish formation of Nb-O-La and Nb-O-B linkages because stretching vibration of these mixed bonds are in the same spectral range.

3. 5. Optical studies

The optical transmittance spectra of synthesized glasses are shown in Figure 4. The glasses are characterized with good transmittance reached to the 65-75 %. As one can see form the Fig. 4 the absorption edge of both glasses is around 350 nm. As the position of the absorption edge is related with the structural rearrangement and oxygen bonds strenght in the glass network [24], the absence of a noticeable shift in the position of the absorption edge with the introduction of Nb_2O_5 into tungstate glass evidenced that its presence does not change significantly the glass structure. This suggestion is also confirmed by the invariable value of the optical band gap energy Eg of both glasses determined from the optical transmittance spectra which is 3.5 eV. Having in mind these results, we can suggest that Nb_2O_5 could have a role as a network former, replacing the tungstate structural units in the glass network as its presence does not reduce the E_g values of glass [25].

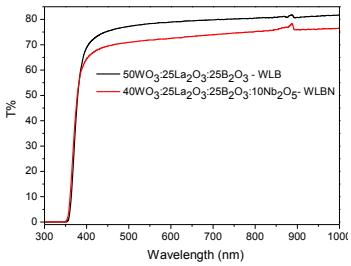

Fig. 4*. Optical transmission spectra at room temperature of $50WO_3{:}25B_2O_3{:}25La_2O_3$ (WLB) and $40WO_3{:}25La_2O_3{:}25B_2O_3{:}10Nb_2O_5$ (WLBN) glasses*

The refractive index (n) for the presented glasses is also established from the optical transmittance spectra. It is found that the refractive index of Nb_2O_5- containing glass is higher (1.97844) as compared with that of Nb_2O_5-free tungstate glass (1.97066) indicating the more densely packed structure in the presence of niobium [26].

3. 6. Photoluminescence spectra of Eu^{3+} ions

The PL spectra at room temperature for both glasses were measured and compared (Fig. 5).

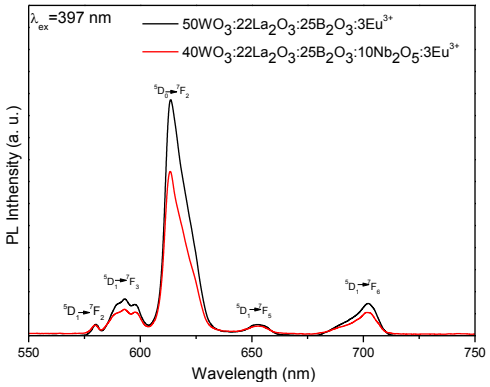

Fig. 5. *Photoluminescence spectra at room temperature of Eu^{3+} ions in the range of 550–750 nm in $50WO_3{:}22La_2O_3{:}25B_2O_3{:}3Eu_2O_3$ (WLBE) and $40WO_3{:}10Nb_2O_5{:}22La_2O_3{:}25B_2O_3{:}3Eu_2O_3$ (WLBNE) glasses.*

The excitation light with wavelength of 397 nm was used. Five different emission peaks assigned to the 4f transition of Eu^{3+} ions, i.e., $^5D_0$-^7F_j (j=0, 1, 2, 3 and 4) are observed. The peak intensity of the $^5D_0$-$^7F_2$ emission at 613 nm is much larger compared with the other ones. It is known that the $^5D_0$-$^7F_2$ emission band due to the electric-dipole transition largely depends on the local symmetry of coordination environments around Eu^{3+} [27]. High intensive peak of the $^5D_0$-$^7F_2$ emission indicates the Eu^{3+} occupies low symmetry site in the glass matrix. Nevertheless, that the addition of Nb_2O_5 slightly reduces the emission intensity of Eu $^{3+}$ions (Fig. 5), the improved glass forming ability and obtaining in a bulk form make Nb_2O_5 containing glass more appropriate material for different optical applications than Nb_2O_5-free tungstate glass. It will be of interest to study the influence of the amount of Eu^{3+} ions on the luminescence properties of the compositions studied here.

4. Conclusions

It has been found that the addition of niobium to tungstate glass modify the structure of the amorphous network. New linkages between NbO_6 and the other structural units are formed increasing the degree of the network connectivity. In this way the addition of niobium even at low concentrations (10 mol%) to tungstate glass has a positive effect on glass forming ability as stabilizes the

amorphous network and increases thermal stability. The Nb_2O_5-contaning glass is characterized with a high refractive index, which benefits for the potential optical applications.

Acknowledgments

The study was performed with financial support of Bulgarian National Science Fund at the Ministry of Education and Science, Contract КП-06-Н29/7

5. References:

1. Suehara S., K. Yamamoto, S. Inoue, A. Nukui, Bonding nature in tellurite glasses. - Phys. Rev. B, 51, 1995, 14919-14922.
2. Narayanan R. A., J. W. Zwanziger, The glass forming ability of tellurites: A rigid polytope approach. - J. Non-Cryst. Solids, 316, 2003, 273-280.
3. Kosuge T., Y. Benino, V. Dimitrov, R. Sato, T. Komatsu, Thermal stability and heat capacity changes at the glass transition in K_2O–WO_3–TeO_2 glasses. - J. Non-Cryst. Solids, 242, 1998, 154 - 164.
4. Aleksandrov L., T. Komatsu, R. Iordanova , Y. Dimitriev. Raman spectroscopic study of structure of WO_3-La_2O_3-B_2O_3 glasses with no color and crystallization of $LaBWO_6$, - Opt. Mater., 34, 2011, 201–206.
5. Aleksandrov L., R. Iordanova, Y. Dimitriev, N. Georgiev, T. Komatsu, Eu^{3+} doped $1La_2O_3$:$2WO_3$:$1B_2O_3$ glass and glass–ceramic. – Opt. Mater., 36, 2014, 1366–1372.
6. Aleksandrov L., T. Komatsu, K. Shinozaki, T. Honma, R. Iordanova, Structure of MoO_3–WO_3–La_2O_3–B_2O_3 glasses and crystallization of $LaMo_{1-x}W_xBO_6$ solid solutions. - J. Non-Cryst. Solids, 429, 2015, 171-177.
7. Nisa K., E. Ahmad, M. A. Chaudry, Niobium doped BGO glasses: Physical, Thermal and Optical Properties, - J. Appl. Phys., 3 (5), 2016, 80-87.
8. Ray N. H., Composition-properties relationship in Inorganic Oxide Glasses, - J. Non-Cryst. Solids, 15, 1974, 423-434.
9. Kawaguchi K., T. Yamaguchi, T. Omata, T. Yamashita, H. Kawazoe, J. Nishi, Phase separation and crystallization in sodium lanthanum phosphate glasses induced by electrochemical substitution of sodium ions with protons, - Phys. Chem. Chem Phys., 1-3, 2015, 1-7.
10. Swapna, G. Upender, M. Prasad, Raman, FTIR, thermal and optical properties of TeO_2-Nb_2O_5-B_2O_3-V_2O_5 quaternary glass system, - Journal of Taiban University for Science, 11, 2017, 583-592.
11. Saddeek Y., M. Azooz, A. Saddek, Ultrasonic investigations of some bismuth borate glasses doped with Al_2O_3, - Bull. Mater. Sci., 38, (1), 2015, 241–246.
12. Saddeek Y., Effject of B_2O_3 on the structure and properties of tungsten-tellurite glassesm, - Philos. Mag., 89 (1), 2009, 41-54.
13. Zhu L., T. F. Xu, Q, H. Nie, X. Shen, Spectral properties and thermal stability of erbium TeO_2-WO_3-La_2O_3 glass, - J. Inorg. Mater., 21, 2006, 351-356.
14. Kaur N., A. Khanna, M. Gónzález-Barriuso, F. González, B. Chen, Effects of Al^{3+}, W^{6+}, Nb^{5+} and Pb^{2+} on the structure and properties of borotellurite glasses, - J. Non-Cryst. Solids, 429, 2015, 153-163.
15. Kaur A., A. Khanna, M. González-Barriuso, F. González, B. Chen, Short-range structure and thermal properties of alumino-tellurite glasses, - J. Non-Cryst. Solids, 470, 2017, 14-18.
16. Cottrell T. L, The Strength of Chemical bonds 2d ed., Butterworth, London, 1958.
17. Hamad A. H., M. A. Marzouk, H. A. ElBatal, The Effect of Bi_2O_3 on Optical, FTIR and Thermal Properties of SrO-B_2O_3 glasses, - Silicon, 8, 2016, 121-131.
18. El-Zaidia M. M., A. A. Ammar, R. A. El-Mallawany, - Infra- Red Spectra, Electron Spin Resonance Spectra, and Density of $(TeO_2)_{100-x}$ – $(WO_3)_x$ and $(TeO_2)_{100-x}$–$(ZnCl_2)_x$ Glasses, - Phys. Stat. Sol., A, 91, 1985, 637-642.
19. Soliman A. A., I. Kashif, Copper oxide content dependence of crystallization behavior, glass forming ability, glass stability and fragility of lithium borate glasses, Phys. B, 405, 2010, 247-253.
20. Petit L., T. Cardinal,, J.J. Videau, Y. Guyot, G. Boulon, M. Couzi, T. Buffeteau, Erbium luminescence properties of niobium-rich oxide glasses, - J. Non-Cryst**.** Solids, 351, 2005, 2076–2084.
21. Jehng Jih-Mirn and Israel E. Wachs, Structural Chemistry and Raman Spectra of Niobium Oxides. - Chem. Mater. ,3, 1991, 100-107.
22. Aronne A., V. N. Sigaev, B. Champagnon, E. Fanelli, V. Califano, L. Z. Usmanova, P. Pernice, The origin of nanostructuring in potassium niobiosilicate glasses by Raman and FTIR spectroscopy, - J. Non-Cryst. Solids, 351, 2005, 3610–3618.
23. Fukumi K., Sumio Sakka Coordination state of Nb^{5+} ions in silicate and gallate glasses as studied by Raman spectroscopy, J. Mater. Sci., 23, 1988, 2819 – 2823.
24. Kamalaker V., G. Upender, Ch. Ramesh, V. Chandra Mouli, Raman spectroscopy, thermal and optical properties of TeO_2-ZnO-Nb_2O_5-Nd_2O_3 glasses, - Spectrochim Acta Part A, 89, 2012, 149-154.
25. Villegas M. A., J. M. Fernandez Navarro, Physical and structural properties of glasses in the TeO_2–TiO_2–Nb_2O_5 system, - J. Eur. Ceram. Soc., 27, 2007, 2715-2723.
26. Masuno A, H. Inoue, K. Yoshimoto, Y. Watanabe, Thermal and optical properties of La_2O_3-Nb_2O_5 high refractive index glasses, - Opt. Mater. Express, 4, 2014, 710-717.
27. H. Lin, W. Qin, J. Zhang, C. Wu, A study of the luminescence properties of Eu^{3+}-doped borate crystal and glass, Solid State Commun., 141, 2007, 436–439.

РОЛЯ НА ИНТЕРАКТИВНИТЕ МУЗЕИ ИЛИ РАЗЛИЧНОТО ПРИЛОЖЕНИЕ НА ТЕХНОЛОГИИТЕ В ТУРИЗМА

THE ROLE OF INTERACTIVE MUSEUMS OR THE DIFFERENT APPLICATION OF TECHNOLOGIES IN TOURISM

Манчева-Али О.[1], Генова Д.[2]
Национален военен университет „Васил Левски“, Велико Търново, България[1]
Великотърновски университет „Св. св. Кирил и Методий“, Велико Търново, България[2]

o.mancheva@ts.uni-vt.bg, dellyanag@abv.bg

Abstract: *in this report a brief analysis of service sector in Bulgaria is presented as an important one both for the formation of GDP and for our country being a popular tourist destination. Tourism provides competitive advantages and it is a resource which challenges the computer and interactive technologies that is a very important factor for the competitiveness of tourism. Interactivity is a factor that is identified by consumers of tourist services as an important and significant one for the development and supply of tourist resources. Such kind of resources are museums. Being an anthropogenic tourist resource they turn to be suitable for modernizing and implementing new interactive technologies. A representation of some of the most popular interactive museums is shown as well as a SWOT analysis which proves that they have highly valuable advantages and potential and in the same time the disadvantages and threats are superable, without influencing their total cost.*

The content of this report divides between authors as follows: Olga Mancheva-Ali develops: 1, 2 and 6 article and Delyana Genova develops: 3, 4 and 5 article.

Keywords: TOURISM, TECHNOLOGY, ADVATAGE, INTERACTIVE MUSEUMS

1. Въведение

Технологиите са неделима част от почти всички сфери на дейност на нашия живот и в по-голямата си част го улесняват. Въпреки твърденията, че технологичните открития оказват негативно влияние върху нас, водят до обезличаване и намаляват социалните ни умения, те имат неопровержими заслуги за развитието на всички бизнес сектори.

Туристическият бизнес не прави изключение, новите технологии го променят и превръщат във възможно, постижимо и интересно преживяване за всякакъв тип потребители. Предлагането на персонализирани продукти и услуги е една от задачите на технологиите в туризма и дори може да стигнем по-далеч, като определим туризма като сектор на икономиката, който дава по-различно и нестандартно приложение на компютърните технологии чрез идеи и предизвикателства за покоряване.

Технологичното усъвършенстване обхваща дейности по внедряване на нови технологии или усъвършенстване на съществуващите.[1] Компютърните технологии могат да обхванат различни аспекти в туризма, като това да служат на бизнеса за повишаване ефективността на управление и анализ на ресурсите или да бъдат част от предлаганата туристическа услуга с цел повишаване конкурентоспособността на туристическия продукт. И важността днес е да обхване „…целесъобразен набор от технологични решения и въведения, които да осигурят процес на активна комуникация с клиента, богато преживяване, даващо ценността на престоя ...“[2]

Настоящият доклад цели да направи кратък анализ на връзката на компютърните технологии и туризма, мястото им в националната икономика и да идентифицира и обобщи примери в музейното дело, популярни с използването на интерактивни технологии. Наред с положителните тенденции, си поставяме и задача да постигнем обективност като направим SWOT-анализ на представените нововъведения в музеите.

2. Компютърните технологии и туризма

Секторът на информационните и комуникационни технологии (ИКТ) се определя като структуроопределящ както самостоятелно, така и като ключов за други дейности. От значение е неговият ръст като % от БВП, който за периода 2014-2017 г. се движи средно около 2.1%. Развитието на ИКТ през последните години се движи както следва: 2014 г. – 15%, 2015 г. – 18 %, 2016 г. – 14%, 2017 г. – 19% (по данни на Софтуерната индустрия в България изготвен от CBN - Pannoff, Stoytcheff & Co. по поръчка на БАСКОМ)[3], което формира среден ръст от 16.5% за сектора за посочения период.

По данни на НСИ през второто тримесечие на 2016 г. брутният вътрешен продукт (БВП) на един зает се увеличава с 1,4% в сравнение със същото тримесечие на предходната година. Заетите лица в икономиката са 3 587,1 хил., а общият брой отработени часове е 1 495,8 милиона. Структурата на заетостта по икономически дейности през второто тримесечие на 2015, 2016 и 2017 г. показва увеличение на относителния дял в сектора на услугите (фиг. 1).

[1] Статев, В., „Икономика на туризма“, Издателство „Фабер“, Велико Търново, 2007. ISBN 978-954-775-779-0, с. 18

[2] Kostadinova, N., The customized conference product in hospitality business, Collection of proceedings from an international scientific conference devoted to the 55th anniversary of College of tourism – Varna Tourism and innovations, Nauka i ikonomika, University of economics - Varna, p. 302, 2018

[3] БАСКОМ - Българската асоциация на софтуерните компании е създадена през 2001 г. Асоциацията е колективен представител на повече от 85 софтуерни фирми – пълноправни членове, и над 120 асоциирани членове, сред които висши училища, фондации, фондове за рисков капитал, стартиращи иновативни компании и др.

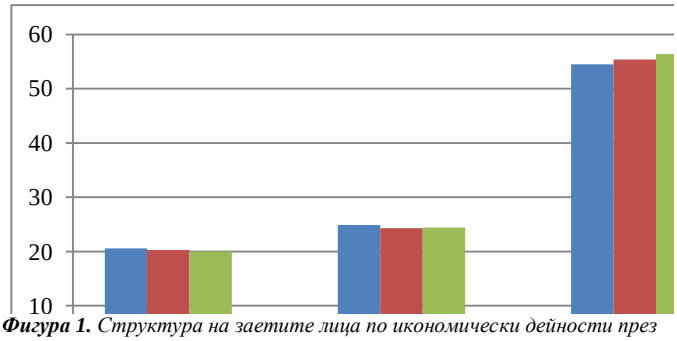

Фигура 1. *Структура на заетите лица по икономически дейности през второто тримесечие на 2015, 2016 и 2017 г. (Данни: НСИ)*

От фигурата може да заключим, че секторът на услугите. генерира повишаване броя на заети лица, като заетите през 2015 г. са 54.5%, през 2016 г. достига 55.4%, а 2017 г. са 56.4%. Това показва ръст с 1.9% заети през 2017 г. спрямо 2015 г.. За сравнение, в аграрния и индустриалния сектор се наблюдава спад за 2017 г. спрямо 2015 г.както следва - с 0.6% и с 0.5%.

От друга страна, търсенето на бизнес услуги в България се повишава и през 2018 година генерира относителен дял от 16.8%, което е повишение с 10,6 % спрямо предходната. (фиг. 2.)

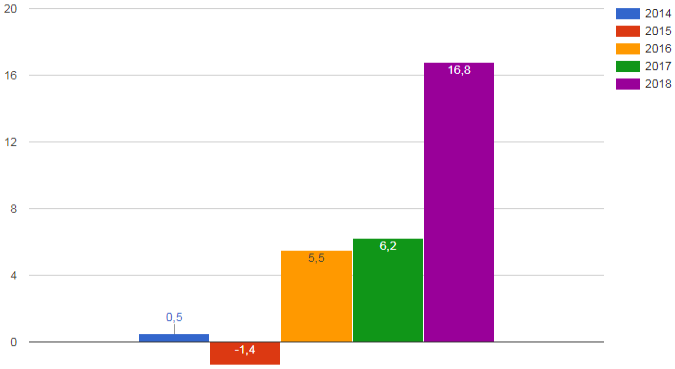

Фигура 2. *Търсене на бизнес услуги 2014-2018 г. (за м. януари на изследваните години, в % по данни на НСИ)*

Фактът, че търсенето на бизнес услуги се е увеличило с 10.6% за 2018 спрямо 2017 г. е ясна индикация, че секторът на услугите е с висок потенциал за развитие и ръстът, който бележи налага особено внимание и анализ на процесите.

Интересно е да се проследят тенденциите в сектора на услугите в страната ни, като във фиг. 3. са представени данните за 5 годишен период от време.

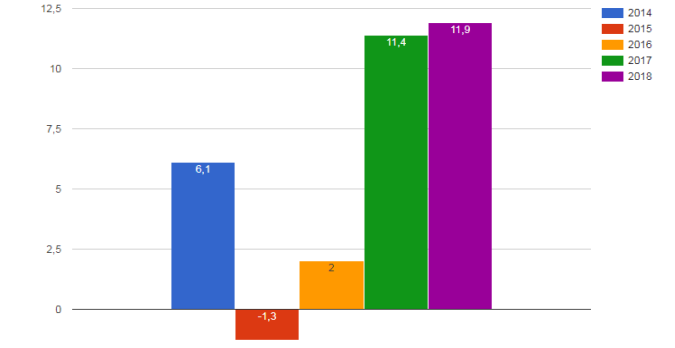

Фигура 3. *Състояние на сектора на услугите 2014-2018 г. (за м. януари на изследваните години, в % по данни на НСИ)*

От данните на НСИ може да обобщим, че се наблюдава положителната тенденция в сектора на услугите и както става ясно от информацията, има повече заети лица, по-голямо търсене и по-добро състояние на сектора за 2018 г., спрямо предходните.

За туризма, всяка година крие рискове въпреки положителната тенденция на развитие, секторът се влияе от различни фактори като част от тях са внедряването на интерактивни и компютърни технологии, модернизиране и подобрение на предлаганите услуги.

3. *Нагласи за интерактивност в туризма*

Проучване на GfK (Growth from Knowledge - изследва пазара и потребителите)[4] за нагласите на „*туриста от бъдещето*" показва, че той очаква повече интерактивност в преживяванията си. Дори начинът на изразяване на впечатления, моменти, спомени се случва по интерактивен начин. Потребителите предпочитат да получават услуги чрез различни приложения, социални медии, електронна поща, онлайн канали и др. Подобна глобализация влияе на туристическият бизнес, тъй като информацията за хотели, събития, дестинации става лесно лесна и достъпна.

Изследването[5] показва, че продажбата на устройства като умни часовници и гривни през 2016 е достигнала стойност от 114 милиона долара. Смята се, че това е в резултат от стремежа за персонализиране и уникалност, което се отразява и на ръста в продажбите на различни туристически пътувания, улеснявайки планирането им. Повече от 25% от потребителите разчитат на социалните мрежи и онлайн канали за споделяне като първа стъпка при планиране на пътуването си.

Интерактивността в туризма може да има и други проявления, поради всеобхватността на предлагане на услуги, но и като сфера на дейност с голяма зависимост и необходимост от човешки ресурси. Като част от интерактивността в туризма може да посочим:

- *За потребители: технологии за виртуалната реалност* (VR), познати също като компютърно-симулирана реалност, която пресъздава среда, истинска или измислена, която симулира физическото присъствие на потребителя по такъв начин, който позволява на използващия устройството да си взаимодейства с околната среда;

- *За служители и потребители: геймифицирането*, като начин на прилагането на елементи от дизайна на игри и включването на принципи от игри в контекста на нещо не-игрално и различно. То е насочено към човешките ресурси и има задачата да реши проблеми, свързани с лоялността, ефективността и желанието за работа на служителите. Това разбира се са само част от проявленията му. Това е и средство за група туристи със специфичен интерес.

Като друг пример за интерактивност в туризма, може да дадем появата на интерактивните музеи, които са нов начин на представяне на музейното дело и начин на модернизиране предлагането на туристически ресурси. Добавената реалност по-често се използва за развиване на образователния потенциал на музейните експозиции. Някои музеи изграждат и специални зали, в които се прожектират 3D филми, посветени на конкретни музейни експонати[6], за да привлекат интереса на посетителите.

4. *Интерактивни музеи по света*

Музеите са учреждения, които събират, съхраняват и публично излагат различни предмети и свързана с тях информация, които представляват обществен интерес. Думата „*музей*" се отнася както за институцията, така и за самата сграда, в която тя се помещава. Законът за културното наследство определя музея като „*културна и научна*

[4] https://www.gfk.com/
[5] Пак там
[6] Varadzhakova, D., Digital reality in tourism industry, Collective Scientific Book of an annual conference Development of the Bulgarian and European Economies – challenges and opportunities, vol. 1, University Press St. St. Cyril and Methodius, Veliko Tarnovo, p. 246, 2018

организация, която издирва, изучава, опазва и представя културни ценности, природни образци и антропологични останки с познавателна, образователна и естетическа цел.“ [7] За нас в туризма, музеят е средство за привличане на туристи със специфични потребности.

Повечето музеи опитват да се възползвате от новите технологии чрез „включването” им в музейни експозиция, което позволява на посетителите да получат повече информация, или да използват интернет за по-пълна картина на музейните колекции и дейности (виртуално представяне в мрежата, виртуален музей).[8]

Ако през 2016 г. „умният” часовник е върхово постижение във внедряването на технологии в туризма, то през 2019 съществуват цели интерактивни музеи. Тези културни центрове разчитат на различни уреди, симулатори, продукти от всички сфери на технологиите и изкуството. Списание Buisnessweek[9] прави класация на най-високотехнологичните музеи в света като определя следните, като представители на новото поколение музеи:

➢ *Музеят на MIT, Масачузетс, САЩ*

Този институт по технологии е американски частен университет, който е едно от най-елитните висши училища в света. В музея му се излагат най-добрите разработки на студенти по време на тяхното обучение. Пример за това са робот за подводни изследвания, ново поколение градски автомобили, триизмерен модел на риба зебра, която ще помогне за разработването на лекарство срещу рак и др.

➢ *Музей на движещите се картини, Ню Йорк, САЩ*

Този музей е посветен на така нареченото поколение на видеоигрите и клиповете в Youtube. В него чрез триизмерни технологии се разполагат експонати от най-известните видеоигри, клипове и кинопродукции. Създадена е и пещера с интерактивна реалност, където всички предмети са триизмерни.

➢ *Музей за роботи, Япония*

Музеят за роботи изглежда като космически кораб. Разполага със стотици експонати от света на роботиката. В него се представят от най-старите изобретения в тази област до бъдещи роботизирани домашни помощници. Освен обичайните снимки и клипове, присъщи за интерактивните музеи, в този се провеждат обучения за управляване на роботи.

➢ *Научен музей, Лондон, Великобритания*

Класическият стил на сградата контрастира с високотехнологичното съдържание на музея, което е едно от най-модерните, познати на човечеството. В него посетителите могат да се насладят на 4D кино с прожекции на филми от различни сфери на науката, да използват различни симулатори. Музеят проследява в хронологичен ред най-значимите исторически и технологични открития. Безплатен е за всички посетители.

➢ *Музей за нови науки, Япония*

Този музей представя изобретения от всякакъв тип, разработвани с помощта на високи технологии. Освен роботи и машини, могат да се разгледат най-високотехологичните превозни средства. В центъра му има огромен глобус, направен от ЛЕД дисплеи, които възпроизвеждат различен тип съдържание.

Уникални музеи в България има в Трявна, Чепеларе, Гурково, Мадан, Перник, Габрово и др.[10], като част от тях вече работят с интерактивни технологии. Такива примери са:

➢ *Музей на индустрията, Габрово, България*

В България също има музеи, представящи експонатите си чрез съвременни експозиционни технологии. Интерактивен музей на индустрията в гр. Габрово притежава атрактивни аудио-визуални приложения, които създават автентична атмосфера. Последната инсталация е симулатор на Ф1.

➢ *Музей Абритус, Разград, България*

Музеят разполага с 12 зали, които превръщат посетителите в древни римляни чрез игри, симулации и филми. Умните стъкла, които издават тайни и шкафчетата, криещи отговори запознават с бита, културата и боговете на Древен Рим.

Всички тези музей по света и в България са доказателство за подобряване представянето и модернизирането на туристически услуги и създаването на високо конкурентна среда за развитие на бизнеса.

По данни на НСИ[11], в България има 191 музея, които за 2017 г. генерират 5 109 хил. посещения, а 1 112 хил. от тях на чуждестранни туристи. Класацията на музеите по области и броя на посещенията има следния вид:

Първо място: София град с 24 музея и 1,039 млн. посещения;

Второ място: Пловдив с 14 музея и 291 хил. посещения;

Трето място: Бургас с 12 музея и 230 хил. посещения;

Четвърто място: тук се нареждат 4 области с по 10 музея – Велико Търново (495 хил. посещения), Габрово (379 хил. посещения), Стара Загора (301 хил. посещения) и Шумен (194 хил. посещения). Уникални музеи са в Трявна, Чепеларе, Гурково, Мадан, Перник, Габрово и др.

Данните са закономерни и анализът показва, че дори на четвърто място по брой на музеи, дестинации като В. Търново, Габрово и Ст. Загора изпреварват Пловдив и Бургас по брой посещения за година. Тук съществена роля има популяризирането на дестинациите и начинът им на представяне пред потенциалните потребители.

За 2017 година в българските музеи са изнесени 55 585 беседи, 2 189 временни изложби, 689 концерта, 490 обсъждания на книги, 13 094 видео прожекции и 141 конкурса.[12] Тази тенденция е положителна за страната ни, а наличието на видео прожекциите е знак за търсене на модерна и интерактивна визия на музейното дело.

5. *SWOT-анализ на интерактивните музеи*

Интерактивните музеи са нов начин за популяризиране на музейното дело, който предлага различна визия на традиционния и автентичен музей като обект на изкуството и културата. В таблица 1. е направен опит за определяне на предимствата, недостатъците, възможностите и заплахите пред интерактивните музеи (SWOT-анализ).

Таблица 1. SWOT-анализ на интерактивните музеи

Предимства	*Недостатъци*
- запомнящо представяне на информацията; - различно преживяване/ усещане; - подходящо за всякакви възрасти.	- възможна загуба на автентично преживяване; - разминаване между очаквания и реалност.

[7] https://www.lex.bg/laws/ldoc/2135623662

[8] Lapteva, M., N. Pikov,Visualization Technology in Museum (From the Experience of SibFU Collaboration with the Museums of Russia), Journal of Siberian Federal University. Humanities & Social Sciences 7 (2016 9), p. 1674

[9] https://www.bloomberg.com/businessweek

[10] Dimitrov, S., CULTURAL AND HISTORICAL HERITAGE OF BULGARIA AS A TOURIST RESOURCE, Научные горизонты № 1(17), 2019, ISSN 2587-618X, p. 69

[11] http://www.nsi.bg/bg/content/3669/музеи

[12] Пак там

Възможности	*Заплахи*
- намаляване разхода за човешки ресурси; - по-лесни за усвоявана на послания и социални каузи.	- отдалечаване от традиционното преживяване в музей; - намаляване на културната стойност и масовизиране.

Една от задачите на музея е да покаже нагледно всички факти и постижения на науката, за които сме чували. Внедряването на високотехнологични методи, тяхното използване за представянето на експозициите, води до по-запомнящо се и ефектно послание за потребителите. Осигурявайки интерактивни преживявания, музеите се превръщат в притегателен център не само за деца, но и за представители на различни възрастови групи.

Както всичко останала, така и интерактивността може да бъде опасна, ако е в прекалено голям процент. Прекалената технологизация крие риск да се изгуби автентичната атмосфера в един музей. Така той би изгубил стойността си на традиционен културен център и би се приел повече като развлекателен. Тъй като музеите са част от обучителната програма на деца, чието ежедневие е заето изцяло от технологиите, трябва да се внимава, за да не се прекали. Това може да доведе до размиване на очаквания и реалност.

Във векът на високите технологии възможностите за развитие са безброй. Такъв тип културни центрове биха се приели по-добре, защото посланието, което носят е по-достъпно и лесно усвоимо. Социални каузи, представени по интерактивен начин биха имали потенциално по-голям успех поради възможността да се покаже нагледно мисията им.

Основната заплаха за музеи, използващи високите технологии, за представяне на експозициите си е да не изгубят истинското преживяване от посещението на такъв тип центрове.

Интерактивните музеи съчетават различни свойства, което ги прави гъвкави и носещи висока добавена стойност в туризма със техните функционални и технологични възможности.

6. *Заключение*

Секторът на услугите е ключов за българската икономика както за формиране на БВП така и за развитието на България като туристическа дестинация. Туризмът носи конкурентни предимства от гледна точка на икономиката и е ресурс, който поражда предизвикателство пред развитието на компютърните и интерактивни технологии.

Интерактивността е фактор, който потребителите на туристически услуги определят като важен и със значение за развитието и предлагането на туристически продукти, услуги и ресурси. Такива са музеите и като антропогенен туристически ресурс се оказват подходящи за модернизиране и внедряване на интерактивни технологии.

SWOT-анализът на интерактивните музеи показва, че предимствата и възможностите пред тях са с висока стойност на полезност, а недостатъците и заплахите са преодолими и подлежат на ограничение, без това да нарушава тяхната стойност.

7. *Източници*

[1] Статев, В., „Икономика на туризма“, Издателство „Фабер“, Велико Търново, 2007. ISBN 978-954-775-779-0, с. 18

[2] Dimitrov, S., CULTURAL AND HISTORICAL HERITAGE OF BULGARIA AS A TOURIST RESOURCE, Научные горизонты № 1(17), 2019, ISSN 2587-618X, p. 69

[3] Kostadinova, N., The customized conference product in hospitality business, Collection of proceedings from an international scientific conference devoted to the 55th anniversary of College of tourism – Varna Tourism and innovations, Nauka i ikonomika, University of economics - Varna, 2018, ISBN 978-954-21-0973-0, p. 302

[4] Lapteva, M., N. Pikov,Visualization, Technology in Museum (From the Experience of SibFU Collaboration with the Museums of Russia), Journal of Siberian Federal University. Humanities & Social Sciences 7 (2016 9), DOI: 10.17516/1997-1370-2016-9-7-1674-1681, p. 1674

[5] Varadzhakova, D., Digital reality in tourism industry, Collective Scientific Book of an annual conference Development of the Bulgarian and European Economies – challenges and opportunities, vol. 1, University Press St. St. Cyril and Methodius, Veliko Tarnovo, 2018, p. 246

[6] Национален статистически институт

[7] Закон за културното наследство

[8] https://www.bloomberg.com/businessweek

[9] https://www.digital.bg/novini/

[10] https://www.gfk.com/

[11] https://imi.gabrovo.bg/BG/

[12] http://travelnews.bg/bg/novite-tehnologii-promenyat-turizma/

INVESTIGATION THE CONDITIONS FOR OBTAINING BULGARIAN YELLOW-COLORED PAVINGS, EQUIVALENT IN COLOR TO THE IMPORTED PRODUCED ON BASE OF SEDIMENTARY ROCK

Assist. Prof. M. Gacheva, Prof. Dr. L. Lakov, Assoc. Prof. Dr. B. Jivov,
Chief Assist. Prof. Dr. St. Yordanov, Assist. Prof. M. Aleksandrova

Bulgarian Academy of Sciences, Institute of Metal Science, Equipment and Technologies with Hydro- and Aerodynamics Centre „Acad. A. Balevski", 67 "Shipchenski Prohod" Blvd, 1574 Sofia, Bulgaria, e-mail: mvgacheva@abv.bg

Abstract. *The development deals with the study of the conditions for appearance of yellow color in ceramic products, obtained from local sedimentary marl rocks from the region of Popovo town, field of Targovishte. Reproduction of the conditions of high temperature liquid-phase synthesis of products such as pavings, tiles, etc., by modifying the composition of the marls. Expanding the sintering interval of rectifying the alkaline-earth oxide content and increasing the phase formation time. The researches are part of the creation and implementation of a technology for production of pavings with equivalent yellow color of the imported standards but with higher tribological and physic-mechanical indicators.*

Keywords: MARL ROCKS, HIGH-TEMPERATURE SYNTHESIS

1. Introduction

The famous „yellow paving stone" known in our country in the center of Sofia have a fine crystalline, dense structure close to that of the semi-porcelain. They were produced in the beginning of the last century in Hungary by marl clays. Sedimentary precipitate marble rocks [1-4] contain more fine fractions than brick clays. They are made up of evenly distributed carbonates and clay minerals - illite and kaolin formed under the existing conditions [5, 6]. The prerequisite for obtaining products corresponding to color and with better physical-mechanical and tribological indicators are marble clays with a certain chemical and grain-size composition. Preliminary laboratory and semi-industrial experiments have been carried out so far to produce experimental samples of yellow colored paving bricks, equivalent in color, shape and size to original historical samples [7-11].

The purpose of this work is to examine and develop suitable formulation compositions and optimum heat treatment mode for prototyping of the so-called „yellow pavers" based on raw materials derived from concrete deposits on the territory of the country. From the studied sedimentary mercury deposits the most promising proved this to the village of Svetlen, Targovishte region. The same raw material is used for the production of building materials (bricks, etc.) in the company „home industry-Popovo" Ltd. Popovo, Targovishte District. The study conducted a series of compositions with the participation of marl clays and technological additives. The formulation of the resulting masses was carried out by applying plastic and semi-dry pressing. An appropriate heat treatment regimen with a maximum temperature of 1150°C and an isothermal fluid retention of 1h is experimentally established.

2. Experimental procedures

The test bodies are prepared using available standard equipment and inventory: KERN scales, porcelain mill with volume 50 l with malt bodies, sets of sieves and others. The experimental heat treatment of molded blanks was carried out in a specially made furnace with homogeneous temperature field and a programmer for setting the speed of increase and lowering of the temperature values and the necessary isothermal fluid retention.

Radiographic Analysis (RFA) was performed using a Philips 1710 X-ray generator (32 kv, 16 Ma, step 0.05, Co-tube with λ 1.78892 Å and range 5 – 55 degrees).

The resulting compositions were conducted differential thermal analysis (DTA) with apparatus STA PT1600 TG-DTA/DSC. The laboratory tests are carried out in an inert gas environment at a temperature range of 20 ÷ 1300°C and an applied heating rate of 10°C/min.

A microscopic examination of the prepared prototypes and the provided benchmarks was conducted and the microphotographs were photographed by binocular ICW binocular microscope Stemi 2000-C and polarizing microscope Amplival Pol D.

At the same time, experimental samples of the surface and volume of the prototypes obtained were examined by a Philips 525 U Scanning Electron Microscope (SEM) with an EDAX 9900 analytical system.

3. Results and discussion

The average chemical and grain size composition of the marsh delivered from a deposit in the village of Svetlen and taken from the technological table for the brick production in "Rodna Industria" in Popovo, in % is: SiO_2 - 42%, Al_2O_3 - 12%, El_2O_3 - 5.14%, CaO - 18.60%, MgO - 2.50%, R_2O - 2.16%, 3H - 1868.

Grain size composition in% by weight:

- fraction below 0.005 – 48;
- fraction from 0.005 to 0.05 – 37;
- fraction above 0,05 – 15.

According to BDS 14175-77, the marl refers to the acidic mergels (Al_2O_3 <15%). Marl with alkaline earth oxides content above 17–18% is determined as high-carbon. By this classification, the marl used by us, with an average content of alkaline earth oxides 20.10 wt%, implies a relatively narrow interval of sleeping and difficulty obtaining fine ceramic products with low voids content. This requires continuous firing and fluid retention at a specified lower temperature. Another possibility is modifying the composition with pure-washed kaolin, but this leads to a certain increase in the final temperature of high temperature liquid phase synthesis. The slow increase in the temperature of the firing of sedimentary mercury clays with high alkaline earth oxides and narrow interval of sleeping is confirmed by companies in Russia, Czech Republic, Holland, etc. We proved that the test fixtures were prepared from a plastic table measuring 5x5x5 cm, made from the light marl clay, heated 7 hours at a temperature of 1120°C, lower than that of the temperature of the high temperature liquid phase synthesis - 1150°C, no yellow color is obtained, but red, despite the large content of Na_2O and K_2O. However, if the grip lasts 40 hours, the colour changes to yellow and the specimens shrink above 15%. The yellow color manifests itself with the appearance of a liquid phase and an intense contraction and compaction of the skull. As a consequence, the quartz grains contained in the marl are attacked superficially and the deformation is avoided.

It is important to develop the yellow color in the oven's gas environment - around the caking temperature is reductive. The effect of reduction can be avoided if Na_2O is added to the marl in the form of Na_2CO_3. The yellow color can be obtained and act favorably when adding a minimum amount of soda to the clay within 02 ÷ 03 wt.% Na_2O as regards the weight of the dry mass. The addition of Na_2O as a stimulating modifier is in the case of baking in a oxidizing

atmosphere. The role of Na_2O, as the deciding factor can be assumed by FeO, the main reason for obtaining which is Fe_2O_3. The available and further formed FeO forms with SiO_2 low-voltage compounds of the type $FeO.SiO_2$ and increases the liquid phase. Na_2O further contributes to the formation of liquid phase. At the same time, in the field of Clinopiroxena, we proved that not diopside is formed, but its variant, known in literature as a façade. Characteristic of the façade is its increased content of aluminum, calcium and trivalent iron. Precisely the rich in trivalent iron fractions are the reason for the yellow color and the imported standards, and the formed and synthesized Bulgarian pavers. Na_2O increases the velocity of the liquid phase and directs the reaction in a solid phase in absorption of SiO_2, which is borne by the reacting environment.

In the presence of MgO, as is the case with sedimentary rocks from the city of Popovo and Svetlen, with the help of X-ray and microscopic analysis with transmitted light through prepared dunncoats of yellow pavers, the mineral phases diopside and anorthite are established. This is a serious circumstance and reason to consider that the cause of the occurrence of the yellow color is Fe^{3+}, which is contained in the pyroxene $CaO.MgO_2.SiO_2$. For the synthesis of diopside MgO is the main component for its formation. According to Zeger sedimentary rocks that do not have in their contents from 1 to 2 mol MgO and 4 mol CaO of Mol Fe_2O_3, their composition so should be modified with additional additives to become 6 mol CaO+MgO of 1 mol Fe_2O_3. In addition, CaO should be in excess of MgO, otherwise it is not yellow, but gray coloring. The molar ratio MgO:CaO should be ≈ 1:7.

In analyzing the influence of the exposed factors, laboratory and semi-industrial experiments have been conducted to obtain experimental samples of yellow-coloured pavers, equivalent in colour, shape and size and superior to the imported standards in physical and mechanical and tribological indicators. For this purpose, local raw materials were used – marls from the town. Popovo and Svetlen, Targovishte. District in clean and modified state. Their chemical compositions are listed in table 1.

Table. 1. *Chemical composition of the raw materials used.*

Row materials	Marls Svetlen	Marls Popovo
Ingredients, wt %		
SiO_2	43,00	42,00
Al_2O_3	12,50	12,00
Fe_2O_3	5,14	5,00
CaO	19,24	18,60
MgO	2,30	2,50
Na_2O+K_2O	2,40	2,16
TiO_2	0,90	0,40
3.H	15,42	19,74

When composing tables for natural coloration of yellow tiles, paving stones, etc. the following raw materials are used as additives: chemically pure, anhydrous Na_2CO_3, glass flour (fraction < 63 microns) and calcined at 550°C washed kaolin. The latter is introduced in order to change the ratio of the alkaline-earth oxides, to increase the fire resistance, to reduce the inclination of the beads to the deformation and to break the caking interval. The remaining materials are added to improve the caking and promote the production of light (yellow) articles (Table 2).

Table 2. *Used raw materials as additives.*

Name of the material	Na_2CO_3 Chem. pure	Glass powder fraction – under 63 μm	Washed kaolin - calcinated at 550°C
Ingredients, wt %			
SiO_2	-	71,00	67
Al_2O_3	-	2,00	33
Fe_2O_3	-	0,22	-
CaO	-	6,75	-
MgO	-	2,60	-
Na_2O+K_2O	58,5	17,78	-
3.H	41,5	-	-

The processing of masses obtained from dry and ground merellni clays and additives, excluding soda, which is in minimal quantities, is carried out by two methods-plastic and semi-dry pressing. The plastic mass, for plastic pressing, is obtained by mixing the materials with 60% water, homogenising in ball mills until the auger is obtained. It matures 24 hours, after which it is passed through a press filter or dewatered in plaster forms to normal molding humidity (20 - 30%). From the resulting plastic mass the products are molded into metal molds of plastic pressing press. The semis is prepared with the materials moistened with 22 – 23% water, and they are mixed and allowed to lie for two days for the swelling of the clay component. From the plastic table are prepared briquettes, which are dry crucible to humidity of 1 – 3% and then grind on a colergant or a ball mill. The resulting sifted powder is granates and moisturizes to 5 - 6%. The following shall be sieving through sieve 2.00 mm for removal of larger fractions. The resulting subsieve fraction has the following granulometric composition: (Table 3).

Table. 3. *Granulometric composition of the subsieve fraction.*

№	**Grain size**	**%**
1	2,0 ÷ 1,25	23
2	1,25 ÷ 0,80	18
3	0,80 ÷ 0,50	17
4	0,50 ÷ 0,25	18
5	0,25 ÷ 0,125	12
6	under 0,125	12

The blanks are molded from the resulting granules of the semi-dry pressing press. The used sedimentary rocks for the production of the masses, as stated above from the deposits in the town of Svetoden and Obzor. Popovo are not suitable for the production of thin-walled products, because they are characterized by a narrow interval of sleep and a pronounced tendency to deformation. Therefore, on both methods are pressed large sample samples of raw ones with dimensions 200 x 100 x from 30 to 50 mm. The sintering was carried out in a specially constructed electric furnace with a homogeneous working volume field and a temperature control program. The ultimate maximal isothermal fluid retention of temperature is within the range of 1140 ÷ 1150°C. As an example, the rates of rise and decrease in temperature and temperature limits are set out in figure 1 for composition 1. Pre-plastic test bodies are dried in a vacuum dryer to residual humidity of 2 – 3%, unlike semi-dry pressing. Despite the slow rate of temperature rise, several isothermal inhibitions were required.

The baking mode is as follows:

- heating speed 2°C/min;
- hold at 100°C and 200°C - 30 min;
- hold at 600°C and 800°C - 20 min;
- maximum temperature of high-temperature liquid phase synthesis 1150°C - hold 1 hour;
- decreasing temperature 4°C/min;
- hold at 600°C - 30 min.

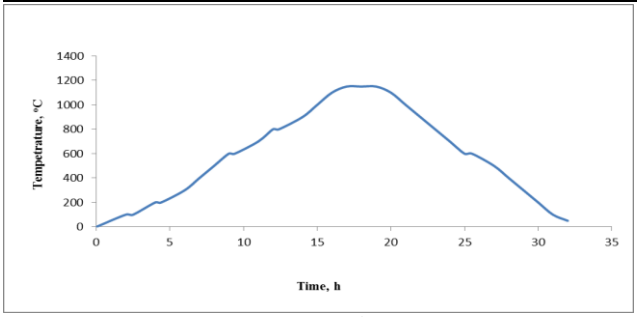

Fig. 1. *Temperature firing curve.*

Table 4 shows the composition of the samples.

Tab. 4. *Experimental compositions tested.*

№	Ingredients	№ of the composition in wt %							
		1	**2**	**3**	**4**	**5**	**6**	**7**	**8**
1	Marls Svetlen	100		95		91		90	85
2	Marls Popovo		100		95		91		
3	Na_2CO_3			4	4				3
4	Glass flour					9	9		
5	Washed kaolin							10	10

The best results with regarding to water absorption were obtained from compositions 1, 5 and 8. By this index, the degree of culling of the skull is best considered. The average values of this indicator for the same curing temperature - 1140°C are given in Table 5.

Table. 5. *Average water absorption values at coagulation temperature - 1140°C.*

Indicator		Water absorption, %
Ingredients	**1**	0,12
	2	0,64
	3	0,48
	4	0,70
	5	0,08
	6	0,80
	7	0,11
	8	0,09

In the basis of the marl base from the village of Svetlen without and with modifiers are better, respectively, and their water absorption is lower.

The solid sintering of the individual masses, with the exception of mass 1, shown in figure 1, is: for mass № 1 - 1150°C; for mass № 2 - 1150°C; for № 3 - 1120°C; for № 4 - 1120°C; for № 5 - 1140°C; for composition № 6 - 1140°C; for composition № 7 - 1160°C and for composition № 8 - 1140 ° C.

The samples obtained are a standard description of the colours on the surface and in depth, through the Munsell Color System. The color nomenclature consists of a separate recording of the nuances, its value and the color to which it refers, which are combined in such a order as to represent the color perception. The samples obtained are characterized by an equivalent yellow colour of the imported standards, the characteristic of which for the individual compositions is from 2.5 y 5/6 to 2.5 y 4/6.

4. Conclusion

Experienced samples of „yellow pavers" of equivalent colour, shape and size have been obtained with the original standards of historical street surface provided for exploration. The prototypes were prepared in laboratory and semi-industrial conditions with the use of local raw materials (marls), extracted from deposits near the city. Popovo and Svetlen, Targovishte District. The new specimens are superior to the physical, mechanical and tribological characteristics of the authentic pavers. On the basis of dry and ground merellni clays are developed table-compositions with the introduction of technological additives: Na_2CO_3, Glass flour (Faction < 63 microns) and thick with 550°C washed kaolin. The molding of the resulting masses is carried out by applying two methods-plastic and dry pressing.

The optimum heat treatment regime (according to the specifics of the tested raw materials) with heating rate of 2°C/min and isothermal inhibitions at different temperature values is established: 100°C and 200°C (30 min), 600°C and 800°C (20 min), maximum temperature 1150°C (1 h). The temperature decrease is achieved at 4°C/min, with a fluid retention of 30 min applied at 600°C.

It has been shown that the experimental specimens obtained on the basis of marl from the village Svetlen (without and with modifiers) are more successful and are characterised by lower water absorption. The obtained experimental bodies outperform the comparative standards in physical and mechanical and tribological indicators. A standard determination of the colour characteristics of the surface and the volume of the prototypes produced is carried out using the Munsell color System and an equivalent yellow colour is established with the original specimens.

Acknowledgement: The authors express their gratitude to the Fund **„**Science Research**"** of the Ministry of Finance for Research project (Contract no № КП-06-ОПР03/4 of 14.12.2018), won in a competition for the financing of fundamental research in public Challenges – 2018.

5. Literature

[1]. Boyadzhieva P., „Ceramic clay in Bulgaria", Report, Sofia, NTITI, 1959, (in Bulgarian).
[2]. Stavrakeva D., P. Grozdanova, „Raw materials and materials in silicate production", Sofia, Technika, 1989, (in Bulgarian).
[3]. Korudellieva S., I. Chomakov, T. Dimova, „Investigation of the possibility of use of marl from the "Popovo" field for the production of Fine Ceramic Products", University of Mining and Geology "St. Ivan Rilski", Yearbook, vol. 47, Scroll I, Geology and Geophysics, Sofia, 2004, pp. 109-111 (in Bulgarian).
[4]. Korudellieva S., I. Chomakov, G. Kolchakova, „Investigation of the influence of raw materials in the synthesis of yellow colored ceramics", Scientific works of the University of Ruse - 2015, Vol. 54, series 10.1, pp. 135-140 (in Bulgarian).
[5]. Boyanov I., D. Kozhuharov, A. Goranov, M. Ruseva, J. Shilyafova, Y. Yanev, Geological map of Bulgaria in M1: 100000, Haskovo. S., Committee on Geology and Mineral Resources, Geology and Geophysics - JSC, 1989, (in Bulgarian).
[6]. Bojilova R., „Analysis of Time Series Geophysical Data through the Least Squares Method. Study of Spectral Characteristics", Journal of Physics and Technology, Plovdiv University Press „Paisii Hilendarski", Vol. 1, No 2, 2017**,** pp.70-73, ISSN 2535-0536.
[7]. Patent Application No. 112274/1304.2016, entitled „Petrugical Material", Authors: P. Tsonev, L. Lakov, V. Vassilev.
[8]. Kandeva M., L. Lakov, P. Conev, V. Vasilev, Kr. Toncheva, „Tribological research of new Bulgarian „yellow paving stones", Scientific Proceedings „NDT days 2016", Year XXIV, No 1 (187), June 2016, pp. 235-240, ISSN 1310-3946 (in Bulgarian).
[9]. Lakov L., Sv. Encheva, P. Conev, V. Vasilev, B. Jivov, Kr. Toncheva, **„**Manufacturing technology, chemical and phase composition of new „yellow brick", obtain on a based of sedimentary rocks", In: Proceedings of the International Scientific Conference on Civil Engineering Design and Construction (Science and Practice), DCB 2016, 15÷17 September 2016, Varna, Bulgaria, pp. 121-127 (in Bulgarian).
[10]. Lakov L., Sv. Encheva, P. Tsonev, B. Jivov, M. Aleksandrova, Kr. Toncheva, „Production of prototypes of "yellow paving stones" in Bulgaria PART I: Physical and chemical properties", Journal of Chemical Technology and Metallurgy, 53, 6, 2018, pp. 1144-1149.
[11]. Lakov L., M. Kandeva, P. Tsonev, V. Vasilev, B. Jivov, M. Aleksandrova, Kr. Toncheva, N. Stoimenov, „Production of prototypes of „yellow paving stones" in Bulgaria PART II: Tribological and mechanical indicators", Journal of Chemical Technology and Metallurgy, 53, 6, 2018, pp. 1150-1156.

CONTEMPORARY MEASURES AGAINST HOSTILE UNMANNED AERIAL VEHICLES

ТЕНДЕНЦИИ В СЪВРЕМЕННАТА БОРБА СРЕЩУ БЕЗПИЛОТНИ ЛЕТАТЕЛНИ АПАРАТИ

Assist. Prof. Atanas Atanasov, Phd
National military university "Vasil Levski" - Veliko Tarnovo, Bulgaria
email: haceto@gmail.com

***Abstract**: The following paper presents some of the cutting edge weapon systems developed and used to counter the actions of the increasing number of different types of UAVs and the capabilities that they provide to hostile operators. All benefits and possibilities of these aerial vehicles are well known to terrorists, and other harm-seeking organizations, which tend to use the unmanned aerial vehicles in order to bring chaos and destruction among the civil population, infrastructure and military staff and bases. Because of this and many more reasons, numerous companies who work in design and manufacture of armaments have been working hard in research and development of Anti-UAV weapons. Such armaments prove to be desired by not only military staff, but also by operators of strategic infrastructure and different law enforcement organizations.*
***KEYWORDS**: UNMANNED AERIAL VEHICLES, ANTI-UAV WEAPONRY, TECHNOLOGY;*

1. Приложения на видовете безпилотни летателни апарати. Безпилотните летателни апарати имат все повече приложения в нашето съвремие. С повишаването на качествата на този вид летателни апарати и техните възможности, както и с постоянно нарастващото им търсене, производителите на различните апарати успяват да ги предложат на достъпни цени, които бяха немислими преди по-малко от десетилетие. Много малко са областите в които тези апарати са неприложими и използването им не е внесло промяна в положителен аспект. С всеки изминал ден ставаме свидетели на нова сфера или бизнес, който се възползва от този "иновативен" подход за повишаване качеството и производителността на предлаганите от него услуги. Продажбите и използването на безпилотни летателни апарати се очаква да нарасне многократно в следващите години.
На фиг. 1 е представен прогнозен ръст на продадени бройки БЛА в световен мащаб.[1]

***Фигура 1** - Прогнозен брой продажби на Безпилотни летателни апарати в световен мащаб (млн.).*

Водени именно от тези фактори, от десетилетия военно-промишлените комплекси осъзнават преимуществата, които биха могли да осигурят БЛА на видовете въоръжени сили, умеещи да ги използват правилно. Поради тази причина и дългогодишното усъвършенстване, използваните БЛА по време на военни конфликти се характеризират с високото си качество и ефикасност на изпълнените задачи. Практически не съществуват модерни Въоръжени сили, които да не разчитат до някаква степен да подобен вид апарати и да не прибягват до тяхното използване в случаите, когато това е възможно. Все по-голямата им достъпност и широката им приложимост не остават незабелязани и от множеството терористични организации действащи в конфликтни зони по Света. Това освен, че за пореден път доказва факта, че безпилотните летателни апарати не са лукс и някакъв вид ексцентризъм, а дори напротив - те са основен и понякога решаващ фактор по време на водене на бойни действия и като такъв средствата за противодействие на тези апарати, следва успешно да могат да се борят с тях. Факт е, че в днешно време средствата за противодействие на различните видове безпилотни летателни са недостатъчно, а там където са налични много често не са способни да се справят с модерните образци летателни апарати от този вид. Един от класическите способи за противодействието тези апарати е посредством т. нар. "хакерска атака" или вмешателство в системите им за управление и контрол, като по този начин се доведе апарата до състояние на неконтролируемо падане или се завземе контрола над него. Този способ се оказва успешен дълги години и се счита за достатъчно добър, съдейки по съществуващи множество примери за успешно извършени подобни операции[2]. Постоянно растящите темпове на научно-техническия прогрес обуславят значително повишаващата роля на информационните потоци при функциониране на сложни военно-технически системи като тези[3]. С напредването на технологиите обаче системите за управление и контрол на борда на апаратите и в командните им центрове стават все по-трудно достъпни и подобни атаки изискват все повече ресурс и време, докато гарантират много по-малка вероятност за успех.
От друга страна персонала, който ги извършва разполага с все по-малко време за реакция, следователно трябва да е много добре обучен и запознат със средството на което ще противодейства, а това е все по-трудно изпълнимо, имайки в предвид постоянно нарастващия брой различни видове апарати. Поради тези и редица други причини става ясно, че конвенционалният начин за унищожаване на летателен апарат може да се окаже по-успешен от "хакерските атаки".

Военно-промишлените комплекси са в надпревара в създаването на различни системи, специфично конструирани за противодействане на БЛА. Съвременните конвенционални системи за ПВО, са изключително скъпи оръдейни системи, с голям брой персонал, скъпи боеприпаси и по своята същност са създадени да противодействат на конвенционалната авиация, поради тези и други причини използването срещу безпилотни летателни апарати от различен вид не винаги е оправдано, имайки в предвид, че някои образи безпилотни летателни

[1] https://www.tractica.com/newsroom/press-releases/consumer-drone-sales-to-increase-tenfold-to-67-7-million-units-annually-by-2021/

[2] Binnie, J. (2013). Iran releases footage from captured RQ-170. IHS Jane's Defence Weekly, 50(10)

[3] Иванов, М. (2016). Основи на геоинформационните технологии, ISBN 978-954-753-236-6

апарати са със стойност по-малка от хилядна на ПВО системата и в следствие на противодействието може да я накара да разкрие собствената си позиция и да я уязви в последствие. Използването на подобни системи много често е немислимо в условията на работа в населени и урбанизирани райони или на места, където трябва да се защити стратегическа инфраструктура и опасността от жертви е много голяма. Най-успешно в такива условия работят средствата за борба с безпилотни летателни апарати, които противодействат пряко на апарата и практически не създават никакви или минимални условия за т. нар. странични щети. Унищожаването на малки и средни БЛА с дозвукова полетна скорост е основна задача пред силите за сигурност, тъй като почти всички БЛА използвани за терористични атаки или атаки срещу инфраструктура и жива сила се извършват именно използвайки подобен тип летателни средства, главно поради ниската им себестойност, простото им устройство и лекотата с която те се управляват.

2. Съвременни средства за противодействие на противникови БЛА.

2.1. Електромагнитните оръжия и в частност електромагнитните пушки се доказват като изключително успешно средство за противодействие. Работата им се заключава в директното смущение на работата и каналите за контрол и пренос на данни на летателния апарат, посредством насочен електромагнитен лъч. В следствие на това апаратурата подкачена на апарата претърпява необратими хардуерни или софтуерни изменения, които правят по-нататъшното използване на този летателен апарат невъзможно. Това е постижимо единствено в случаите, когато отношението на мощността на смущението, попадащо в лентата на пропускане на апаратурата на БЛА надвишава дори и минимално силата на сигнала на каналите за контрол и пренос на данни към БЛА.[4] В зависимост от типа апарат, оператора на т. нар. пушка може да използва различни налични заглушители, които да влияят на апарата. Основно предимство на подобен способ противодействие се явява изключителната мобилност и лекота на използване на тези оръжия, както и сравнително ниската им себестойност и заменяемост. Като основен недостатък може да се счита ограничената дистанция на която могат да въздействат, както и по-голямата възможност за допускане противников безпилотен летателен апарат, въпреки опита за противодействие. Най-често този вид средства за противодействие се използват в райони за временно дислоциране или в такива в които е възникнала критична ситуация по изключение и те се очаква да бъде преодоляна напълно в кратки срокове.

2.2 Успешно оръжие срещу безпилотните летателни апарати използва лазер за унищожаването апаратите. Лазерният лъч който се използва е с голяма мощност и нанася непоправими щети по корпуса на летателния апарат, като прави невъзможен по-нататъшния му полет. Поради изключително бурното развитие на възможностите предоставяни от различните видове лазери, бъдещето пред този вид средства за противодействие се очертава като многообещаващо, подобна технология монтирана именно на безпилотни летателни апарати се счита за един от бъдещите способи за противодействие на последното поколение между континентални балистични ракети. Тези системи са много по-сложни конструктивно, стационарни или трудни за дислоциране, поради особеностите на компонентите, които са вложени в изделието, те са скъпоструващи, използват системи за локализиране на обектите и тяхното непосредствено съпровождане, като много често могат да работят напълно самостоятелно (напр. в зони забранени за полети). Характерно за тяхната работа е, че е необходима много по-голяма инвестиция, трудни са за разполагане без предварителна подготовка и в кратки срокове. Основни предимства се явяват високата точност с която работят, възможността да работят в отдалечени и безлюдни райони самостоятелно т.е. без персонал непосредствено при изделието. Практически при правилната работа с подобен вид оръжие се гарантира изключително висока успеваемост при борба с противникови БЛА. Лазерната борба с летателни апарати се счита за бъдещ основен способ на противодействие. Теоретично ограниченията пред възможностите предоставяни от подобна технология не са достигнати и се очаква все по-голям дял от бъдещите средства за борба с всички видове летателни апарати да разчитат именно на тази или подобна технология.

2. 3. В случаите в които не е възможно използването на електромагнитни или лазерни средства за противодействие, като например в гъсто населени урбанизирани райони или в близост до обекти, характеризиращи се с чувствителност към гореизложените способи на въздействие, изключително успешно се използва т. нар. способ "anti-drone drone" показано на изображение 1, който по своята същност представлява използването на собствен безпилотен летателен апарат или апарати с чиято помощ да се противодейства на действията на противниковия БЛА. Използвайки собствени летателни средства за тази цел се дава възможност на оператора да "залови" противниковия БЛА, посредством мрежа или друг вид захващане, предоставяйки възможност за обследване на

Изображение 1 *Anti-drone drone*

заловения летателен апарат, евентуално последвано от инкриминиране на действията на оператора на това летателно средство. Този на пръв поглед архаичен способ за противодействие се доказва като изключително надежден срещу т. нар. "VTOL Drones" или безпилотни летателни апарати с вертикално излитане и кацане, поради сравнително по-ниската им полетна скорост, по-голямата възможност за успешно противодействие и далеч не толкова подходящ за борба срещу БЛА с конвенционален или т.нар. летищен способ на излитане/кацане с висока полетна скорост.

Ниската експлоатационна цена на апаратите и практически почти несъществуващите ограничения на използването им ги правят предпочитан избор на много места. Като друг основен недостатък на този вид противодействие може да се счита необходимостта от опитен оператор на собствения безпилотен летателен апарат, който да умее да борави отлично с предоставената му техника.

2.4. На този принцип съществуват също така и специално разработени пушки, изстрелващи мрежа във въздуха, която улавя апарата и предотвратява полета му, изобразени на фиг. 2.

[4] Lazarov L.,General Terms and Conditions for the Radio Connection Jamming, International conference on High Technology for Sustainable Development HiTECH 2018, ISBN: 978-1-5386-7039-2

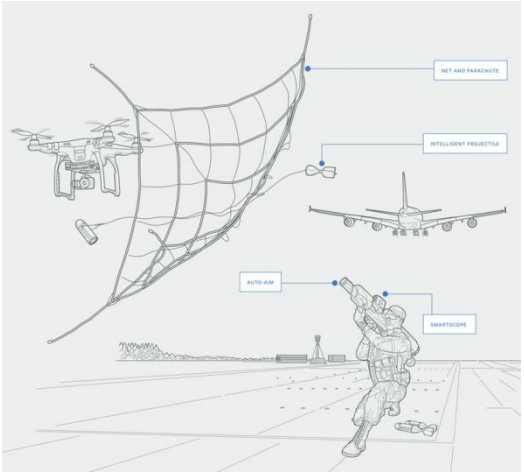

Фигура 2 *- Примерен модел на пушка изстрелваща мрежа за противодействие на БЛА*

Този вид противодействие, подобно на използвания от борда на БЛА е подходящ за борба с "VTOL drones" и се доказва като незаменим особено при борба с нелегалния трафик на стоки и други нерегламентирани дейности над гранични бразди и други обекти с контролиран достъп. След успешното улавяне на БЛА от мрежата се разтваря парашут, който предотвратява излишното унищожение на вече заловения летателен апарат Като недостатък може да се характеризира сравнително малката дистанция на която може да се въздейства на летателния апарати, както трудното локализиране на малки и микро БЛА. В този случай отново наличието на добре обучен персонал е гаранция за постигането на високи нива на ефикасност при използването на метода.

2.5. В случаите когато периметъра който трябва да се контролира за нерегламентиран достъп от страна на БЛА е сравнително малък и не търпи изменения за голям времеви период е оправдана инвестиция в т. нар небесна стена, изобразена на фиг. 3.

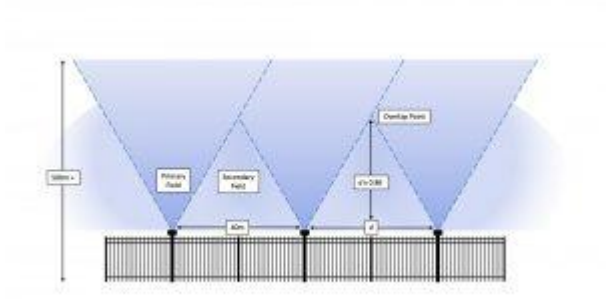

Фигура 3 - Система за противодействие тип "небесна стена"

По своята същност една подобна система представлява постоянно работещи или автоматично активиращи се насочени нагоре множество излъчватели подредени един до друг в определен периметър и припокриващи се, които имат за цел да смущават управлението на прелитащи над тях безпилотни летателни апарати, които нарушават определения периметър. В допълнение на това системата може да се оборудва с допълнителни компоненти, които да проследяват обратния полет на засечените нарушители в случаите в които контролиращите ги се опитат да си ги върнат, като по този начин разкрият местоположението си. Системи от този тип се доказват като изключително подходящи при охраната на затвори и други обекти с контролиран достъп към които често има опити за пренос на нерегламентирани стоки посредством БЛА. В случаите в които се използва подобна система инвестицията която се прави е значителна и следва да се изготви прецизен анализ за бъдещи инфраструктурни изменения по периметъра който се оборудва със системата, поради факта, че последвало изменения е съпътствано със допълнителни разходи, които в повечето случаи са значителни. От друга страна подобна система се характеризира с много високо ниво на защита и работи практически автономно и без необходимост от постоянно човешко присъствие.

2.6. Използването на жива животинска сила за борба с безпилотните летателни апарати може би звучи нетрадиционно и неефективно, но пазара показва, че съществуват редица предприемачи, които се концентрират изключително върху дресирането и продажбата на едри грабливи птици, обучени в залавянето на БЛА. Този метод на противодействие буди множество дискусии и полемики както от морална така и от чисто прагматична гледна точка. Птиците използвани за тези цели често стават жертва на летателните апарати или на операторите им които ги отстрелват, за да не могат да им пречат те. От друга страна е необходимо да има човек, който да познава животните и да умее да работи с тях винаги щом е необходимо. Именно поради тези и други причини този метод на противодействие не е популярен сред търсещите противодействие на БЛА, но все пак намира своята пазарна ниша.

3. Заключение. Широкия спектър от задачи които се поставят пред съвременните безпилотни летателни апарати не остава скрит за престъпния свят. Възможностите които предоставят тези летателни апарати на операторите без да ги поставят под пряка заплаха правят използването им все по-често срещано. Този вид апарати стават все по-достъпни и надеждни като придобиването им в днешно време съвсем не е лукса, който те са представлявали само преди няколко години. Именно поради тези и други причини заплахите които могат да представляват БЛА нарастват пропорционално с тяхното разпространение. Тези заплахи не могат да бъдат оставени безответни и в ситуацията в която системите за противодействие на конвенционална авиация се оказват неподходящи или тяхното използване неоснователно се налага да бъдат разработени и произведени един напълно нов тип оръжия, а именно тези за борба с безпилотните летателни апарати. Търсенето на този тип оръжие нараства с всеки изминал ден и тяхното усъвършенстване е един процес, който логически следва този на подобряване възможностите предоставяни от най-новите образци безпилотни летателни апарати. Въоръжените сили на страните и силовите структури в самите страни инвестират изключително сериозни средства в системи, гарантиращи сигурността им срещу нежелани безпилотни летателни апарати, осъзнавайки материалните и нематериални щети, които могат да нанесат те. Този вид летателни апарати и средствата за борба с тях естествено ще се усъвършенстват едновременно. Летателните апарати ще стават по-надеждни, по-бързи, по-добри ,а средствата за борба с тях ще стават по-прецизни, по-ефективни и по-разпространени. Моментът в който се подценяваха и пренебрегваха възможностите, които дава подходящия безпилотен летателен апарат на неподходящия оператор е останал безвъзвратно в миналото и никога няма да се върне. Никоя сериозна организация за в бъдеще няма може да си позволи лукса да прояви неблагоразумието да остане незащитена от този съвременен вид летателни средства в ситуацията в която се намира Светът.

4. Литература

1.https://www.tractica.com/newsroom/press-releases/consumer-drone-sales-to-increase-tenfold-to-67-7-million-units-annually-by-2021/

2. Binnie, J. (2013). Iran releases footage from captured RQ-170. IHS Jane's Defence Weekly, 50(10)

3. Иванов, М. (2016). Основи на геоинформационните технологии, ISBN 978-954-753-236-6

4. Lazarov L.,General Terms and Conditions for the Radio Connection Jamming, International conference on High Technology for Sustainable Development HiTECH 2018, ISBN: 978-1-5386-7039-2

AMPLIFIED SPONTANEOUS EMISSION IN FIBER OPTIC LINES USING RAMAN AMPLIFIERS

Chief ass. prof. Eng. Penev Penyo PhD
Aviation Faculty, National Military University „Vasil Levski“, Dolna Mitropolia, Bulgaria

penyo_g_penev@abv.bg

Abstract: *New methods for a regeneration and an enhancement of the optical signal have been developed all over the world. The main reason is the increasing bit rate and optical fiber length. A new method for optical amplifiers based on nonlinear effects is discussed in this report. Amplification changes are surveyed as a function of the signal power at different pump configurations and different wavelength.*

Keywords: Fiber Raman Amplifier (FRA), Amplified Spontaneous Emission (ASE), Optical noise, Raman amplification, Raman Gain Coefficient.

1. Introduction

Communication systems are used to transfer information both within a country, continent and for intercontinental transmission. Systems development and the growing information traffic require a new traffic area like fiber optic to be involved.

As nowadays Wavelength Division Multiplexing (WDM) systems are those with growing bit rate information and the length of fiber optic lines and use of repeaters leads to limitation of bandwidth, it is necessary to use another type of units to replace these devices.

Retransmission limitation also influences the transmission of information in modern multilateral (MLAT) systems that are increasingly used in radar-free areas. The limitations of the radio channels used in MLAT systems also contribute to the involving of optical lines in this type of surveillance system [7, 6].

For these reasons, alternative approaches to loss decrease are required in optical amplifiers that amplify the optical signal directly without requiring transformation in the electrical signal [4].

One of the most effective methods of amplifying optical signals is the use of the non-linear effects of Stimulated Raman scattering and Stimulated Brillouin scattering. Optical amplifiers built on these effects, and in particular the Raman effect, can successfully replace optical repeaters, and even massive used Erbium-Doped Fiber Amplifier (EDFA) [4].

At the beginning of the 21st century, almost any long distances optical system (usually defined from 300 to 800 km) or ultra-long distances once (typically defined over 800 kilometers) uses the Raman Optical Amplifier (FRA).

A great FRA advantage is a very wide bandwidth amplifying which allows that to be used in various optical systems using the existing optical lines. The gain is accomplished in the fiber itself with significantly better figure noise resistant.

FRA gain using the transmission fiber as a carrier is an advantage technology in DWDM optical telecommunication systems. To amplify signal more pump power is needed, but thus the noise of Amplified Spontaneous Emissions (ASE) increases and other noises generated in the amplifier also reduces the power of the input signal to the amplifier. So, ASE takes an important part in transmitting the optical signal to the receiver [4, 5].

It is important to research the gain variation as a function of the signal power in the different pump configurations and fiber lengths. One of the main noises, namely ASE, can be used in the FRA. By adding ASE to the amplification process, it is possible to improve the amplifier operation and increase the gain of the amplifier [8].

2. Mathematical models on ASE influence on Raman Amplifier gain coefficient.

The FRA bandwidth is above 40 THz, with a dominant peak at 13.2 THz relative to the pump frequency (Figure 1) [3, 9].

The gain coefficient g_r is related to Raman's spontaneous scattering cross section, which is measured experimentally and generally depends on the optical fiber characteristics, and is also highly dependent on the polarization state between the pump and the signal. For a fiber of several tens of meters in length, propagation of the signal and the pump through it will cause the two states of polarization to decrease g_r.

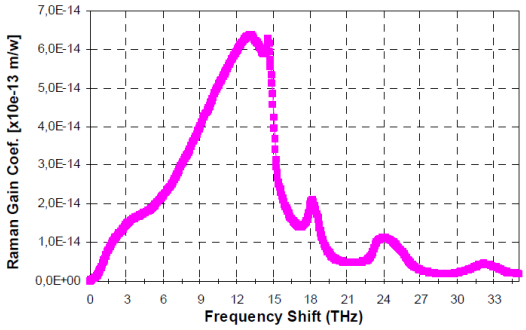

Figure 1. *The Raman amplifier gain coefficient g_r for the wavelengths of the signal and of the pump [3, 9].*

We examine the simplest case of spreading a beam entering in the optical fiber used for amplification.

It is necessary to calculate the amplification of Raman's amplifier signal with or without spontaneous emission.

2.1 Raman gain without amplified spontaneous emission.

The amplification of the signal and propagation of the pump signal along the length of the optical fiber is described by the following equations:

$$\frac{dP_s}{dz} = -\alpha_s P_s + \frac{g_r}{A_{eff}} P_p P_s \qquad (1)$$

$$\frac{dP_p}{dz} = -\alpha_p P_p + \frac{g_r}{A_{eff}} \frac{\omega_p}{\omega_s} P_p P_s \qquad (2)$$

where P_s and P_p are the signal power and pump power;

g_r is the gain coefficient to the Raman amplifier;

α_s and α_p are the optical fiber attenuation coefficients for the wavelengths of the signal and the pump;

ω_s and ω_p are carrier of signal waves and pump waves.

Second part of the equation (2) represents the transmitted power from the pump if we ignore it and solve the equation and replace in (1) the following expression:

$$\frac{dP_s}{dz} = -\alpha_s P_s + \frac{g_r}{A_{eff}} P_p(0)\exp(-\alpha_p z) P_s \qquad (3)$$

Where $P_p(0)$ is pump power at $z = 0$.

After reading the length of the optical fiber, meaning $z = L$ and by the equation (3) is obtained

$$P_s(L) = P_s(0)\exp\left(\frac{g_r P_p(0) L_{eff}}{A_{eff}} - \alpha_s L\right) \qquad (4)$$

where L_{eff} the effective length of interaction between the signal and the pump is determined by the equation:

$$L_{eff} = \frac{1-\exp(-\alpha_p L)}{\alpha_p} \qquad (5)$$

After integrating equation (4) for Raman gain coefficient [dB] is obtained:

$$G_s[dB] = -\alpha_s L + \frac{0{,}434 g_r P_p(0) L_{eff}}{A_{eff}} \qquad (6)$$

where L_{eff} is effective length of interaction between the signal and the pump in meters.

2.2 Raman gain with amplified spontaneous emission.

ASE is a typical noise in optical amplifiers. FRA is used to increase amplification of the optical amplifier.

ASE is added to the signal power in equation (1). Then equation (1) takes the following form:

$$\frac{dP_s}{dz} = -\alpha_s P_s + \frac{g_r}{A_{eff}} P_p\left(P_s + P_{ASE}\right) \qquad (7)$$

where $P_{ASE} = 2 n_{sp} h \upsilon_s \Delta V_R$ and $h = 6{,}6260.10^{-34}[m^2 kg/s]$ is Planck's constant.

$n_{sp} = \frac{1}{1-\exp\left(\frac{-h\Omega}{K_B T}\right)}$ is the spontaneous emission factor.

$$\frac{dP_s}{dz} = -\alpha_s P_s + \frac{g_r}{A_{eff}} P_p P_s + \frac{g_r}{A_{eff}} P_p 2 n_{sp} h \upsilon_s \Delta V_R \qquad (8)$$

After reading the length of the optical fiber, meaning $z = L$ and integrating an equation (8) the gain with added ASE is obtained:

$$G_{ASE}[dB] = 0{,}434\left(-\alpha_s L - \frac{g_r P_p(0) L_{eff}}{A_{eff}} - \frac{P_{ASE} g_r P_p(0)\left(1-\exp\left(\alpha_s - \alpha_p\right)\right)L}{A_{eff} P_s(0)\left(\alpha_s - \alpha_p\right)}\right) \qquad (9)$$

3. Simulations and results.

In order to study the impact of ASE on the FRA gain ratio, two types fiber optics, Standard single mode fiber (SMF) [1] and Non-zero dispersion-shifted fiber (NZ-DSF) [2] were used. The fiber parameters are given in Table 1.

Table 1. Fiber optic parameters

Optical fiber	Attenuation coefficients α_s [dB/km]	Wavelengths λ_s [nm]	Raman gain coefficient g_r [1/mW]	Fiber effective area A_{eff} [μm²]	Fiber optic length [km]
SMF	0,13 dB/km	1550 nm	$4{,}2.10^{-14}$	80 μm²	100 km
NZ-DSF	0,18 dB/km	1550 nm	$4{,}2.10^{-14}$	72 μm²	100 km

To calculate the effective length of interaction between the signal and the pump, it is more convenient to translate the equation (5) L_{eff} into decibels.

It is more convenient to use an equation in which the attenuation coefficient set in the reference data in dB/km is used directly. Then (5) acquires the following form:

$$L_{eff} = \frac{4{,}343}{\alpha_p}\left(1-\exp\left(-0{,}23\alpha_p L\right)\right) \qquad (10)$$

Figure 2 shows the results of the equation (10) of the effective length of the signal and pump interaction depending on the length of the optical fiber.

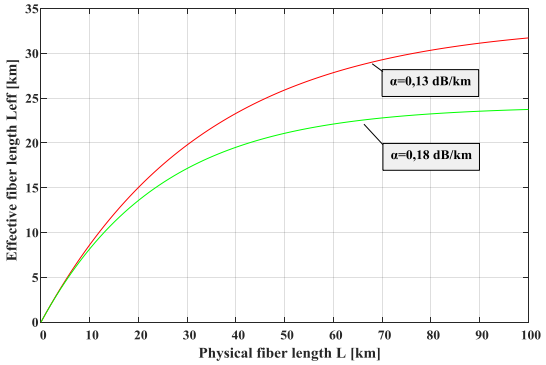

Figure 2. *Effective fiber length L_{eff} for both fiber types.*

The figure shows that L_{eff} depends on the attenuation coefficient, i.e. from fiber type.

Figure 3 shows the results obtained for the gain ratio using a pump with power *Pp=500mW* and different wavelength. In the figure, the first graph is obtained with the pump attenuation coefficient $\alpha_p = 0{,}13 dB/km$, and the second with the attenuation coefficient $\alpha_p = 0{,}18 dB/km$.

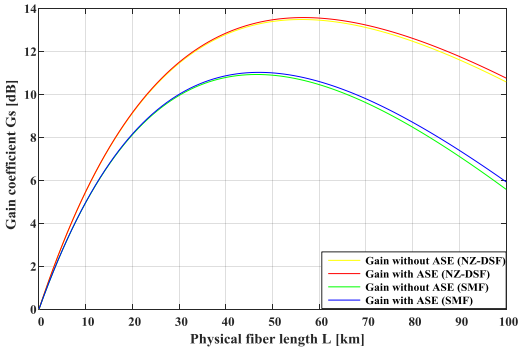

a) with $\lambda_p = 1450nm$

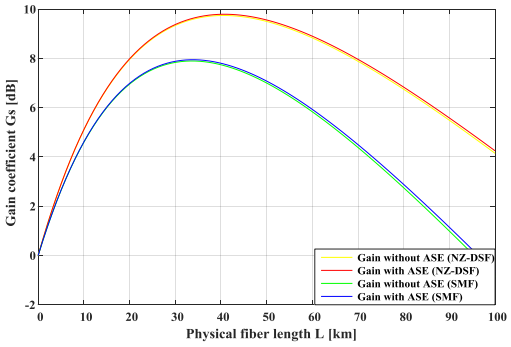

b) with $\lambda_p = 1460nm$

Figure 3. *The Raman amplifier gain coefficient with Pp=500mW.*

Figure 4 shows the results obtained for the gain ratio using a pump with power *Pp=1000mW* and different wavelength. In the figure, the first graph is obtained with the pump attenuation coefficient $\alpha_p = 0{,}13dB/km$, and the second with the attenuation coefficient $\alpha_p = 0{,}18dB/km$.

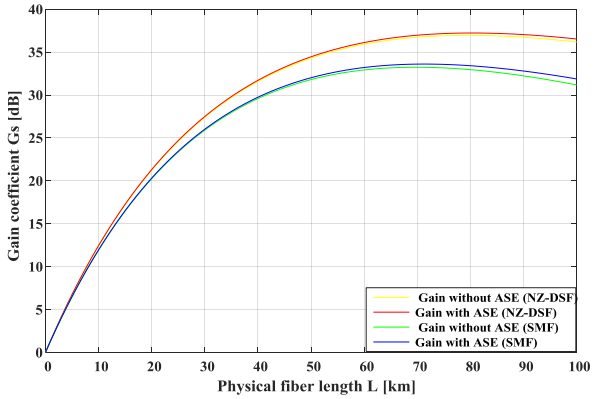

a) with $\lambda_p = 1450nm$

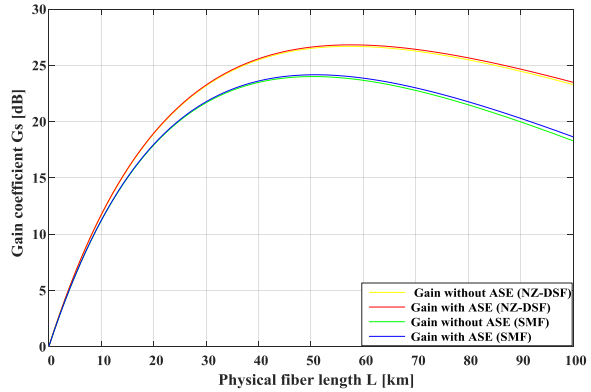

b) with $\lambda_p = 1460nm$

Figure 4. *The Raman amplifier gain coefficient with Pp=1000mW.*

Figure 5 shows a graph of the difference between ASE and non-ASE gains of different fiber types. The attenuation coefficient for the both pumps are respectively $\alpha_p = 0{,}13dB/km$ and $\alpha_p = 0{,}18dB/km$.

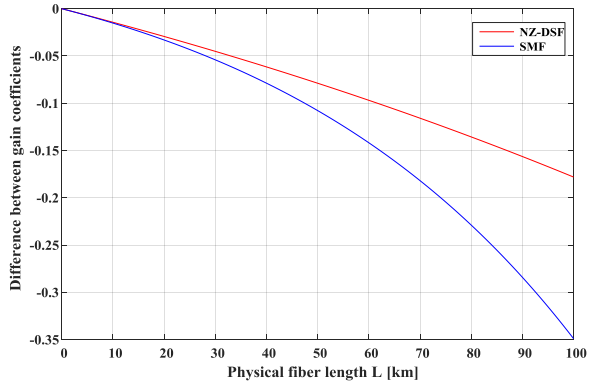

a) with $\lambda_p = 1450nm$

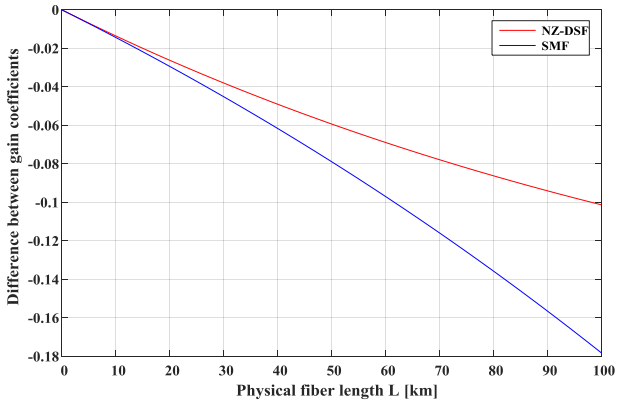

b) with $\lambda_p = 1460nm$

Figure 5. *Subtraction the Raman amplifier gain coefficient with Pp=500mW.*

Figure 6 shows a graph of the difference between ASE and non-ASE gains of different fiber types. The attenuation coefficient for the both pumps are respectively $\alpha_p = 0{,}13dB/km$ and $\alpha_p = 0{,}18dB/km$.

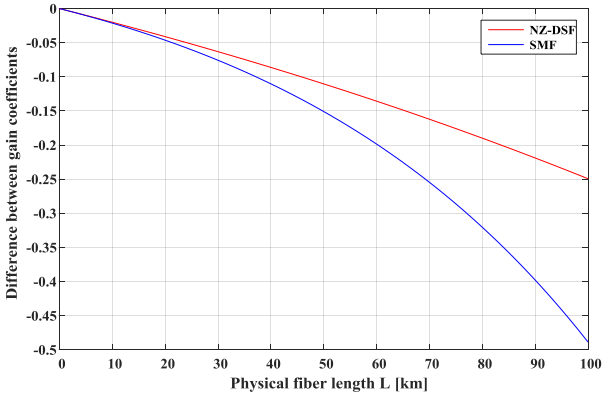

a) with $\lambda_p = 1450nm$

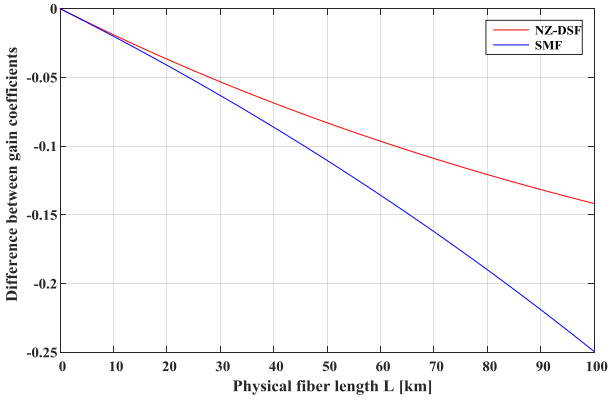

b) with $\lambda_p = 1460nm$

Figure 6. *Subtraction the Raman amplifier gain coefficient with Pp=1000mW.*

From the results obtained, it is seen that in order to achieve a higher amplification of the signal, higher pump power is required. At pump power Pp=1000mW the gain is greatest.

The results show that the gain coefficient for both fiber types is higher when ASE is added in the amplification process.

When a specified wavelength of the pump is used, the ASE gain ratio is approaching the gain coefficient without ASE.

From the results derived for the difference between the gains for the two fiber types, it can be seen that the gain rate also depends on the fiber type.

4. Conclusion.

Choosing a suitable laser as a pump can reduce the number of amplifiers used in the long lines. Increasing the power of the pump also leads to a reduction in the number of amplifiers, but so far there are not as many powerful lasers to use in the FRA.

To achieve greater amplification, the selection of an appropriate laser is very important. By selecting a laser with appropriate wavelengths and an attenuation coefficient for a specific fiber type, we achieve a greater effect than ASE.

Using an appropriate fiber type will make a greater use of ASE in the amplification process.

The results obtained and the conclusions drawn show that long and ultra-long lines require a more detailed spontaneous emission study in order to increase the regeneration areas and reduce the number of amplifiers.

5. References.

1. Characteristics of a single-mode optical fibre and cable, Recommendation ITU-T G.652, 2009.

2. Characteristics of a non-zero dispersion-shifted single-mode optical fibre and cable, Recommendation ITU-T G.655, 2009.

3. D. B. M. Pereira, A. L. Teixeira……, Raman Amplifiers for Use in WDM Systems, Revista Do Detua, vol. 3, №8, January 2003.

4. Islam M. N., "Raman amplifiers for telecommunications 1: Physical principles", Springer-Verlag, New York, Inc., 2004.

5. K. Rottwitt and M. Nissov, Detailed analysis of Raman amplifiers for long-haul transmission. In Proceedings of the Optical Fiber Communication Conference, Technical Digest, Conference EditionWashington DC: Optical Society of America, TuG1, 1998.

6. Marinov M. Peneva V., Opportunities for MLAT systems using in air traffic management and control, II International scientific conference CONFSEC, Borovets, 2018, pp. 243-245.

7. Peneva V., Aviation safety development by optimization of airspace, XXVI International scientific conference on transport, road-building, agricultural, hoisting & hauling, Borovets, 2018, pp. 387-389.

8. R. Sharma, S. K. Raghuwanshi, RAMAN amplifier gain dynamics with ASE: Numerical nalysis and simulation approach, International Journal of Engineering, Science and echnology Vol. 7, No. 3, 2015, pp. 52-57, 2015.

9. VPIcomponentMaker™ Optical Amplifiers User's Manual, Virtual Photonics Incorporated, 2002.

CHELATING EXTRACTION TECHNOLOGY IN REMOVING AND RECOVERING HEAVY METALS FROM MUNICIPAL SLUDGE

Professor Dr. Valdas Paulauskas
Aleksandras Stulginskis University, Lithuania
valdas.paulauskas@asu.lt

APPROACH FOR MODEL DRIVEN DEVELOPMENT OF MULTI-AGENT SYSTEMS FOR AMBIENT INTELLIGENCE

Prof. Dr. Idilia Batchkova
Dept. of Industrial Automation
UCTM-Sofia